SYNTHETIC AND STRUCTURAL STUDIES OF NOVEL β-SHEET MODELS

a thesis presented by

Nigel Pitt

to the

UNIVERSITY OF ST. ANDREWS

in application for

THE DEGREE OF DOCTOR OF PHILOSOPHY

St. Andrews July 2000

Declaration

I, Nigel Pitt, hereby certify that this thesis, which is approximately 51,000 words in length, has been written by me, that it is a record of work carried out by me and that it has not been submitted in any previous application for a higher degree.

date 20/7/00 signature of candidate

I was admitted as a research student in October 1995 and as a candidate for the degree of Ph.D. in October 1996; the higher study for which this is a record was carried out at the University of St. Andrews between 1995 and 1999.

date 20/7/00 signature of candidate

I hereby certify that the candidate has fulfilled the conditions of the Resolution and Regulations appropriate to the degree of Ph.D. in the University of St Andrews and that the candidate is qualified to submit this thesis in application for that degree.

date 20 July 2000 signature of supervisor

Copyright

Acknowledgements

I would firstly like to thank the Universities of St. Andrews and Birmingham for financial support and providing excellent working facilities. I would also like to thank Professor David Gani for supervision, Drs Mahmoud Akhtar, Amit Mehrotra for proof-reading this thesis and Dr Nigel Botting for friendly and helpful advice throughout the preparation of this work. I am also grateful to Drs Benson Kariuki and Philip Lightfoot for providing X-ray crystal structures, Mel Smith and Dr Neil Spencer for excellent NMR support, Peter Ashton and Nick May for mass spectrometry data, Dr Jenny Tang for invaluable advice on HPLC, Dr Thierry Jenn and Michael O' Donnell for synthetic advice, Lynn Blake for friendly chats and all my laboratory co-workers (Iain, Saqib, Pui Shan, Duane, Serge, Shuyan, Dave, Jonathan and Martin) for creating such a friendly working atmosphere.

Finally, I would like to thank my parents for their patience, generosity and support during the researching and writing of this thesis.

Abstract

β-Turns and β-sheets are important structural features of many biologically active peptides and proteins, and are involved in a diverse range of processes from protein dimerisation to substrate recognition by proteolytic enzymes. In spite of their importance, however, the factors behind β-sheet nucleation and stabilisation are still not well understood. A small well-behaved model system would allow the structural detail of a β-sheet to be studied spectroscopically in the absence of the tertiary interactions of a protein. When isolated, oligopeptide sequences with a known propensity to form β-sheet within their native protein environment generally adopt a random-coil conformation and frequently hydrogen-bond to neighbouring strands to form heterogeneous aggregates that cannot be analysed spectroscopically.

Computer modelling studies have suggested that acetylene-based pseudo amino acids, when incorporated into peptides, have the potential to stabilise an isolated β-sheet structure. The phenylacetylene-based pseudo amino acids, methyl (2*R*)-2-[2'-(3"-*tert*-butoxycarbonylamino-prop-1"-ynyl)-phenylamino]-propanoate (Boc-APPP-OMe), methyl (2*R*)-[2'-(3"-*tert*-butoxycarbonylamino-prop-1'-ynyl)-phenylamino]-4-methyl-pentanoate (Boc-APPMP-OMe), methyl (2*S*)-[2'-(3"-*tert*-butoxycarbonyl-amino-prop-1"-ynyl)-phenylamino]-3-phenyl-propanoate (Boc-APPPP-OMe) and methyl (2*S*)-2-[2'-(3"-*tert*-butoxycarbonylamino-prop-1"-ynyl)-phenylamino]-butanoate (Boc-APPB-OMe) were each prepared in 6 steps from propargylamine, iodoaniline and a range of amino or α-hydroxy acids. Solution phase synthetic routes were devised for the incorporation of these units into a cyclic hexapeptide analogue [cyclo(APPP-APPMP); 6 steps] and a cyclic decapeptide analogue [cyclo(APPPP-Ala-Val-APPB-Thr-Leu); 17 steps]. The synthesis of a large cyclic tetradecapeptide analogue [cyclo(APPPP-Ala-Abu-Thr-Leu-APPPP-Ala-Val-Ile-Ala)] employed a combination of solution and solid phase techniques (14 steps). 2D NOE studies in C^2HCl_3 indicate that the cyclic hexapeptide and decapeptide analogues adopt an intramolecularly H-bonded β-sheet structure. Although no NOE data was available for the cyclic tetradecapeptide analogue, its rate of cyclisation was comparable to the other, smaller cyclic systems, indicating that a degree of β-sheet pre-formation may be present in the acyclic precursor.

X-ray crystal structure data for the pseudo amino acid Boc-APPB-OMe and the immediate precursor, 2-(3'-*tert*-butoxycarbonylamino-prop-1'-ynyl)-phenylamine, is also presented and discussed.

Contents

List of Figures

List of Schemes

List of Tables

Amino acid codes

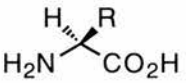

Amino acid	*Abbreviation*	*1-letter code*	*-R*
Alanine	Ala	A	$-CH_3$
Arginine	Arg	R	$-(CH_2)_3NHC(=NH)NH_2$
Asparagine	Asn	N	$-CH_2CONH_2$
Aspartic acid	Asp	D	$-CH_2CO_2H$
Cysteine	Cys	C	$-CH_2SH$
Glutamine	Gln	Q	$-(CH_2)_2CONH_2$
Glutamic acid	Glu	E	$-(CH_2)_2CO_2H$
Glycine	Gly	G	-H
Histidine	His	H	$-CH_2$(4-imidazolyl)
Isoleucine	Ile	I	$-CH(CH_3)CH_2CH_3$
Leucine	Leu	L	$-CH_2CH(CH_3)_2$
Lysine	Lys	K	$-(CH_2)_4NH_2$
Methionine	Met	M	$-(CH_2)_2SCH_3$
Phenylalanine	Phe	F	$-CH_2Ph$
Serine	Ser	S	$-CH_2OH$
Threonine	Thr	T	$-CH(CH_3)OH$
Tryptophan	Trp	W	$-CH_2$(3-indolyl)
Tyrosine	Tyr	Y	$-CH_2$(4-hydroxyphenyl)
Valine	Val	V	$-CH(CH_3)_2$
Proline	Pro	P	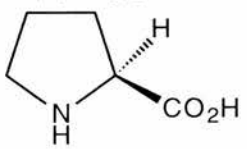

Abbreviations

Bn	benzyl
BOC	*tert*-butoxycarbonyl
CD	circular dichroism
Cbz	benzyloxycarbonyl
COSY	correlation spectroscopy
CTAB	cetyltrimethylammonium bromide
CVFF	consistent valence force field
DMAP	4-dimethylaminopyridine
DMF	*N*,*N*'-dimethylformamide
DMS	dimethylsulfide
DMSO	dimethylsulfoxide
DNA	deoxyribonucleic acid
EDCI	*N*-(3-dimethylaminopropyl)-*N*'-ethylcarbodiimide hydrochloride
FMDV	foot-and-mouth disease virus
Fmoc	9-fluorenylmethoxycarbonyl
HPLC	high performance liquid chromatography
NMM	*N*-methyl morpholine
NMR	nuclear magnetic resonance
NOE	nuclear Overhauser enhancement
NOESY	NOE correlation spectroscopy
PyBOP	benzoptriazolyloxy-*tris*[pyrrolidino]-phosphonium hexafluorophosphate
RNA	ribonucleic acid
mRNA	messenger ribonucleic acid
tRNA	transfer ribonucleic acid
SPPS	solid phase peptide synthesis

TASP	template assembled synthetic protein
TFA	trifluoroacetic acid
TFMSA	trifluoromethane sulfonic anhydride
TMSI	trimethylsilyl iodide
THF	tetrahydrofuran
TLC	thin layer chromatography

1. INTRODUCTION

1.1 Proteins and Peptides

1.1.1 Introduction

"Could the search for ultimate truth really have revealed so hideous and visceral-looking an object?". This was a statement made by Perutz in 1964 in relation to the first X-ray crystal structure of a protein.[1] Perutz was expressing the disappointment he felt when he observed the structure of the protein, sperm whale myoglobin. Rather than the highly ordered and symmetrical structure many scientists anticipated, the protein appeared to be a chaotic tangle of peptides, with few clues as to the factors controlling its shape.[1]

In the last 30 years, with the advent of higher resolution X-ray crystallography, a greater appreciation of peptide and protein structure has developed. Proteins are now viewed as graceful structures, containing elegant and well-ordered helices, sheets and ribbons of peptide that twist and turn throughout the macromolecule. One remarkable feature of proteins is that every one of these elaborate sub-structures has a specific role in defining the overall shape, structure and function of the protein.

As well as being the primary constituent of proteins, peptides also constitute small, biologically active molecules[2] which regulate almost every important biochemical process by binding to membrane bound proteins in a cell. Examples include angiotensin II and renin which together regulate blood pressure;[2] tachykinins, responsible for neuromodulation in parts of the central and peripheral nervous system; cholecystokinin, which increases the release of insulin, and opioid peptides which possess analgesic properties.[2-9] There are also peptides that have general antimicrobial properties such as cecropins, bombinins defensins and protegrins.[10]

Like larger proteins, the 3D structure of biologically active peptides is essential for defining their function. The elucidation of the relationship between peptide sequence and 3D structure of both peptides and proteins is an area of intense interest with potential applications in the development of new peptide based therapeutic agents. What now follows is a summary of the processes behind protein and peptide biosynthesis and an overview of the key structural motifs that define their shape and function.

1.1.2 Synthesis of proteins and peptides from DNA

DNA, a sugar-phosphate polymer with heterocyclic bases attached, contains all the necessary information for creating the many hundreds of thousands of proteins and peptides found in living organisms. The process by which genetic information is converted into proteins is central to molecular biology, and follows a well defined 3-step process (Scheme 1.1).

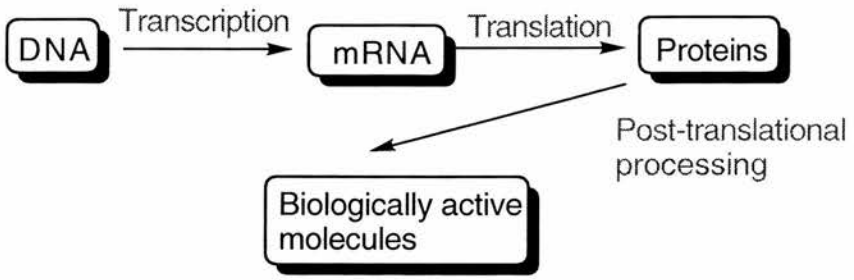

Scheme 1.1: *Origin of biologically active peptides*

Transcription is the process by which a segment of DNA double helix unwinds and exposes the bases of the 2 strands (Fig. 1.1). Ribonucleotides line up in the proper order by hydrogen bonding to their complementary base on the DNA template strand. This DNA strand contains promoter sites which are specific base sequences that bind RNA polymerase, the protein responsible for the polymerisation of messenger RNA (mRNA), thus signalling the start of a gene. Similarly, other base sequences at the end of the gene terminate this synthesis.[11]

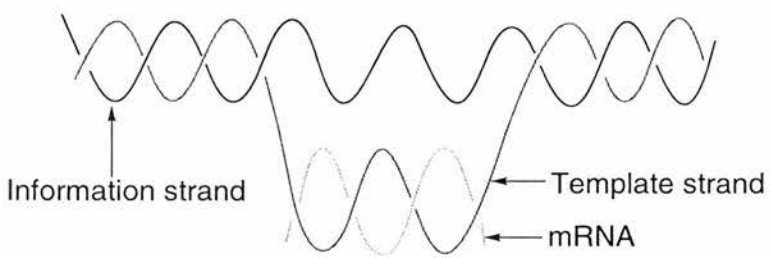

Figure 1.1: *Schematic representation of the biosynthesis of mRNA from DNA*

Once the mRNA molecule is synthesised, the process of translation can begin. This takes place on the ribosome, a complex structure composed of proteins and

ribosomal RNA (rRNA), where the mRNA serves as a direct blueprint for the peptide or protein sequence. Groups of three nucleotides on the mRNA molecule (the codon) code for a specific amino acid on the protein and this is read by transfer RNA (tRNA). There are over 60 different tRNA molecules, one for every codon combination. Each tRNA acts as a carrier to bring a particular amino acid into place so that it can be transferred to the growing protein chain by enzyme mediated transfer;[11] the exact sequence of protein/peptide synthesis is detailed below (Scheme 1.2).

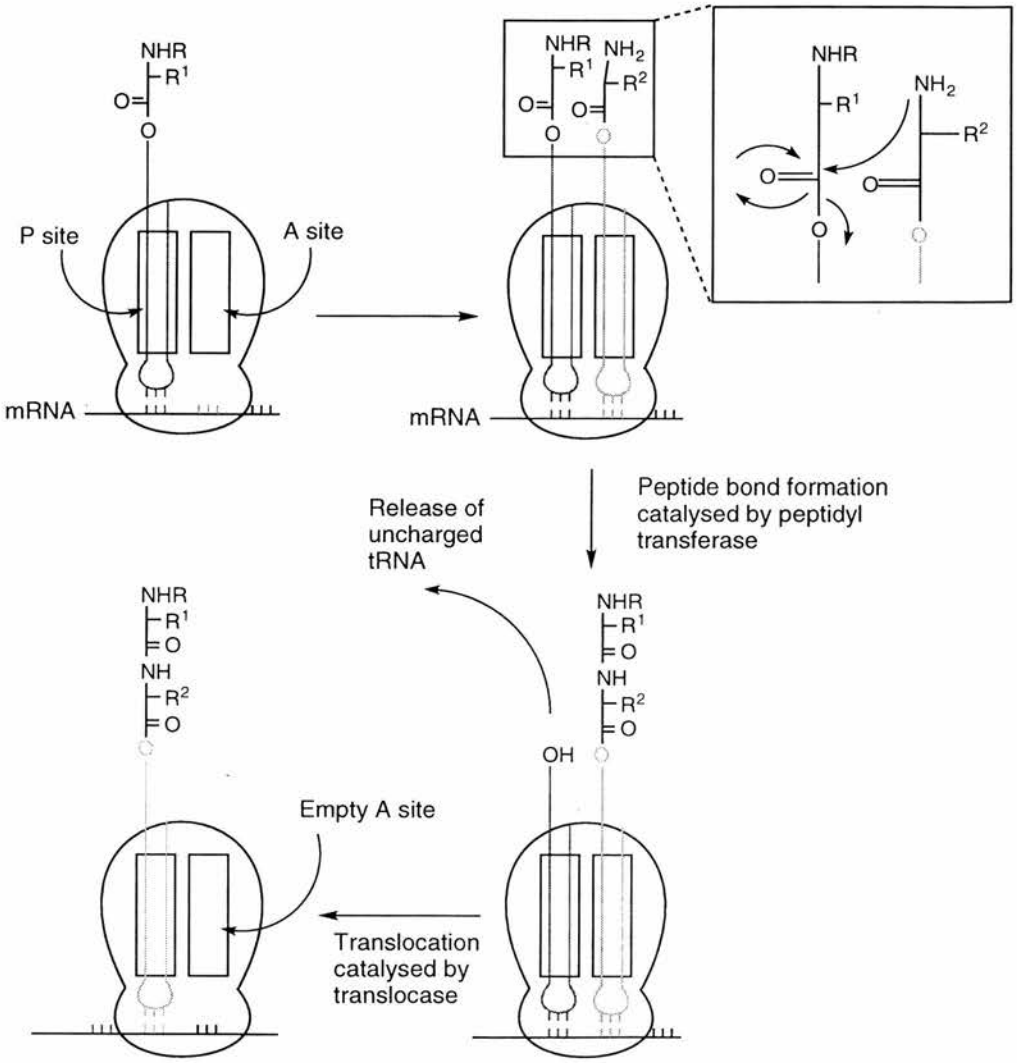

Scheme 1.2: *Simplified scheme detailing peptide synthesis on the ribosome*

Initially, a peptidyl-tRNA molecule occupies the P site. An aminoacyl-tRNA molecule then complexes to the A site and enzyme mediated peptidyl transfer of the acyl group of R^1 to the amino group of the R^2 occurs to give a deacylated tRNA in the P site. The next phase is *translocation*. The uncharged tRNA is released, the peptidyl-tRNA moves from the A site to the P site, and mRNA moves a distance of three nucleotides exposing the next codon for reading by the incoming aminoacyl-tRNA and starting another round of elongation.

Once translated, the shape of peptides and proteins is defined by the primary sequence of proteins and peptides and the surrounding environment. The primary sequence can also influence the way in which a protein or peptide is translated [*e.g.* FMDV polyprotein processing (see Section 1.7)]

Unlike proteins, small, biologically active peptides are not usually translated directly in the ribosome. Instead, tripsin-like processing enzymes cleave polyproteins at the *N*-terminus of key peptide sequences (e.g. Arg-Arg, Lys-Lys or Lys-Arg) to form the appropriate molecules. As well as cleaving precursor proteins at specific amide bonds, certain enzymes can modify the termini of particular peptide sequences. For example, the amidated *C*-termini of vasopressin and oxytocin are a result of an enzyme controlled removal of *C*-terminal glycine from the precursor peptide *via* dehydrogenation, to give the imine, and then subsequent hydrolysis (Scheme 1.3).

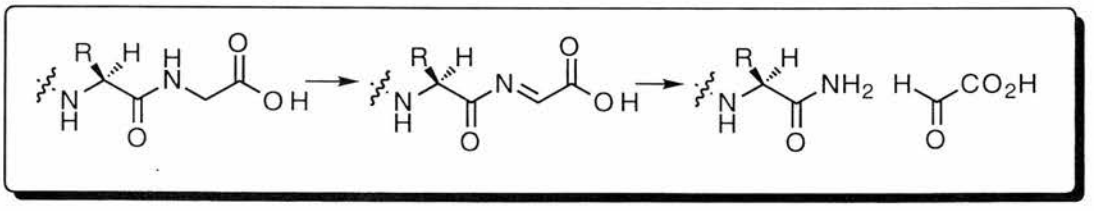

Scheme 1.3: *Mechanism of enzyme-mediated C-terminal amide formation on a peptide*

Biologically active peptides originate from precursor proteins and are not translated directly for two reasons:

- *Solubility* - Small peptide messengers, when compared to their precursor peptides are often only slightly soluble under neutral conditions. The insolubility of these small peptides could conceivably be problematic if they were the synthesised directly on the ribosome;

- *Self-stimulation.* - If the cell secreting the biologically active agent also has complementary receptors, a potentially lethal self-stimulation might result. Precursor molecules are generally much less potent thus preventing this problem.

1.1.3 General anatomy of proteins

1.1.3.1 Water soluble proteins

Proteins are often found in an aqueous environment, indeed, the first protein to be observed in atomic detail was the water soluble protein myoglobin.[12] Like most water soluble proteins, they are globular - a result of segments of polypeptide chain making sharp bends at the surface, changing the peptide direction by up to 180° and connecting well-defined units of secondary structure such as α-helices and β-sheets.

Myoglobin, the protein responsible for oxygen transport in muscle, is made up of α-helices - rod-like structures composed of tightly coiled peptide, with peptide turns to be found in between the helices (Fig. 1.2). The interior is non-polar and consists of non-polar residues like methionine and leucine, while the exterior consists of a mixture of both polar and non-polar residues. The folding of myoglobin is driven by the tendency of hydrophobic groups to be excluded from water and cluster together. In order to bury the highly polar peptide main chain in the hydrophobic interior, all the polar NHs and carbonyls have to be masked in some way. This is achieved by hydrogen bonding and in myoglobin, is conveniently accomplished in the extended structures of the α-helix.[12]

Figure 1.2: *Structure of myoglobin, a water soluble protein*

Another example of a water soluble protein is ribonuclease S, a pancreatic enzyme which hydrolyses RNA. It is a small protein, consisting of only 124 residues and like myoglobin, has a non-polar interior stabilised by β-sheets and disulfide bonds.[13]

1.1.3.2 Membrane proteins

Membrane proteins are responsible for most of the dynamic processes carried out on cell membranes.[14, 15] They can act as pumps, gates, receptors and enzymes. The protein content of most cell membranes is around 50%, but there are exceptions; myelin, a membrane that serves as an insulator around nerve fibres, has a low content of protein (18%), while membranes involved in energy transduction such as internal membranes of mitochondria and chloroplasts have the highest protein content (75%).

There are 2 major classes of membrane proteins; integral and peripheral. Integral proteins, as their name suggests, traverse the lipid bilayer while peripheral membrane

proteins are bound to the integral membrane proteins by electrostatic, H-bond or covalent interactions (Fig. 1.3).

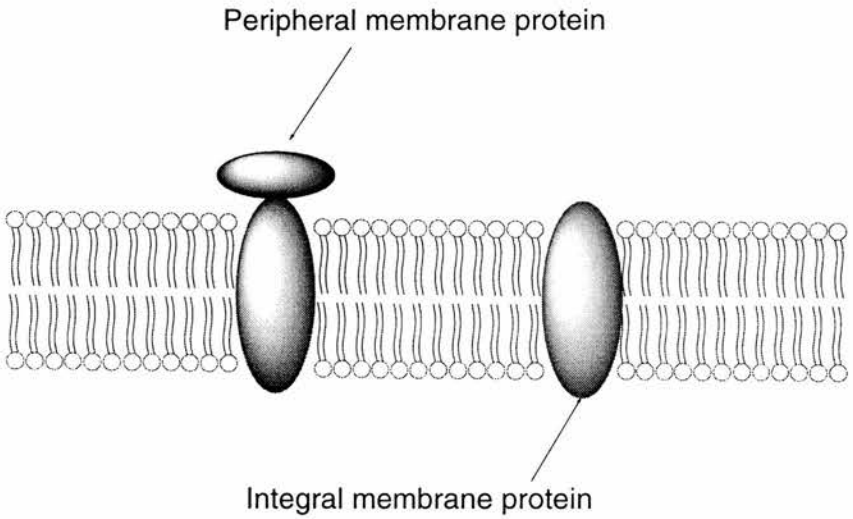

Figure 1.3: *The different protein types in cell membranes*

Glycophorin A was the first integral membrane protein to be sequenced. Through a combination of proteolytic degradation and chemical modification studies, it was discovered that the protein consists of an amino terminal with attached carbohydrate units, a hydrophobic region, comprised of α-helices, where backbone hydrogen bonds are internally satisfied and polar surfaces are shielded from the lipid environment of the membrane, and a region containing ionised and polar residues which resides in the cytosolic side of the membrane.[11]

Another example of an integral membrane protein is bacteriorhodopsin, a 25 kDa protein which converts the energy of light into a transmembrane proton gradient that is used to synthesise ATP.[16] It was the first protein that was observed directly by electron microscopy and the part of the protein that traverses the lipid bilayer also consists largely of trans-membrane α-helices.

The transmembrane segment of proteins can also adopt elaborate β-barrel structures (see Section 1.2.3.4). These structures appear to be associated exclusively with the outer membranes of bacteria and mitochondria.[17]

Gp120 is an example of a peripheral membrane protein and is found on the surface of the AIDS virus.[18] It is connected to the integral membrane protein gp41 by a disulfide bridge and has recently been the focus of studies to develop peptide based therapeutics against the disease.

1.2 Peptide Structure

1.2.1 Introduction

The three dimensional structure of proteins is directly related to the conformation of the peptide chains that compose them. The folding of these peptide chains is complex and is governed by different interactions ranging from covalent (disulfide bridges) to electrostatic (hydrogen bonds, salt bridges) and hydrophobic interactions (clustering of non-polar groups).[19] Each of these types of interaction is involved to a greater or lesser extent in defining stable peptide and protein conformations.

Peptide structure is usually complex, so for the purposes of simplification the description of these structures can be sub-divided into four categories:[20]

- *Primary structure*, the amino acid sequence;
- *Secondary structure,* the folding of the amino acid sequence into well defined structural motifs *via* electrostatic and hydrophobic interactions (*e.g.* α-helix, β-sheet and β-turn);
- *Tertiary Structure,* the overall packing of the secondary structure motifs;
- *Quaternary structure,* how large units of tertiary structure interact with each other in proteins composed of more than one sub-unit.

Most biomedical research is directed at understanding the relationship between primary and secondary structure in small peptides, because it is these two features which define how well a peptide can interact with a protein receptor (and *vice versa*) and hence exert a biological effect (see Section 1.3).[4]

The secondary structure of peptides is defined by a set of torsion angles for each residue within the chain (Fig. 1.4).[1]

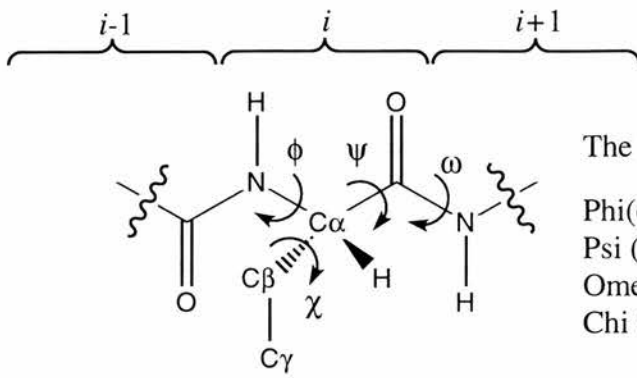

The key torsion angles are:

Phi(ϕ), around the N-Cα bond;
Psi (ψ), around the Cα-CO bond;
Omega (ω), around the CO-N bond;
Chi (χ), around the Cα-Cβ bond.

Figure 1.4: *Definition of dihedral angles in peptide backbone*

The torsion angle can be calculated by taking four atoms in sequence (Fig. 1.5), looking along the bond of the two central atoms (B & C) and then, using the end atom (A) as the 0° reference, measuring the relative position of the end atom (D) with respect to the position of atom A. The sign of the torsion angle is determined by the direction of rotation bond AB has to move in order to eclipse bond CD. If the direction is anticlockwise, then the sign is negative, and if the direction is clockwise, the sign is positive.

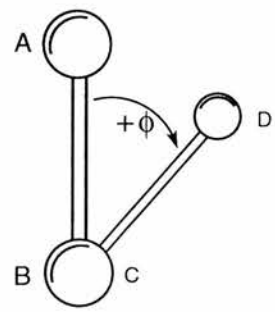

Figure 1.5: *Standard convention for defining a torsion angle*

The residues within the different classes of secondary structure (*i.e.* α-helices, β-sheets and peptides turns) adopt characteristic torsion angles. The two most important parameters ψ and ϕ can be plotted on a Ramachandran plot,[21] a graphical representation of the low energy torsion angles allowed for residues in a peptide (Fig. 1.6). The enclosed areas represent the allowed torsion angles for residues in particular secondary structures. The bottom left quadrant contains right-handed

helices (α_R), the top left quadrant β-structures (which include all β-turns and β-sheets) and the top-right quadrant contains left-handed α-helices (α_L).

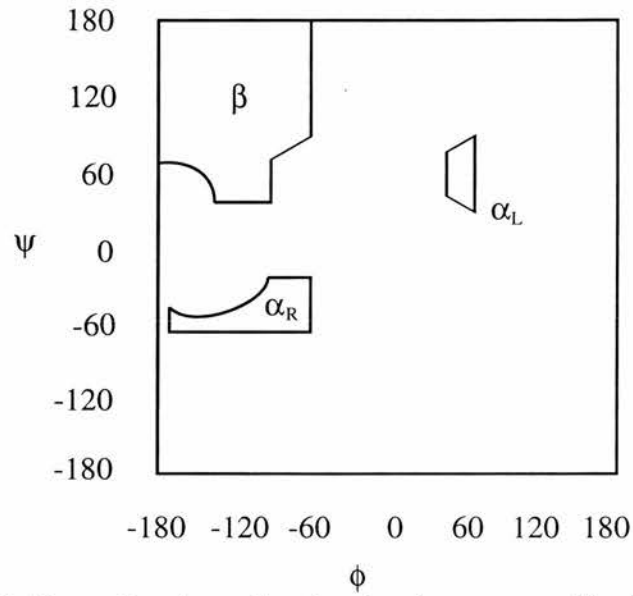

Figure 1.6: *Ramachandran plot showing low-energy dihedral angles*

Although less than half the area of the plot is defined by β-structures and α-helices, these structures account for the majority of conformations adopted by peptides and proteins and can be considered as the primary structural units of almost every enzyme, hormone and bioactive peptide; defining both structure and function.

1.2.2 Predicting protein secondary structure: Chou Fasman Rules

Predicting the folding pattern of a protein or peptide from its primary structure alone is a challenging task and there is still no way of predicting the folding pattern of a peptide/protein sequence with absolute certainty. After a statistical survey of 15 proteins, Chou and Fasman[22, 23] developed a set of simple rules which allowed the prediction of protein secondary structure with a reasonable degree of accuracy (70-80%). These rules are based on the assignment of unique α-helix and β-sheet conformational parameters, P_α and P_β respectively, for every amino acid, where:

$$P_\alpha = f_\alpha / \langle f_\alpha \rangle, \quad P_\beta = f_\beta / \langle f_\beta \rangle$$

The variables f_α and f_β are the frequency of a residue in the α-helix and β-sheet regions of 15 proteins of known structure, while $\langle f_\alpha \rangle$ and $\langle f_\beta \rangle$ are the average

frequency of all residues in the helix and β-regions of these 15 proteins. Using the above equation, every amino acid can be classified as a *secondary structure former* or *breaker* depending on the value of P_α and P_β. From this, a profile showing regions of high helical and β-sheet potential can be mapped for any peptide (Table 1.1). Short sequences (1-4 amino acids) of secondary structure formers (H_α or H_β) and breakers (B_α and B_β) signal areas in which secondary structure can be nucleated and terminated respectively.

Table 1.1: *Assignment of amino acids as formers and breakers for α-helical and β-sheet regions in proteins based on P_α and P_β values of 15 proteins*

Helical residues[a]	P_α	Helical assignment	β-Sheet residues[b]	P_β	β-Sheet assignment
Glu	1.53	H_α	Met	1.67	H_β
Ala	1.45	H_α	Val	1.65	H_β
Leu	1.34	H_α	Ile	1.60	H_β
His	1.24	h_α	Cys	1.30	h_β
Met	1.20	h_α	Tyr	1.29	h_β
Gln	1.17	h_α	Phe	1.28	h_β
Trp	1.14	h_α	Gln	1.23	h_β
Val	1.14	h_α	Leu	1.22	h_β
Phe	1.12	h_α	Thr	1.20	h_β
Lys	1.07	I_α	Trp	1.19	h_β
Ile	1.00	I_α	Ala	0.97	I_β
Asp	0.98	i_α	Arg	0.90	i_β
Thr	0.82	i_α	Gly	0.81	i_β
Ser	0.79	i_α	Asp	0.80	i_β
Arg	0.79	i_α	Lys	0.74	b_β
Cys	0.77	i_α	Ser	0.72	b_β
Asn	0.73	b_α	His	0.71	b_β
Tyr	0.61	b_α	Asn	0.65	b_β
Pro	0.59	B_α	Pro	0.62	b_β
Gly	0.53	B_α	Glu	0.26	B_β

[a]Helical assignments: H_α, strong α-helix former; h_α, α-helix former; I_α, weak α-helix former; i_α, α–helix indifferent; b_α, α-helix breaker; B_α, strong α-helix breaker.
[b]β-Sheet assignments: H_β, strong β-helix former; h_β, β-helix former; I_β, weak β-helix former; i_β, β–helix indifferent; b_β, β-helix breaker; B_β, strong β-helix breaker.

This principle, along with the rules described below, can frequently establish the folding pattern of a protein.

- *Rule 1 - Helix prediction.* Any segment of 6 residues or longer in a peptide sequence with $\langle P_\alpha \rangle \geq 1.03$ and $\langle P_\alpha \rangle \geq \langle P_\beta \rangle$ is helical;

- *Rule 2 - β-Sheet prediction.* Any segment of 3 residues in a peptide sequence with $\langle P_\beta \rangle \geq 1.05$ and $\langle P_\beta \rangle \geq \langle P_\alpha \rangle$ is a β-sheet structure;

- *Rule 3 - Cases of ambiguity.* Any segment containing overlapping α and β-regions is resolved through conformational boundary analysis, *i.e.* specific residues that typically occur only at the *C* and *N*-termini of secondary structures are located at both ends of the sequence and the $\langle P_\alpha \rangle$ and $\langle P_\beta \rangle$ values are recalculated within this region with the larger value dictating the overall conformation

These rules serve as a useful guide to structure prediction but they should not be relied on too heavily as there are still many sequences that do not fall into any of the three categories above. Also, these rules do not take into account the longer range tertiary interactions which can have a crucial effect on defining and stabilising protein secondary structure.

1.2.3 Protein and peptide conformations

1.2.3.1 The α-helix

The α-helix is a rod-like structure in which a tightly coiled polypeptide forms the inner part of the rod with the side chains extending outwards in a helical array. The α-helix is stabilised by hydrogen bonds between the amino NH and carbonyl groups of the main chain. More specifically, the carbonyl group of a residue *i* usually hydrogen bonds to the NH of an amino acid four residues away ($i + 4$) (Fig. 1.7).

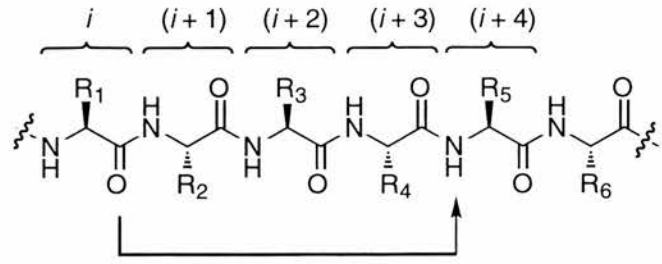

Figure 1.7: *Hydrogen bonding pattern of a standard α-helix*

The overall effect is to create a coiled spring-like structure where each residue is related to the next by a translation of 1.5 Å along the helix axis and a rotation of 100°, giving an average of 3.6 amino acid residues per turn. The α-helix is also sometimes referred to as a 3.6_{13}-helix where 3.6 is the number of residues per turn (n) and 13 is the number of atoms in each hydrogen bonded loop.[1, 20] The residues within this repetitive structure all adopt identical (ϕ, ψ) values of -57° and -47° respectively. Other helix types are also possible, the 3_{10} helix, the γ-helix, where n = 5.14 and each residue is related to the next by a translation (h) of 0.98 Å, the π-helix (n = 4.4, h = 1.15) and the ω-helix (n = 4, h = 1.32), a notable example of an α-helix with a left handed screw sense. Although there is generally a large unfavourable loss of entropy in aqueous media when a fully solvated, extended peptide adopts α-helical structure, the hydrogen bonds within the core of the helix have a stabilising influence by occupying polar amide groups which do not suit this non-polar environment.

All the carbonyl groups of an α-helix are aligned in the same direction which gives the whole helix a significant dipole, with the positive end of the dipole at the *N*-terminus and the negative end at the *C*-terminus. While this is a destabilising factor, it is offset by the enthalpic gain from hydrogen bonding.

Particular amino acids can stabilise or destabilise an α-helix depending on where in the structure they are situated, *i.e.* residues that are favoured at the termini may be disfavoured at internal positions and *vice versa.* Internal residues tend to have hydrophobic side chains which can prevent water disrupting the hydrogen bonding in

the helix backbone.[24-27] Examples of amino acids that are found in this region are alanine and leucine.

At the helix termini, the last four NH groups at the *N*-terminus and the last four CO groups at the *C*-terminus lack hydrogen bond partners. Consequently, residues that are found at the ends of helical structures tend to have polar side chains that can supply H-bond partners for unpaired main chain NH and CO groups.[28-32] Residues at the *N*-terminus tend to have either small polar side chains (*e.g.* Asn, Ser, Thr) which provide H-bonding partners for unsatisfied main chain NH and CO groups, or negatively charged side chains (*e.g.* Asp, Glu) which can interact with the positive end of the helix macrodipole. Glycine can also be found at the *N*-terminus because its small size means that it does not impede the access of solvent which can H-bond to unpaired NH groups,[28-32] while proline has a high *N*-terminus propensity because its ϕ angle is fixed to the α-helical value of -60° and requires no H-bonding partner because it does not have an NH group.[33]

Residues at the *C*-terminus commonly have positive charges which interact with the negative end of the helix macrodipole. Examples include lysine, histidine and arginine.[32]

Electrostatic or hydrophobic interaction between different residues in a helix can also impart stability. Side chain→side chain hydrogen bonds are commonly found in helices between residue i and residue $(i + 4)$ where the residue side chains lie close to one another on the same face of the helix [*e.g.* $(i, i + 4)$ = (Gln, Asp) or $(i, i + 4)$ = (Phe, His)].[34, 35] Salt bridges between oppositely charged side chains also stabilise helices [*e.g.* $(i, i + 4)$ = (Glu, Lys)][36] as can the packing of non-polar side-chains [*e.g.* $(i, i + 4)$ = (Tyr, Leu)].[36]

In order to define helix stability in a concise way, Zimm and Bragg defined two parameters, the helix initiation constant σ, and the propagation constant s. The initiation constant reflects the probability of aligning the first three residues in an α-helical conformation and generally has low values (*i.e.* $<10^{-3}$, where σ=1 indicates

that the first three residues are fixed in an α-helical conformation). The propagation constant *s* is a measure of an amino acid's ability to adopt α-helical torsion angles (ψ, ϕ) when attached to a pre-existing helix. Values for *s* of >1 indicate that the residue is a helix making amino acid (*e.g.* alanine) while values <1 indicate that the residue helix-breaking (*e.g.* proline).[37, 38]

1.2.3.2 The β-turn

Like the α-helix and β-sheet, the β-turn is essential for defining the overall shape of proteins and biologically active peptides.[39-42] As well as connecting areas of secondary structure such as α-helices and β-sheets, β-turns, directly or indirectly, are an important recognition motif in many biological processes. They play a role in the recognition necessary for post-translational modification of proteins, *e.g.* phosphorylation and glycosylation,[43] and can potentially be a site of high antigenicity; for example, the glycoprotein gp120 of the human immune deficiency virus (HIV) contains a turn which is referred to as the immunodominant loop[18] (see Section 1.4.2). The structural diversity of β-turns is huge, and reflects their importance in all aspects of protein and peptide structure and function.

β-Turns, also known as hairpin bends and 3_{10} bends, are composed of 4 amino acid residues in which each amino acid possesses a well defined set of torsion angles (ϕ, ψ). β-Turns are usually stabilised by a H-bond between the CO of residue *i* and the NH of residue (*i*+3), forming a 10-membered ring with the interatomic distance of the C-α atoms of residues, *i* and (*i*+3), normally less than 7 Å (Fig. 1.8). Statistical treatment of protein crystal data suggests that short polar residues (*e.g.* Asn and Ser) as well as proline and glycine, favour β-turn formation, with the latter two residues frequently residing in the (*i*+1) and (*i*+2) positions of the turn.[44, 45] Model studies indicate that the 10-membered ring formed by the hydrogen bond is enthalpically favoured with a near optimal hydrogen-bond geometry,[46] but entropically disfavoured because chain flexibility is reduced.[47]

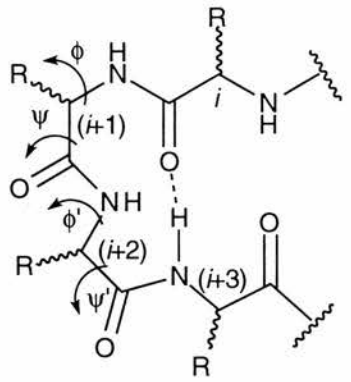

Figure 1.8: *Assignment of torsion angles in a β-turn*

The large number of β-turns found in proteins are categorised by the back-bone torsion angles, φ, ψ, φ' and ψ' which define the conformation of the two amino acid residues in the middle part of a β-turn [*i.e.* residues (*i*+1) and (*i*+2), Fig. 1.8].[48] Each class of turn has a unique set of torsion angles; the torsion angles φ and φ' are the dihedral angles around the N-C-α bonds of residues (*i*+1) and (*i*+2) respectively, while ψ and ψ' are the torsion angles around the corresponding C=O-C-α bonds (Fig. 1.8).

The first three turn types in Table 1.2 (types I to III) were identified by Venkalachalam in 1968.[1] Types I, I', II and II' are often found at the ends of antiparallel β–sheets.[49] Type III turns have the same ψ and φ torsion values as turns in 3_{10}-helices and are sometimes referred to as helical turns. Types I', II' and III' are simply mirror images of I, II and III. Five other turn types were later defined. The type IV turn has two or more angles which differ by at least 40° from the definitions of β-turn types I, I', II, II' and III, III' and it is generally considered as a miscellaneous category, types V and V' are unusual variations of types II and II', type VI has a *cis* proline at the third position (*i*+2) and type VII turns have either φ' near 180° and ψ<60° or *vice versa*.[1]

Table 1.2: *Classification of β-turns by the torsion angles* φ, ψ, φ' and ψ'

Turn Type	φ	ψ	φ	ψ'
I	-60	-30	-90	0
I'	60	30	90	0
II	-60	120	80	0
II'	60	-120	-80	0
III	-60	-30	-60	-30
III'	60	30	60	30
IV	see text	-	-	-
V	-80	-80	80	-80
V'	80	-80	-80	80
VI	see text	-	-	-
VII	see text	-	-	-

Although well established, the method of classifying β-turns by their back-bone torsion angles is rather cumbersome not to mention imperfect as many β-turns reside in ill defined categories such as IV and VII. Another problem with categorising β-turns in this way is that it does not take account of side chain orientation. There is mounting evidence that side chains play an important role in peptide-receptor interaction, so the synthesis of constrained β-turn mimetics based on the traditional method of β-turn classification may not accurately reproduce the overall topography of the turns they are mimicking. This oversight may ultimately be a hindrance to the construction of useful non-peptidic bioactive molecules based on β-turns. In this sense, an alternative method proposed by Ball *et al.*[50] based on side chain orientation, may be far more useful, not just in the design of bioactive molecules, but for understanding β-turn topography in general.[48]

Observation of several β-turn models, with backbones torsion angles set to the ideal types detailed in Table 1.2, revealed that despite large differences in the peptide backbone, the relative positions of bond 1, bond 2 and atom C(3) remained similar (Fig. 1.9). Likewise it was observed that the relative positions of bond 3, bond 4 and atom C(2) also appeared to constitute a single conformational unit. The only difference between the various β-turn types, with respect to bonds 1, 2, 3 and 4 was the dihedral angle between these two conformationally invariant units. Ball defined

this torsion angle as β, and he used this parameter to neatly describe the general topology of almost any β-turn.

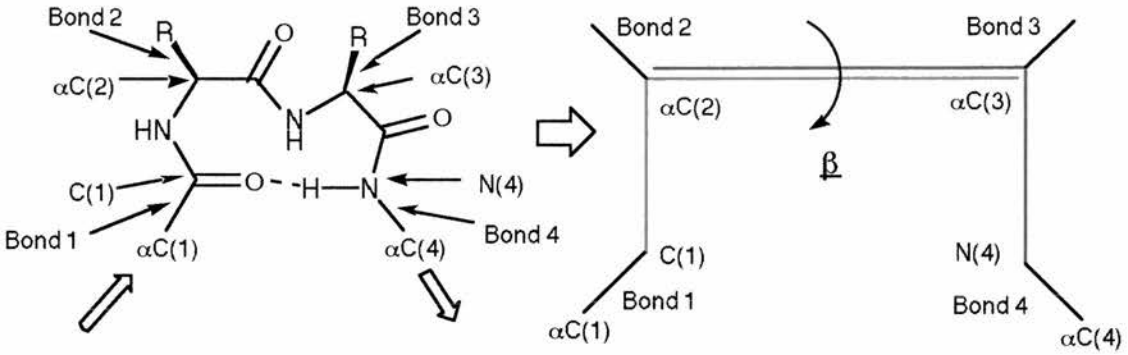

Figure 1.9: *The simplification of a β-turn down to two invariant units, highlighted in red and green*

Re-classification of all β-turns by their β-value gave some interesting results. Any relationship between the parameter β and the standard β-turn types was found to be virtually non-existent, with many different turn types having the same β-value. For example, type III, type IV, type I and type V' turns all had the same β value (β=55). As well as β, there are several other parameters that Ball defines to fully describe the geometry of the β-turn (Fig. 1.10).

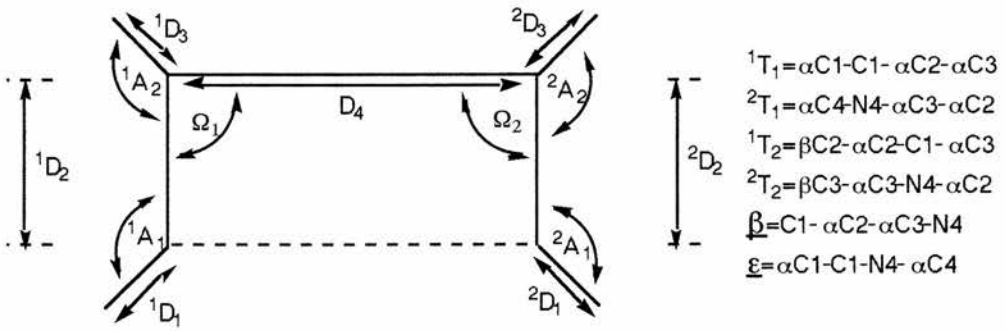

Figure 1.10: *Definitions of the distances (D), angles (A, Ω) and dihedral angles (T, β and ε) in a β-turn*

These other parameters are essential to avoid any ambiguity between different turns that might have the same β-value. The need for extra parameters is demonstrated in Fig. 1.11; both turns have β-values of 0°, but the dihedral angles

between bonds one and four (ε) differ by 60°. Without ε, these very different peptide motifs would be classed as the same which is clearly not the case.

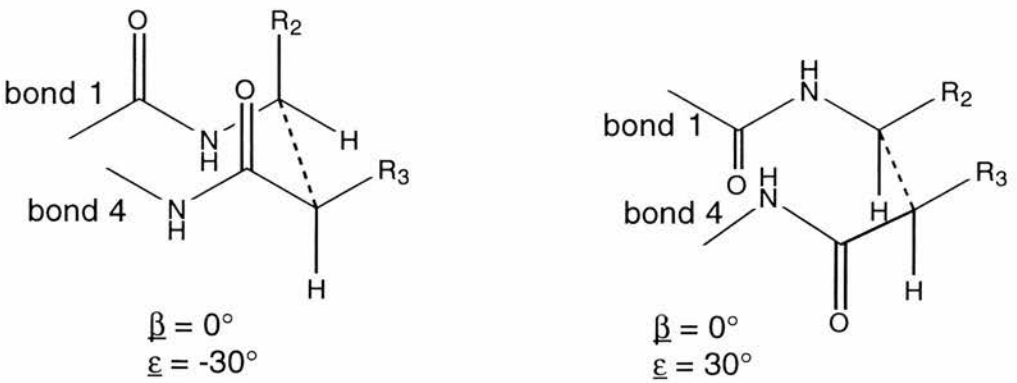

Figure 1.11: *Two different β-turns with identical β values*

Although Ball's method provides a simplified method of β-turn classification and takes greater account of the side-chain orientation, it remains to be seen whether it will supersede the traditional method of classification.[50] One drawback is that it does not take account of peptide back-bone conformation, a major factor in peptide structure and function which is amply demonstrated in the vastly altered receptor-binding properties of retroinverso peptides compared to native peptides.[51]

1.2.3.3 The β-sheet

β-Sheets consist of adjacent polypeptide chains hydrogen bonding to each other and are found in two main forms; parallel β-sheets, where adjacent bonds run in the same direction [Fig. 1.12(*a*)] and anti-parallel β-sheets where adjacent chains run in opposite directions [Fig. 1.12(*b*)]. In both cases, the side chains are oriented orthogonal to the sheet surface with adjacent side chains adopting an antiperiplanar conformation. The physical dimensions of β-sheets are generally consistent from one protein or peptide to the next; antiparallel β-sheets have an interstrand distance of 5 Å, the strands are almost fully extended and the repeat period is 7.0 Å per residue pair with the interstrand hydrogen bonding pattern forming alternating 10 and 14 membered rings. In proteins, these systems are composed of a minimum of 2 strands and, on average, have approximately six residues per strand. Parallel β-sheets have a

repeat period of 6.5 Å per residue pair and the hydrogen bonding pattern is composed of 12 membered rings only.[52]

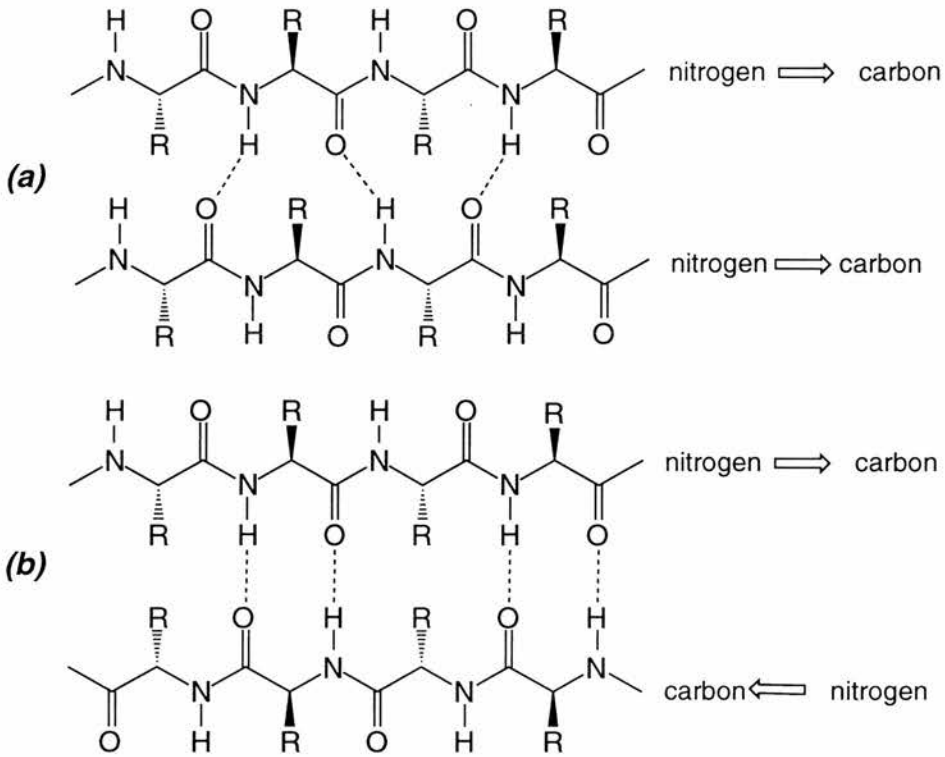

Figure 1.12: *Schematic diagrams of (a) parallel and (b) antiparallel β-sheets*

Antiparallel β-sheets are usually formed when polypeptides change direction and fold on themselves. This phenomenon is often induced by β-turns and in the most common cases arises when the carbonyl group of residue *i* in a polypeptide, hydrogen bonds to the NH group of residue (*i*+3). An antiparallel sheet which is 'capped' in this way is sometimes referred to as a β-hairpin and is almost always nucleated by 'prime turns', in particular, type I' and type II' turns (Fig. 1.13).[53-60]

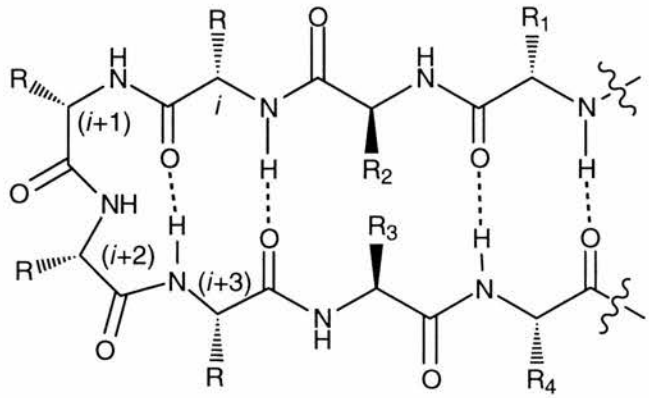

Figure 1.13: *Example of a β-hairpin*

As well as playing an important role in defining the shape of proteins, β-sheets, both parallel and antiparallel, feature in many biochemical features and processes. For example, it has been known for some time that enzymes can bind their inhibitors and substrates by generating β-sheet type interactions,[52] while the formation of β-sheets has also been implicated as the cause of the insoluble amyloid fibrils associated with Alzheimer's disease (see Section 1.4.3).[61, 62]

1.2.3.4 β-Sheet structures in proteins and biologically active peptides

Parallel β-sheets are statistically less common than antiparallel ones because, for a parallel β-sheet to form, two peptide segments which are not close in sequence must be brought together. This can involve elaborate crossover loops with the intervening peptide strand sometimes adopting secondary structure itself (the minimum requirement for an antiparallel β-sheet to form is simply that there is a β-turn motif present to reverse the chain direction). Furthermore, the longer loops that are required to connect parallel β-strands are kinetically and thermodynamically unfavourable which may explain the lower statistical frequency of parallel β-sheet structure in proteins [Fig. 1.14(*b*) and 1.14(*c*)].[52]

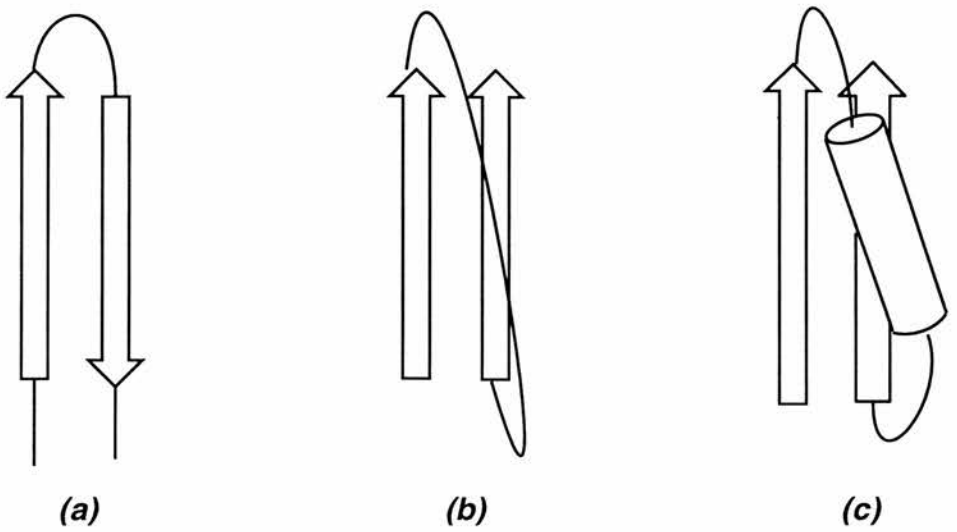

Figure 1.14: *The different connecting loops in parallel and antiparallel β-sheets; (a) antiparallel; (b) and (c) parallel*

β-Sheets are not strictly planar; in reality, they adopt a right handed twist from 0-30°. [63] This angle is defined by the orientation of the backbone of the β-strand relative to the adjacent strand and arises because it is energetically more favourable than a completely flat, planar structure. There are two main reasons for this; firstly, the amide NH in peptides has a small tetrahedral distortion which can only be accommodated into an extensive β-sheet hydrogen bonding pattern by a twist in the sheet itself, and secondly, the presence of twist in a β-sheet allows greater packing of hydrophobic groups. It should be noted, however, that twisting of a β-sheet is opposed by interchain electrostatic interactions, with the most favourable orientation of peptide dipoles occurring in a non-twisted structure.[52]

Statistical analysis of a range of peptides indicates that twisted antiparallel β-sheets are more stable when composed of small unbranched residues like glycine, alanine and aminobutyric acid, while twisted parallel sheets are stabilised by β-branched and γ-branched residues such as valine, isoleucine threonine and leucine, polar groups like serine, aromatic residues such as tyrosine and phenylalanine, and residues with long side chains like lysine.[52]

β-Sheet structures can adopt a range of exotic topologies within proteins. The commonest of these is the β-sandwich which is composed of two sheets separated by a distance of 8.3 - 10.3 Å and oriented in such a way that the strands of the 'bottom sheet' are rotated by 20°- 50° relative to the strands of the 'upper sheet'. Interestingly, side chains from the top and bottom sheets are aligned even though the peptide backbone of the β-strands is not. To accommodate this geometry, the β-sandwich structure must adopt a significant twist. The driving force behind the formation of these structures is the hydrophobic interactions between the faces of interacting sheets. Approximately 60% of residues involved in β-sandwich interaction are Leu, Val, Ile and Phe, the reason being that these residues allow for smooth well packed hydrophobic surfaces, important for a stable β-sandwich structure (Fig. 1.15).[52]

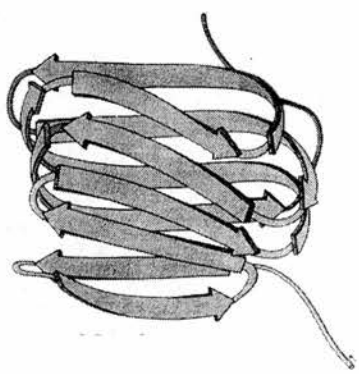

Figure 1.15: *β-Sandwich in a tomato bushy stunt virus protein*

β-Sheets also sometimes 'wrap around' to form cylindrical structures which are referred to as β-barrels. These structures, which contain hydrophobic interiors, are composed of 5 - 13 strands and have a right handed twist of approximately 36° relative to the axis of the barrel (Fig. 1.16) and are commonly found in the transmembrane segments of membrane proteins. α/β-Barrel proteins are a variation of this theme, with intervening strands composed of α-helices rather than short peptide loops.

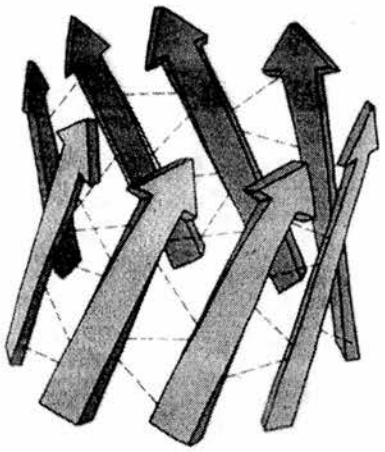

Figure 1.16: *β-Barrel;the dotted lines represent hydrogen bonds*

1.2.3.5 β-Sheet sub-structures: The β-bulge and β-bend

β-Sheets contain two important features which have a significant effect on their structure; the β-bend and the β-bulge. Like all structural motifs, bulges and bends contribute to the function of proteins by directing peptide folding and the orientation of peptide side chains, especially at substrate binding sites.[64]

A β-bulge is formed when two residues on one peptide strand are positioned opposite a single residue on a neighbouring strand (Fig. 1.17). β-Bulges are generally only found in antiparallel β-sheets and, because a strand containing a β-bulge cannot propagate a β-sheet, are always found near to or on an edge strand.[65]

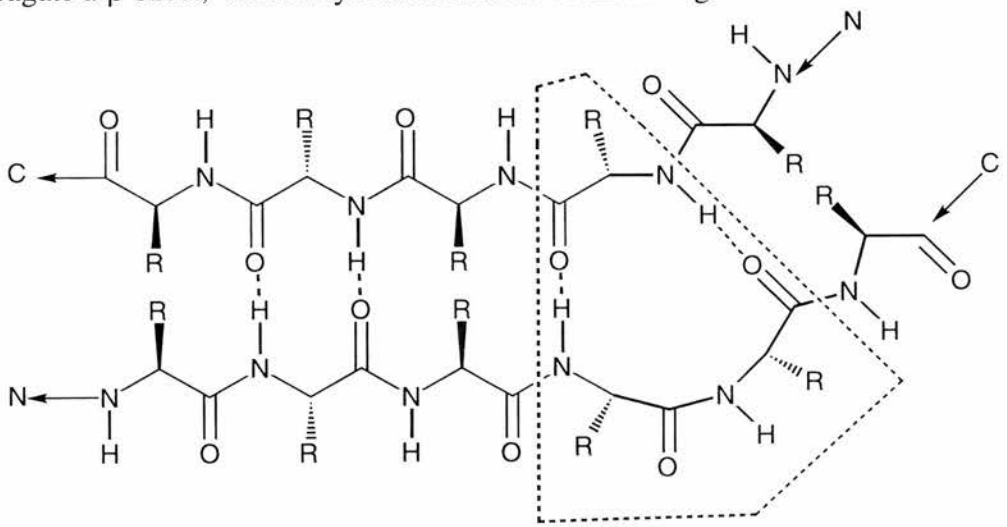

Figure 1.17: *β-Bulge region in an antiparallel β-sheet; the β-bulge is highlighted by a dotted line*

β-Bends, as their name suggests, introduce a bend or kink in the backbone of a peptide chain. They feature prominently in β-sheet structures with perhaps up to 85% of all β-sheets containing them. They occur most commonly in antiparallel strands of more than five residues, residing inside a sheet of three strands or more. Proline is often present in these β-sheet bends in which strands can bend by 90° without disturbing the hydrogen bonding pattern. Although surprising, Kemp and Li confirmed that this is perfectly possible with the development of a small β-sheet model containing proline on one of the strands (Fig. 1.18).[66]

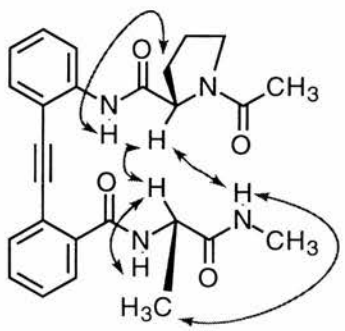

1

Figure 1.18: *β-Sheet model by Kemp and Li; NOE crosspeaks (in $C^D{}_2Cl_2$) indicate a stable β-sheet hydrogen bonding pattern*

1.2.3.6 Amino acid propensities within β-sheets

Statistical studies of proteins of known structure reveal that β-branched and aromatic amino acids occur frequently in β-sheets. However, this may simply indicate a hydrophobic requirement rather than any β-sheet forming propensity, since β-sheets frequently occur in the hydrophobic core of proteins anyway. β-Sheets have also been found to be amphiphilic, with one face solvent exposed and the other contributing to a hydrophobic core within a protein. In cases such as this, it is not uncommon for polar residues such as lysine to reside within the β-sheet.

The ability of a residue to block a peptide from solvent interactions has been suggested by Bai and Englander as a prerequisite for its β-sheet propensity. They propose that, in the random coil, the destabilisation of H-bonding of the peptide

backbone to water, induced by the steric bulk of hydrophobic side chains, confers an enthalpic stabilisation to intramolecular hydrogen bonds in the range of 0-0.9 kJ mol^{-1} (relative to alanine). Although other contributions such as conformational entropy, steric factors and hydrophobic interactions are also involved in β-sheet stabilisation, the indirect role of side chains on electrostatic interactions and H-bonding may be an important factor in controlling β-sheet stability.[67]

The pattern of distribution of amino acids in a peptide sequence is also central to secondary structure stability. A study reported in a paper by Xiong *et al.* compared the propensities of amino acid residues to the hydrophobic periodicity of the sequence in order to determine which interaction would dominate the folding process. To achieve this, two peptides were synthesised from amino acids with α-helix propensities (peptides 1A and 1B) and two were synthesised from amino acids with β-sheet propensities (2A and 2B). The pattern of polar and non-polar residues in peptides 1A and 2A corresponded to that expected for an α-helical peptide, while 1B and 2B had a periodicity corresponding to that of a β-sheet. CD studies of all four peptides revealed that the periodicity of the peptide governed the overall secondary structure regardless of the intrinsic properties of the amino acid residues within each peptide; *i.e.* 1B and 2B were β-structures while 1A and 2A were α-helical.[68]

1.2.3.7 γ-Turns

A variation of the β-turn, the γ-turn (Fig. 1.19), is composed of three residues rather than four with a hydrogen bond between the carbonyl of residue *i* and the NH of residue *i*+2, forming a seven membered ring ψ_i=120°, $\phi_{(i+1)}$=-65°, $\psi_{(i+1)}$=80°, $\psi_{(i+2)}$=-120°). Model studies in the absence of tertiary interactions indicate that the γ-turn has a lower enthalpic stability than the β-turn, nevertheless, γ-turns are believed to be present in the bioactive conformations of many biologically active peptides.[69-71]

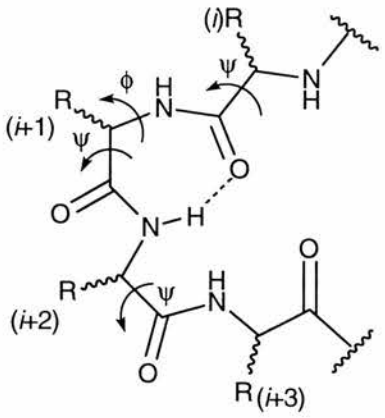

Figure 1.19: *Torsion angles in a γ-turn*

1.3 Peptides as Therapeutic Agents

1.3.1 Introduction

Peptides are central to almost all biochemical processes in living systems. They regulate functions in the cardiovascular, gastrointestinal, immunological and central nervous systems, operating as chemical messengers and eliciting a physiological response in a cell by interacting with membrane bound receptors.

Angiotensin II (**2**),[72-75] bradykinin (**3**),[76] a vasodilator and bronchioconstrictor, and opioid peptides (endorphins, enkephalins and dynorphins) (**4**)[5, 77-82] are but a handful of biologically important peptides that have been studied in recent years (Fig. 1.20).

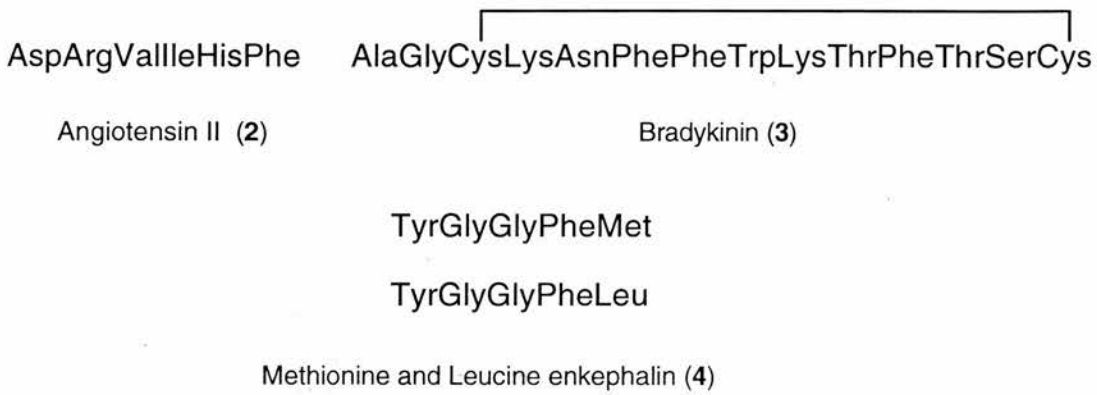

Figure 1.20: *Biologically active peptides*

1.3.2 Introduction of conformational constraints

Proteins and peptides interact with molecular receptors to initiate biological events. When it is desirable to interrupt these processes (*i.e.* the treatment of diseases or unpleasant symptoms), antagonists can be developed which block the native ligand from binding to its receptor, but elicit no response themselves. The first stage for antagonist development involves determining the smallest sequence of peptide or protein that interacts with a receptor through screening peptide fragments for receptor affinity. The second stage evaluates the 3D conformation of the receptor-bound peptide. This is achieved by introducing conformational constraints and determining

whether the constrained peptide retains affinity for the receptor; if it does, the analogue can be considered as a pharmacophore model. Further conformational adjustment can ultimately lead to the design of potent antagonists with useful therapeutic properties (Scheme 1.4).[6, 83-88]

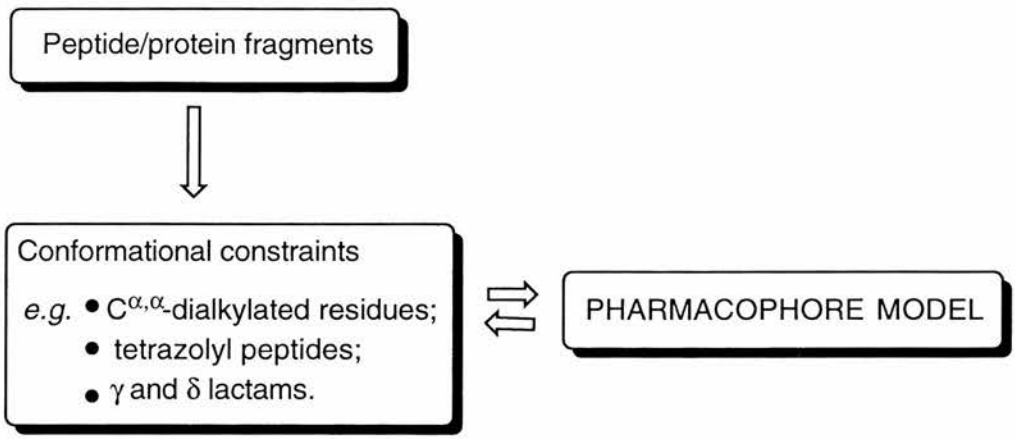

Scheme 1.4: *General strategy for the development of peptide based therapeutics*

Conformational constraints such as C-α,α-dialkylated residues, tetrazolyl peptides and γ and δ lactams are commonly introduced into bioactive peptides to hold the peptide backbone in its receptor bound conformation and, hopefully, impart greater selectivity and potency.

Conformational restriction, however, need not only be restricted to the peptide backbone. Hruby *et al.* devised tyrosine analogues with restricted side-chain dynamics around the χ_1 and χ_2 torsion angles (Fig. 1.21).[89, 90]

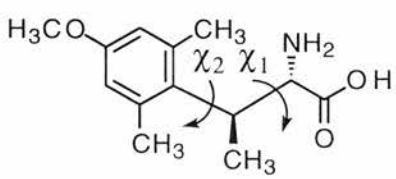

5

Figure 1.21: *2', 6'-dimethyl-β-tyrosines exhibit restricted rotation around the Cα-Cβ and Cβ-Cγ bonds*

These can be used to study the roles of side-chain orientation in peptide receptor interactions, particularly with respect to tyrosine containing peptides such as leucine

or methionine enkephalin.[9] Indeed, conformational restriction of any form offers several benefits:

- *Increased receptor affinity*, as the peptide is fixed in the receptor bound conformation and entropic losses are greatly reduced;
- *Minimal side-effects*, since other receptors which trigger undesirable responses are unable to bind to the constrained peptide;
- *Increased stability to peptidases*, which may be unable to bind to the fixed conformation even if a peptide backbone is present, thus preventing peptide degradation.

The diagram below illustrates how conformational constraints limit undesirable effects by limiting the peptide to only the bioactive conformation (Scheme 1.5).

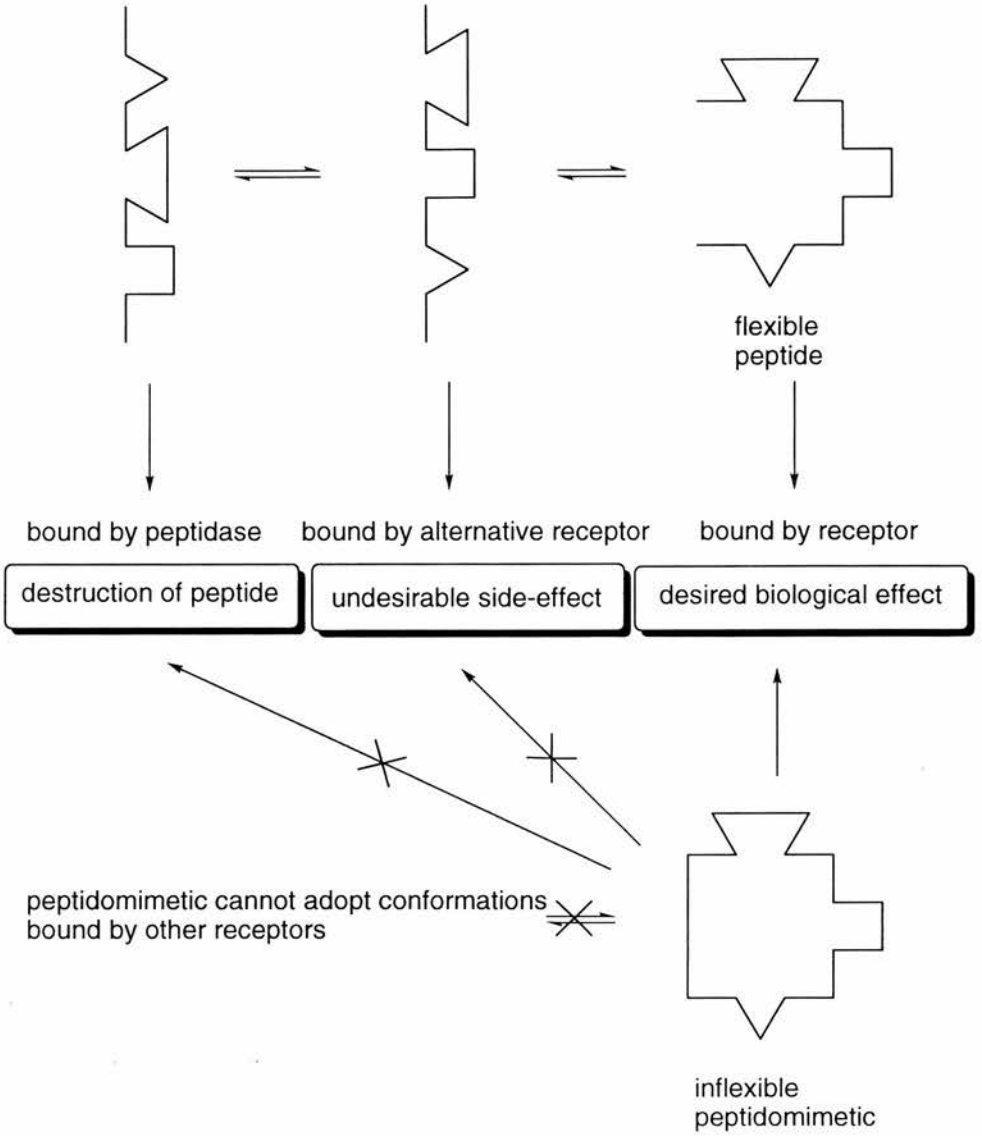

Scheme 1.5: *Behaviour of a peptide and peptidomimetic in a biological system*

1.3.3 Development of alternatives to the peptide backbone

When designing drugs based on peptides two problems have to be addressed. Firstly, the lack of membrane transport systems means that peptides are rapidly degraded by peptidases in the stomach and gut and are poorly absorbed into the bloodstream due to their peptide back-bone and relatively high molecular mass. Secondly, their conformational flexibility means that they are capable of binding to several different receptors, some of which could result in undesirable side-effects.

In recent years a range of strategies aimed at overcoming these shortcomings have evolved. One of these is the alteration or replacement of the amide unit in the peptide back-bone to render it invulnerable to peptidases.[91-96] Hydrophobic backbones have also been developed to make drug molecules more lipophilic and therefore allow them to cross cell membranes. Some of the commonest approaches are described below:

- *Retro-amide peptide design*, the inversion of the amide bonds of a peptide whilst maintaining residue side-chain sequence and geometry;[51]
- *Isosteric bond replacements*, swapping the amide unit for CH=CH, CF=CH, or thioamide bonds (NHCS);[97-99]
- *Peptoids*, the preparation of oligomers of *N*-substituted glycines (Fig. 1.22). These systems are conformationally more flexible than peptides due to a lack of chirality and H-bonding but show improved stability to peptidases.[100]

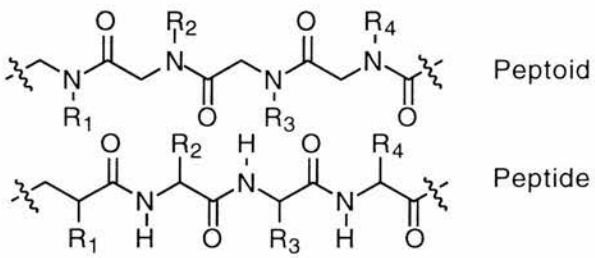

Figure 1.22: *Comparison of a peptide and peptoid*

The importance of peptides in all biological processes means that peptide backone mimics are of enormous medical interest. However, if therapeutic agents based on peptides are to be developed, there must first be a solid understanding of the interplay between biologically active peptides, protein function and disease states. The following chapter details some of the roles which peptide β-structures such as β-strands, β-sheets and β-turns play in key biological processes and describes some novel therapeutic strategies based on our current understanding of protein secondary structure.

1.4 The Role of β-Sheet in Disease States

1.4.1 Introduction

β-Structures can be found in a huge variety of peptides and proteins ranging from very small biologically active peptides like gramacidin S,[101] to proteins (*e.g.* ribonuclease S).[13] They are extremely important to the structure and biological activity of the systems they occupy and are involved in many processes ranging from electron transfer and protein dimerisation to substrate recognition by proteolytic enzymes. They are also associated with disease states and many therapeutic strategies are targeted at interfering with β-structure formation.

1.4.2 β-Sheets and HIV-1 protease

Work by Kent *et al.* has revealed that HIV-1 protease, a key component required for the replication of the AIDS virus, self-assembles into a homodimeric structure, which in turn generates the catalytic centre of the enzyme and also the substrate binding pocket.[102] The dimer is stabilised at the interface by the interdigitation of pairs of peptide strands on each half of the dimer, forming a four-stranded β-sheet (Fig. 1.23).[103]

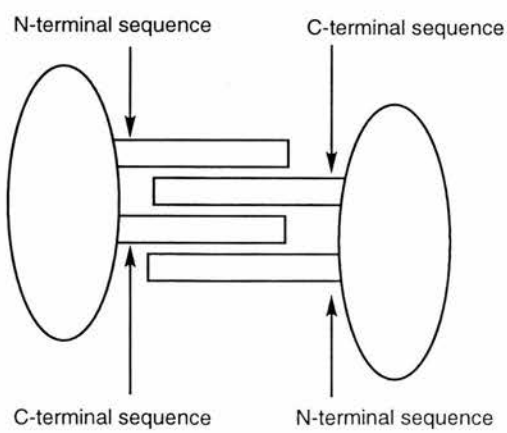

Figure 1.23: *Schematic of the HIV-1 protease homodimeric structure*

Chemielewski and co-workers successfully interfered with the processes behind β-sheet formation and stabilisation by developing a set of HIV-1 protease inhibitors which were composed of the N and C-terminal portions of the protease coupled to an alkyl chain of methylene groups (Fig. 1.24).[103] By adjusting the length of the alkyl tether it was possible to change the degree to which these oligopeptides inhibited dimerisation of the protease and therefore probe the structural requirements of the peptide when bound to the protease monomer.

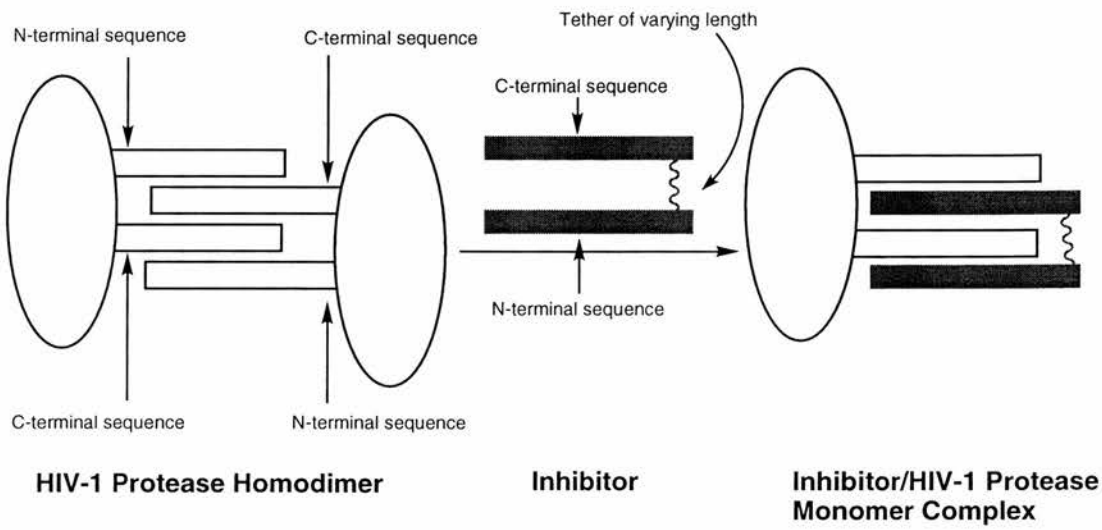

Figure 1.24: *Prevention of HIV-1 protease dimer formation*

Inhibition of the protease monomer blocked formation of the biologically active dimer which in turn resulted in a decrease of HIV-1 protease activity and a decrease in the amount of protease dimer in solution as measured by size exclusion chromatography and protease fluorescence studies. This strategy of interfering with β-sheet formation offers a unique way of inhibiting HIV-1 protease and is a promising step towards finding a treatment for AIDS.

Another strategy, developed by Long and Moeller, uses a constrained mimetic to mimic the conformation of the peptide sequence found in the V3 loop of the gp120 protein of HIV-1, the protein which forms part of the principal neutralising determinant of HIV-1.[18] It is known that the V3 loop adopts a type II β-turn

conformation (as observed by X-ray crystallography of an antibody bound to the V3 loop). In order to maintain the secondary structure of the peptide analogue, a cyclic constraint was introduced between the α-C of proline and the neighbouring amido NH (Fig. 1.25) in effect, restricting the ϕ, ψ and ω torsion angles (see Section 1.5.3.4).[18]

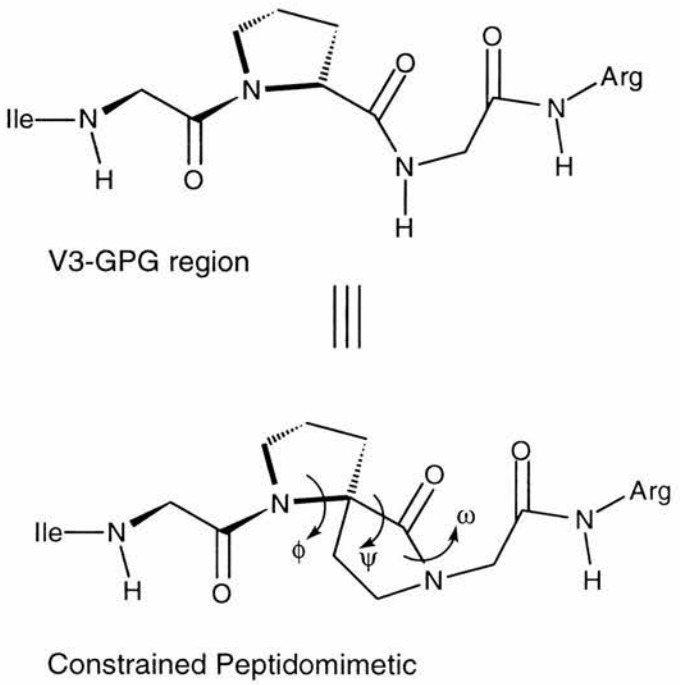

Figure 1.25: *Constrained peptidomimetic of the V3 loop peptide sequence*

It was found that antibodies raised against the constrained V3 loop peptidomimetic bound the gp120 protein to almost the same extent as antibodies raised against the antigen without the additional constraint. This suggests that spiroketal units could be useful conformational constraints for studying the 3D conformational requirements of antibody-antigen interactions in HIV-1, as well as a useful tool in the development of vaccines for targeting other small epitopes of proteins.

1.4.3 β-Sheets and Alzheimer's disease

Alzheimer's disease is primarily a disease associated with old age and is undoubtedly the commonest form of dementia. Because of this, it is expected that the increase in life expectancy in the global population will be accompanied by a huge rise in brain disorders. Alzheimer's is triggered by the development of an abnormal protein in the brain which is a mutation of the brain protein amyloid beta. The deformed proteins have the ability to hydrogen bond to each other to form extended β-sheets, forming insoluble plaque deposits which destroy nerve cells and ultimately lead to dementia.[61, 62]

The brain tissue of patients with Alzheimer's disease were found to contain insoluble plaques in regions involved in memory processes. These plaques are a mixture of damaged neurones, proteins, peptides and debris from lysed neurones. One underlying feature of all plaques is the presence amyloid fibrils, the proteinaceous fibrous material which is believed to play an important in the in the events leading to cell death. The build up of this material is caused by proteolysis of an amyloid precursor protein APP, a transmembrane protein of unknown function (Scheme 1.6).[61, 62]

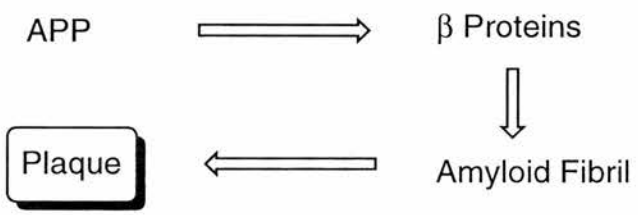

Scheme 1.6: *Principle steps in the formation of AD plaques*

The β-proteins that are formed as a result of APP proteolysis, hydrogen bond to each other to form extended β-sheet structures which are the primary constituent of amyloid plaques. The structure of amyloid plaques has not been successfully determined by high resolution crystallographic methods, however the X-ray

diffraction patterns of amyloid fibrils is believed to resemble those of the cross-β-silk fibril which is primarily composed of β-sheet.[61]

Lansbury has developed a model which depicts the nucleation and polymerisation of amyloid fibrils.[62] A series of entropically unfavourable associations take place to form a nucleus containing *n* monomers. This is followed by a series of favourable equilibria (Kg) which lead to amyloid fibril formation (Scheme. 1.7).

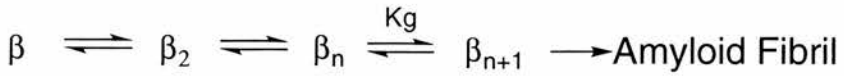

Scheme 1.7: *Lansbury model for amyloid fibril formation*

Another contributory factor to Alzheimer's disease is neurofibrillary tangles. Using CD spectroscopy, Fasman and Moore have shown that peptide fragments of human neurofilament NF-M17 change conformation from an α-helix to a β-sheet upon addition of Al^{3+}, with large quantities of Al^{3+} triggering formation of insoluble β-sheet aggregates.[104]

1.5 Strategies of Peptidomimetic Design

1.5.1 Introduction

In recent years peptidomimetics have been used extensively to probe the role and function of peptide segments in proteins by replacing particular amino acid sequences with non-native molecules. These mimetics are generally used to stabilise the secondary structure of an isolated segment of peptide, thus allowing a detailed study of protein secondary structures by NMR, IR spectroscopy and X-ray crystallography.[105]

1.5.2 α-Helix templates

One of the most successful strategies for stabilising α-helices has been the development of the helix template (Fig. 1.26). The overall strategy involves the synthesis of a template (usually a cyclic peptide) in which a set of parallel carbonyl groups are presented in an α-helical conformation. Subsequent attachment of the peptide can result in hydrogen bonding of the amide NHs of the peptide to the template carbonyls, reducing the entropic penalty that occurs in helix stabilisation.

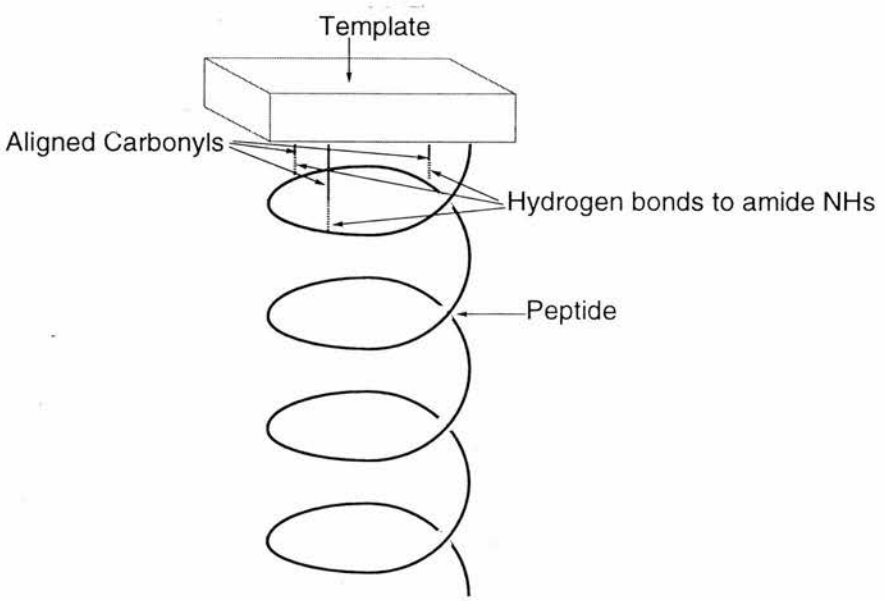

Figure 1.26: *Stabilisation of an α-helix via an N-terminal template*

Some recent examples of helix templates are shown below (Fig. 1.27). The diproline based template **6** prepared by Kemp *et al.*, constrained by a two atom bridge between position 4 of proline 1 and position 5 of proline 2, holds the ϕ and ψ torsion angles of the dipeptide to approximately those found in a classical α-helix and provides 3 amide carbonyls that can assume the correct α-helical pitch and spacing.[37] NMR studies revealed that peptides attached to this unit assumed a helical conformation in C^DCl_3, CD_3CN, d_2-DMF and d_6-DMSO.[37]

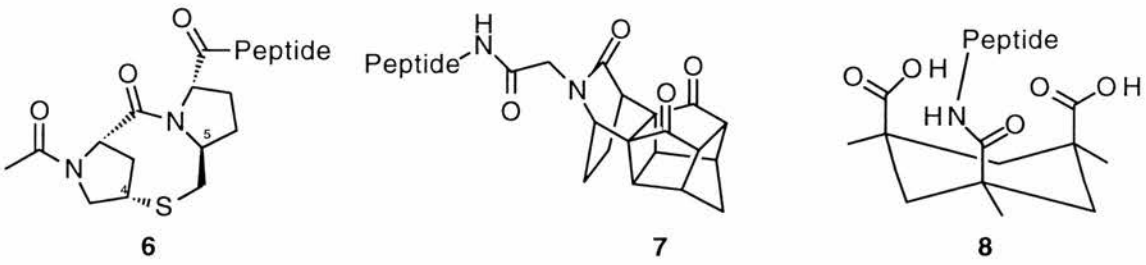

Figure 1.27: *Examples of α-helix stabilising templates*

The cage compound **7** and the cyclic compound **8** are both very recent additions to the helix template library.[106] CD spectroscopy indicated that an Ala and Aib containing nonapeptide attached to **7** exhibited a greater degree of helicity than the unattached peptide, while X-ray studies on peptide conjugates of triacid **8** revealed that the attached peptides adopt a 3_{10} helical structure.

Helix stabilising templates have also been synthesised within our own group. The (2*R*)-*N*-propionyl-(2*S*)-Pro-(2*R*)-Ala-(2*S*)-Pro thioether macrocycle attached to a trialkylammonium ion (Fig. 1.28) was found to adopt two rapidly interconverting conformational isomers.[37, 107, 108]

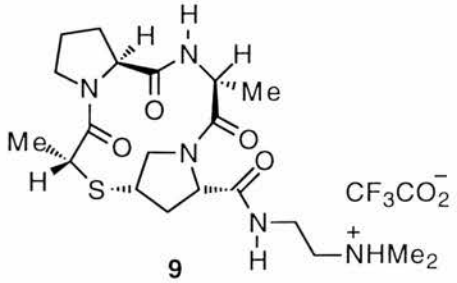

Figure 1.28: *(2R)-N-propionyl-(2S)-Pro-(2R)-Ala-(2S)-Pro thioether macrocycle*

At low temperature (-80 °C), NMR studies indicated that the minor isomer (40%) has four carbonyl groups aligned in an α-helical conformation suitable for helix propagation, while in the other conformer, the Pro^2 carbonyl dipole was anti-aligned with the other three dipoles. The positive charge acts as a counter charge, interacting favourably with the helix dipole and stabilising the desired alignment of the carbonyl groups in the macrocycle which would otherwise be destabilised by repulsive dipole-dipole interactions (see Section 1.2.3.1).

1.5.3 β-Turn mimetics

A β-turn peptidomimetic is commonly prepared by constraining the geometry of an existing β-turn peptide motif that is found in proteins and biologically active peptides. One of the most well established strategies for creating conformationally stable β-turn mimetics is to restrict rotation around the φ, ψ and ω torsion angles of a dipeptide unit.[106] This can be achieved in several ways by:

- Linking residue side chains together with a covalent bond;
- Introduction of α,α-disubstituted amino acids;
- Introduction of cyclic amino acids, e.g. proline.

There are a huge number of constrained peptidomimetics in the literature that serve as β-turn mimetics.[109-114] Some are constrained around only one torsion angle while others are constrained around two or more giving elaborate systems with extensive molecular scaffolding. The following sections detail some of the strategies that have been employed to introduce a stable β-turn into a short peptide.

1.5.3.1 Restriction of ϕ_i torsion angle

One of the simplest ways of preparing a constrained peptide is to introduce an *N*-alkyl cyclic amino acid in which the φ torsion angle is constrained. Examples include the artificial amino acids, homoproline **10** and 5,5-dimethylthiazolidine-4-carboxylic acid (DTC) **11**.[106]

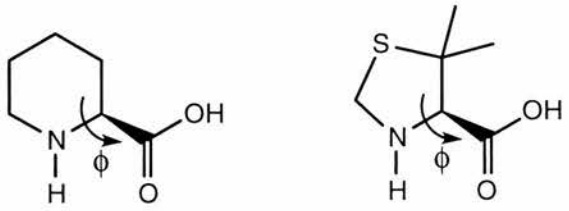

10 **11**

Figure 1.29: *Examples of ϕ constrained peptidomimetics*

1.5.3.2 Restriction of ψ_i torsion angle

The ψ_i torsion angle can be constrained by forming a lactam between neighbouring residue side chains. Friedinger prepared the β-turn peptidomimetic **14** by cyclizing a dipeptide sulfonium salt (Scheme 1.8). This was subsequently incorporated into a peptide sequence to form an analogue of a luteinizing hormone-releasing hormone constrained in its bioactive conformation (**15**).[109, 115]

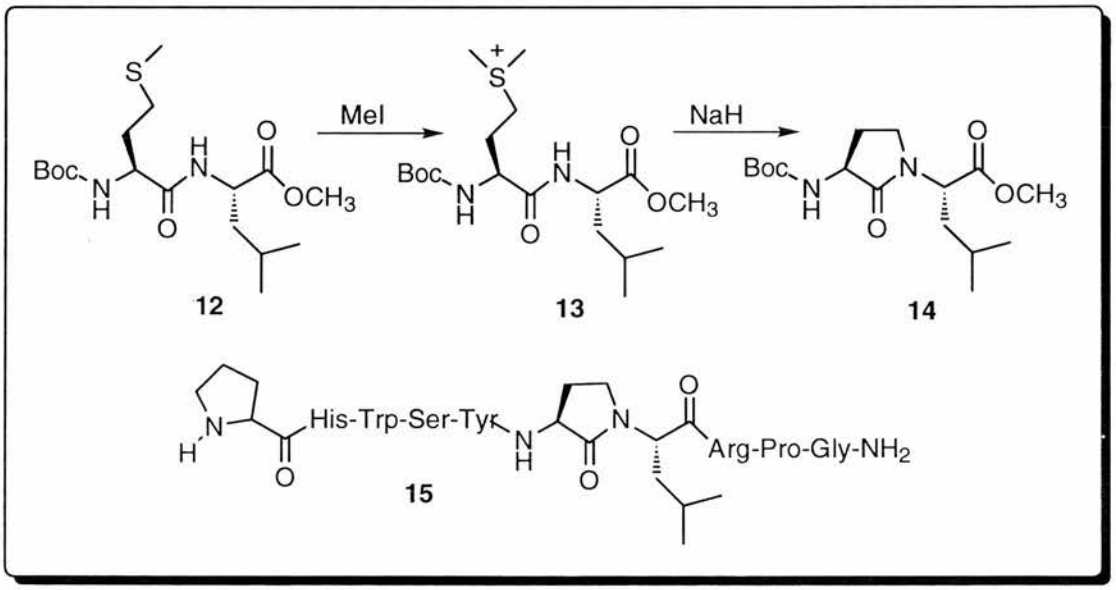

Scheme 1.8: *Preparation of Friedinger peptidomimetic*

1.5.3.3 Restriction of ω_i and $\phi_{(i+1)}$

Torsion angles ω_i and $\phi_{(i+1)}$ can be effectively constrained by introducing a thiazoline **16**, imidazoline **17** or oxazoline **18** moiety into the peptide backbone and many naturally occurring cyclic peptides such as ascidiacyclamide and ulitiacyclamide contain these structures.[106]

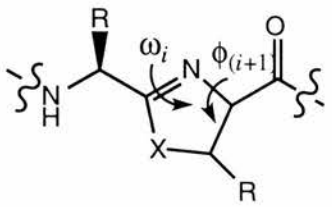

16 X=S
17 X=N
18 X=O

Figure 1.30: *Examples of ω_i and $\phi_{(i+1)}$ constrained peptidomimetics*

1.5.3.4 Restriction of ϕ_i, ψ_i and ω_i

A spirolactam **19** unit can be employed to simultaneously restrict the ϕ_i, ψ_i and ω_i torsion angles.[18, 116] These spirolactam units are good mimics of type II β-turns and peptide analogues of bioactive molecules containing this moiety often exhibit comparable biological activity. This was demonstrated by Long and Moeller who prepared a spirolactam-based peptide mimic of a key bioactive sequence in HIV-1 (see Section 1.4.2).[18]

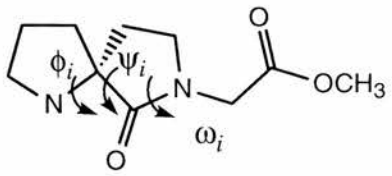

19

Figure 1.31: *Example of a ϕ_i, ψ_i and ω_i constrained peptidomimetic*

1.5.4 γ-Turn mimetics

A γ-turn forms a pseudocyclic hydrogen-bonded 7-membered ring system (see Section 1.2.3.7) and like any other peptide motifs, can be a key component in biologically active peptides, for example angiotensin II.[70, 73, 74] A number of γ-turn mimetics have been synthesised, including non-peptide mimetics by Huffmann *et al.* which replace the H-bond participating carbonyl and NH moieties with an ethylene bridge (Fig. 1.32).[69] Such systems have the required γ-turn torsion angles and have applications in the development of inhibitors of platelet aggregation by mimicking the *C*-terminal region of RGD antagonists.

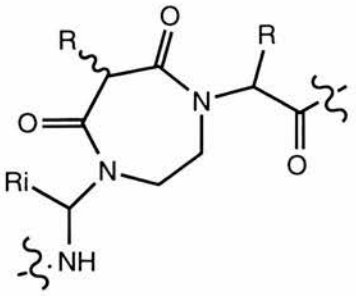

Figure 1.32: *Huffman γ-turn peptidomimetic*

1.5.5 Turn inducers

Some turn templates bear no structural resemblance to the native motifs they are mimicking. So called turn inducers cannot be classified like other β-turn mimetics because all topological similarities (*i.e.* ϕ, ψ and ω torsion angles) with β-turn peptides is virtually absent.[101, 117, 118] Feigel prepared one of the first examples of this class of compounds - a spacer prepared from phenoxathin-*S*-dioxide (**20**), Fig. 1.33). Since then, many unusual ring systems have been developed and incorporated into peptides.[119] Notable examples include, 3-amino benzoic acid (**23**), 2-aminocyclopentane carboxylic acid (**24**), and polycyclic amino acids **21** and **22**. All have successfully induced peptide folding and nucleated hydrogen bonding between adjoining strands.

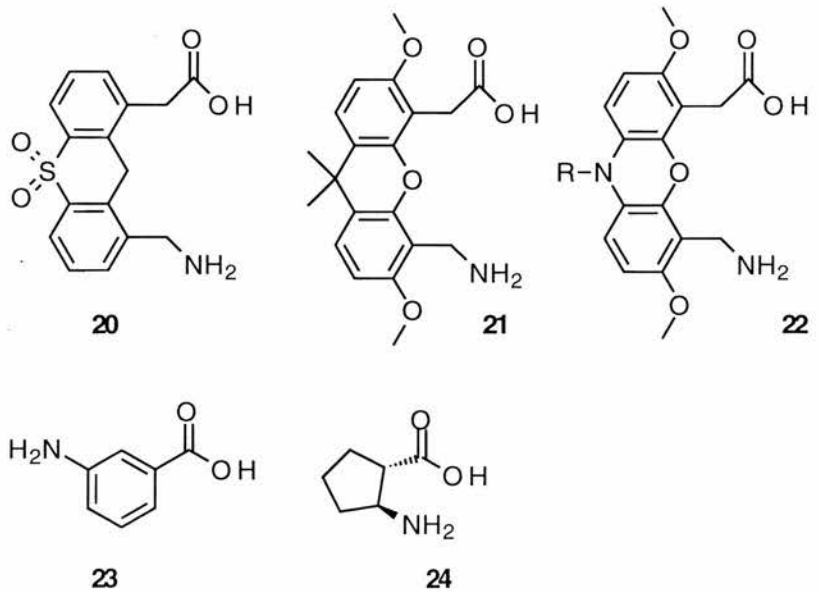

Figure 1.33: *Some peptide turn inducers*

1.5.6 β-Strand mimetics

Like the α-helix and the β-turn, the peptide backbone within a β-sheet has well defined torsion angles. This stable conformation, referred to as a β-strand, is a product of the intrinsic geometry of peptides and the constraining influence of the intrastrand hydrogen bonding within the β-sheet.

β-Strand models can be generated by attaching peptide strands to a constrained template which directs the attached peptide strands to hydrogen bond to each other (see Section 1.5.7) and adopt a β-strand conformation within the context of a β-sheet.

In some cases, rigid mimics of β-strands can be used to initiate β-sheet structure. For example, Kemp's diacylaminoepindolidione template, discussed later in Section 1.5.7, simulates a β-strand and also helps to stabilise a three stranded antiparallel β-sheet.[120]

Smith and Hirschmann have also developed a cyclically constrained non-peptide scaffold based on 3,5-linked polypyrrolin-4-ones (Fig. 1.34).[121, 122]

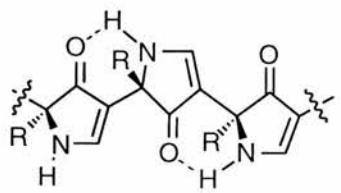

Figure 1.34: *β-Strand mimic based on 3,5-linked polypyrrolin-4-ones*

This peptidomimetic adopts an extended conformation in solution which is stabilised by intramolecular H-bonds between adjacent pyrrolin-4-one rings, constraining the ϕ torsion angle at approximately 205°.

Finally, Schrader and Kirsten used aminopyrazole as a β-strand mimetic to stabilise a dipeptide in a β-strand conformation *via intermolecular* hydrogen bonding (Fig. 1.35).[123]

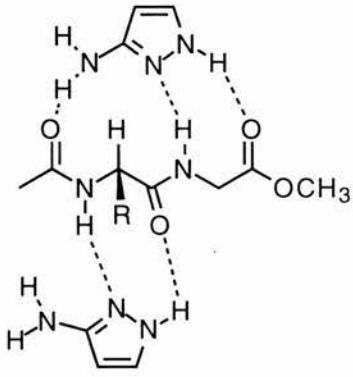

Figure 1.35: *Stabilisation of a dipeptide using aminopyrazole*

In general, β-strand mimetics are a useful for β-sheet stabilisation. By acting as a conformational template, they can propagate a stable conformation from an ordered region - the template, to a disordered region - the peptide. Furthermore, because they frequently lack amide bonds, they are less susceptible to cleavage by proteolytic enzymes, making them promising candidates for the development of biologically stable peptide based therapeutics (see Section 1.3.3).[96]

1.5.7 β-Sheet models

The construction of well defined β-sheet models and templates provides an excellent basis for determining the factors behind β-sheet nucleation and stabilisation by separating tertiary context effects from the intrinsic sources of secondary structure stability.[124] Isolated β-sheet systems are also easier to study experimentally by NMR, IR and CD spectroscopy than protein bound motifs.

All β-sheets are stabilised by hydrogen bonds between the amido NH and carbonyl groups of residue pairs on neighbouring peptide chains. Although the anatomy of β-sheet structure is generally straightforward, predicting whether or not a peptide will participate in a β-sheet structure is far less certain. In helices, the phenomena of nucleation and propagation are easy to understand in terms of H-bonding because we are dealing with H-bonding units that lie at regular intervals along a sequence. It is a great deal harder to identify potential β-sheet sequences because these structures can be formed by residues far apart in the primary sequence. It is certainly true that certain amino acids appear to have a high propensity for β-sheet structures and that side chain-side chain hydrophobic interactions play a role in β-sheet stabilisation,[52, 125, 126] but the importance of these factors is ultimately controlled by the location of amino acids in the primary sequence. All this means is that it is difficult to predict the folding pattern of a peptide solely in terms of its amino acid sequence. This is often referred to as the *protein folding problem.*

If we are to understand β-sheet nucleation and propagation, we must first understand the factors that control folding. This is difficult to determine without a well defined β-sheet model that is accessible to spectroscopic analysis. It is generally difficult to make systems based solely on peptides because their folding is complex, with intermolecular association often comparable in rate to intramolecular β-sheet folding, leading to insoluble heterogeneous aggregates (Scheme 1.9). Furthermore, the small free energy difference that stabilises the folded state of a protein over the unfolded state (3-15 kcal mol^{-1}) is difficult to attain in a small polypeptide as the free

energy difference between the folded and unfolded states arises from the difference between two large values representing enthalpic and entropic contributions from both the solvent and the peptide chain. Since the magnitude of these contributions are context dependent and dictated by electrostatic and hydrophobic interactions, it is difficult to design a polypeptide whose thermodynamic stability can be predicted empirically. Although there are a number of fully peptidic model systems that have a well defined secondary structure (Yan and Erickson, Balaram, and Searle have produced some notable examples),[125-127] it is reasonable to say that this strategy is generally rather unpredictable.

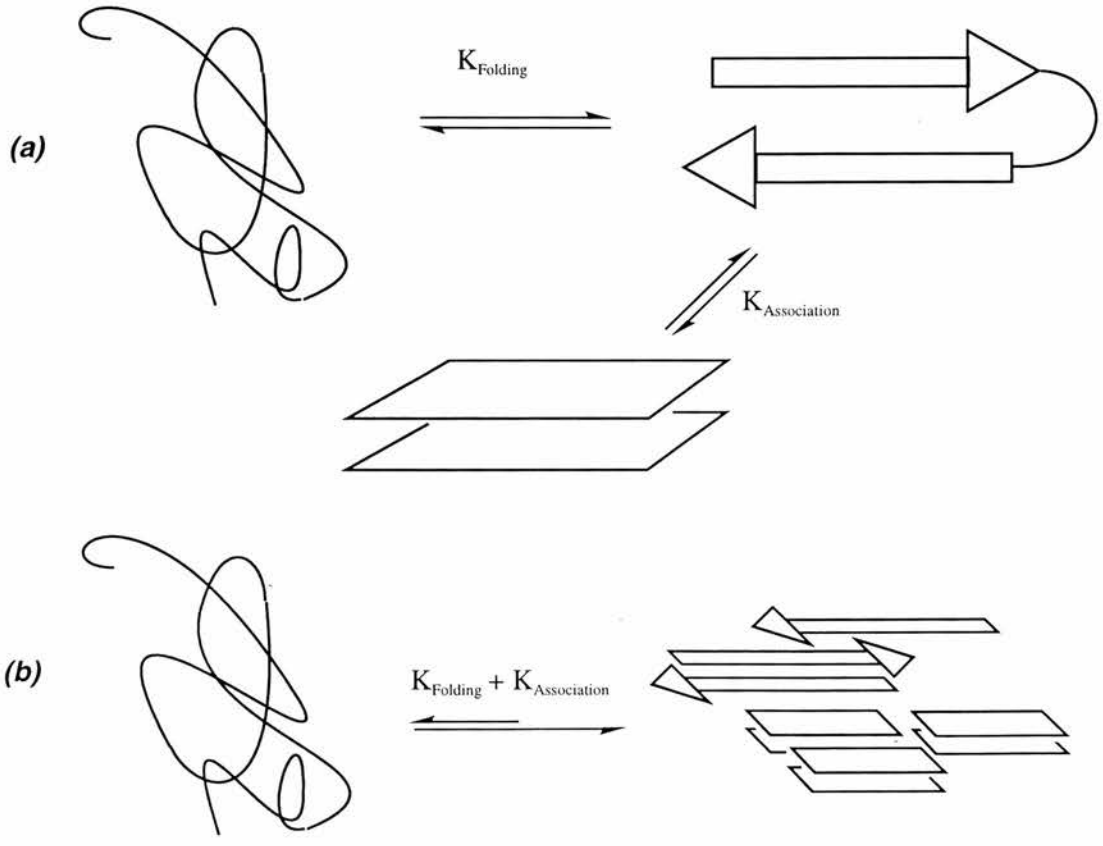

Scheme 1.9: *Peptide folding; (a) Intramolecular folding preceding self-association to give a homogeneous β-sheet structure; (b) Intramolecular folding and self-association can have comparable rates which leads to an insoluble aggregate*

Conformationally constrained templates can assist in the creation of stable, well defined systems that are accessible to spectroscopic analysis by lowering the unfavourable entropy difference between the folded and unfolded states. In turn, quantitative data can be collected that will help us to understand the factors behind β-sheet nucleation and propagation and ultimately enable the development of artificial peptides that interfere in disease states where β-sheet formation is important such as Alzheimer's disease and AIDS (see Sections 1.4.2 and 1.4.3) as well as prion-based diseases such as scrapie, CJD and BSE.[62]

In recent years there has been an increase in research relating to peptide folding and sheet formation. One result of this work is the development of β-sheet models which can give us new insight into the structural detail and stability of this important motif.[64, 128] The commonest type of β-sheet model mimics a two-stranded anti-parallel β-sheet, and is usually prepared by anchoring a pair of peptide strands to a turn-inducing template. The template has fewer degrees of freedom than the fully peptidic β-turns often found 'capping' natural β-sheets in proteins - which means that it can impart some degree of secondary structure stability to a system which might otherwise adopt a random coil conformation in the absence of long range tertiary interactions. This is a concept which is also used with respect to α-helix stabilisation (see Section 1.5.2).[104]

Feigel *et al.* prepared prepared one of the first parallel β-sheet models (Fig. 1.36). It was composed of phenoxathiin-4,6-dicarboxylic acid and a sulphone based diamine connected to each other by a pair of amino acids.[128, 129]

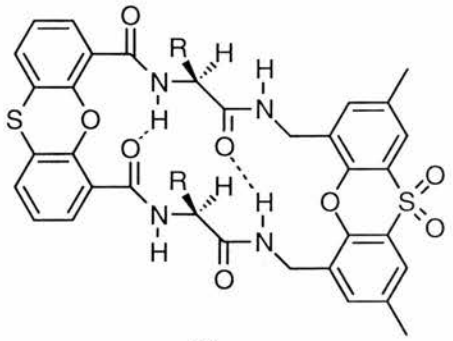

25

Figure 1.36:*Parallel β-sheet model by Fiegel*

Molecular modelling studies suggested that this system should adopt a parallel β-sheet conformation and ^{1}H ROESY NMR studies of **25** in $CDCl_3$ solution at -61°C showed crosspeaks consistent with a parallel β-sheet structure. Fiegel also constructed antiparallel β-sheet models from 2-biphenyl templates, one of which is shown below (**26**, Fig. 1.37).[130, 131]

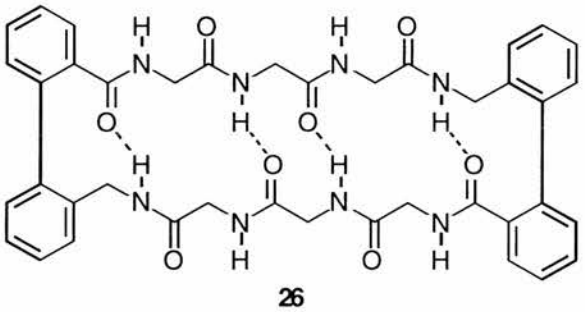

26

Figure 1.37: *Antiparallel β-sheet model by Fiegel*

Unfortunately, spectroscopic analysis was complicated by the fact that the biphenyl template imparts an element of atropisomeric chirality to the macrocycle which means it exists as a mixture of *RR*, *SS* and *RS* diastereoisomers in d_6-DMSO solution. Temperature dependent chemical shift studies suggested that the *RR* atropisomer is dominant and adopts an antiparallel β-sheet conformation. In any event, this added complication means that the biphenyl template is not ideal for preparing β-sheet models, and serves to highlight the importance of rigidity in the design of β-sheet templates.

Kelly utilised hydrophobic interactions to form a hydrophobic cluster which nucleated a β-sheet in aqueous solution.[132, 133] The dibenzofuran unit is designed with flexible alkyl 'arms' so that it can fold onto the first pair of flanking amino acid side chains, forming an area of hydrophobicity which in turn nucleates a β-sheet (**27**, Fig. 1.38).[134] Kelly's system was one of the first β-sheet models that maintained a stable structure in aqueous solution. It is also monomeric as determined by equilibrium ultracentrifugation studies at pH 4.1. This was an important result because β-sheets generally aggregate in aqueous solution.

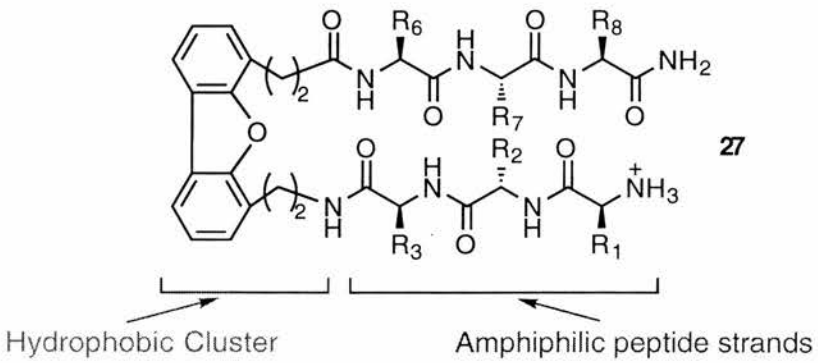

27

Figure 1.38: *Antiparallel β-sheet by Kelly*

Kemp took a somewhat different approach to β-sheet stabilisation by preparing a three stranded β-sheet consisting of a central β-strand mimic attached to two dipeptide strands by two Pro-D-Ala β-turns and urea linking groups (**28**, Fig. 1.39).[120] This approach is distinct from other examples in that it uses a β-strand mimic to stabilise a β-sheet rather than a turn inducer.

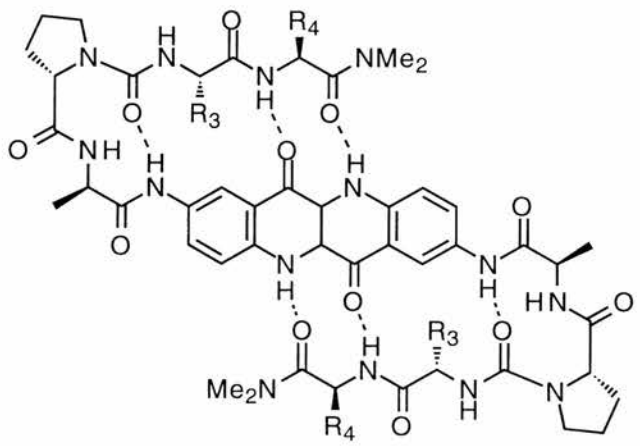

28

Figure 1.39: *Three stranded β-sheet stabilised by an epindolidione unit*

This so-called 'β-meander' motif features prominently in many other peptide β-sheet models and provides a useful starting point for probing the stability of β-sheets composed of more than two strands.[135, 136]

Nowick *et al.* prepared a range of anti-parallel and parallel multistranded β-sheet models using an oligourea scaffold.[137-140] One example, the three-stranded

antiparallel β-sheet shown below (Fig. 1.40), also uses a β-strand mimic to provide additional stability.

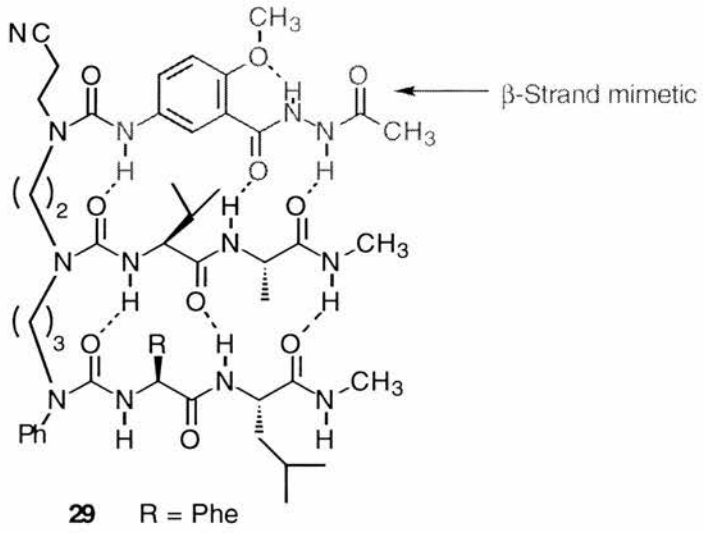

Figure 1.40: *Three-stranded parallel β-sheet by Nowick*

Some other examples of sheet stabilising templates include a tetrasubstituted trans-alkene template (**31**, Fig. 1.41) prepared by Gellman *et al.* which adopts a β-hairpin conformation in CD_2Cl_2,[117] a norbornene based β-sheet template (**32**)[141, 142] prepared by North *et al.* and a diphenylacetylene template (**30**) developed by Kemp and Li which induces β-sheet formation between two attached peptide strands in a variety of organic solvents.[141]

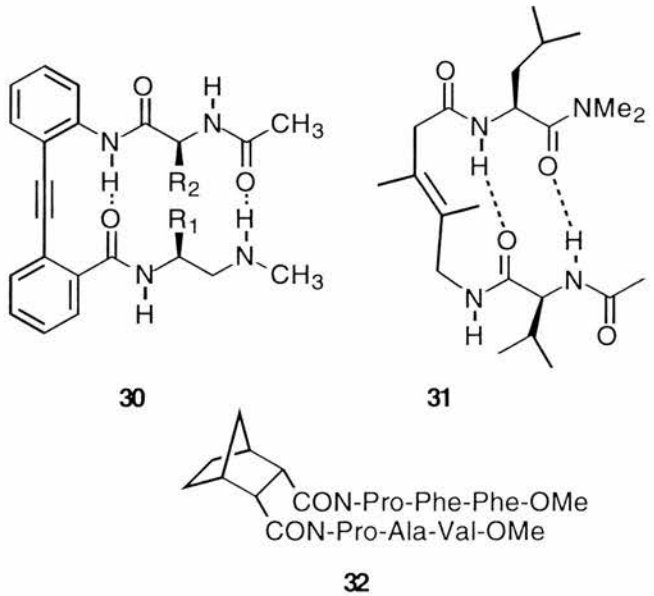

Figure 1.41: *Small artificial antiparallel β-sheet models*

All the aforementioned β-sheet models share the same characteristics. They are all prepared from rigid or semi-rigid templates to which two or more peptide strands are attached. The template effectively induces β-sheet formation by directing the peptide strands in a favourable orientation for β-sheet formation with the result that a planar β-sheet model is formed.

β-Sheets need not be limited to planar two dimensional systems. Ghadiri *et al.* adopted a different approach towards the preparation of β-sheet models. By taking advantage of the strong hydrogen bonding between flat cyclic peptides composed of alternating D and L amino acids, he templated covalent bond formation between separate peptides and assembled cylindrical β-sheets (Scheme 1.10).

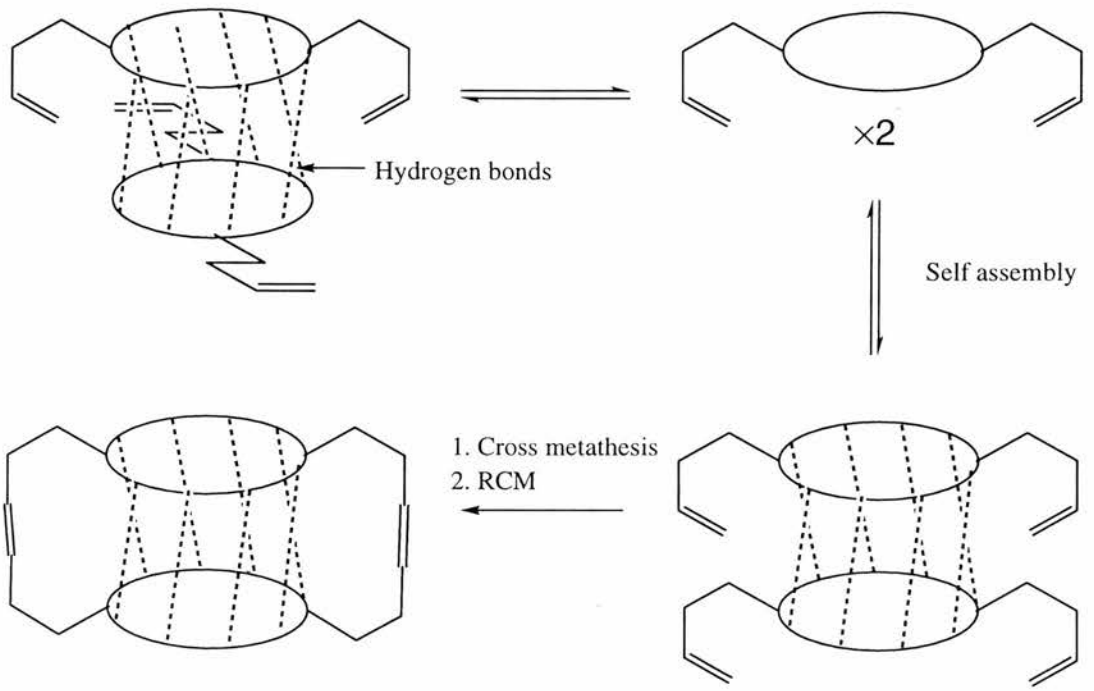

Scheme 1.10: *Synthesis of cylindrical β-sheet assemblies*

Furthermore, by selective incorporation of *N*-alkylated residues, on one side of the cyclic peptide, Ghadiri managed to limit β-sheet self-assembly to the formation of discrete dimeric systems which were then stabilised by covalent capture, producing systems which were unable to aggregate and therefore more accessible to spectroscopic analysis.[142, 143] Hollow, tubular structures are well documented in

natural systems. Notable examples include transmembrane channel proteins and the tobacco mosaic virus. Ghadiri's systems provide a useful starting point for the analysis of the processes behind their formation and stabilisation. Moreover, by measuring the degree of self-assembly with respect to different amino acids, these dimer-forming DL peptides could prove useful as well-behaved systems for the evaluation of amino acid β-sheet propensities.

1.5.8 Larger model systems: Miniprotein models

The design and synthesis of small artificial proteins by self-assembly processes is an area of research that has been growing rapidly in recent years and provides a means of probing the relationship between secondary and tertiary structure.[144, 145] Several research groups have now taken important steps toward the development of artificial proteins that have a well defined folding topology. The concept of template assembled synthetic proteins (TASP), developed by Mutter *et al.*, is one of the first examples of a synthetic approach to the construction of artificial proteins (Fig. 1.42).[146-148]

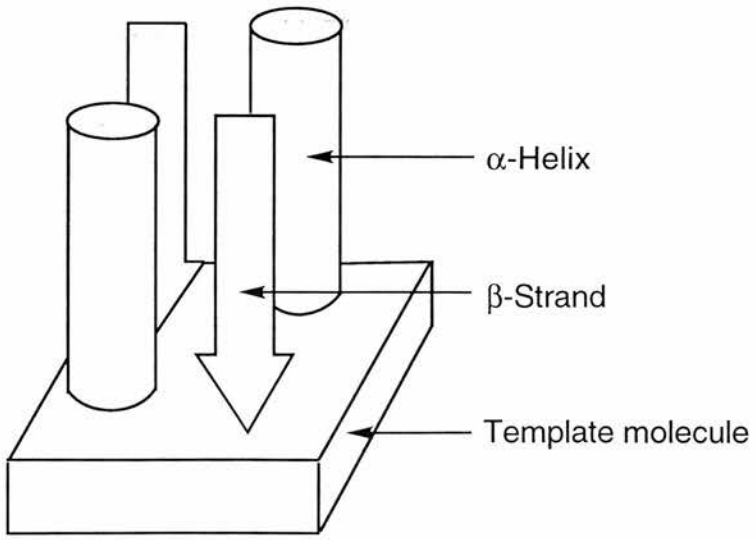

Figure 1.42: *TASP concept: Template induces attached peptides to fold into an α-helical or β-sheet/strand conformation*

TASP works by anchoring the first amino acid in the proper orientation for helix or β-sheet/strand initiation, thus overcoming the entropically unfavourable nucleation step in secondary structure formation. Any molecule can be used as the stabilising template (*e.g.* cyclic peptides) with the only criterion being that the attachment sites are in the appropriate positions and oriented correctly. The TASP concept has been used to generate a range of artificial proteins; DeGrado *et al.* synthesised a four helix bundle proton channel using tetraphenyl porphyrin as a template and Mutter synthesised a membrane channel forming protein derived from the bee venom Melittin.

One limitation of TASP is that it relies heavily on interstrand interactions to stabilise the secondary structure of the attached peptide strands. It does not allow for the study of isolated secondary structure motifs in the absence of longer range forces, limiting the range of potential protein models to bundles of α-helices, β-sheets/strands or both. They have, however, been very useful in understanding the relationship behind secondary and tertiary structure with respect to multiple-helix transmembrane proteins such as Bacteriorodopsin (Fig. 1.43) as the TASP approach is ideally suited to emulating structures of this type.

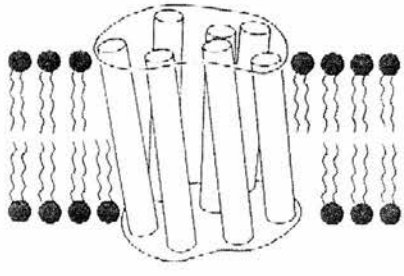

Figure 1.43: *Representation of the α-helical transmembrane segment of Bacteriorodopsin*

1.6 Synthesis of Peptides Containing Uncoded Amino Acids

Many biologically active peptides and secondary structure models contain unusual amino acids which are either *N*-methylated, C-α-disubstituted, β-branched or bear no resemblance to conventional amino acids at all. Synthesising peptides which incorporate bulky, non-native β-turn inducers can be particularly problematic because their steric bulk can often impede the formation of amide bonds between template and peptide.[149] There is also the additional problem of ensuring that any functionality within uncoded units are not affected by the peptide coupling conditions.

In general, peptides are synthesised from an *N*-protected segment with a free carbonyl group and a C-protected segment with a free amino group (Scheme 1.11).[150]

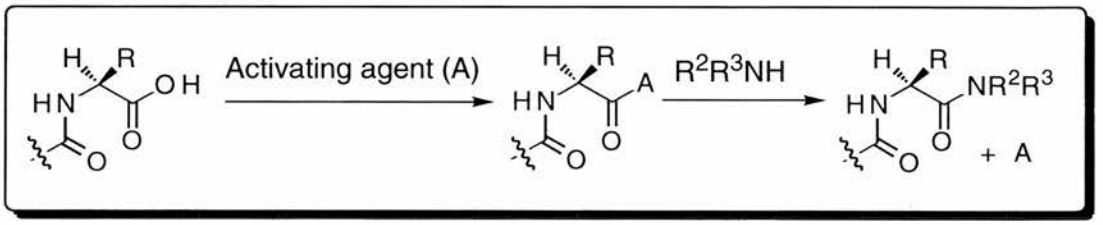

Scheme 1.11: *General mechanism of synthetic formation of an amide bond*

The free acid is activated by a coupling reagent, usually *via* the formation of a mixed anhydride,[150] making the carboxyl group more electrophilic. This species then reacts with the incoming amine moiety of an amino acid, forming an amide bond and displacing the activating agent. If the residue to be acylated it sterically hindered (*e.g.* α or β disubstituted or *N*-alkylated) the reaction rate slows down and side reactions that would normally be too slow to cause problems become competitive, for example diketopiperazine formation, first reported by Huang and Niemann in 1950,[151] and racemisation.

Alkyl chloroformates and simple carbodiimide-based coupling reagents are commonly used for peptide coupling (Fig. 1.44), however, these reagents are often ineffective when coupling hindered residues.

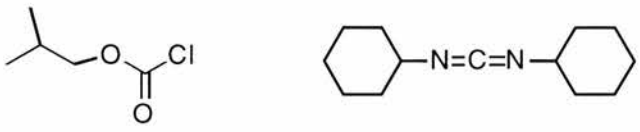

33 **34**

Figure 1.44: *Isobutylchloroformate (33) and DCC (34)*

More powerful coupling reagents have been developed in recent years. Uronium and phosphonium salts such as HBTU (**35**), TBTU (**36**) and PyBOP (**37**) (Fig. 1.45), as well as modified versions of carbodiimide reagents [*e.g.* EDCI (**38**)], all give higher yields with a decrease in racemisation and are increasingly being used for couplings involving sterically demanding residues such as Pro, Aib, and *N*-methylated residues.[152]

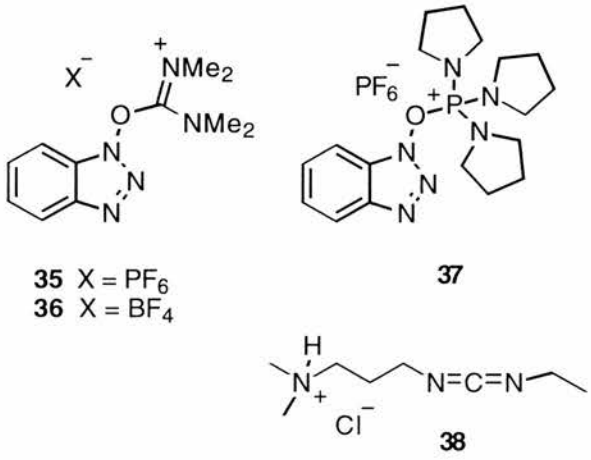

35 X = PF_6
36 X = BF_4

37

38

Figure 1.45: *Some peptide coupling reagents*

Coupling reagents, **35**, **36**, and **37** react with the carboxyl group of an amino acid to produce an active oxyuronium or oxyphosphonium species. A hydroxybenzotriazole anion (**39**) is displaced and this reacts with the oxyuronium or oxyphosphonium intermediate to give an oxybenzotriazole ester (**40**) which is the active amine acylating agent (Fig. 1.46). Because this species is relatively stable compared to other activated esters, the α-proton adjacent to the activated carbonyls is less acidic than it might otherwise be, therefore the likelihood of enolisation, and hence racemisation, is diminished greatly. These active esters can also be prepared by

using hydroxybenzotriazole (**41**) in conjunction with other coupling reagents, for example EDCI (**38**).[153]

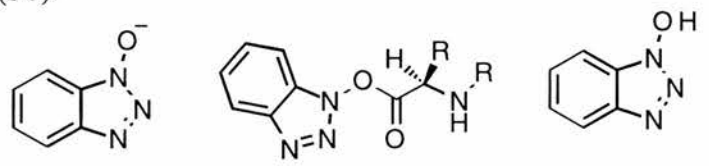

39 **40** **41**

Figure 1.46: *Hydroxybenzotriazole anion (**39**), oxybenzotriazole ester (**40**) and hydroxybenzotriazole (**41**)*

Unfortunately, the reduced reactivity of oxybenzotriazole esters can be problematic, particularly in difficult couplings where yields can be diminished. This was addressed by the development of HATU (**42**) by Carpino *et. al.*[154, 155]

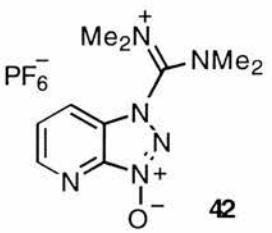

42

Figure 1.47: *HATU*

Peptide couplings with HATU gave high yields and low levels of racemisation, even in extremely hindered cases.[149, 156-159] Its efficiency is due to a favourable complex (**43**) between the azabenzotriazolyl ester and the incoming amine function which brings it into close proximity to the activated carbonyl (Fig. 1.48). Like HOBt esters, this active ester can also be produced by using 7-azabenzotriazole with other coupling reagents.[154, 155]

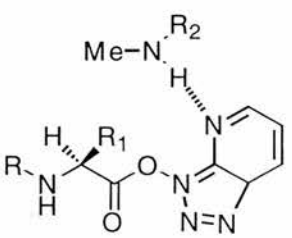

43

Figure 1.48: *HATU coupling complex*

Finally, mention should be made of DPPA (**44**), a phosphoryl azide based reagent first used for peptide couplings in 1972 by Yamada and co-workers.[160]

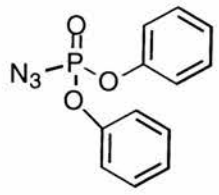

44

Figure 1.49: *DPPA*

It has proven to be effective in reactions were the peptide side-chains might otherwise participate in unwanted side-reactions (*e.g.* threonine, asparagine and glutamine) and has also been used extensively in peptide cyclisations.[160, 161]

1.7 Foot and Mouth Disease Virus (FMDV)

Foot and Mouth Disease is an acute viral infection of cloven footed animals with symptoms consisting of fever and the formation of painful vesicles on the mouth and on the feet. This disease prevents weight gain in cattle and reduces milk yields in dairy cows with obvious economic consequences.[162]

The Foot and Mouth Disease Virus (FMDV) is a member of the picornaviruses, a group of small RNA viruses. A common characteristic of this family of viruses is that they are based on a single strand of positive sense RNA consisting of around 8400 base pairs, surrounded by an icosahedral capsid. This capsid is composed of 20 faces, each consisting of 60 copies of each of the 4 capsid proteins. During replication, the viral capsid is discarded and the RNA strand passed into the host cell were the RNA strand acts as a messenger RNA on cellular ribosomes. Translation takes place, resulting in the production of various viral proteins which consist of capsid proteins and replicative proteins (including RNA polymerase, a replicative enzyme which catalyses the synthesis of new RNA strands). The overall result is the production of new copies of the original virus particle which can then leave the cell.

The replicative process begins with the production of a large polyprotein which is processed into smaller encapsulative and replicative proteins *via* a series of proteolytic cleavage reactions (Fig. 1.50), a process usually carried out by proteases embedded within the protein itself, in this case, L3 and L. In the 16 amino acid 2A polyprotein region, however, molecular biology studies have ruled out such a mechanism. This has been proven by the synthesis of the plasmid pCAT2AGUS which coded for a polyprotein in which the 2A sequence was inserted between two unrelated protein sequences CAT and GUS. The translation products were cleaved into CAT2A and GUS, showing that the process does not require the presence of any other part of the FMDV polyprotein. Moreover, it was observed that more CAT2A was produced than GUS, suggesting that this cleavage is not a proteolytic event akin to those catalysed by the L and 3C proteases (as this would have produced equal amounts of both products), but instead occurs while the 2A region is still attached to

the tRNA on the ribosome. In other words, the 2A region is an esterase unlike the L and 3C regions which are embedded proteases.[163]

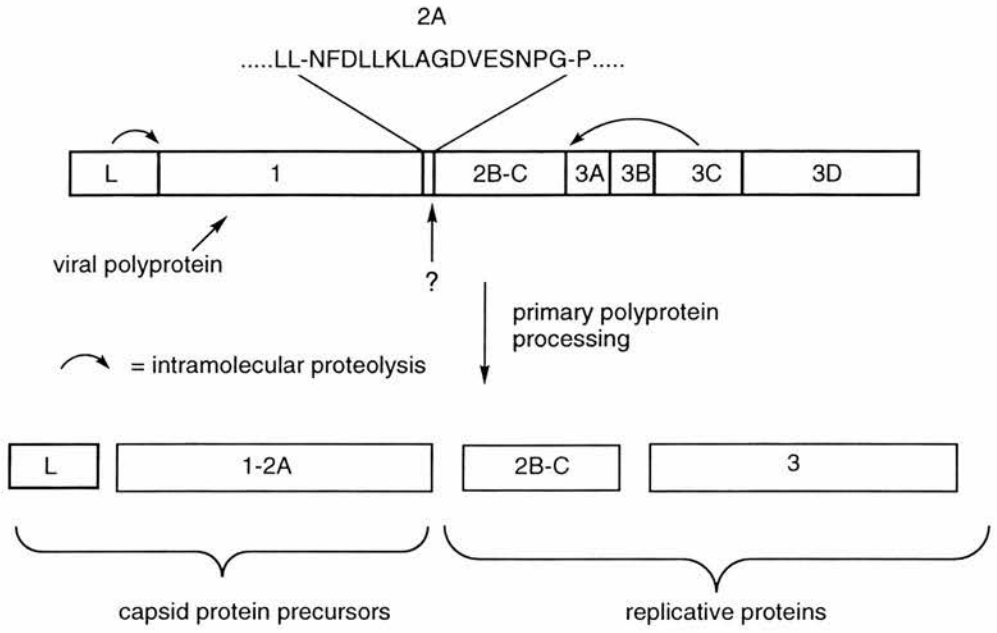

Figure 1.50: *Polyprotein processing of the foot and mouth disease virus*

Like all peptides and proteins, the 3D structure of the 2A region is important in defining how it cleaves the polyprotein. Molecular modelling studies and Chou Fasman rules indicate that this region is composed of an alpha helix throughout the *N*-terminal region with a type VI β-turn in the Ser-Asn-Pro-Gly sequence. The α-helical structure is stabilised by a series of $[i \rightarrow (i+3)]$ or $[i \rightarrow (i+4)]$ side-chain interactions; a salt-bridge ($Asp^3 \rightarrow Lys^6$); hydrogen bonds ($Lys^6 \rightarrow Asp^{10}$ and $Asp^{10} \rightarrow Asn^{14}$) and a set of side-chain hydrophobic interactions. The helix is also amphiphilic, with hydrophobic residues grouped on one face and hydrophilic residues on the other.

The highly structured 2A peptide possibly disturbs the position of the Mg^{2+} ions required for peptidyltransferase activity such that peptidyl transfer is suppressed in favour of attack of the scissile Gly^{16}-RNA bond by a Mg^{2+}-bound water molecule. The Mg^{2+} ion could reside at the base of the helix where it could bind to the acylated vicinal diol moiety of the adenosyl ribofuranosyl fragment at the end of the tRNA

acceptor stem, stabilise the helix through a charge-dipole interaction, and position a Mg^{2+}-coordinated water molecule for attack on the 3'-ester carbonyl group. [Fig. 1.51(*a*)].[163]

Unfortunately, in the absence of the ribosomal polypeptide exit channel, isolated 2A peptides lack a stable secondary structure so it is presently not possible to directly observe and verify this cleavage event. We intend to investigate the mechanism of this process by constructing an isolated 2A sequence stabilised by peptidomimetics. This involves using an *N*-terminal helix template, to stabilise helical structure, and a β-turn mimetic to stabilise the turn region. An RNA analogue can then be attached to the 2A peptide analogue and the extent of ester cleavage can be studied chemically, thus establishing if the proposed bioactive structure is accurate [Fig. 1.51(*b*)].[164] If this proves to be the case, major advances can be made in the elucidation of the mode of action of these self-cleaving peptides.

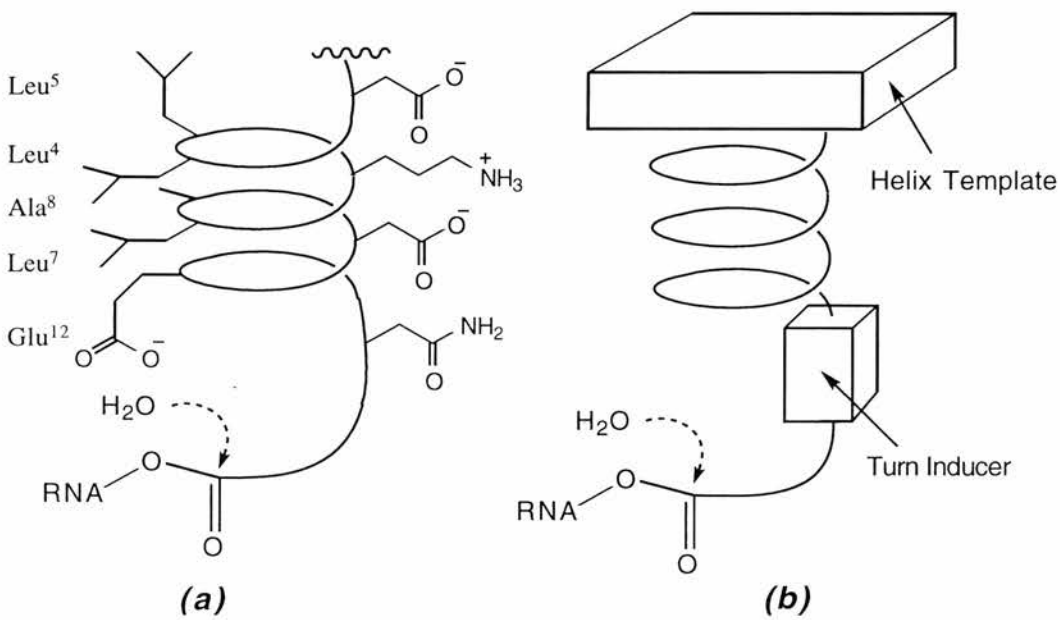

Figure 1.51: *(a) Proposed conformation of 2A polyprotein in ribosome (Mg^{2+} not shown); (b) miniprotein model*

In recent years, many *N*-terminal α-helix templates have been developed that have enabled us to stabilise helical structure in isolated peptides, thus allowing us to probe

the processes behind helix nucleation and propagation.[165] Unfortunately, similar progress has not been made in our understanding of β-structures; *i.e.* β-turns, hairpin bends and β-sheets. This gap in our understanding inspired us to develop novel turn inducing templates, not only in the context of the FMDV 2A polyprotein, but also with the synthesis of extended β-structures and their associated applications in mind.

2. RESULTS and DISCUSSION

2.1 Synthesis of Peptidomimetics for the Stabilisation of β-Sheets

2.1.1 Introduction

The β-hairpin structure highlights the relationship between the β-turn and the β-sheet. It was probably the main inspiration for the strategy, pioneered by Feigel, of using turn inducing templates with the sole purpose of stabilising a β-sheet.[129-131, 166] Unlike peptidomimetics designed to mimic the geometry of a particular turn, for example, in a bioactive peptide, the side-chain and backbone topology of general β-sheet stabilising templates is not of great importance. The most important requirement is the ability to hold two or more attached peptide strands at the optimum interstrand distance required for interstrand H-bonding. Other aspects of the template are also important such as rigidity, ease of synthesis and chemical stability. The criteria for a good β-sheet template can be condensed into three main points:[141]

- The template should be tailored to the geometry of the β-sheet, that is, it should hold the attached peptide strands apart at the optimum orientation and distance for hydrogen bonding;

- it should be synthetically accessible and easily incorporated into a peptide without affecting the structure of the host peptide or the template;

- it should possess a stable, well-defined conformation.

In our own group, modelling and computer aided design indicated that peptides containing 5-amino-3-pentynoic acid (APA) (**47**), or derivatives of this moiety, would adopt a β-hairpin structure in which attached peptide strands would adopt the optimum C-α to C-α interstrand distance of 4.5-5.3 Å required for antiparallel β-sheet formation (Fig. 2.1).[167]

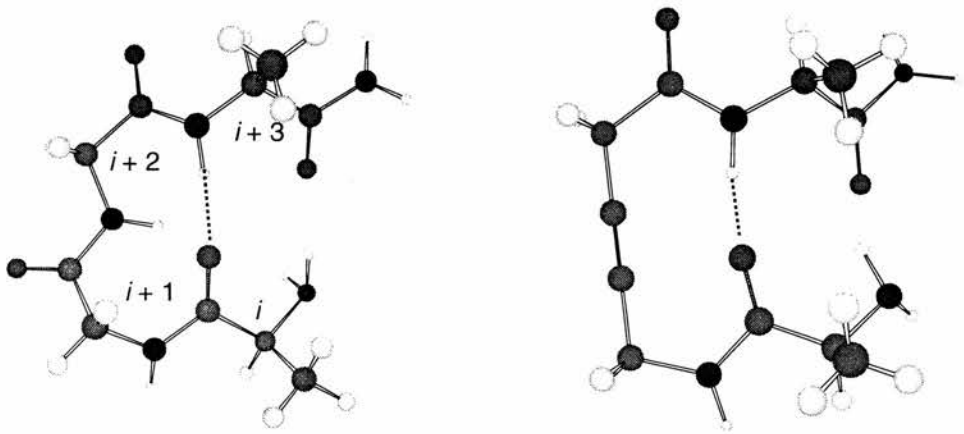

Figure 2.1: *Natural and artificial β-turns; (a) Reverse turn showing the H-bond and the potential to form antiparallel β-sheet. Amide and α-carbon hydrogen atoms are shown and the central two residues (i +1 and i + 2) are glycine to allow comparison with structure (b); (b) Reverse turn analogue derived from 5-amino-3-pentynoic acid*

2.1.2 Synthesis of APA - a first generation β-sheet template

As part of a study to synthesise analogues of GABA, an inhibitory transmitter at receptor sites in mammalian central nervous systems, Allan *et al.* synthesised peptidomimetic **47** in very low overall yield (~3 %) from the acetylenic diol **45** *via* Jones oxidation followed by treatment under Schmidt conditions with sodium azide and concentrated H_2SO_4 (Scheme 2.1).[168]

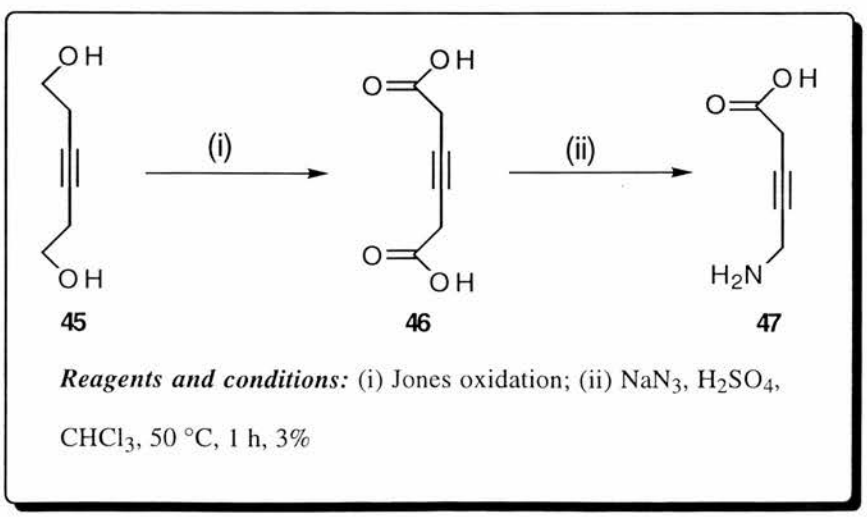

Scheme 2.1: *Synthesis of APA by the method of Allan et al.*

As one of the criteria for a β-turn mimetic is its ease of synthesis, an alternative method had to be found. In conjunction with Dr Basil Hartzoulakis, a higher yielding protocol was developed which produced the *N*-Cbz aminopentynoic acid **50** in 30% overall yield. It was prepared by reacting the sodium acetylide of propargylamine with ethylene oxide in liquid ammonia, forming an alcohol and, without further purification, was *N*-protected using benzylchoroformate to form benzylurethane **49** in 65% yield after chromatographic purification. Oxidation of the alcohol with potassium dichromate in acetone gave the target compound **50** (HRMS: found [M + H]$^+$, 247.0841. $C_{13}H_{15}O_3N$ requires 247.0844) in 55% yield as a white solid with a mp of 76 °C (Scheme 2.2).

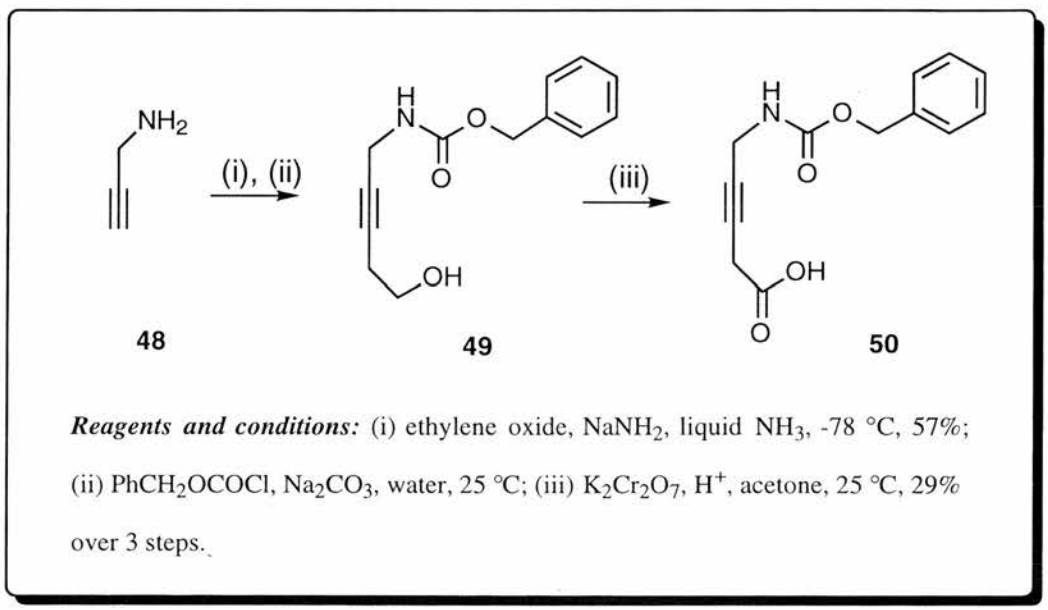

Reagents and conditions: (i) ethylene oxide, $NaNH_2$, liquid NH_3, -78 °C, 57%; (ii) $PhCH_2OCOCl$, Na_2CO_3, water, 25 °C; (iii) $K_2Cr_2O_7$, H^+, acetone, 25 °C, 29% over 3 steps.

Scheme 2.2: *Preparation of N-Cbz-5-amino-3-pentynoic acid (**50**)*

Studies by Hartzoulakis *et al.* revealed that, although it was synthetically possible to incorporate 5-amino-3-pentynoic acid into a hairpin peptide, overall yields were low because of the labile nature of the CH_2 hydrogens α to the carbonyl under basic conditions. This frequently resulted in the conversion of the alkyne group to an allene during synthetic elaborations of the *C* and *N*-termini (Scheme 2.3).[167]

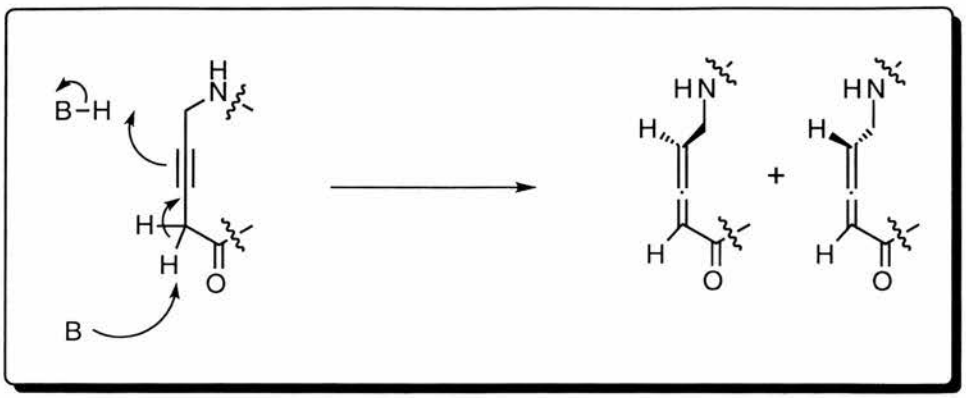

Scheme 2.3: *Mechanism of allene formation from APA under basic conditions*

This allene formation is clearly not desirable in **50** or any associated derivative, because an allene bond would hold any attached peptide strands orthogonal to each other and effectively eliminate any possibility of β-sheet formation. Furthermore, NMR studies of peptide analogues containing intact APA did not appear to adopt the expected β-hairpin/β-sheet conformation because of a lack of conformational constraint in the template.

2.1.3 Synthesis of 2-(3'-amino-prop-1'-ynyl)-phenylamine - a second generation β-sheet template

An alternative reverse turn without these vulnerable α-protons, was investigated. Replacement of the α-protons with a vinyl side chain was viewed as a reasonable approach to the problem and attempts were made to synthesise ethyl 3,3-dimethyl-2-(3'-*tert*-butoxycarbonylamino-prop-1'-ynyl)-2-propenoate (**51**, Scheme 2.4).

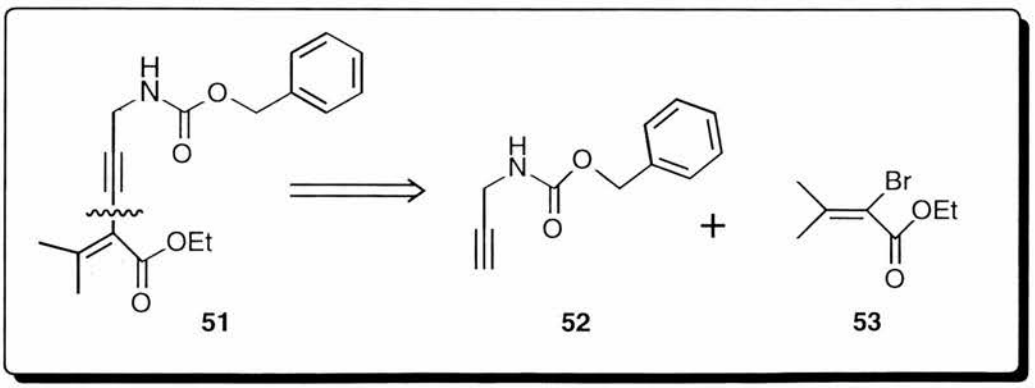

Scheme 2.4: *Disconnection of* ***51***

Retrosynthetic analysis of **51** indicated that it could be synthesised from *N*-Cbz-propargylamine (**52**) and 3,3-dimethylvinyl bromide (**53**) using Heck chemistry.[169-172] Schinzer and co-workers have already demonstrated that vinyl bromides containing vinylic and allylic silane groups (**54** and **55**) undergo a regiospecific Stephens-Castro coupling (a variation of the Heck reaction) with derivatives of terminal propargylic alcohols to form polyunsaturated silanes (**56** and **57**, Scheme 2.5).[173]

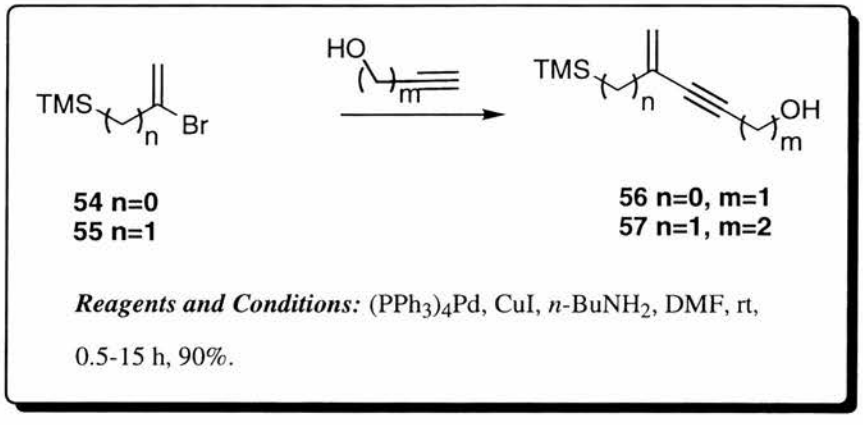

Scheme 2.5: *Stephens-Castro coupling of halogenated vinylic and allylic silanes with (homo)propargylic compounds*

Using a similar strategy, Myers *et al.* prepared functionalised enynes by a Pd(0)-catalysed cross-coupling of terminal acetylenes with ethyl (*Z*)-2,3-dibromopropenoate (**58**), forming ethyl (*Z*)-2-bromo-5-(trimethylsilyl)-2-penten-4-ynoate (**59**, Scheme 2.6).[174, 175]

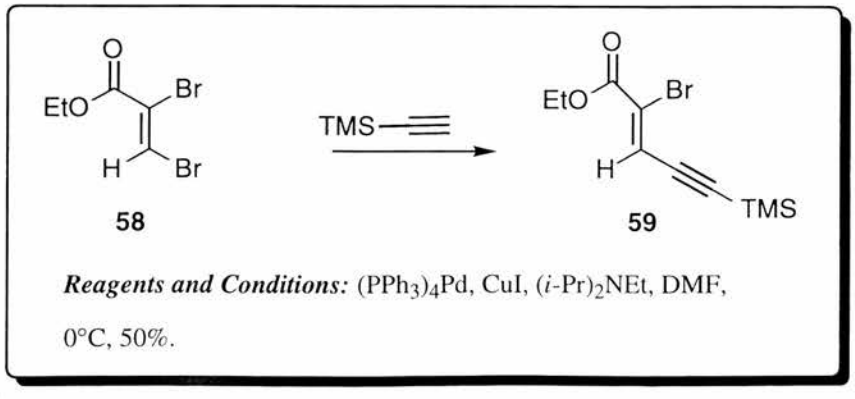

Scheme 2.6: *Stephens-Castro coupling of TMS acetylene with a dibromoester*

Indeed, Heck chemistry has been extensively used to prepare functionalised enynes from vinyl halides and terminal acetylenes. Using a similar conditions, reaction Scheme 2.7 was proposed for the synthesis of enyne **51**.

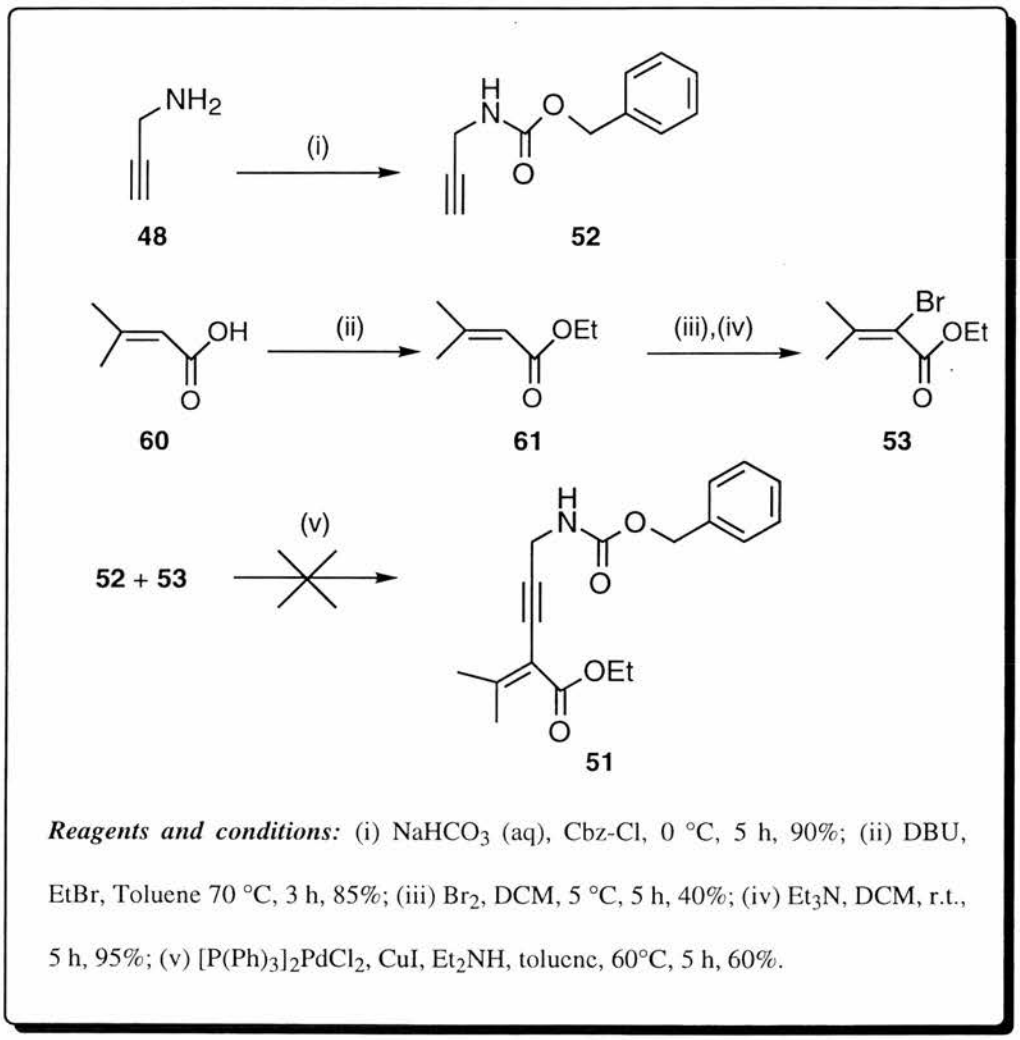

Reagents and conditions: (i) $NaHCO_3$ (aq), Cbz-Cl, 0 °C, 5 h, 90%; (ii) DBU, EtBr, Toluene 70 °C, 3 h, 85%; (iii) Br_2, DCM, 5 °C, 5 h, 40%; (iv) Et_3N, DCM, r.t., 5 h, 95%; (v) $[P(Ph)_3]_2PdCl_2$, CuI, Et_2NH, toluene, 60°C, 5 h, 60%.

Scheme 2.7: *Proposed synthetic scheme for the synthesis of **51***

Urethane **52** was prepared from propargylamine and benzylchloroformate to give, after aqueous work-up with dilute acid, the product in good yield (90%) as a colourless oil which readily solidified on standing.

Attempts to esterify vinylic acid **60** under standard acidic conditions in alcohol proved unsuccessful due to the sensitivity of the vinyl group. However, using the methodology of Ono *et al.*, ethyl ester **61** was synthesised from ethyl bromide and DBU in excellent yield (85%).[176] Normally the reaction of carboxylic acids with

alkyl halides in the presence of amine bases such as triethylamine is too slow to be useful; but the increased reactivity when using DBU can be attributed to the greater solubility in toluene of the DBU-carboxylic acid complex compared to the triethylamine complex, which arises because of the larger and more charge delocalised cation that is formed (Fig. 2.2).

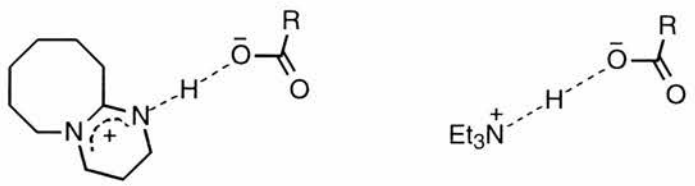

Figure 2.2: *Comparison of DBU and triethylamine carboxylic acid complexes*

Addition of bromine across the double bond of **61** and elimination of HBr from the dibromo intermediate with triethylamine gave vinyl bromide **53** as a colourless oil in 38% yield over two steps. Unfortunately, after trying a variety of reaction conditions and reagents, the desired product from the coupling reaction between urethane **52** and vinyl bromide **53** could not be isolated, and in most cases starting materials were recovered. Furthermore, when less hindered bases were tried (*e.g. n*-butyl amine), a Michael addition reaction took place between the base and the vinyl bromide **53** to yield a significant quantity of aziridine **62** after elimination of HBr from the α-bromo ester (Scheme 2.8). The presence of **62** was confirmed by ^{1}H and ^{13}C NMR spectroscopy.

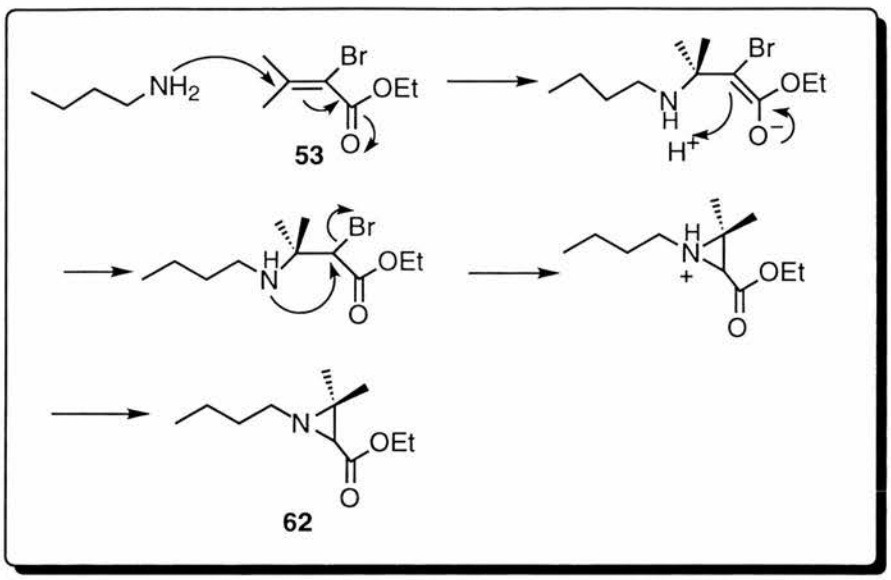

Scheme 2.8: *Mechanism of formation of aziridine* ***62***

This reaction is similar to the Gabriel-Cromwell reaction of primary amines with 2-bromo acrylates that was used by Filigheddu *et al.* to synthesise aziridine based β-sheet templates for parallel β-sheets (Scheme 2.9).[177]

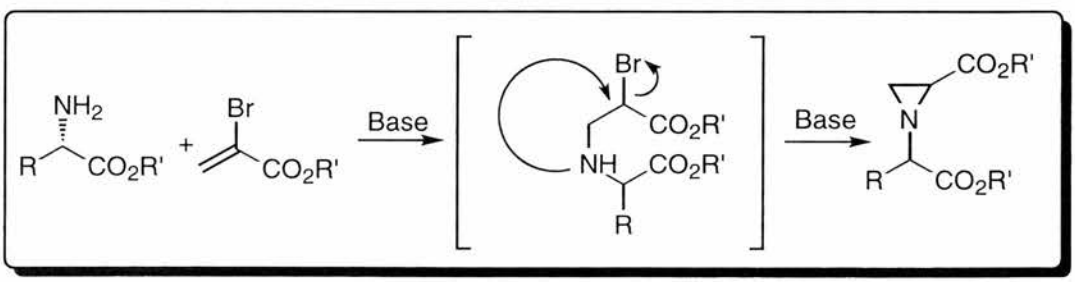

Scheme 2.9: *Gabriel-Cromwell reaction*

Variation of reaction temperature and the use of different secondary and tertiary amine bases, such as diisopropylamine and triethylamine, resulted only in the recovery of starting materials. However, analogous reactions, in which vinyl bromide **53** was exchanged for iodoaniline, were more successful resulting in the diamine **66** (Scheme 2.10).

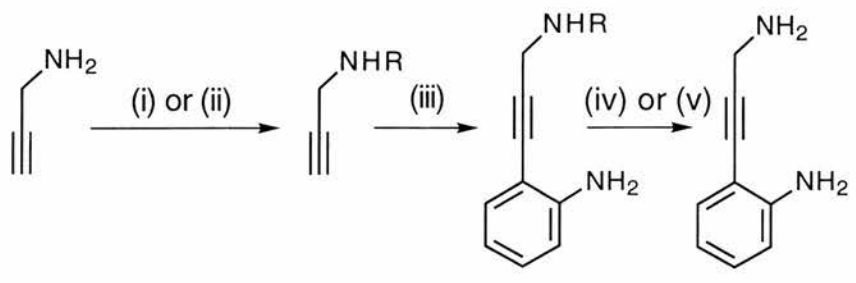

48 **52** R=Cbz, **63** R=Boc **64** R=Cbz, **65** R=Boc **66**

Reagents and conditions: (i) $NaHCO_3$(aq), $(BOC)_2O$, dioxane, water, 0 °C, 5 h, 79%; (ii) $NaHCO_3$ (aq), Cbz-Cl, 0 °C, 5 h, 80%; (iii) 2-iodoaniline, $(PPh_3)_4Pd$, CuI, Et_3N, DMF, 25 °C, 12 h, (**64**, 40%; **65**, 45%); (iv) BF_3.OEt, DMS, DCM, rt, 3 h, 78%; (v) TFA, EtOAc, -20 °C, 20 min, 99%.

Scheme 2.10: *Synthesis of 2-(3-amino-prop-1-ynyl)-phenylamine (**66**)*

The synthetic strategy was the same as for enyne **51**, but using iodoaniline instead of 3,3-dimethylvinyl bromide. At first, *N*-BOC protection of the iodoaniline nitrogen was considered necessary to prevent consumption of this substrate during the reductive elimination of HI in the Heck reaction [step (*iii*), Scheme 2.10], however, yields of the BOC-protected aniline were low using standard *N*-BOC protection methodology, so Heck coupling without any *N*-protection on iodoaniline was attempted. The reaction of terminal acetylenes **52** and **63** with unmasked iodoaniline gave phenylacetylenes **64** and **65** in reasonable yield (~40%) as pale yellow solids. Portions of phenylacetylenes **64** and **65** were then deprotected with BF_3.OEt/DMS[178] and TFA respectively to give **66** as the free diamine (78%) and TFA salt (99%) respectively [HRMS (free diamine): found M^+, 146.0838. $C_9H_{10}N_2$ requires 146.0844].

2.2 Incorporation of 2-(3'-amino-prop-1'-ynyl)-Phenylamine into Peptides

2.2.1 Introduction

Any peptide template if it is to be useful, must be accompanied by an efficient and reliable protocol for its incorporation into a peptide sequence (see Section 2.1.1). In other words, the reaction conditions and reagents used to remove template protecting groups and attach oligopeptides should not interfere with either the structure of the peptide or the template and ideally, the overall yield for the synthesis of the peptide analogue should be high (>80%).

For 2-(3'-amino-prop-1'-ynyl)-phenylamine to be used as a reverse turn inducer in an antiparallel β-sheet, further modification of the amino moiety of aniline was necessary. In its current form, diamine **66** would not be a viable template because if it were to be incorporated into an oligopeptide, the peptide chains on either side of the template would effectively be out of phase by one atom and the characteristic H-bonding pattern of the antiparallel β-sheet would not be formed. To circumvent this problem, the incorporation of a pseudo amino-acid moiety on the aniline nitrogen to give a tripeptide analogue was necessary (Fig. 2.3). In order to minimise any potential complications during synthesis, no functionality (*e.g.* a carboxylate or amino group) was included on the side-chain R of the pseudo amino acid residue.

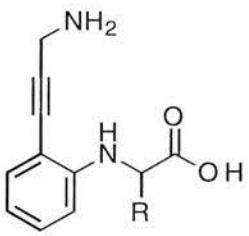

Figure 2.3: *General structure of a β-sheet stabilising tripeptide analogue*

2.2.2 *N*-Alkylation of 2-(3'-amino-prop-1'-ynyl)-phenylamine

Alkylation of the aniline amino group proved problematic due to delocalisation of the nitrogen lone pair into the aromatic ring. This reduced nucleophilicity meant that a reactive alkylating agent had to be found. Trial reactions on *N*-Cbz masked diamine

64, using methyl bromoacetate as the alkylating agent, gave very poor yields and in some cases the reaction conditions resulted in a partial saponification of the methyl ester [step (*i*), Scheme 2.11]. Alkylation under non-aqueous conditions also gave poor yields [step (*ii*), Scheme 2.11]. Mashraqui *et al.* had demonstrated that aryl thiols could be *S*-alkylated in good yield with alkyl bromides in aqueous micelles,[177] but unfortunately, nucleophilic *N*-substitution of **64** with alkyl halides in the presence of cetyltrimethylammonium bromide (CTAB) micelles under a variety of conditions yielded only starting materials [step (*iii*), Scheme 2.11].[179]

Lemaire's one-pot strategy of imine formation between an aniline and aldehyde, followed by catalytic reduction with palladium under a 50 bar atmosphere of H_2, was also considered.[180] However, this procedure offered no control over the stereochemistry of the product and the extreme reaction conditions would undoubtedly have resulted in complete hydrogenation of the triple bond.

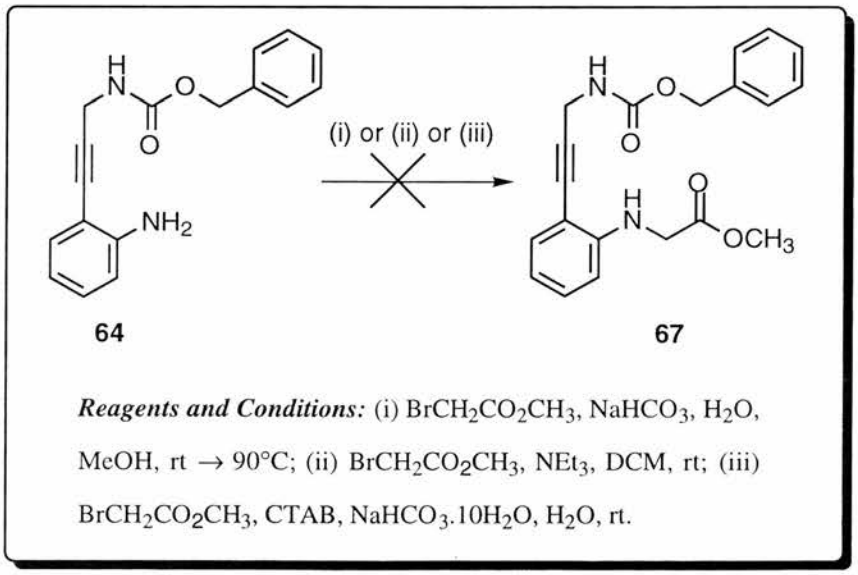

64 **67**

Reagents and Conditions: (i) $BrCH_2CO_2CH_3$, $NaHCO_3$, H_2O, MeOH, rt → 90°C; (ii) $BrCH_2CO_2CH_3$, NEt_3, DCM, rt; (iii) $BrCH_2CO_2CH_3$, CTAB, $NaHCO_3.10H_2O$, H_2O, rt.

Scheme 2.11: *Attempted N-alkylations of* ***64***

An alternative strategy involving intramolecular S_N2 displacement of bromide from bromo amide **68** (Scheme 2.12), followed by cleavage of the peptide bond in lactam **69** also proved unsuccessful. This was simply because the aniline nitrogen was held too far away from its target by the rigid acetylenic bond.

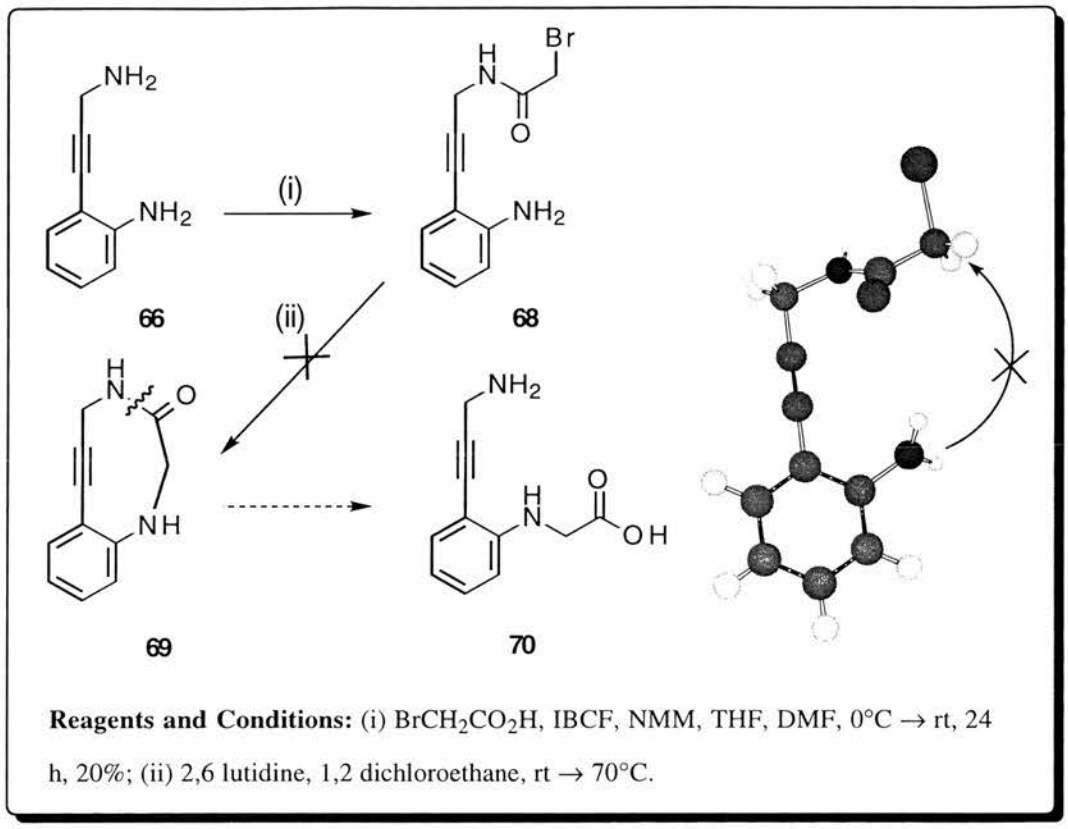

Reagents and Conditions: (i) $BrCH_2CO_2H$, IBCF, NMM, THF, DMF, 0°C → rt, 24 h, 20%; (ii) 2,6 lutidine, 1,2 dichloroethane, rt → 70°C.

Scheme 2.12: *Attempted alkylation of* ***66*** *by a cyclisation/lactam cleavage strategy and a 3D model of* ***68*** *prior to cyclisation*

In a report by Effenberger *et al.*, which studied the synthesis of *N*-substituted amino acids, the reactivity of various α-substituted ethyl propionates towards benzylamine in CH_2Cl_2 were compared (Scheme 2.13).[181] Several α-substituents were tested, ranging from halogens to the toluenesulfonyloxy group. The trifluoromethanesulfonyloxy group was found to be the most efficient leaving group with α-trifluoromethanesulfonyloxy propionate being converted quantitatively into the corresponding *N*-substituted amino acid in 93% yield after only 20 min. This high yield suggests that trifluoromethanesulfonates are a more effective alternative to bromides for the synthesis of *N*-substituted anilines.[182]

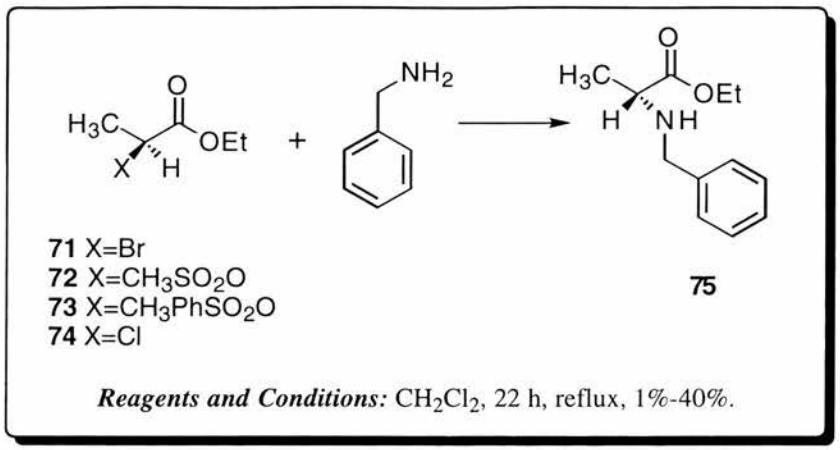

Scheme 2.13: *Preparation of N-substituted amino acids with activated α-hydroxycarboxylates **71-74***

Kogan *et al.* used triflates (**77**) derived from valine to prepare (-)-indolactam-V (**79**) (Scheme 2.14). This method proved very effective in alkylating the aniline nitrogen, giving good yields (>75%) of the *N*-alkylated product **78**.[183]

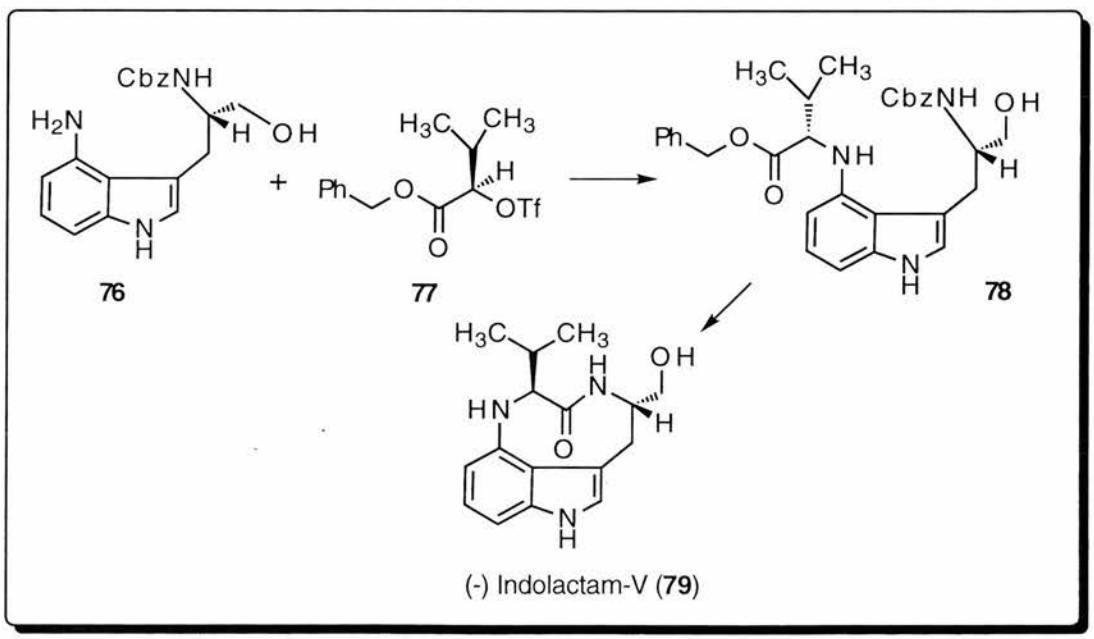

Scheme 2.14: *Preparation of (-)-indolactam-V*

Using a similar methodology, three phenylacetylene based tripeptide analogues, **89**, **90** and **91** were prepared in good overall yield (Scheme 2.15). A range of amino acid side-chains, from glycine to leucine were incorporated into the tripeptide analogues in order to test the reliability of the protocol. As well as varying the pseudo amino-acid side chain, the *N* and *C*-terminus protecting groups were varied as

well. As we have already demonstrated that *N*-Cbz groups can be removed from **64** with $BF_3.OEt_2$/DMS, it was reasonable to assume that *C*-terminus benzyl protecting groups could be removed under similar conditions. Tripeptide analogues **89** and **90**, protected at the *N* and *C*-termini with Cbz and benzyl groups respectively, would be removed globally with $BF_3.OEt_2$/DMS prior to incorporation into the host peptide. In the event that this strategy proved unsuccessful, a tripeptide analogue with an orthogonal methyl ester protecting group (**91**) would be prepared which, prior to removal of the Cbz group with $BF_3.OEt_2$/DMS, can be easily unmasked at the *C*-terminus by base saponification.

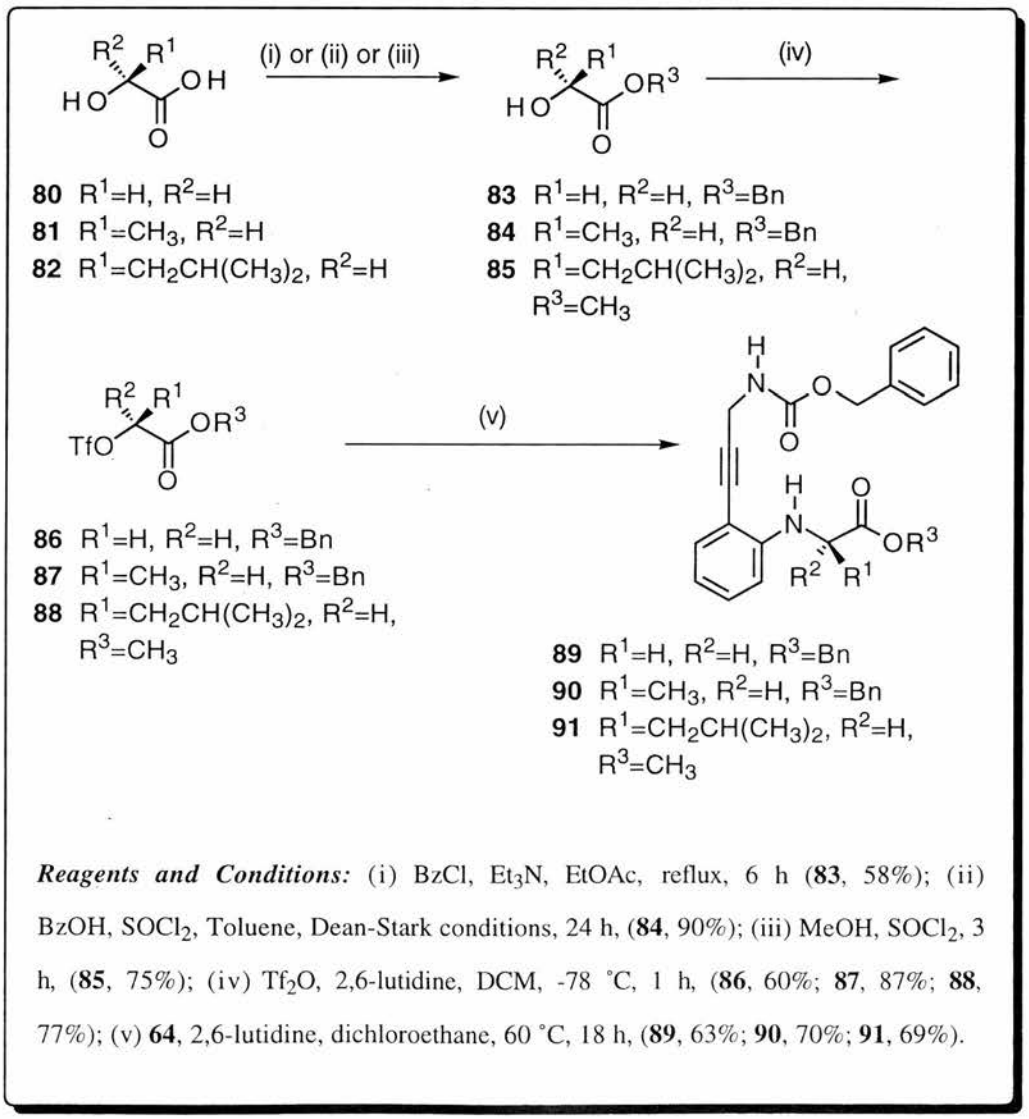

Scheme 2.15: *Synthesis of tripeptide analogues **89**, **90** and **91***

Tripeptide analogue **89** was prepared by benzylation of glycolic acid with benzyl chloride and triethylamine to give benzyl ester **83** in quantitative yield.[72] Reaction with trifluoromethane sulfonic anhydride (TFMSA) at -78 °C in DCM gave the corresponding triflate **86** which was reacted with phenylacetylene **64** without delay (due to its instability) to give tripeptide analogue **89** (HRMS: found M^+, 428.1727. $C_{26}H_{24}N_2O_4$ requires 428.1736) in 69% yield. In a similar manner, tripeptide analogue **90** (HRMS: found M^+, 442.1887. $C_{27}H_{26}N_2O_4$ requires 442.1892) was prepared from (2*S*)-lactic acid in 65% yield, but unlike **89**, the benzylation step [step (*ii*), Scheme 2.15] was carried out under Dean Stark conditions with thionyl chloride and benzyl alcohol to give the benzyl ester **84** in higher yield (90%) than before. Tripeptide analogue **91** (HRMS: found M^+, 408.2058. $C_{24}H_{28}O_4N_2$ requires 408.2049) was prepared from triflate **88** to yield a pale yellow oil in 70% yield. In all three cases, the alkylation step proceeds *via* an S_N2 mechanism, resulting in an inversion of configuration at the chiral centre.

2.2.3 Deprotection of *C* and *N*-termini of template

To our disappointment, attempted global deprotection of the Cbz and Bn groups on tripeptide analogues **89** and **90** using $BF_3.OEt_2$/DMS or HBr/AcOH resulted in reduction of the triple bond, as observed by ^{13}C NMR spectroscopy (Scheme 2.16). A similar problem was also encountered during *N*-Cbz deprotection of tripeptide analogue **91**. These results were surprising because, under similar conditions, removal of the *N*-Cbz group on phenylacetylene **59** presented no problems. It was decided that a change in both *N* and *C*-termini protecting groups was necessary to allow the exploration of a new range of unmasking conditions that would not affect functionality within the template.

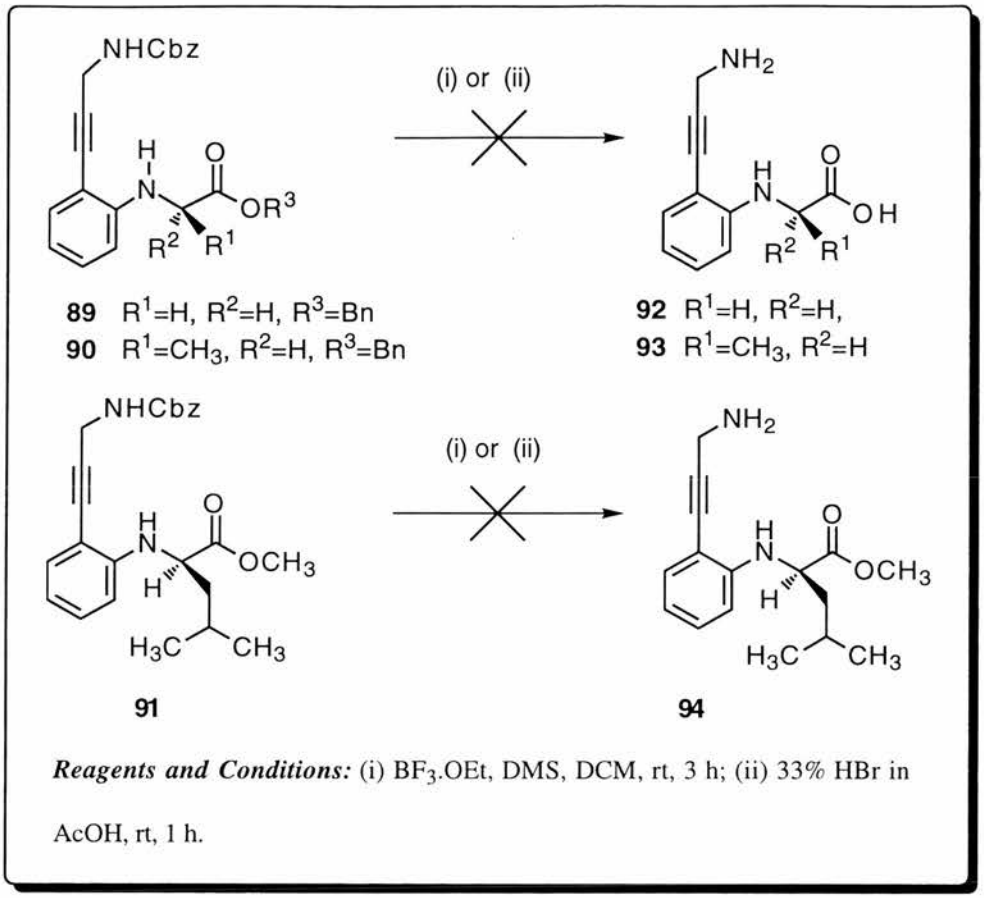

Scheme 2.16: *Attempted N and C-terminus deprotection of tripeptide analogues **89**, **90** and **91***

For the preparation of tripeptide analogues **105** to **109**, protected at their *N* and *C*-termini with BOC and methyl ester groups respectively (Scheme 2.17), it was necessary to prepare, under diazotisation conditions with aqueous sulphuric acid (0.5 mol dm^{-3}), α-hydroxy acids **82**, **95** and **96** from leucine, phenylalanine and α-aminobutyric acid respectively.

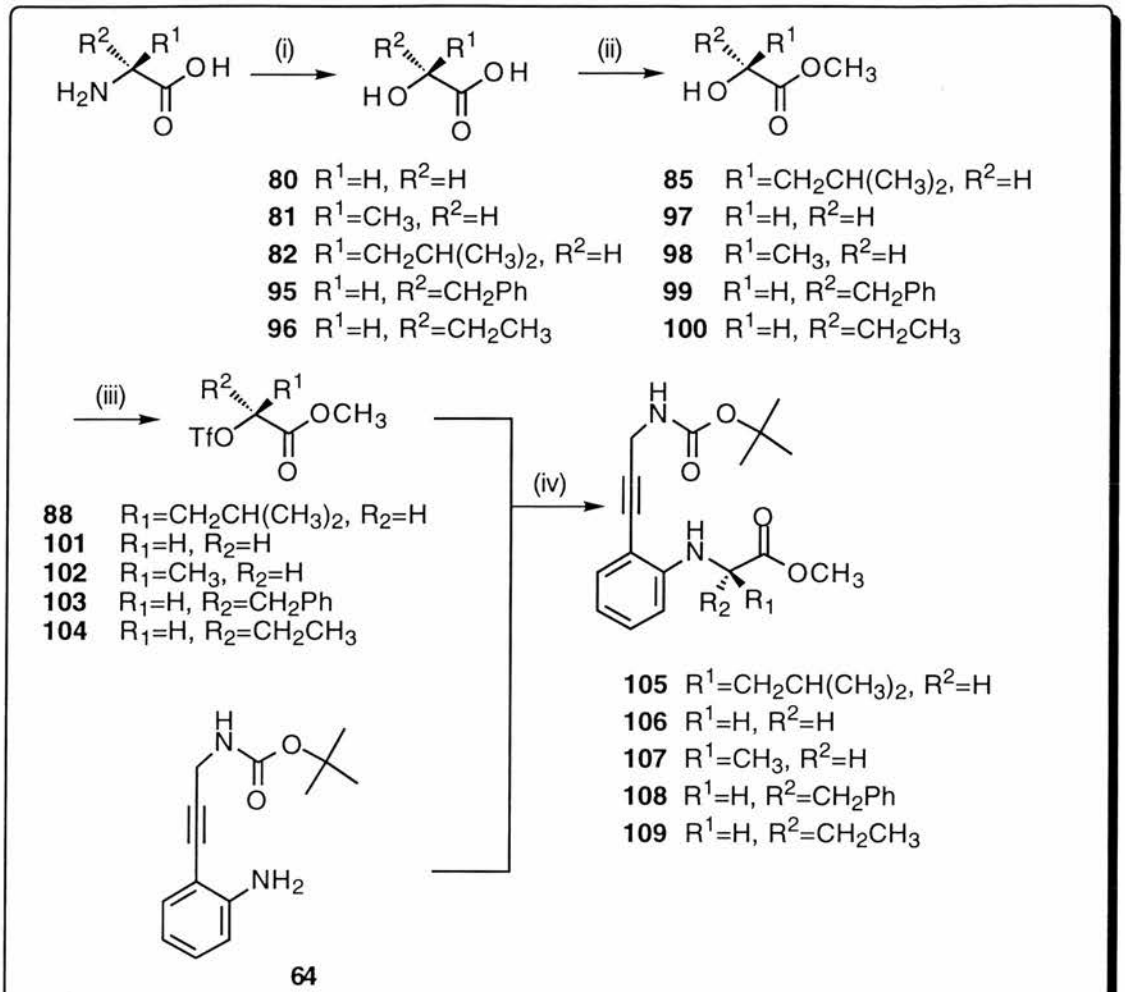

Reagents and Conditions: (i) $NaNO_2$, H_2SO_4 (0.5 mol dm^{-3}), 0 °C → rt, 12 h, (**82**, 75%; **95**, 54%; **96**, 66%); (ii) $SOCl_2$, MeOH, reflux, 2 h, (**85**, 84%; **97**, 63%; **98**, 37%; **99**, 82%; **100**, 57%); (iii) Tf_2O, 2,6-lutidine, DCM, -78 °C, 1 h, (**88**, 82%; **101**, 78%; **102**, 71%; **103**, 79%; **104**, 75%); (iv) 2,6-lutidine, dichloroethane, 60 °C, 18 h, (**105**, 84%; **106**, 77%; **107**, 81%; **108**, 62%; **109**, 77%).

Scheme 2.17: *Synthesis of tripeptide analogues **105** to **109***

These reactions proceed *via* the α-lactone with a double inversion of configuration, resulting in overall retention of stereochemistry in the product (Scheme 2.18).[183]

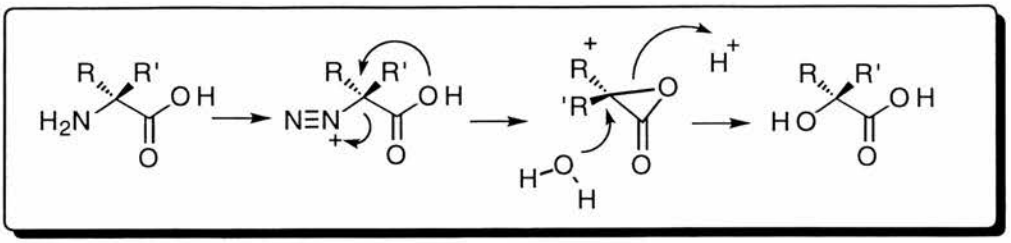

Scheme 2.18: *Diazotisation mechanism of amino acids*

α-Hydroxy acids **82, 95** and **96** were obtained in good yield (>50%) from (2*S*)-leucine, (2*S*)-α-aminobutyric acid and (2*S*)-phenylalanine respectively. However, there was concern that diazotisation of phenylalanine would produce tropic acid as a significant by-product. It has been shown by Yamada *et al.* that ethyl phenylalanate can be converted to tropic acid ethyl ester in the presence of sodium nitrite and acetic acid (Scheme 2.19) under conditions very similar to those described for the conversion of (2*S*)-leucine, (2*S*)-α-aminobutyric acid and (2*S*)-phenylalanine into their respective α-hydroxy acids[184, 185] In the diazonium intermediate **110**, reaction at C-3 with an acetate ion is accompanied by a concerted migration of the phenyl group from C-3 to C-2, displacing N_2 to give *O*-acetyl **111**. Fortunately, there was no evidence of tropic acid formation with phenylalanine, presumably because α-lactone formation is kinetically more favourable than migration of the phenyl group (Scheme 2.19).

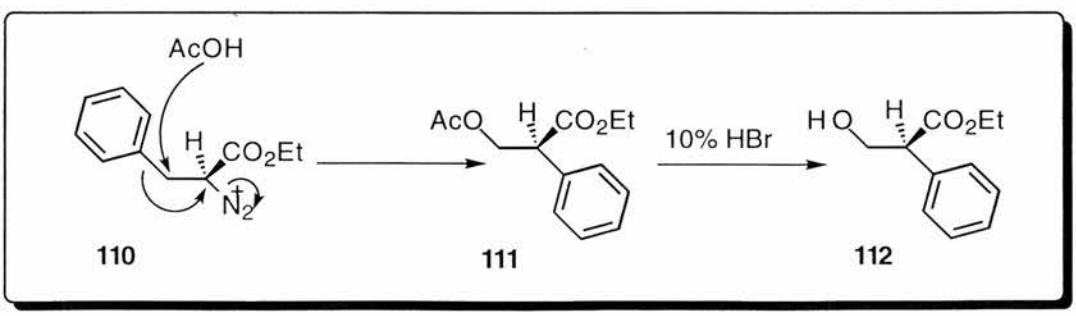

Scheme 2.19: *Tropic acid, ethyl ester formation from ethyl phenylalaninate*

During the preparation of α-hydroxy esters **85, 97, 98, 99** and **100** [step (*ii*), Scheme 2.17], it is essential to neutralise any strong acids present before

concentration under reduced pressure or distillation, otherwise condensation by ester interchange could arise, resulting in the formation of alcohol and long chain polymers (Scheme 2.20). To avoid this, $NaHCO_3$ was used to quench the reaction prior to further work-up.

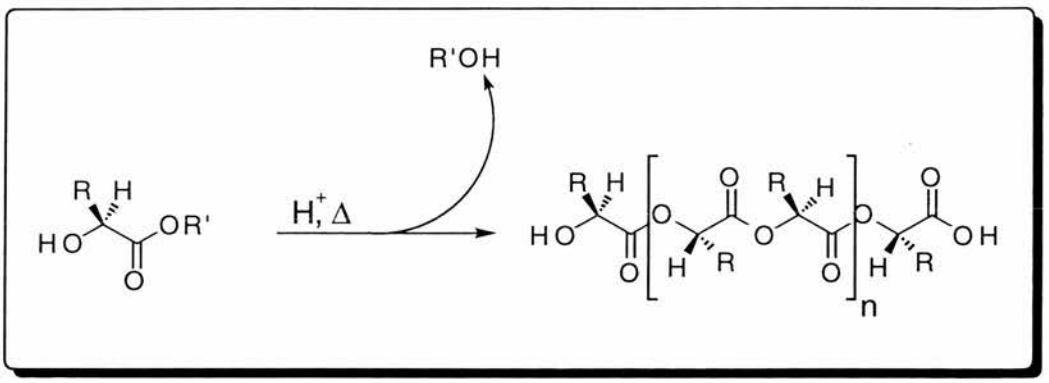

Scheme 2.20: *Polymerisation of α-hydroxy acids under acidic conditions*

All the α-hydroxy methyl esters prepared were volatile, except methyl 2-hydroxy-3-phenyl propanoate (**99**) which was obtained as a white solid in 79% yield. Preparation of the volatile esters, **85**, **97**, **98** and **100** involved refluxing α-hydroxy acids with thionyl chloride in methanol for several hours, neutralisation of the reaction mixture ($NaHCO_3$) and distillation of the suspension under reduced pressure to yield the methyl esters as colourless oils in 37% - 84% yield. Conversion of the α-hydroxy esters to triflates was effected with trifluoromethane sulfonic anhydride and 2,6-lutidine in dichloromethane at -78°C to give the triflates **88** and **101-104** in excellent yield after chromatographic purification (>70%). Each triflate was stirred with phenylacetylene **65** in 1,2-dichloroethane in the presence of 2,6-lutidine at ~70 °C for 24 h to give tripeptide analogues **105** - **109** in good yield (62% - 84%).[183]

Test reactions on phenylacetylene **65** showed that the BOC protecting group could be successfully removed from this phenyl acetylenic precursor using trifluoroacetic acid (TFA) at -20 °C, giving the free diamine **66** as the trifluoroacetate salt (Scheme 2.10). However, attempts to remove the BOC group of **105** with TFA were unsuccessful and resulted in the addition of water across the triple bond, forming a

ketone - a result supported by ^{13}C NMR spectroscopy with a peak at 199.97 ppm (**113**, Scheme 2.21). This suggests that the alkyl group has an electronic effect on the triple bond, feeding electrons into the triple bond *via* the nitrogen and making it more susceptible to protonation by acid, forming a highly conjugated allene intermediate which is subsequently attacked by water (Scheme 2.21). A range of reaction temperatures, from -78 °C to rt, and reaction times, from 30 seconds to 2 h, were tested but none had any noticable effect on circumventing the problem of ketone formation.

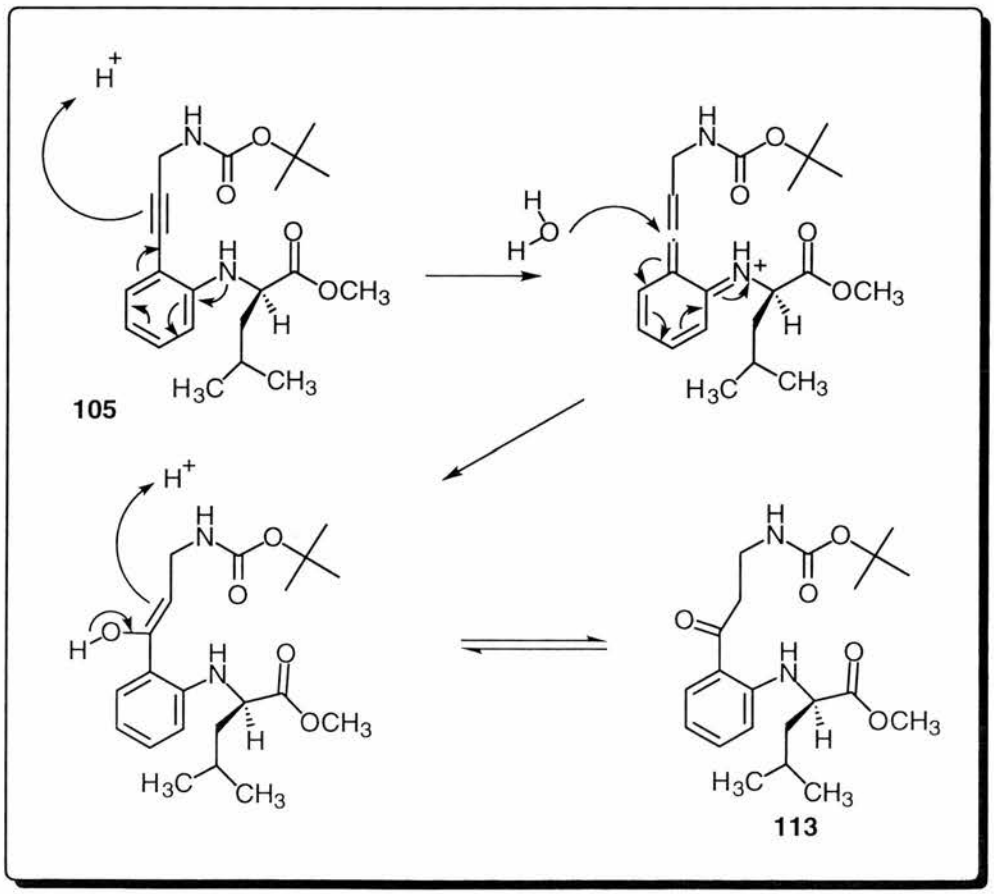

Scheme 2.21: *Formation of ketone during BOC deprotection using TFA*

Other, less-acidic conditions were considered. BOC-group removal under mild conditions in the presence of an acid-labile thioamide moiety had been successfully acheived by Safford *et al.* and Schutkowski *et al.*,[186] however in both cases rather toxic tin chlorides were used as the principal unmasking reagent.

Eventually, dry HCl gas in ethyl acetate was found to remove the BOC group on **105** without destruction of the triple bond, furnishing the dihydrochloride salt (HRMS: found M^+, 274.1688. $C_{16}H_{22}N_2O_2$, requires 274.1681) in excellent yield (>99%) as a white solid ready for further elaboration at the *N*-terminus (Scheme 2.23, Section 2.3.2). This procedure was also successfully applied to tripeptide analogues **106**, **107**, **108** and **109** (yield >99% in all cases) which suggests that HCl, being stronger than TFA, readily protonates the aniline nitrogen, preventing the reaction sequence that leads to ketone formation (Scheme 2.21).

C-Terminal deprotection of tripeptide analogues **105-109** presented few problems and was acheived in good yield under standard saponification conditions (1 mol dm^{-3} LiOH, MeOH) to yield the corresponding carboxylic acids as pale yellow foams after workup with aqueous mineral acid. The deprotection of three of these tripeptide analogues, **107**, **108** and **109**, is shown in Schemes 2.23 (Section 2.4.2), 2.32 (Section 2.5.2) and 2.33 (Section 2.5.2).

Thus, a stable acetylene-based reverse turn template had been synthesised and an efficient, reliable protocol for its *C* and *N*-deprotection has been established. In the folowing chapters, the incorporation of these tripeptide analogues into three, progressively larger, cyclic β-sheet models is discussed, along with details of strucutural analyses.

2.3 The Design and Structural Evaluation of β-sheet Models

2.3.1 Introduction

The flexibility of small peptides means that their conformational freedom must be limited if they are to be effective secondary structure models. Hartzoulakis *et al.* demonstrated that, by itself, a rigid or semi-rigid template may not be sufficient to stabilise a folded hairpin structure in short peptides, in the absence of tertiary protein interactions.[167] The occurance of small cyclic β-sheet peptides in nature (*e.g.* the decapeptide antibiotic gramacidin S[101] or the α-amylase inhibitor, tendamistat[187]) suggest that cyclisation may be the additional constraint required to stabilise short oligopeptides in a β-sheet conformation.[188, 189] Furthermore, there are some notable examples of artificial β-sheet models which, along with the sheet stabilising template, are constrained globally by cyclisation. With this in mind, three antiparallel β-sheet models were designed, all cyclic, and all stabilised by two phenylacetylene-based turn inducers (Fig. 2.4).

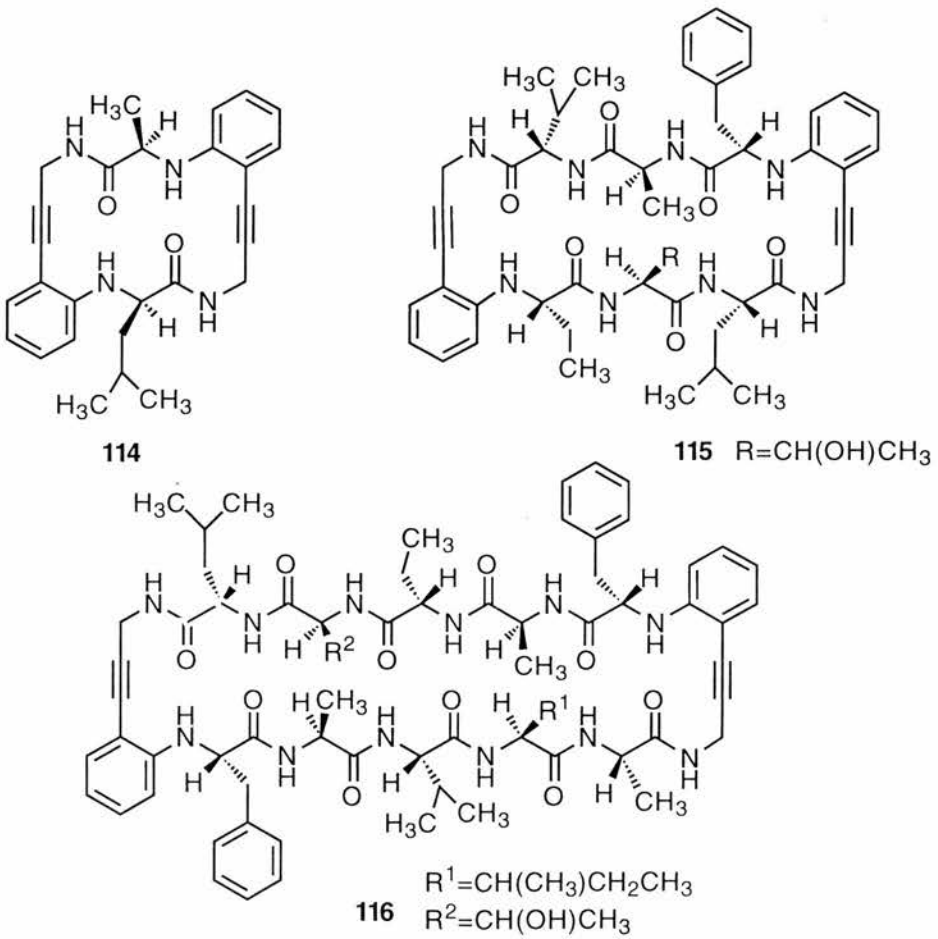

Figure 2.4: *β-Sheet targets*

2.3.2 Structural analysis of β-sheets

2.3.2.1 NMR

Nuclear magnetic resonance (NMR) spectroscopy can provide detailed information about molecular conformations and has been applied extensively to the determination of protein and peptide secondary structures. Nuclear Overhauser effect spectroscopy (NOESY) experiments are particularly useful in analysing β-sheet structures. The most useful pieces of information can be derived form the presence of the long range NOEs; $d_{\alpha N}(i,j)$, $d_{NN}(i,j)$ and $d_{\alpha\alpha}(i,j)$ and $d_{\alpha N}(i, i+1)$ (Fig. 2.5), which are always strongly supportive of β-sheet structure.[52, 128, 137-140, 190]

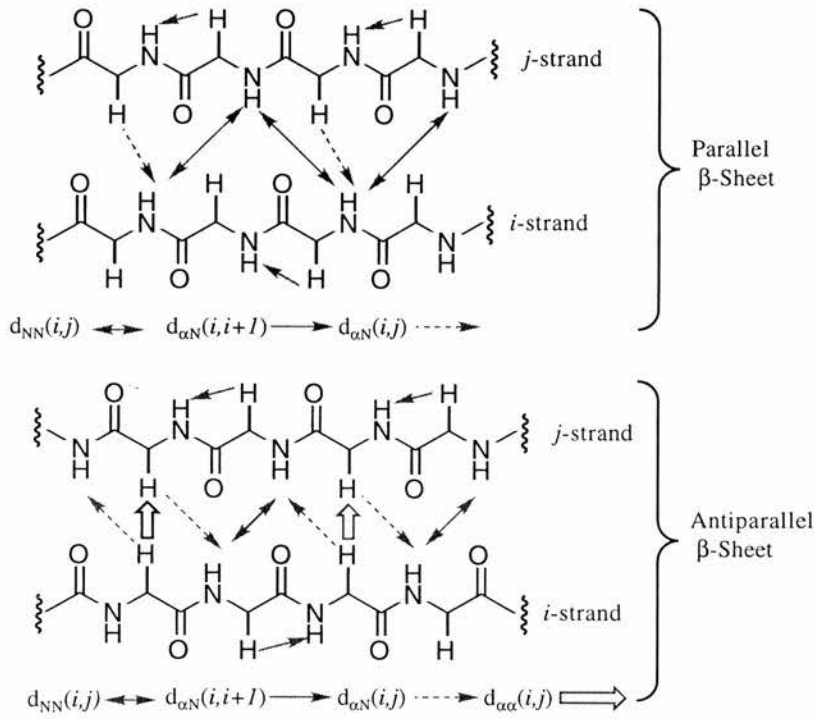

Figure 2.5: *Schematic representation of an antiparallel and parallel β-sheet showing the intra- and inter-strand NOEs*

NOEs between protons separated by distances ranging from less than 2 Å to more than 4 Å can be detected. Since the magnitude of NOEs decrease as a function of the sixth power of internuclear separation, proteins separated by 4 Å produce very weak NOEs that are not always detectable. Different β-sheet structures give characteristic

patterns of NOEs. Figure 2.5 illustrates typical interresidue NOEs involving the main chains of parallel and antiparallel β-sheets. The patterns of long range NOEs involving the α-H and NH protons of adjacent peptide strands can establish whether residues are in an antiparallel or parallel β-sheet structure. Interstrand NOEs involving amino acid side chains can provide additional evidence for β-sheet formation, while strong NOEs between the α-H and NH protons of adjacent residues are consistent with a β-strand conformation. The latter NOEs must be interpreted with caution, however, since unstructured peptides also give NOEs between sequential α-H and NH protons.[128]

NOEs arise between magnetic nuclei that can interact through space [*i.e.* in close proximity (≤ 5 Å)] and manifest themselves as an increase or decrease in the signal intensity of nuclei in close proximity to a nucleus irradiated at its resonance frequency. The theory behind the nuclear overhauser effect is summarised in Figure 2.6 below. Two nuclei A and X relaxing each other, but not coupling, interact to set up four populated energy levels. Transitions W_A lead to the lines associated with the A nucleus and transitions W_X lead to lines associated the nucleus X. If a sample is irradiated at the resonance frequency of the X nucleus, population of energy levels 1 and 2 grow by an amount +Δ and 3 and 4 decrease by the same amount.[191]

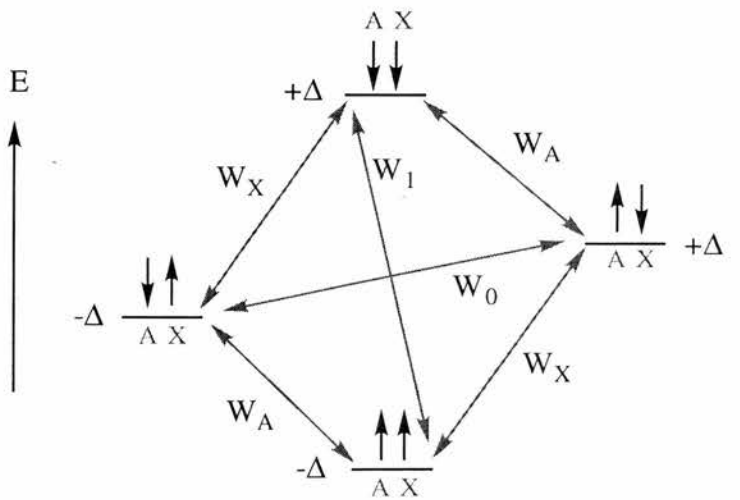

Figure 2.6: *Evolution of the Nuclear Overhauser Effect*

The relaxation pathway W_1 is stimulated by the tumbling of molecules with a molecular weight in the region of 100-400 Daltons, within the magnetic field, increasing the population of energy level 4 at the expense of energy level one. The overall effect is to decrease the population of energy levels 1 and 3 relative to 2 and 4, effectively increasing the difference in population between energy levels 2 and 4, and between 1 and 3. Also, because the intensity of the A signal is related to the difference in populations of these 2 groups of levels, the signal is increased in intensity (positive NOE). Molecules with a molecular weight in the region ≥1000 Daltons tumble more slowly and the W_0 relaxation pathway is stimulated, increasing the population of energy levels 1 and 3 relative to 2 and 4 and resulting in a reduced signal (negative NOE). Molecules between these two molecular weights will show very weak or non-existent NOEs. This may account for the weak NOEs observed in **115** and why some expected NOEs are not observed at all.[191]

All NMR signals in the cyclic peptide analogues **114** and **115** were assigned using correlated spectroscopy (COSY) and heteronuclear single quantum correlation (HSQC) experiments. NOESY experiments were then used to reveal which protons were in close proximity to each other to create a picture of the solution conformation. In the NOESY experiment, the indroduction of a delay time in the pulse sequence prior to collecting the FID ensures that COSY peaks do not complicate the spectum; the result is that only signals between nuclei interacting through space are observed.

Like NOE experiments, the chemical shift of NH protons in a peptide can give useful information about the hydrogen-bonding pattern, and therefore conformation, of a system. Protons that are intramolecularly H-bonded to a carbonyl in a neighbouring peptide strand or H-bonded to a polar solvent appear downfield of protons that are not. In non-H-bonding solvents like $CDCl_3$, hydrogen-bonded amide protons appear at *c.a.* 8 ppm while non hydrogen-bonded amide protons resonate at approximately 6 ppm. In strongly H-bonding solvents (*e.g.* d_6-DMSO or D_2O) this pronounced difference is not usually observed.

^{1}H NMR coupling constants can provide information about the conformation of the peptide main chain. In particular, vicinal coupling constants between NH and α-H (^3J) can supply information about the dihedral angle between these protons and hence the ϕ angle of the peptide residue. Vicinal coupling constants greater than 7 Hz, whilst not proof of β-sheet structure, are consistent with this conformation, while coupling constants less than 6 Hz are generally only found in α-helical structures.

2.3.2.2 X-ray crystallography

X-ray crystallography is one of the most powerful techniques for studying molecular structure and can provide a definitve answer to the conformation and structure of many molecules including peptides and proteins. Although attempts to make suitable crystals of β-sheets **114**, **115** and **116** for structural analysis were unsuccessful, it was possible to generate good quality crystals of phenyl acetylene **65** and the associated tripeptide analogue **109**. Unfortunately, analysis of their X-ray crystal structures revealed that neither molecule had a propensity to adopt a β-turn conformation (*i.e.* no hydrogen bonding was observed between the anilino NH and the carbonyl of the urethane, Fig. 2.7). Although disappointing, it was not a serious concern as X-ray crystallography is unable to identify the range of conformations that a molecule might adopt in solution. Furthermore, crystal packing forces can often adversely affect the conformation of a molecule in the solid state.

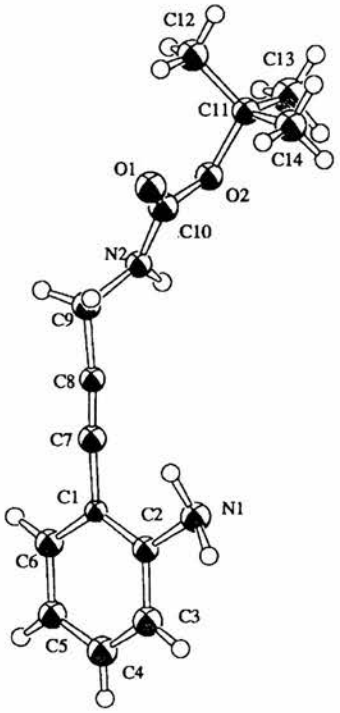

(*a*) *2-(3'-tert-Butoxycarbonylamino-prop-1'-ynyl)-phenylamine*

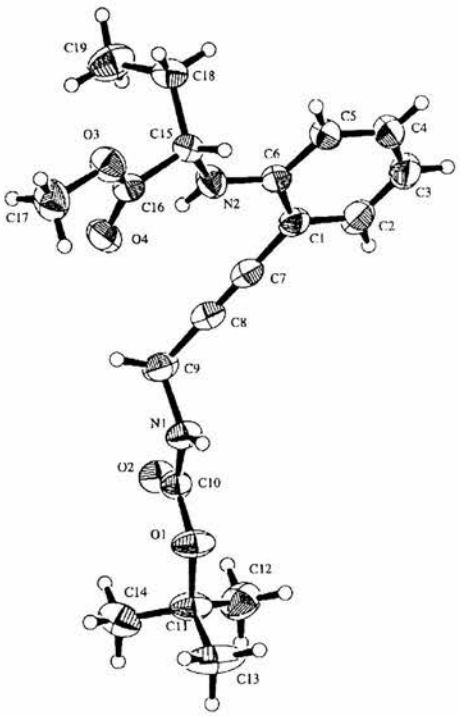

(*b*) *Methyl (2S)-2-[2'-(3''-tert-butoxycarbonylamino-prop-1''-ynyl)-phenylamino]-butanoate*

Figure 2.7: *X-ray structures of (a)* ***65*** *and (b)* ***109***

2.3.2.3 Circular Dichroism

Circular dichroism (CD) spectroscopy is the differential absorption of circularly polarised radiation by a non-racemic sample. In peptides, it is the interaction between adjacent amide groups during light adsorption which accounts for most of the CD bands observed. The key structural elements that are responsible for the wavelength and intensity of these bands are the relative orientations of the amide groups within the peptide. When a peptide adopts a well defined secondary structure, by forming intramolecular H-bonds, absorption of radiation by the oriented chromophores is enhanced. This leads to the appearance of more intense CD bands at characteristic wavelengths. CD spectroscopy has been used extensively to study peptide conformations in aqueous solution. Helices and β-sheets each have a distinct spectroscopic signature; α-helices exhibit maxima at 191 nm and minima at 208 and 222 nm while β-sheets exhibit maxima at 195 nm and minima at 197 nm. Unfortunately, CD spectroscopy is not compatible for our studies because β-sheet models **114**, **115** and **116** are soluble only in organic solvents like $CHCl_3$ and DMSO which absorb UV light near these wavelengths. Also, the chromophores in the phenylacetylene template can generate unpredictable and misleading contributions in the CD spectrum.[52]

2.4 Synthesis and structural studies of hexapeptide analogue 114

2.4.1 Introduction

The smallest possible cyclic β-sheet model incorporating two 2-(3'-aminopropynyl)-aniline templates, is the cyclic hexapeptide analogue **114**. This system was chosen as the initial synthetic target in order to evaluate whether such a small system could adopt a stable β-sheet conformation. It also offered the opportunity to develop the synthetic methodology required for the larger cyclic decapeptide analogue **115** and cyclic tetradecapeptide analogue **116**. The choice of amino acids for all three systems was governed by three rules; the amino acids should have hydrophobic side chains (β-sheets are commonly found in the hydrophobic interiors of proteins and contain hydrophobic residues like leucine and valine); there should be a good variation of amino acids to allow separation of key NMR signals in the NMR spectrum (this simplifying NOE assignment and structural determination) and finally, the residues should be stable to the reaction conditions used for assembly of the β-sheet models (*i.e.* no acid or base sensitive side-chains).

2.4.2 Synthesis of hexapeptide analogue 114

The disconnection detailed in Scheme 2.22 shows that **114** can be readily prepared from two tripeptide analogues *via* a peptide coupling and cyclisation reaction.

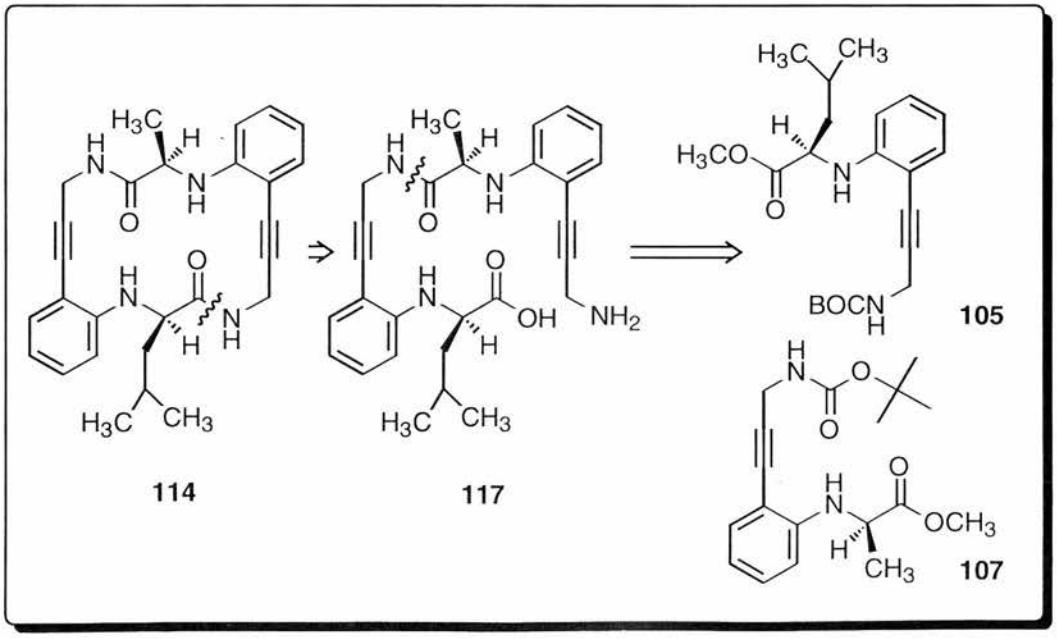

Scheme 2.22: *Disconnection of hexapeptide analogue **114***

Tripeptide analogue **107** was umasked at the *C*-terminus with aqueous LiOH (1 mol dm^{-3}) to yield carboxylic acid **119** (HRMS: found: M^+, 318.1580. $C_{17}H_{22}N_2O_4$ requires 318.1588) in 90% yield and **105** was deprotected at the *N*-terminus with dry HCl gas in ethyl acetate to yield dihydrochloride salt **118** (HRMS: found: M^+, 274.1688. $C_{16}H_{22}N_2O_2$ requires 274.1681) in 99% yield as a white solid. Both compounds were judged to be pure (>95%) by ^{13}C NMR (Scheme 2.23).

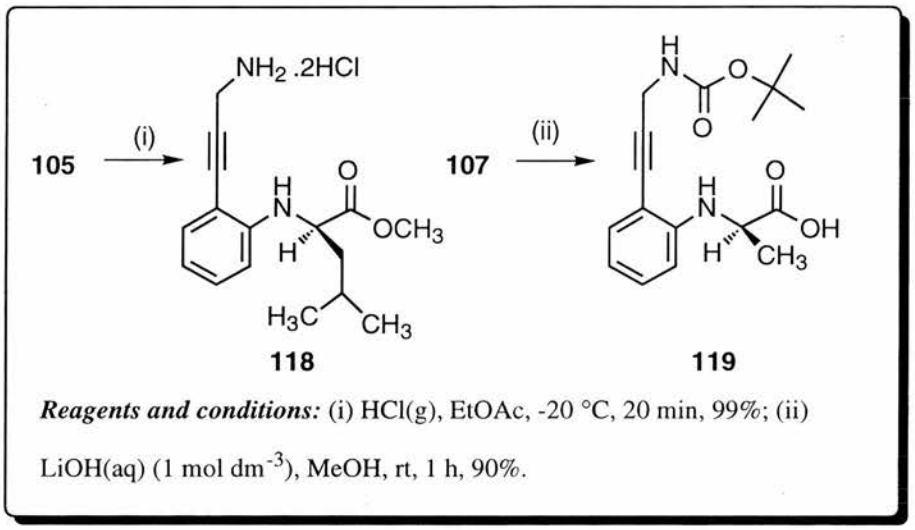

Reagents and conditions: (i) HCl(g), EtOAc, -20 °C, 20 min, 99%; (ii) LiOH(aq) (1 mol dm^{-3}), MeOH, rt, 1 h, 90%.

Scheme 2.23: *Synthesis of tripeptide analogues **118** and **119***

Standard mixed anhydride conditions (IBCF, NMM and DMF/THF) were initially used for the coupling of carboxylic acid **119** with amine dihydrochloride **118**. The reaction was high yielding but the ^{13}C NMR spectrum was more complicated than expected. A similar result was observed when the coupling reagent, TBTU, was used with a protocol reported by Dourtoglou and Gross for HBTU couplings.[152] Not all the signals could be accounted for by conformational effects, which suggested that diastereoisomers were present. This was also borne out by TLC which indicated the crude product contained two compounds with very similar R_f values. As the chiral integrity of tripeptide analogues **105** and **107** was not in doubt (see Section 2.3.2.2) two possibilities were considered to be the most likely; racemisation was taking place during the coupling reaction between **118** and **119**, or tripeptide analogue **107** was racemising during saponification. The latter possibility was discounted when EDCI

was found to give acyclic hexapeptide analogue **120** (HRMS: found $[M + H]^+$, 575.3225. $C_{33}H_{43}N_4O_5$ requires 575.3233) in moderate yield (52%) with no epimerisation as judged by ^1H and ^{13}C NMR spectroscopy (Scheme 2.24).

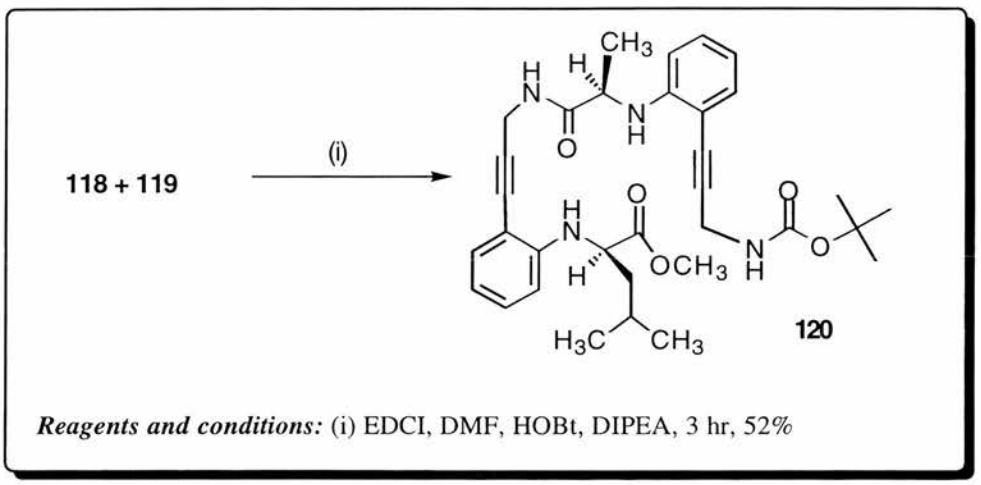

Scheme 2.24: *Synthesis of hexapeptide analogue **120***

Initially, we attempted to cyclise hexapeptide analogue **120** by removing the BOC group with dry HCl gas and stirring the resulting trihydrochloride salt (**121**) under basic conditions in DMF (Scheme 2.25).

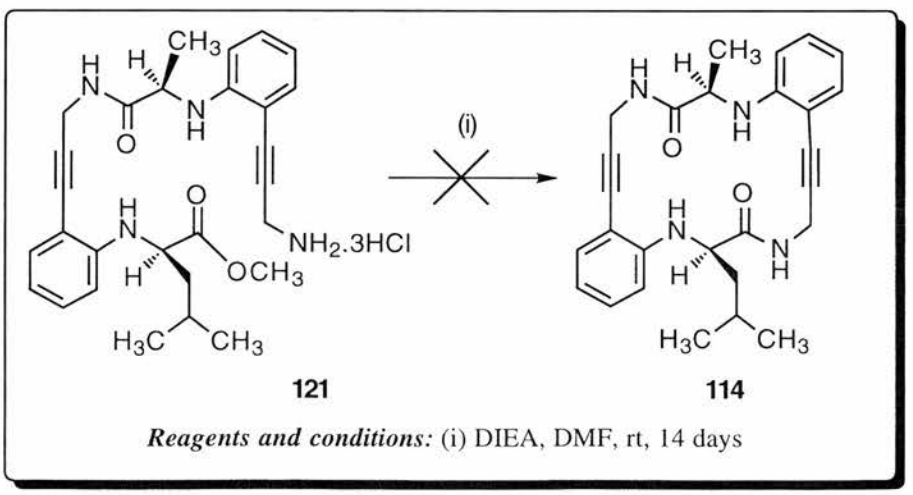

Scheme 2.25: *Attempted synthesis of **114** from trihydrochloride **121***

Adrián *et al.* had demonstrated that polyazamacrocycles can be efficiently cyclised (~60%) if β-turn pre-formation is present in the acylic precursors;[192] therefore it was hoped that any degree of β-sheet preformation in **121**, induced by the

phenylacetylene turn templates, would help position the ester carbonyl in close proximity to the free primary amine, resulting in the rapid elimination of MeOH and the formation of the cyclic hexapeptide analogue **114** *via* a second order tetrahedral mechanism ($A_N + D_N$) (Fig. 2.8).

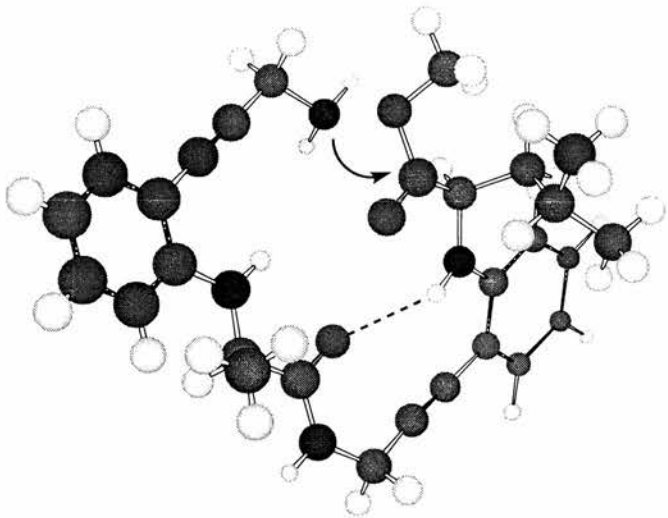

Figure 2.8: *3D representation of acyclic hexapeptide analogue **121** in a suitable conformation for cyclisation by an $A_N + D_N$ mechanism*

Unfortunately this strategy was unsuccessful, and subsequent NMR analysis of acyclic hexapeptide analogue **120**, in $CDCl_3$, revealed no significant downfield shift of the anilino NHs compared to those of tripeptide analogues **105** and **107**, suggesting that **120** does not adopt a β-sheet conformation - in a non-polar environment at least.

Instead, peptide analogue **120** was deprotected at both the *C* and *N*-termini, with aqueous LiOH and HCl gas respectively, and attempts were made to cyclise the deprotected hexapeptide analogue with a range of carbonyl activating agents. Initially, saponification of **120** resulted in partial racemisation of the peptide analogue, as judged by ^{13}C NMR spectroscopy - methyl esters are relatively stable protecting groups and the conditions required for their removal can be very vigorous, increasing the likelihood of unwanted side reactions. The problem was compounded by the fact that *C*-terminus deprotection of hexapeptide analogue **120** proceeded more slowly than expected. This was probably a consequence of the steric bulk of the

leucine side chain next to the methyl ester hindering access of hydroxide ions to the ester carbonyl, prolonging the reaction time and with it the risk of racemisation.

Racemisation during saponification arises because a competing reaction takes place whereby the proton α to the ester carbonyl is removed by base to form a planar enolate anion intermediate which can be re-protonated on either side of this sp^2 centre to give a racemic mixture (Scheme 2.26).

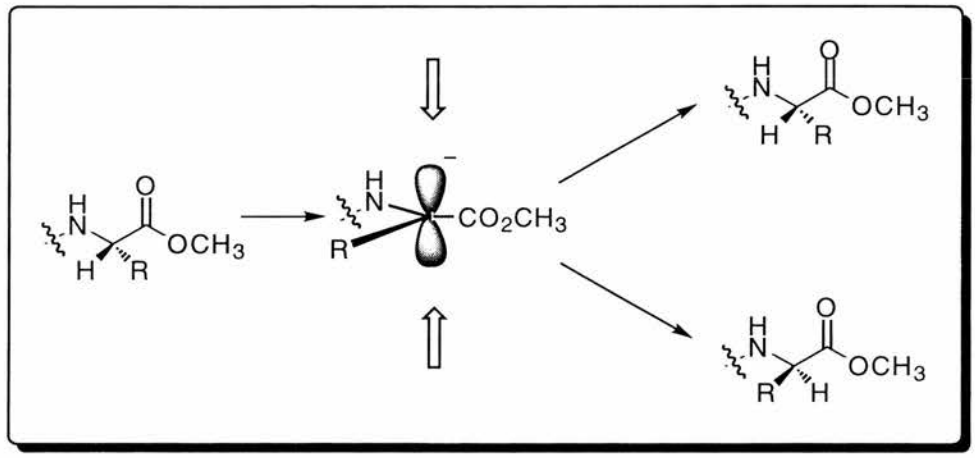

Scheme 2.26: *Mechanism of racemisation during saponification*

Alternative, less basic, reagents for the deprotection of ester functional groups were investigated. Trimethylsilyl iodide (TMSI) was particularly appealing because of the mild reaction conditions and simple experimental protocol. Furthermore, this reagent is an efficient urethane deblocking agent which means that global deprotection of the hexapeptide analogue, prior to cyclisation, should be possible.[193-198] Unfortuately, test reactions with TMSI on tripeptide analogue **105** removed only the urethane protecting group even after heating to 80°C (Scheme 2.27).

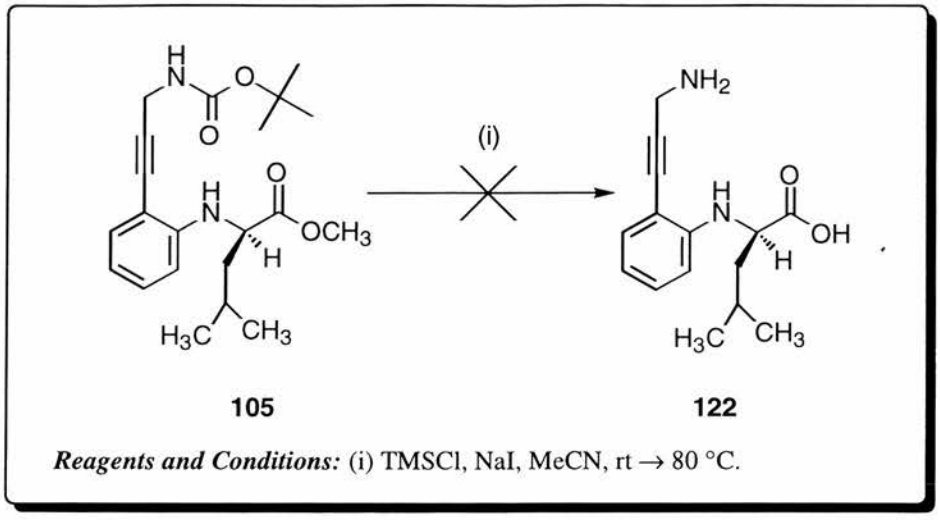

Reagents and Conditions: (i) TMSCl, NaI, MeCN, rt → 80 °C.

Scheme 2.27: *Attempted global deprotection of **105** with TMSI*

It was decided that saponification of acyclic hexapeptide analogue **120** under closely monitored conditions was probably the most effective method of ester removal. It was found that the methyl ester could be completely removed after 1.5 days with aqueous LiOH (1 mol dm^{-3}) in methanol at room temperature to give, after aqueous work-up, the free acid with the minimum of racemisation as judged by ^{13}C NMR spectroscopy. This compound was then deprotected at the *N*-terminus with dry HCl in ethyl acetate to give the fully deprotected hexapeptide analogue **117** (HRMS: found $[M + Na]^+$, 483.2381. $C_{27}H_{34}N_3O_3$ requires 483.2372) as the trihydrochloride salt in 98% yield (Scheme 2.28) and was judged to be pure (>95%) by ^{13}C NMR spectroscopy.

Cyclisation of hexapeptide analogue **117** to give cyclic hexapeptide analogue **114** proved to be problematic. A number of trial cyclisations were carried out on hexapeptide analogue **117** using a range of coupling reagents. Both EDCI[161] and BOP-Cl[199, 200] proved ineffective, giving no cyclic product as judged by mass spectrometry, but diphenylphosphoryl azide (DPPA), first used by Yamada *et al.* for peptide coupling, gave the desired cyclic product **114** (HRMS: found $[M + H]^+$ 443.2447. $C_{27}H_{31}N_4O_2$, requires 443.2451) in 28% yield after chromatographic

purification (Scheme 2.28) and was found to be pure by analytical HPLC (Scheme 2.28)[160, 201]

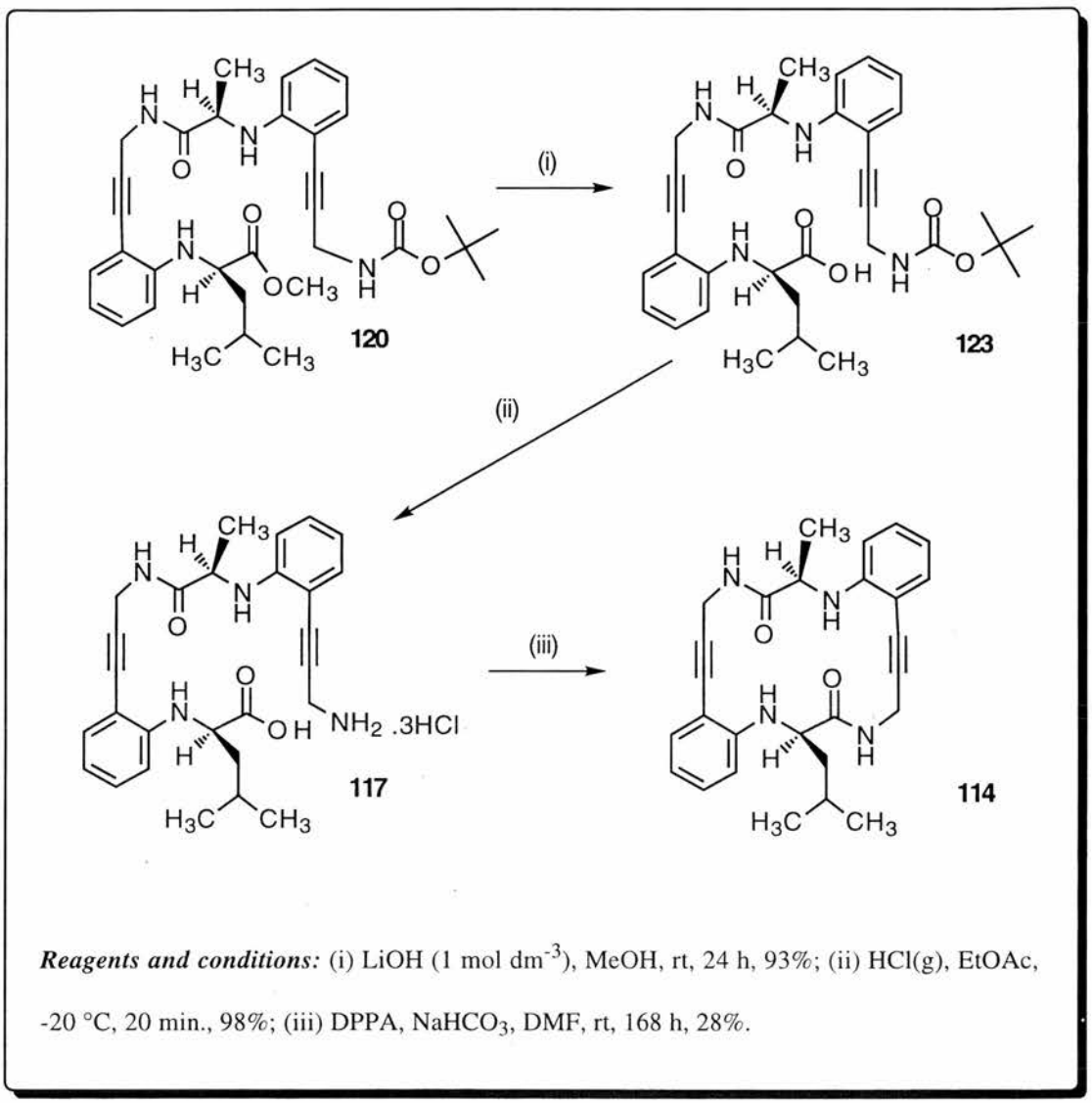

Reagents and conditions: (i) LiOH (1 mol dm^{-3}), MeOH, rt, 24 h, 93%; (ii) HCl(g), EtOAc, -20 °C, 20 min., 98%; (iii) DPPA, $NaHCO_3$, DMF, rt, 168 h, 28%.

Scheme 2.28:*Synthesis of hexapeptide analogue* ***114***

This low yield could be accounted for, in part, by unreacted starting material (*i.e.* acyclic hexapeptide analogue **117**). However, there was mass spectrometric evidence that water was adding across the triple bonds of the hexapeptide analogue **114**, forming significant quantities of mono-ketones **125** and **126** {*m/z* (CI+) $[M + H]^+$ = 461, 11%} and diketone **124** {*m/z* (CI+) $[M + H]^+$ = 479, 13%} during

chromatographic purification (a consequence of the mildly acidic silica used, Fig. 2.9).

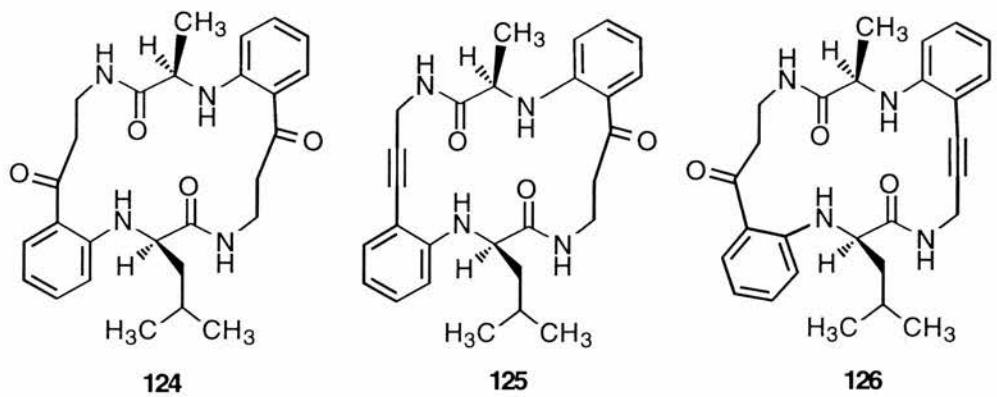

124 **125** **126**

Figure 2.9: *Side products from preparation of* ***114***

During cyclisation, other side reactions can diminish the yield further. This is because the key intermediate of a DPPA mediated cyclisation is an acyl azide which is produced by the transfer of the azido group from DPPA to the carboxylic acid. The azide is subsequently displaced by the incoming amine group and an amide bond is formed (Scheme 2.29). Sometimes problems can arise at this stage; the intermediate acyl azide is also prone to Curtius rearrangement, forming an isocyanate which, if traces of water are present, may be converted to a carbamic acid and then subsequently decarboxylated to the amine, rendering cyclisation impossible (Scheme 2.30).

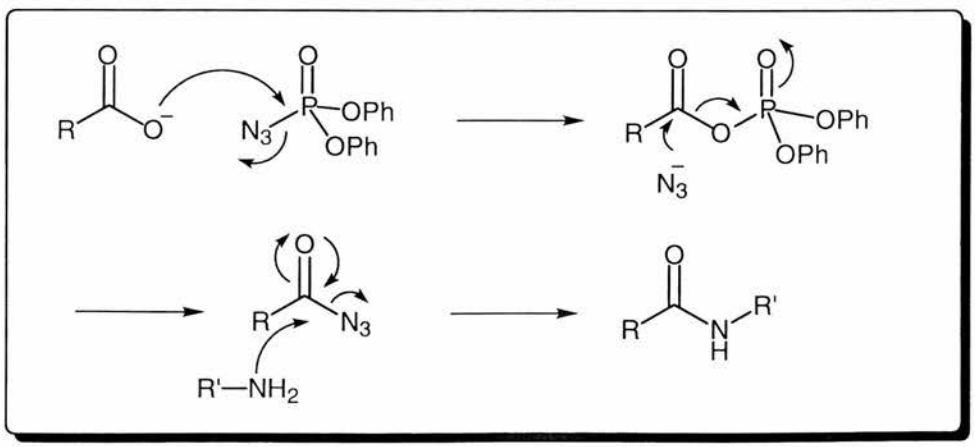

Scheme 2.29: *Mechanism of amide formation using DPPA*

Alternatively, the isocyanate may be attacked by the incoming amine, forming a cyclic urea (Scheme 2.30). Fortunately, mass spectrometry indicated that none of these side-products had formed during the cyclisation of **114**, or the larger tetradecapeptide **116** (see Section 2.6.3). However, following the preparation of decapeptide analogue **115**, traces of cyclic urea were detected by mass spectrometry (see Section 2.5.2).

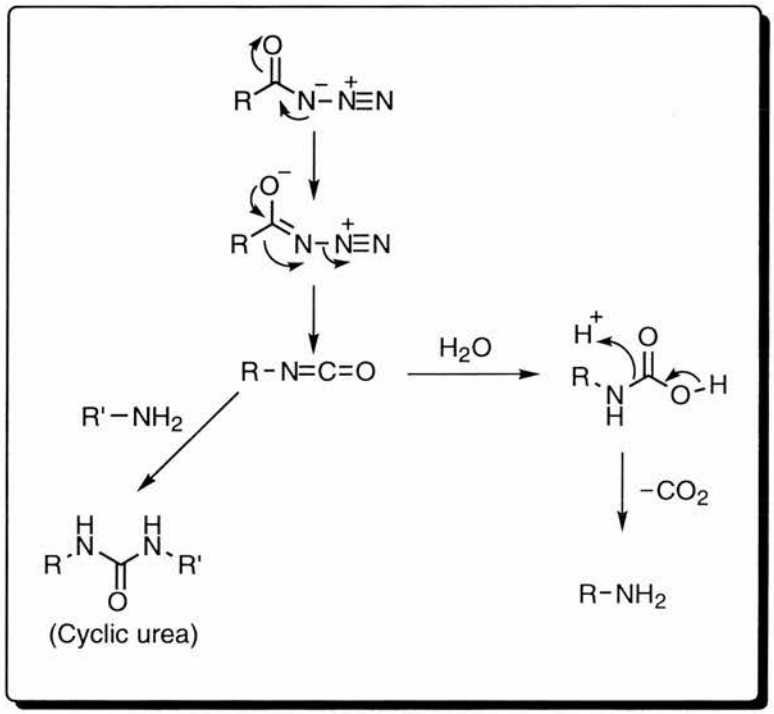

Scheme 2.30: *Possible side-reactions of DPPA*

One other possibility is cyclodimerisation. Cyclisation of the acyclic peptide analogue **141** reduced traces of cyclic dimer - even under high dilution conditions (< 0.1 mM, see Section 2.5.2).

2.4.3 NOE studies: cyclic hexapeptide analogue 114

All proton chemical shifts were assigned using HSQC and total correlation spectroscopy (TOCSY) experiments. The diagram in table 2.1 shows five key NOEs observed in $CDCl_3$ which suggest a β-sheet conformation is present.

Table 2.1: *NOESY crosspeaks observed for cyclic hexapeptide analogue* ***114***

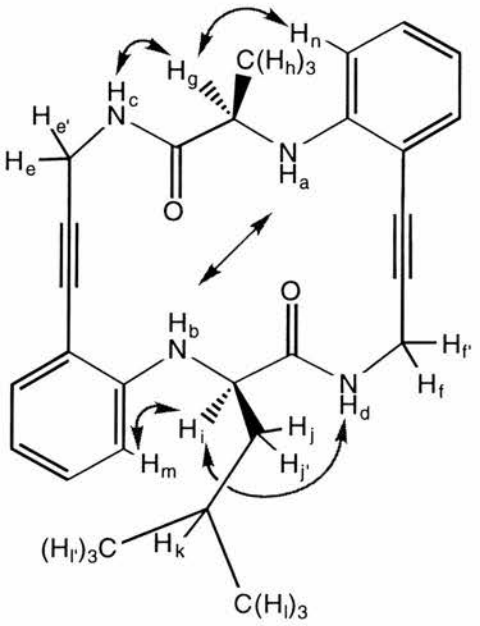

Proton	NOESY cross-peaks[a-c]
H_a	H_b (w), H_g (m),
H_b	H_i (w), H_a (w), $H_{j/j'}$ (m), H_m (w), H_d (w)
H_c	H_g (s), $H_{e/e'}$ (s), H_a (w)
H_d	H_i (s), $H_{f/f'}$ (s), H_a (w), H_b (w)
$H_{e/e'}$	H_c (s)
$H_{f/f'}$	H_d (s)
H_g	H_n (m), H_h (m), H_c (s), H_a (m)
H_h	H_g (m)
H_i	H_d (s), H_m (m), $H_{j/j'}$ (s), H_k (m), $H_{l/l'}$ (w), H_b (w)
$H_{j/j'}$	H_i (s), $H_{l/l'}$ (s), H_b (m)
H_k	$H_{l/l'}$ (s), H_i (m)
$H_{l/l'}$	H_i (w), $H_{j/j'}$ (s), H_k (s)
H_m	H_i (m), H_b (w)
H_n	H_g (m)

[a]14 mM solution in $CDCl_3$, 295 K. [b]Geminal NOEs are not listed. [c]Crosspeaks were identified as strong (s), medium (m) or weak (w) on the basis of their relative intensities.

The $^3J_{NH(amine)-\alpha-H}$ coupling constants were 7.5 Hz in $CDCl_3$ and 7.9 Hz in 8% CD_3OD/CH_3OH. Both are within the acceptable range for a β-sheet (7.5-

10.0 Hz).[128, 133] In $CDCl_3$, the weak $H_a \leftrightarrow H_b$ NOE cross-peaks, strong α-H $\leftrightarrow$ NH(amide) crosspeaks and strong $H_m \leftrightarrow H_i$ and $H_n \leftrightarrow H_g$ NOE cross-peaks are consistent with hexapeptide analogue **114** adopting a β-sheet conformation in $CDCl_3$. The amide NH resonances experience a large downfield shift of 1.4 ppm on conversion from $CDCl_3$ to the more polar 8% CD_3O^2H/CH_3OH medium indicating exposure to solvent, whereas the anilino NH groups only exhibit a very small downfield shift of 0.2 ppm which suggests that they are solvent inaccessible and supports their involvement in intramolecular H-bond formation. In 8% CD_3OD/CH_3OH, NOE difference spectra of **114**, in which the irradiating frequency is set at the resonant frequency of H_a and H_b, indicate that these protons are in close proximity in more polar media as well.[202]

An energy minimised model of hexapeptide analogue **114** (Fig. 2.10) is broadly consistent with observed NOEs.

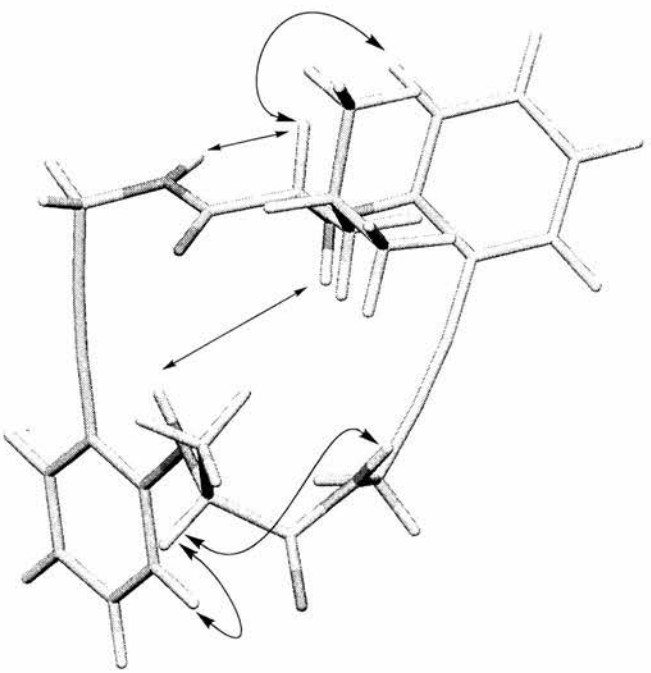

Figure 2.10: *Model of artificial β-sheet **114** in a minimum energy conformation as calculated using INSIGHT II with the CVFF force field*

2.5 Synthesis and structural studies of decapeptide analogue 115

2.5.1 Introduction

Unlike the hexapeptide analogue, decapeptide analogue **115** contains 'real' peptide sequences and is therefore a more realistic β-sheet model. Disconnection of this molecule gives rise to two tripeptide analogues (**129** and **132**) and dipeptides, H-Ala-Val-OH (**130**) and H-Thr-Leu-OH (**131**) (Scheme 2.31).

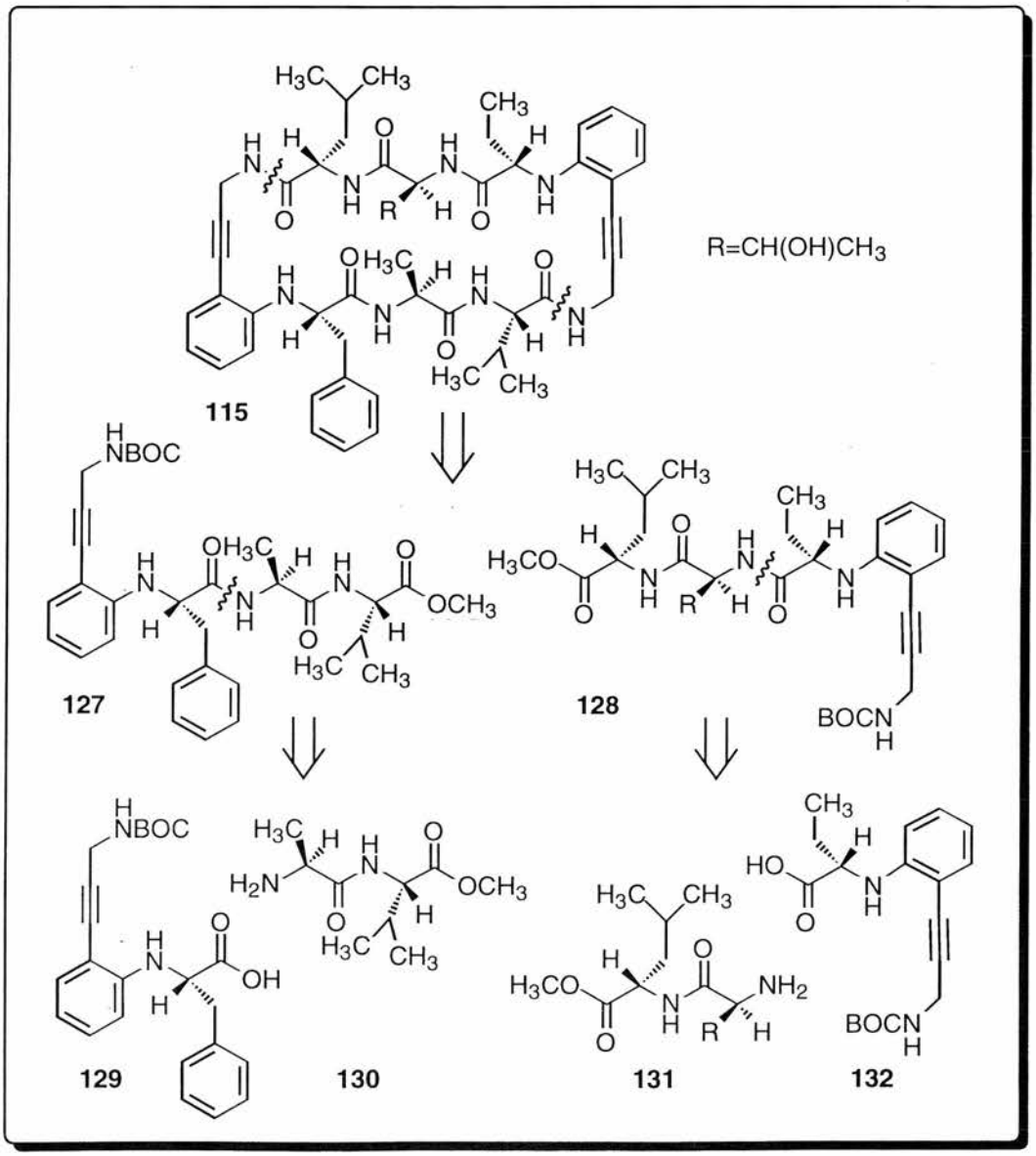

Scheme 2.31: *Disconnection of cyclic decapeptide analogue **115***

2.5.2 Synthesis of decapeptide analogue

Synthesis of macrocycle **115** began with the preparation of the fully protected pentapeptides **127** and **128** (Schemes 2.32 and 2.33 respectively). The dipeptide unit **135** was prepared from *N*-BOC-alanine (**133**) and valine methyl ester hydrochloride (**134**), with TBTU as the coupling reagent, to give the dipeptide **135** as a colourless oil in satisfactory yield (81%). This dipeptide was then unmasked at the *N*-terminus, with dry HCl gas, to give the dipeptide hydrochloride salt **130** in good recovery (~99%). Tripeptide analogue **108** was unmasked at the *C*-terminus with aqueous LiOH (1 mol dm^{-3}) and coupled to dipeptide **130** (coupling reagent: TBTU) to give pentapeptide analogue **127** (HRMS: found $[M + Na]^+$, 601.3019. $C_{32}H_{42}N_4O_6$ requires 601.3002) in 60% yield after column chromatography (Scheme 2.32) and was judged to be pure (>95%) by ^{13}C NMR spectroscopy. Dry HCl gas was used to remove the BOC group on **127** to give dihydrochoride salt **136** as a white solid in 99% recovery (Scheme 2.32).

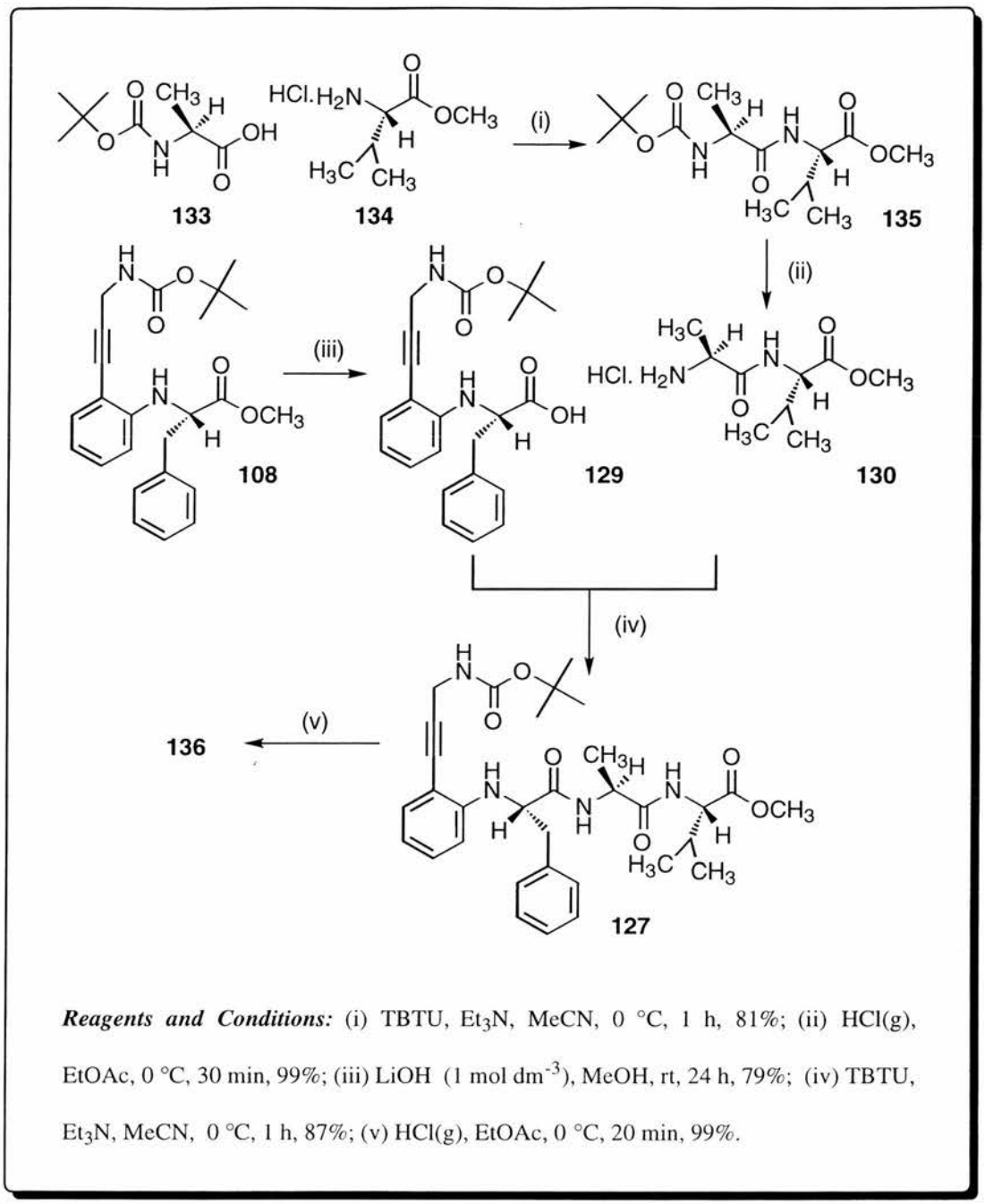

Reagents and Conditions: (i) TBTU, Et_3N, MeCN, 0 °C, 1 h, 81%; (ii) HCl(g), EtOAc, 0 °C, 30 min, 99%; (iii) LiOH (1 mol dm^{-3}), MeOH, rt, 24 h, 79%; (iv) TBTU, Et_3N, MeCN, 0 °C, 1 h, 87%; (v) HCl(g), EtOAc, 0 °C, 20 min, 99%.

Scheme 2.32: *Synthesis of decapeptide analogue **115**; part (i)*

Using similar methodology, dipeptide **139** was prepared in 90% yield from *N*-BOC-threonine (**138**) and leucine methyl ester hydrochloride (**137**) (Scheme 2.33). The resulting dipeptide was then unmasked at the *N*-terminus to give the dipeptide hydrochloride salt **131** in excellent recovery (99%). Tripeptide analogue **109** was unmasked at the *C*-terminus and coupled to dipeptide **131** (coupling reagent: TBTU) to give pentapeptide analogue **128** (HRMS: found $[M + H]^+$, 561.3296. $C_{29}H_{45}N_4O_7$ requires 561.3288) in 60% yield after recrystallisation from ethyl acetate/hexane and

was judged to be pure (>95%) by ^{13}C NMR spectroscopy. Pentapeptide analogue **128** was unmasked at the *C*-terminus with LiOH (1 mol dm^{-3}) in methanol to give, after aqueous work-up with mineral acid, the free acid **140** in 90% yield (Scheme 2.33).

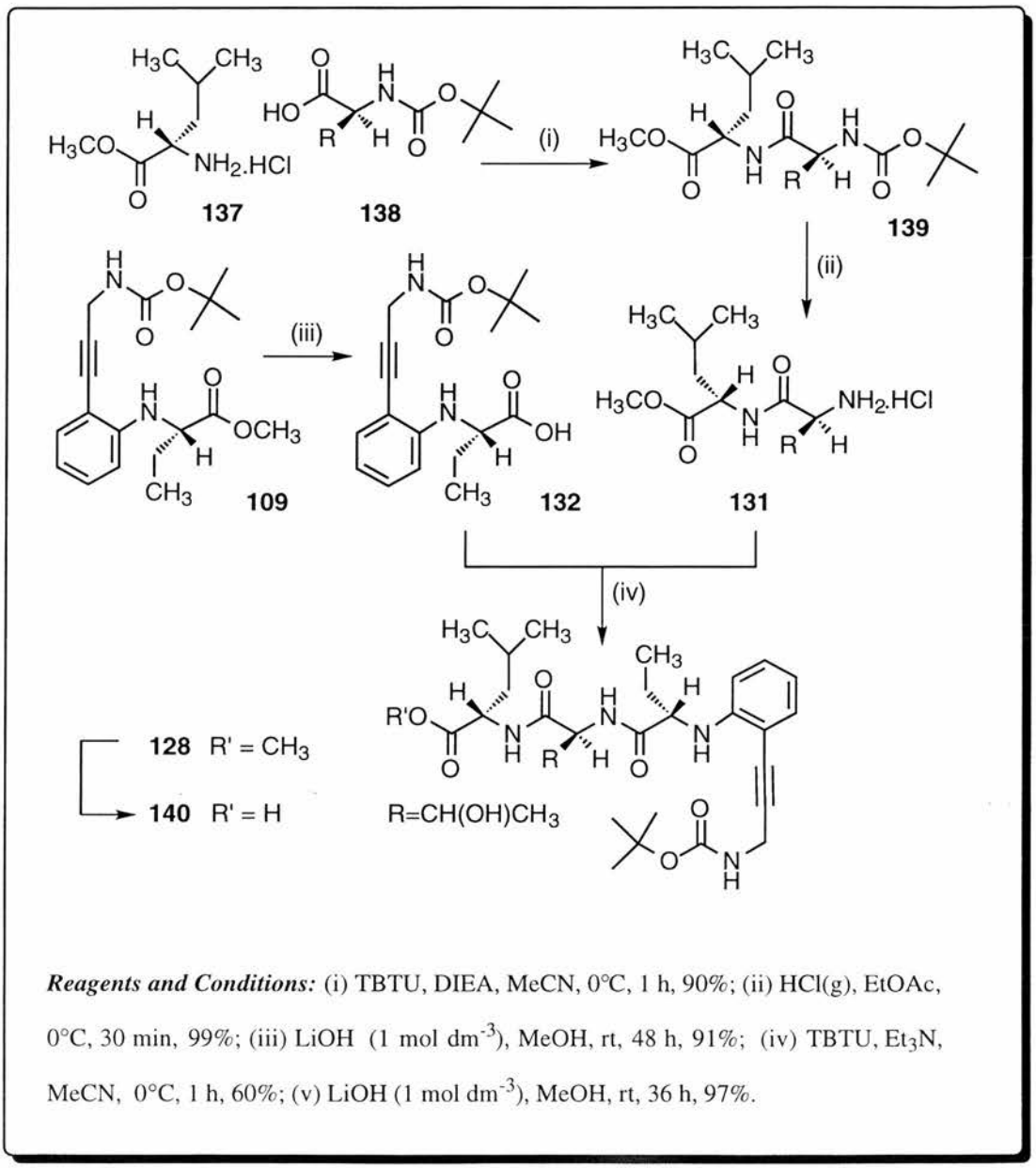

Reagents and Conditions: (i) TBTU, DIEA, MeCN, 0°C, 1 h, 90%; (ii) HCl(g), EtOAc, 0°C, 30 min, 99%; (iii) LiOH (1 mol dm^{-3}), MeOH, rt, 48 h, 91%; (iv) TBTU, Et_3N, MeCN, 0°C, 1 h, 60%; (v) LiOH (1 mol dm^{-3}), MeOH, rt, 36 h, 97%.

Scheme 2.33: *Synthesis of decapeptide analogue **115**; part (ii)*

Peptide analogues **136** and **140** then underwent an EDCI mediated coupling in DMF to give acyclic decapeptide analogue **141** in 81% yield, following chromatographic purification (Scheme 2.34). After deprotection of the *C* and *N*-termini with methanolic LiOH (1 mol dm^{-3}) and dry HCl gas respectively, cyclisation

was effected with DPPA and solid sodium bicarbonate to give, after aqueous work-up and HPLC purification, the cyclic decapeptide analogue **115** (HRMS: found [M + Na]$^+$ 897.4648. $C_{49}H_{62}N_8O_7$, requires 897.4639) as a white solid in good yield (20%).

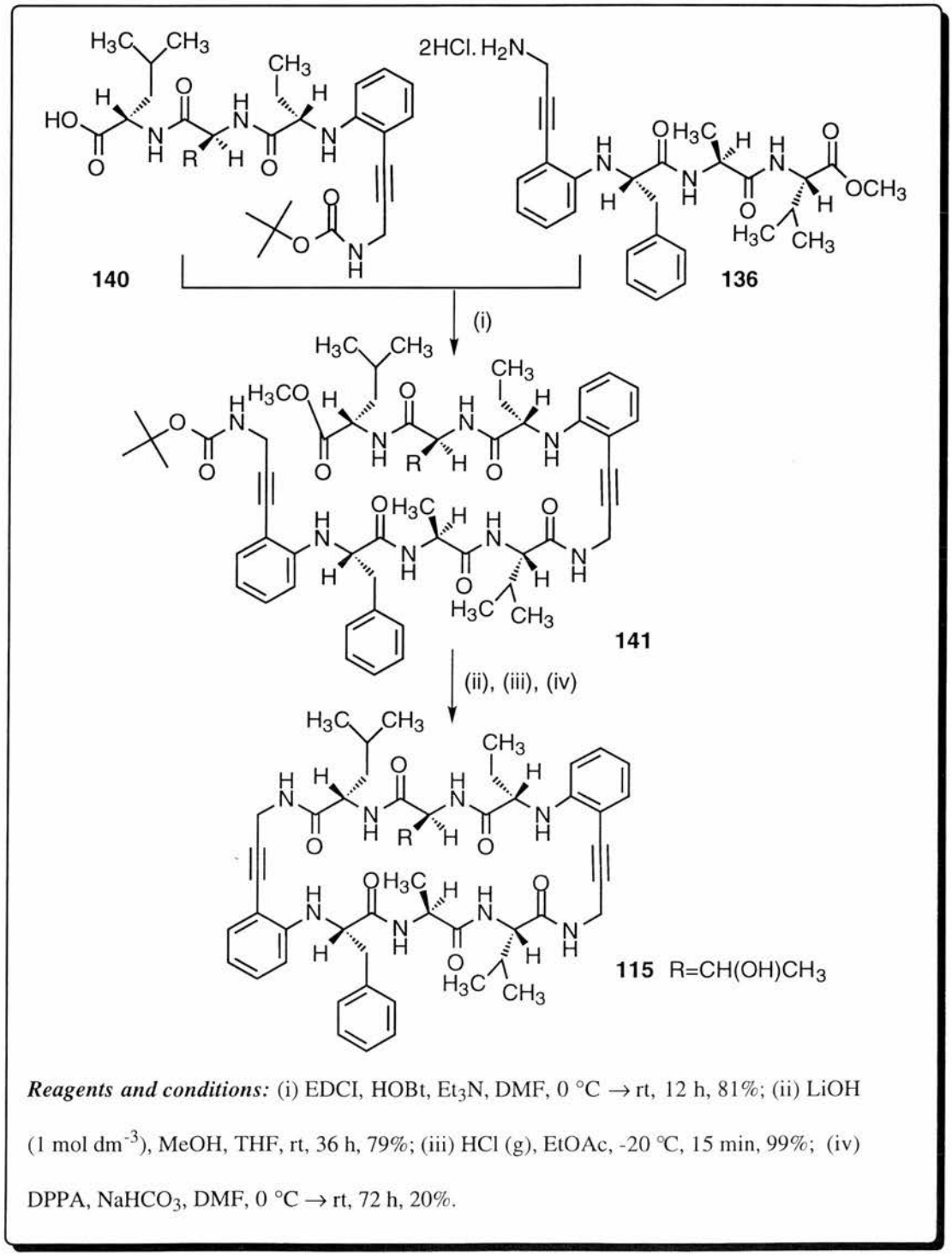

Reagents and conditions: (i) EDCI, HOBt, Et_3N, DMF, 0 °C → rt, 12 h, 81%; (ii) LiOH (1 mol dm^{-3}), MeOH, THF, rt, 36 h, 79%; (iii) HCl (g), EtOAc, -20 °C, 15 min, 99%; (iv) DPPA, $NaHCO_3$, DMF, 0 °C → rt, 72 h, 20%.

Scheme 2.34: *Synthesis of decapeptide analogue **115**; part (iii)*

Mass spectrometry of the crude reaction mixture of **115** indicated the presence of some side-products; cyclic urea **142** {*m/z* (FAB) $[M + Na]^+ = 912$, 25%} (Fig. 2.11) and a cyclic dimer {*m/z* (FAB) $[2M + H]^+ = 1750$, 1%}.

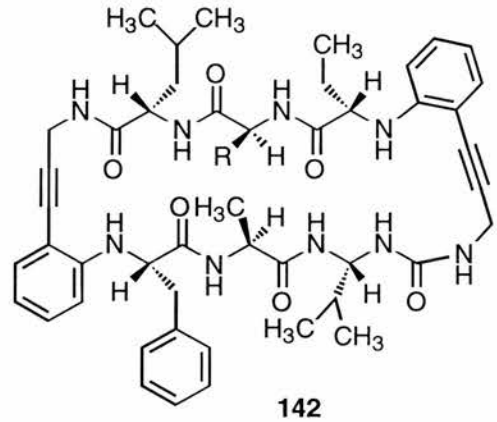

142

Figure 2.11: *Cyclic urea **142***

Unlike the cyclic hexapeptide analogue **114**, purification of the decapeptide analogue **115** was not possible by column chromatography. This was because traces of impurities, primarily diastereoisomers, had R_f values too similar to the target molecule to be clearly visualised as separate products on a TLC plate. C_{18} Analytical reverse-phase HPLC of the crude cyclodecapeptide, under gradient conditions (99.9% water/0.01% TFA to 99% MeCN/0.99% water/0.01% TFA) over 30 min, revealed a mixture of two main products [Fig. 2.12(*a*)]. Isolation of these peaks and subsequent electrospray MS, indicated that both products had the same mass and were probably diastereoisomers. The possible site of epimerisation in **115** was most likely to be around the α-C of leucine, a consequence of the rather harsh conditions initially used during deprotection of the methyl ester of **141** [LiOH (1 mol dm^{-3}), MeOH, 40 °C, 72 h]. This problem was alleviated when a less polar co-solvent (THF) was added to unfold the peptide and make the methyl ester more accessible to base, lowering the required reaction time and temperature [step (*ii*), Scheme 2.34]. Analytical HPLC of the crude cyclic product prepared in this way revealed only one major product which had the correct mass by ES+ [Fig. 2.12(*b*)].

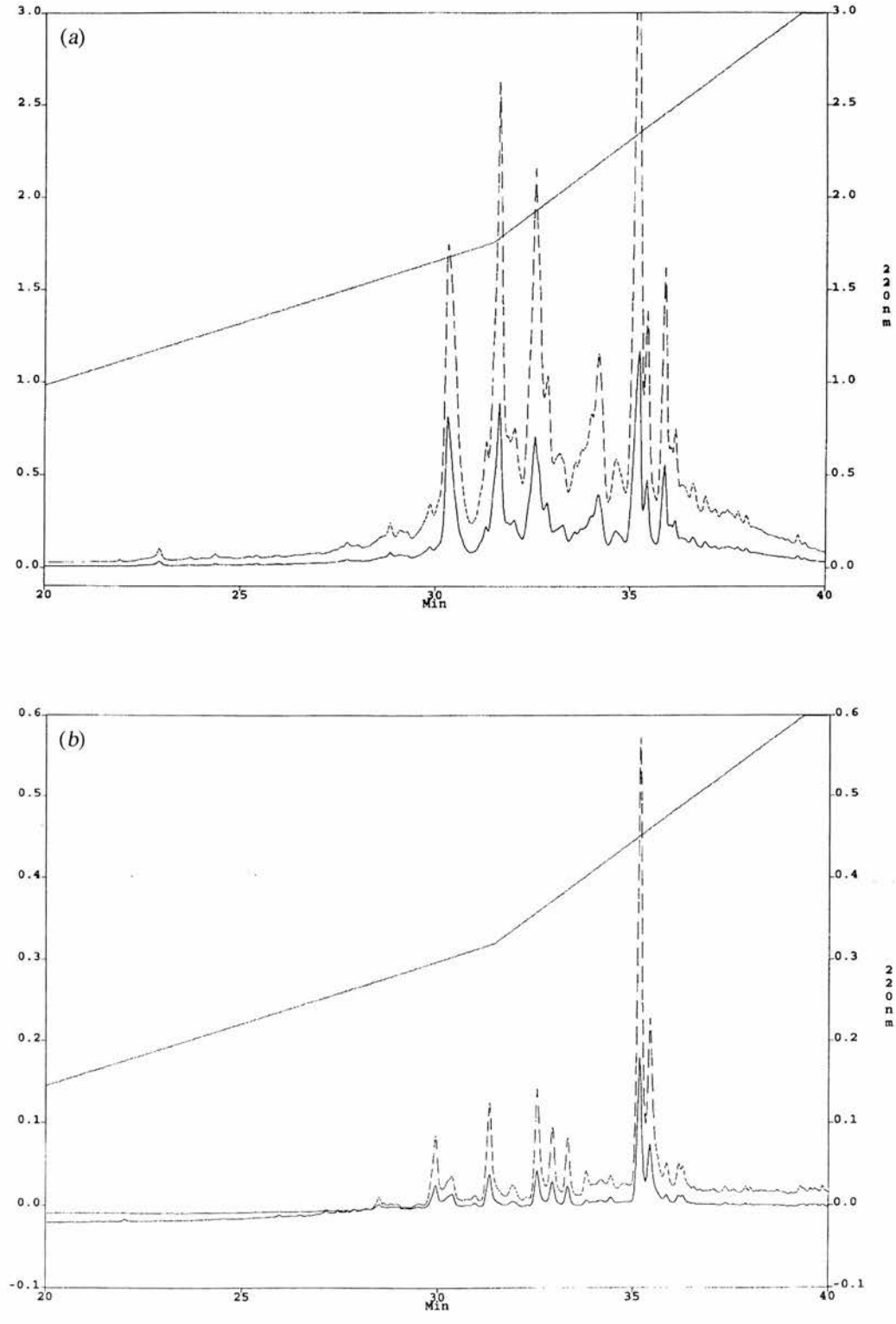

Figure 2.12: *HPLC traces of crude decapeptide analogue* ***115*** *prepared via saponification of* ***141*** *under different conditions: (a) LiOH (1 mol dm^{-3}), MeOH, 40°C, 72 h; (b) MeOH, THF, rt, 36 h (dashed line: 220 nm, solid line: 254 nm).*

However, we still encountered purification problems. Analytical C_{18} HPLC of the product after isolation of the major peak still revealed significant impurities [see Fig. 2.14(*a*)]. Furthermore, these impurities were quite different in their retention times from both the major product and impurities in the crude material, suggesting that crude material was decomposing on the column. Mass spectrometry of material after purification indicated that ketones **143** and **144**, {*m/z* (ES+) $[M + Na]^+ = 915$, 25%} and diketone **145** {*m/z* (ES+) $[M + Na]^+ = 933$, 3%} (Fig. 2.13) were present. Neither compound was detected in the crude material prior to HPLC.

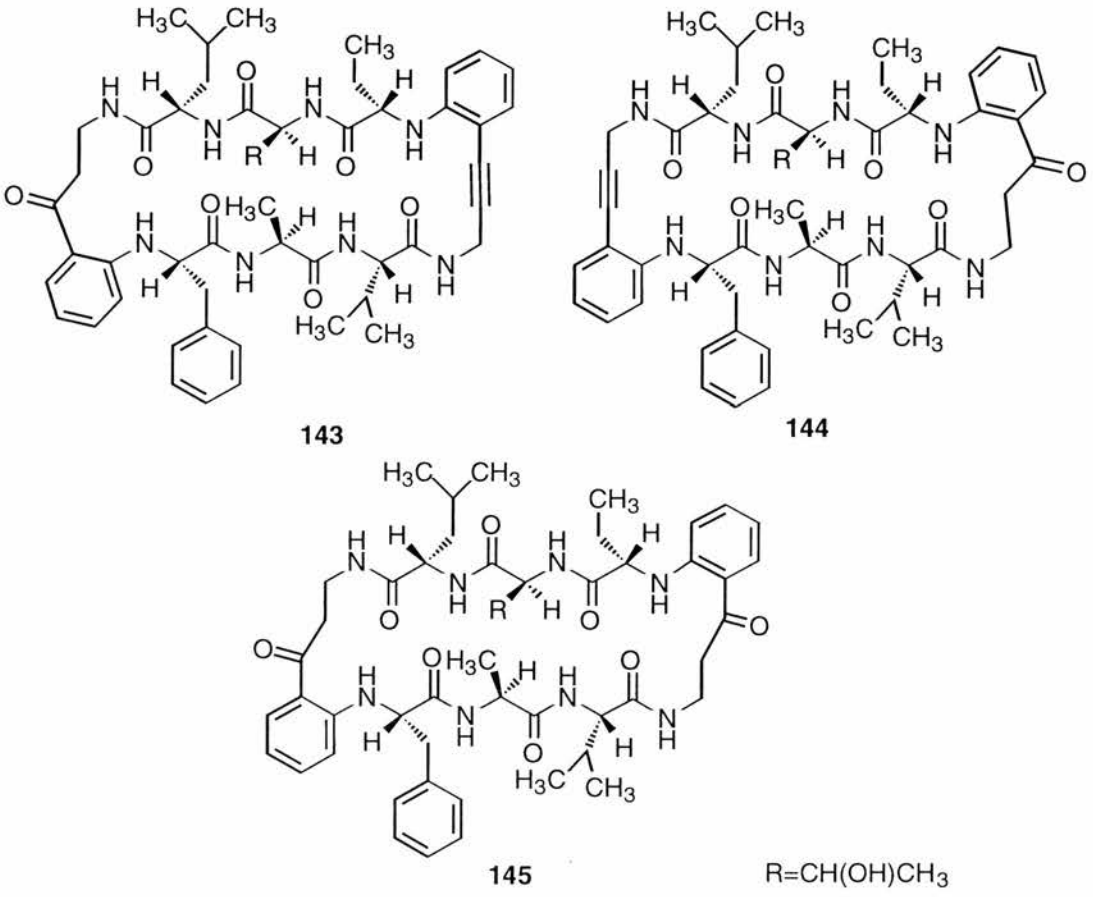

Figure 2.13: *Side products from preparation of decapeptide analogue* ***115***

These observations confirmed that the substrate was decomposing on the column, perhaps as a result of the 0.1% TFA in the eluting solvent. It had been demonstrated earlier (Scheme 2.21) that TFA readily attacks the triple bond of methyl ester **105** to give a ketone. Initially we were reluctant to attempt reverse-phase HPLC purification

without TFA because the very small quantities used in the eluent serve a useful function as an ion pairing agent, improving resolution and separation as well as helping to extend the column lifetime. However, attempts to purify the compound on a non-TFA dependent normal-phase column were not successful as resolution and peak separation were very poor. Consequently, purification of crude material was attempted on a semi-preparative C_{18} reverse phase column without TFA. To our surprise, despite the reduced resolution of the procedure, the major impurities were well separated and subsequent analyses of purified material revealed no further impurities [Fig. 2.14(*b*)].

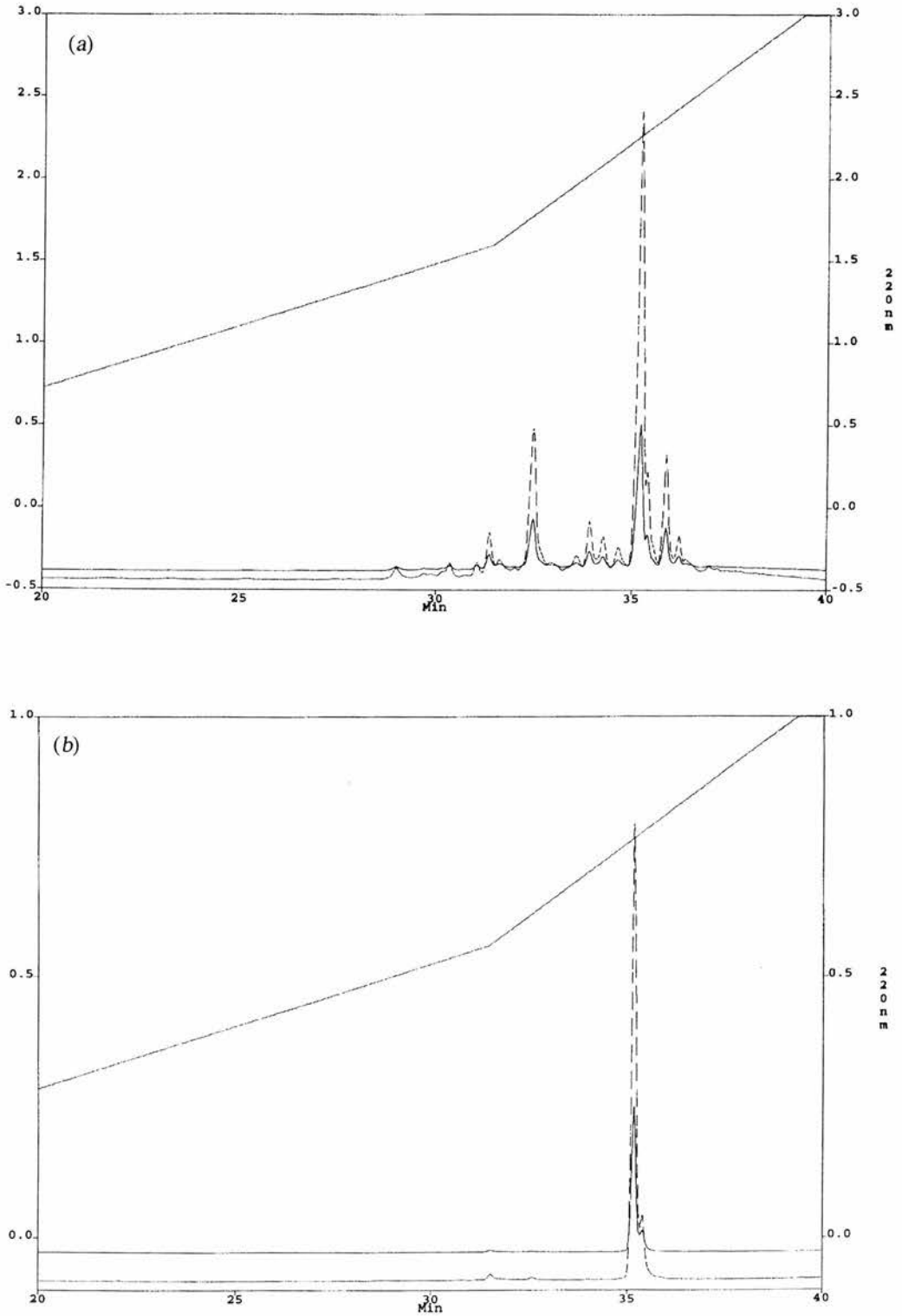

Figure 2.14: *Analytical HPLC traces of decapeptide analogue* ***115****: (a) HPLC trace of decapeptide analogue* ***115*** *purified with 0.1% TFA in eluent; (b) HPLC trace of material purified without TFA*

2.5.3 NOE studies: acyclic decapeptide analogue 141

There is the possibility that the acyclic precursors of both **115** and **116** may, to a certain extent, adopt a β-sheet conformation in solution, thus facilitating cyclisation. In order to determine whether this is indeed the case, the NOE spectra of acyclic precursors to both **115** and **116** were analysed in d_6-DMSO solution.

NOE studies of the acyclic decapeptide analogue **141** in d_6-DMSO, revealed no significant long range NOEs. Only short-range sequential NOEs were observed [*i.e.* 5 × NH(i) ↔ α-H(i + 1), Ar-H ↔ α-H(Phe) and Ar-H ↔ α-H(Abu)] suggesting that acyclic decapeptide analogue **141** may not form an intramolecularly hydrogen-bonded β-sheet to any significant extent in non-protic organic solvents (Fig. 2.15).

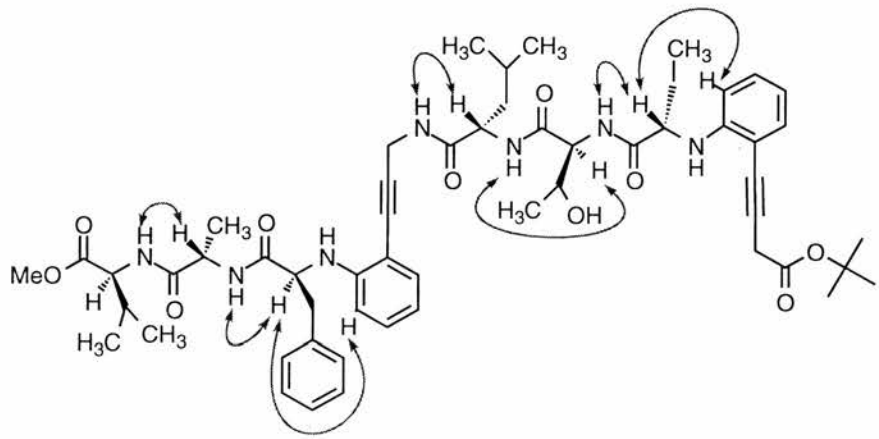

Figure 2.15: *NOE crosspeaks observed for decapeptide analogue **141** in d_6-DMSO*

2.5.4 NOE studies: cyclic decapeptide analogue 115

NOE results for cyclic decapeptide analogue **115** in $CDCl_3$ (Table 2.2), suggest that intrastrand H-bond formation occurs. The dashed lines indicate NOEs that could not be uniquely assigned due to resonance overlap.

Table 2.2: *NOESY crosspeaks observed for cyclic decapeptide analogue* ***115***

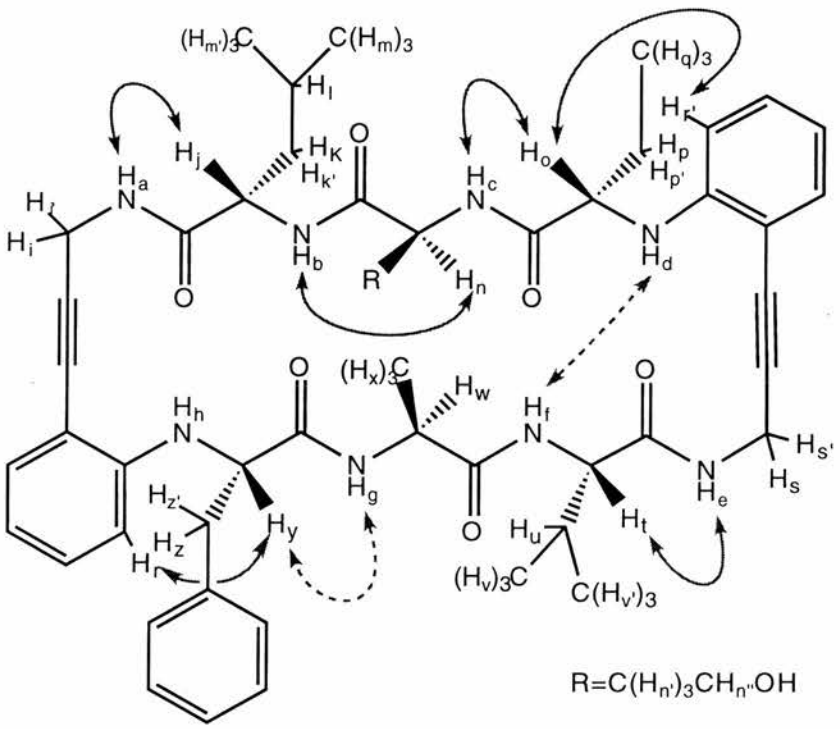

Proton	NOESY cross-peaks[a-d]
H_a	H_j (m), $H_{i/i'}$ (m)
H_b	H_j(w), H_n(m), H_l (w)
H_c	$H_{n'}$ (m), $H_{n''}$ (m), H_n (m), $H_{k/k'}$ (w), OH (m), H_o (m)
H_d	H_q (w), $H_{p/p'}$ (w), H_o (w), H_e (w), H_f (w), H_g(w), H_o(w), $H_{n''}$(m)
H_e	$H_{s/s'}$ (w), H_d (w), H_t (m)
H_f	H_d (w), H_t (w)
H_g	H_h (m), H_w (m), H_y (m), H_x (m), $H_{z/z'}$(m), H_d(w), $H_{v/v'}$
H_h	$H_{z/z'}$ (w), H_y(w), H_g (m), H_r (m)
$H_{i/i'}$	H_a (m)
H_j	H_b (w), H_a (m), $H_{k/k'}$ (w), H_l (w), $H_{m/m'}$ (m)
$H_{k/k'}$	H_c (w), H_l (s), $H_{m/m'}$ (s), H_j(w)
H_l	H_b (w), H_j (w), $H_{m/m'}$ (s), H_j(w), $H_{k/k'}$(s)
$H_{m/m'}$	H_l (s), H_j (m), $H_{k/k'}$ (s)
H_n	H_b (m), H_c (m), $H_{n''}$ (m), $H_{n'}$ (m), OH (m)
H_o	H_d (w), $H_{r'}$ (m), $H_{p/p'}$ (m), H_q (m), H_c(m)
$H_{p/p'}$	H_d(w), H_o (m), H_q (s), $H_{r'}$ (w)
H_q	$H_{p/p'}$ (s), H_d (w), H_o (m)
H_r	H_h (m), H_y (w), $H_{z/z'}$ (w)
$H_{r'}$	$H_{p/p'}$ (w), H_o (m)
$H_{s/s'}$	H_e (w)
H_t	H_e (m), H_f (w), H_u (m), $H_{v/v'}$ (m)
H_u	H_t (m), $H_{v/v'}$ (s)
$H_{v/v'}$	H_t (m), H_u (s), H_g (w)
H_w	H_x (m), H_g (m)
H_x	H_w (m), H_g (m)

H_y	H_r (w), $H_{z/z'}$ (m), H_g (m), H_h (w)
$H_{z/z'}$	H_y (m), H_h (w), H_r (w), H_g (m)

[a]7.5 mM solution in $CDCl_3$, 295 K. [b]Geminal NOEs are not listed. [c]Crosspeaks were identified as strong (s), medium (m) or weak (w) on the basis of their relative intensities. [d]Due to resonance ovelap, some NOEs could not be unambiguously assigned and have therefore not been listed.

^{1}H NMR variable temperature studies can offer additional insight into hydrogen-bonding pattern of decapeptide analogue **115**. In an attempt to observe a low energy conformation in which more interstrand NOEs were more prominent, a 7.5 mM solution of **115** in $CDCl_3$ was cooled to 0 °C and then to -20 °C. Unfortunately, at lower temperatures, fewer NOEs were detected and the resolution of each spectrum grew progressively worse, making accurate assignment of most signals difficult. During these experiments it was possible, however, to measure the chemical shift temperature dependence of the NH_h and NH_d protons. It was found that NH_d and NH_h exhibited temperature dependencies of -3.0×10^{-3} ppm K^{-1} and -1.0×10^{-3} ppm K^{-1} respectively. In a non-competitive solvent, such as $CDCl_3$, a small temperature dependence ($-\Delta\delta/\Delta T \leq 2 - 3 \times 10^{-3}$ ppm K^{-1}) indicates that a proton is either completely hydrogen-bonded or completely non-hydrogen-bonded while a large temperature dependence ($-\Delta\delta/\Delta T \geq 4 - 5 \times 10^{-3}$ ppm K^{-1}) indicates that a proton participates in an equilibrium between hydrogen-bonded and non-hydrogen-bonded states.[128] With this in mind, the values obtained for NH_d and NH_h support the NOE data in Table 1.2 and is consistent with a partial β-sheet structure between the aminobutyric acid and valine residues. Due to signal overlap, it was difficult to obtain vicinal coupling constants for the amide NH protons, however NH_h and NH_d were well separated and their $^3J_{NH\text{-}\alpha\text{-}H}$ coupling constants were both approximately 8.5 Hz, consistent with a β-sheet structure.

Fig. 2.16 shows a model of decapeptide analogue **115** in a minimum energy conformation with sequential and long-range NOEs highlighted. The sequential α-H

$\leftrightarrow$ NH NOEs that are a characteristic of β-sheets are highlighted, but the ideal antiparallel β-sheet structure appears to be disrupted by H-bonding between NH_e and the oxygen of the threonine side-chain. This may account for the absence (or weakness) of characteristic β-sheet interstrand NOEs, in particular, the $H_d \leftrightarrow H_f$ and $H_b \leftrightarrow H_h$ NOEs as well as the NOEs between α-protons ($H_n \leftrightarrow H_w$, $H_o \leftrightarrow H_t$ and $H_j \leftrightarrow H_y$). There is also the suggestion of NH_i to CO_{i+2} H-bonding along the peptide main chain, in which a series of γ-turns are formed. This would also disrupt the H-bonding pattern of the antiparallel β-sheet.

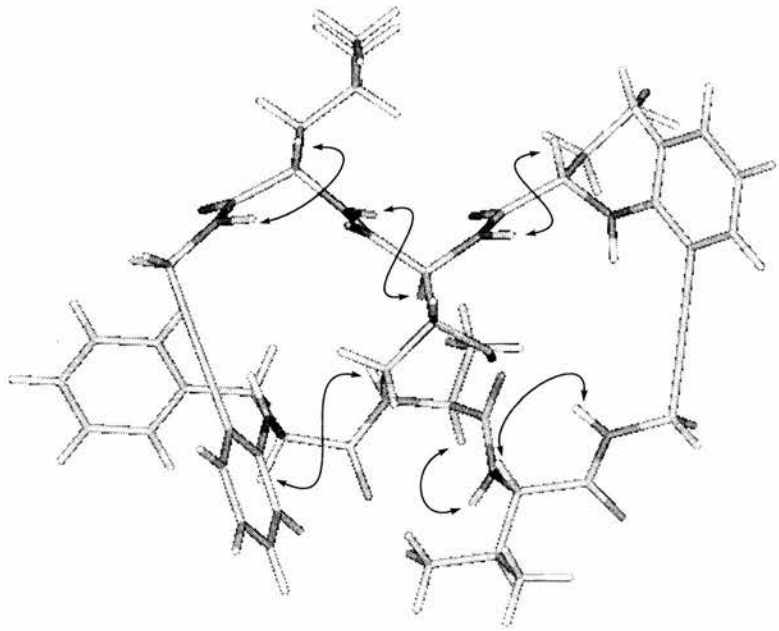

Figure 2.16: *Model of artificial β-sheet **115** in a minimum energy conformation as calculated using INSIGHT II with the CVFF force field*

2.5.5 Spectral broadening

When a spectroscopic sample of decapeptide analogue **115** in $CDCl_3$ was cooled to 0 °C and then further to -20 °C, the spectrum was considerably broadened, making it difficult to extract any meaningful data.

These results can be explained in terms of efficient relaxation of ^1H nuclei and the Heisenberg uncertainty principle which states that if a state has a lifetime τ_m, then there is an uncertainty in its energy given by:[191]

$$\delta E \propto 1/\tau_m$$

Since the relaxation rate of a given nucleus is is equal to τ_m^{-1}, then the larger the relaxation rate is, the larger the uncertainty in its energy (δE). Therefore from Planck's law ($\Delta E = h\nu$), an uncertainty in energy will also produce an uncertainty in the frequency of the nucleus, manifesting itself as a broader line in the NMR spectrum.

The process of relaxation is governed by fluctuations in the local magnetic field surrounding the nucleus. These fluctuations are, in turn, related to the rate a molecule tumbles within the magnetic field, with molecular tumbling rates of *ca.* 10^8 s^{-1} promoting the most efficient relaxation.

Molecules with a molecular weight of 100 have a tumbling frequency of 10^{11} s^{-1} which is too fast for efficient ^1H relaxation and NMR lines are sharp (ν is small). However, molecules approaching a molecular weights of 1000 or more, such as **115** and **116**, have a slower tumbling frequency (*ca.* 10^9 s^{-1}) which produces fluctuating magnetic fields close to the natural resonant frequency of the nucleus. This results in a faster relaxation rate and hence a broader signal. Solvent viscosity can also greatly influence the molecular tumbling frequency and this would explain why the resolution of the spectrum of **115** varies so significantly with temperature (Fig. 2.17).

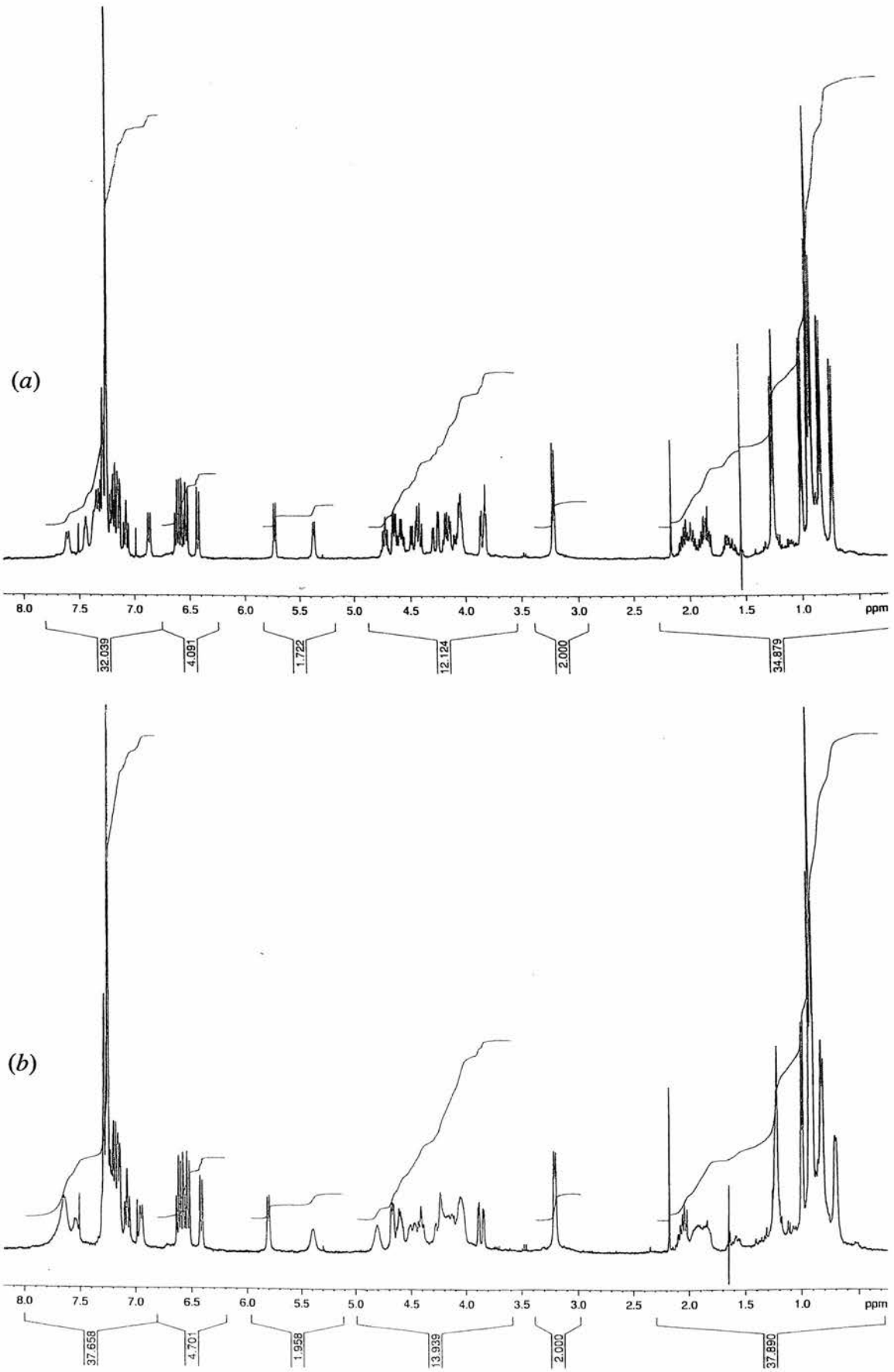

Figure 2.17: *^1H NMR spectrum of decapeptide analogue **115** at (a) 25°C, (b) 0°C*

2.6 Synthesis and Structural Studies of Larger β-sheet Models

2.6.1 Introduction

The synthetic strategy used for the synthesis of potential β-sheet targets **114** and **115** could feasibly be applied to β-sheet models of any size, but clearly, any solution phase synthesis of systems larger than decapeptide analogue **115** would be very time consuming. Solid phase peptide synthesis (SPPS), however, can enhance the efficiency of oligopeptide synthesis and this was used in conjunction with solution phase techniques, for the preparation of cyclic tetradecapeptide **116**.

2.6.2 Solid phase peptide synthesis

The synthesis of peptides on a solid support was introduced by R. B. Merrifield in 1963. Merrifield resin is a chloromethylated polystyrene (Fig. 2.18) and peptide synthesis on this system begins with the immobilisation of a *N*-BOC-protected amino acid *via* a reaction with the chloromethyl groups on the polystyrene polymer. Subsequent *N*-deprotections and couplings are usually carried out with TFA and DCC respectively. Cleavage of the completed peptide is commonly effected with TFA.

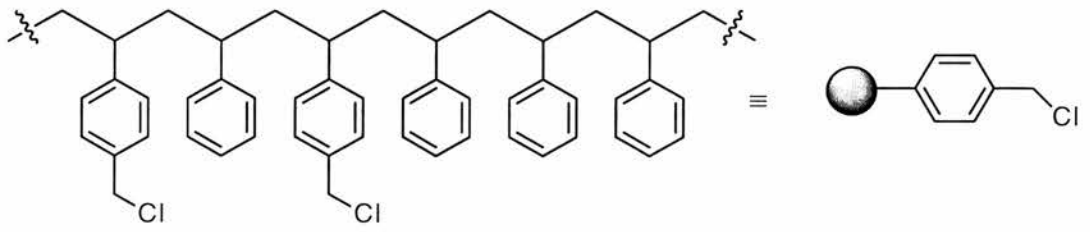

Figure 2.18: *Merrifield resin*

There are several different resins and reagents available for peptide synthesis but the overall strategy remains the same (Scheme 2.35): An *N*-protected amino acid is attached to an insoluble polymer support *via* a linker, the protecting group is removed (usually under mild conditions) and the next amino acid, also *N*-protected, is coupled to the first amino acid in the presence of an activating agent (*e.g.* PyBOP, TBTU, HATU, DCC *etc*). This strategy can also be applied to whole segments of peptides

(termed fragment or segment condensation). After coupling, the resin bound dipeptide (or oligopeptide) is washed with solvent and the deprotection/coupling procedure is repeated until the desired sequence of amino acids is generated, at which point the peptide is cleaved from the resin using an appropriate reagent (*e.g.* TFA or HF).

The solid phase peptide synthesis method developed by Wang utilises the base-labile fluorenylmethoxycarbonyl (Fmoc) group for *N*-terminus protection and can be rapidly removed by 20-50% piperidine/DMF solution where the DMF is used as a polar medium to ensure facile Fmoc removal (Scheme 2.35).

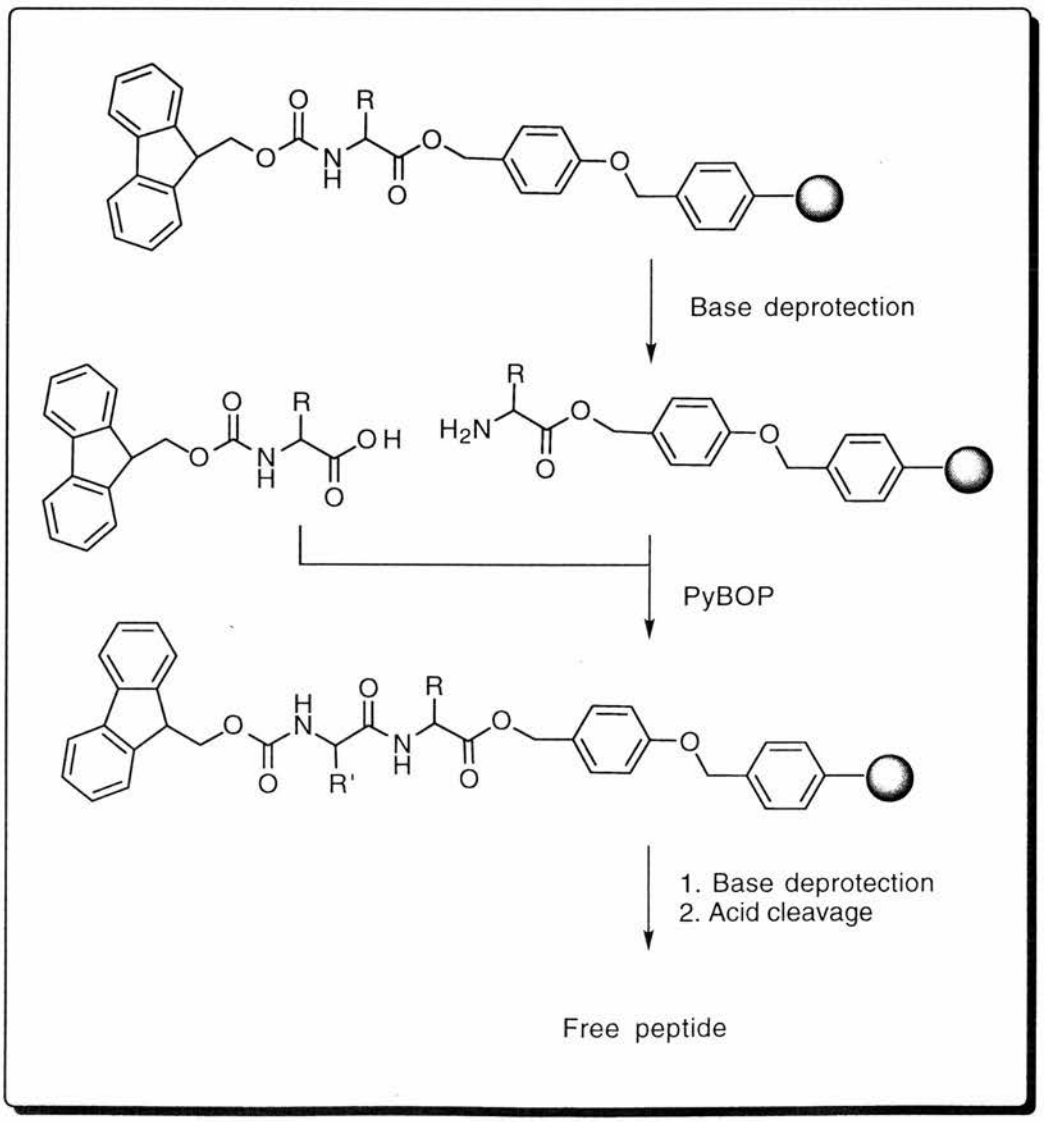

Scheme 2.35: *General strategy of peptide synthesis on Wang resin*

The electron withdrawing fluorene ring system of the Fmoc group renders the hydrogen on the β-carbon very acidic, and therefore susceptible to removal by weak bases. It can be removed, *via* β-elimination, to form dibenzofulvene and a free amino group (Scheme 2.36).

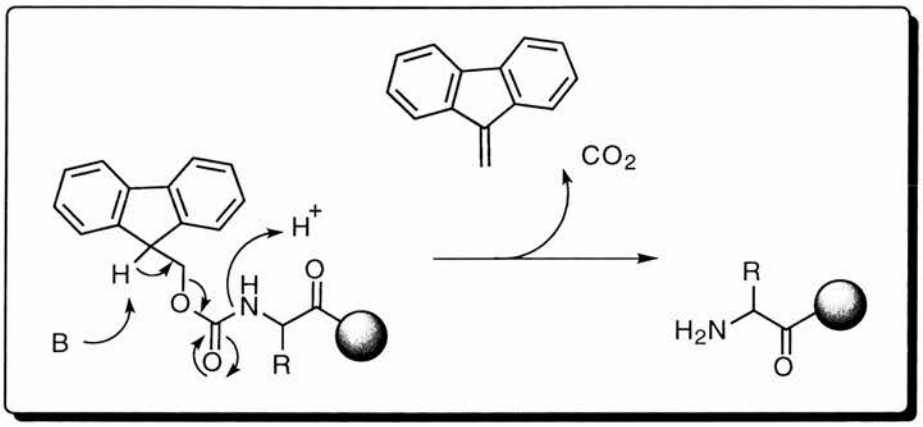

Scheme 2.36: *Fmoc deprotection under basic conditions*

The Fmoc amino acid acylation reactions must be efficient to ensure homogeneous peptide products and a good overall yield, therefore a large excess of PyBOP and Fmoc amino acid is often used (~5 eq. each) to ensure each reaction step goes to completion. Efficient solvation of the peptide immobilised resin is also important for successful SPPS. The solvation of the cross-linked polystyrene polymer of the resin leaves the linear peptide chain as accessable as if free in solution. The ability of the peptide resin to swell increases with increasing peptide length due to a net decrease in free energy from solvation of the linear peptide chains, so theoretically, there should be no size limit to the peptides prepared on SPPS, provided that proper solvation conditions exist. Polar solvents such as DMF enhance resin swelling and are therefore commonly used in SPPS.

The final stages of SPPS on Wang resin involve removal of the Fmoc group with piperidine and then cleavage of the complete peptide from the resin using TFA. A small amount of triethylsilane (2.5%) is added to the TFA to prevent unwanted side reactions during cleavage.

2.6.3 Synthesis of cyclic tetradecapeptide analogue 116

Since the principle method of cleaving oligopeptides from Wang resin is TFA, the phenyl-acetylenic moiety was not included in the solid phase synthesis of tetradecapeptide **116** due to its vulnerability to mild acids. Instead, a combination of solid and solution phase chemistry was employed. The cyclic tetradecamer was prepared by the same convergent synthesis that was used for both the previous β-sheet targets **114** and **115**, using SPPS for the synthesis of the peptidic portions and solution phase chemistry to introduce the β-sheet templates into the oligopeptide (Schemes 2.37-2.39).

The tetrapeptide H-Ala-Val-Ile-Ala-OH (**146**) was synthesised on Wang resin in high yield (>98%) and its TFA salt isolated as a white solid after trituration with cold ether. The *C*-terminus was subsequently protected as a methyl ester, using dimethoxypropane and concentrated HCl solution, to give methyl ester **147** in good yield (95%) as the hydrochloride salt (HRMS: found $[M + Na]^+$, 411.2202. $C_{17}H_{32}O_6N_4Na$ requires 411.2220) (Scheme 2.3.7).[203] TBTU mediated coupling of methyl ester **147** with tripeptide analogue **129** yielded heptapeptide analogue **148** as a white solid in 95% yield after trituration with cold ether (HRMS: found $[M + Na]^+$, 785.4223. $C_{41}H_{58}N_6O_8Na$ requires 785.4214). Subsequent saponification of ester **148** furnished the free acid **149** in 79% yield (HRMS: found $[M + Na]^+$, 771.4053. $C_{40}H_{56}O_8N_6Na$ requires 771.4057). Peptides **147**, **148** and **149** were judged to be pure (>95%) by ^{13}C NMR spectroscopy.

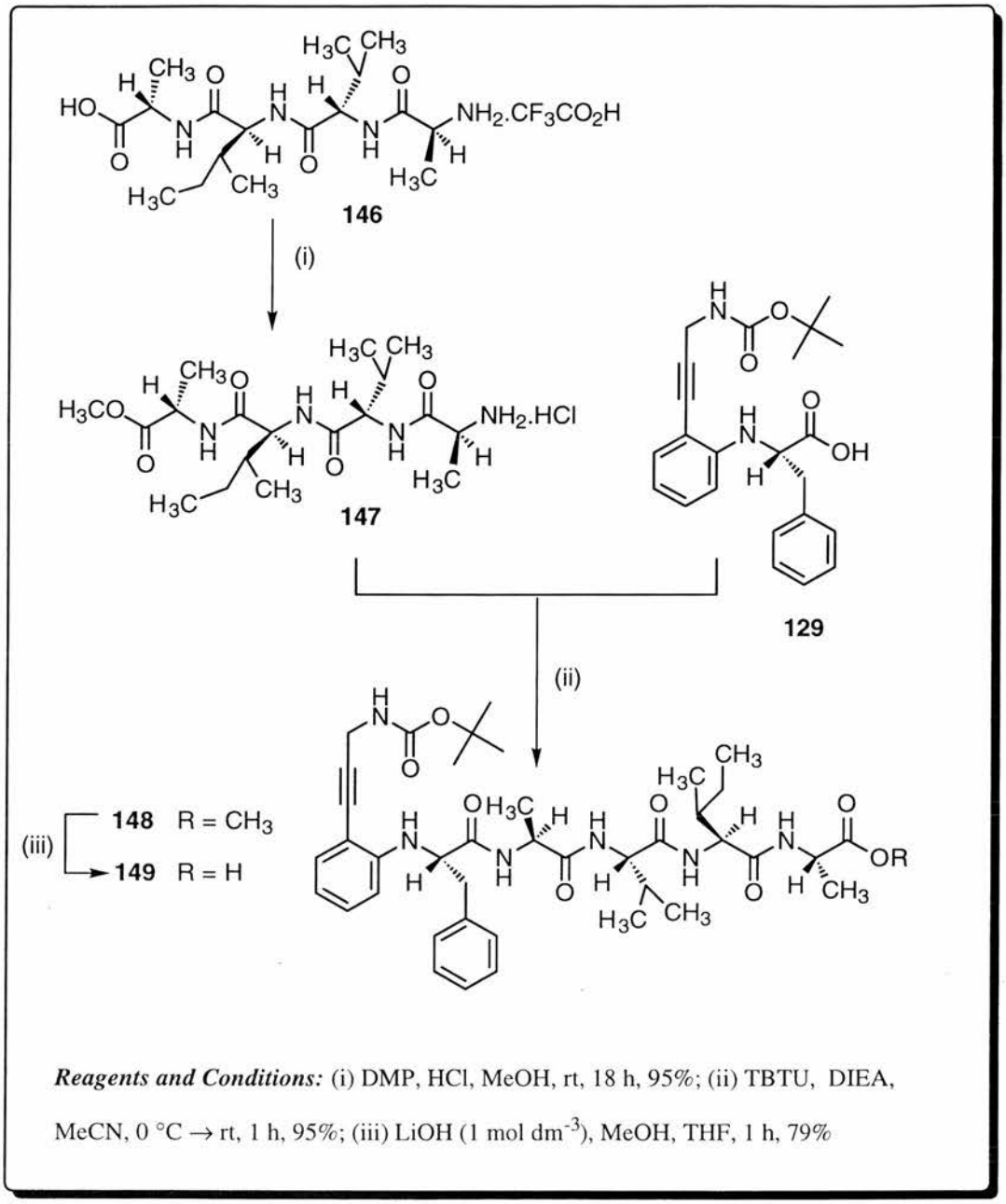

Reagents and Conditions: (i) DMP, HCl, MeOH, rt, 18 h, 95%; (ii) TBTU, DIEA, MeCN, 0 °C → rt, 1 h, 95%; (iii) LiOH (1 mol dm^{-3}), MeOH, THF, 1 h, 79%

Scheme 2.37: *Synthesis of tetradecapeptide **116**; part (i)*

The tetrapeptide H-Ala-Abu-Thr-Leu-OH (**150**) was prepared in a similar manner to tetrapeptide **146** and its TFA salt was again isolated as a white solid after trituration with cold ether. The *C*-terminus was subsequently protected as a methyl ester to give tetrapeptide **151** in good yield (99%) as the hydrochloride salt (HRMS: found [M + Na]$^+$, 425.2368. $C_{18}H_{34}N_4O_6Na$ requires 425.2376) (Scheme 2.3.8).[203] This was followed by EDCI mediated coupling of ester **151** with tripeptide analogue **129** yield to heptapeptide analogue **152** as a white solid in 52% yield after column chromatography (HRMS: found [M + Na]$^+$, 801.4155. $C_{41}H_{58}N_6O_9$ requires

801.4163). Both **151** and **152** were pure (>95%) by ^{13}C NMR spectroscopy. Finally, the *N*-terminus BOC group was removed to yield heptapeptide analogue **153** as a dihydrochloride salt in 99% recovery.

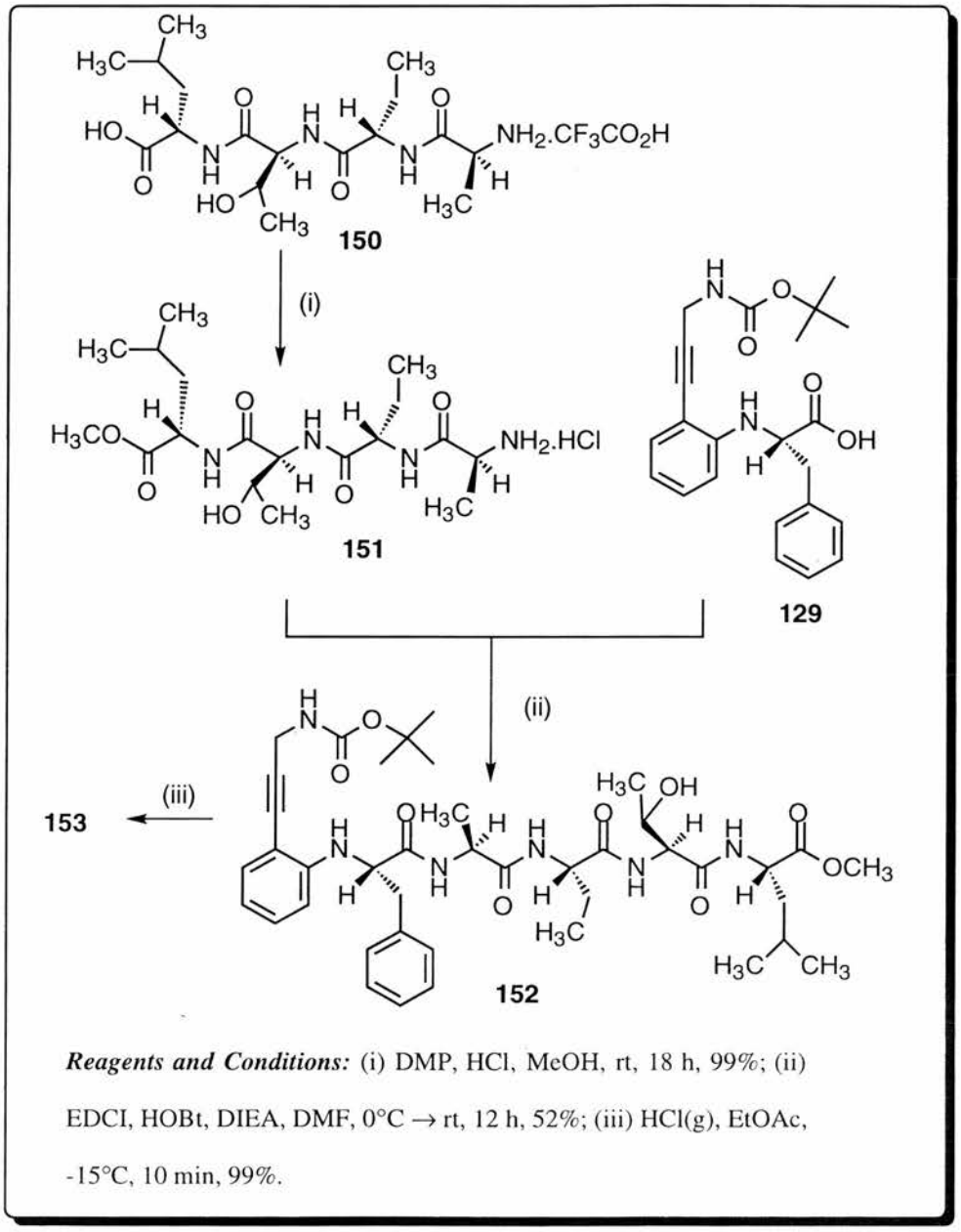

Scheme 2.38: *Synthesis of tetradecapeptide **116**; Part (ii)*

Both heptapeptide analogues **149** and **153** were combined (coupling reagent: EDCI) to furnish the acyclic tetradecapeptide analogue **154** in 35% yield as a white solid after washing with methanol (Scheme 2.39). A solution of this compound was dissolved in DMSO and added to a solution of LiOH (10 eq) in MeOH and water

(1:1). The reaction was judged complete by TLC after 2 days and gave, after aqueous acid work-up, the free acid **155** in 83% yield. This was followed by BOC deprotection [HCl(g), EtOAc] to give the fully deprotected acyclic tetradecamer **156** as a white solid in 99% yield. Cyclisation was effected with DPPA and, after 1 day, cyclised material was detected by electrospray MS; by the fourth day the reaction appeared to be complete.

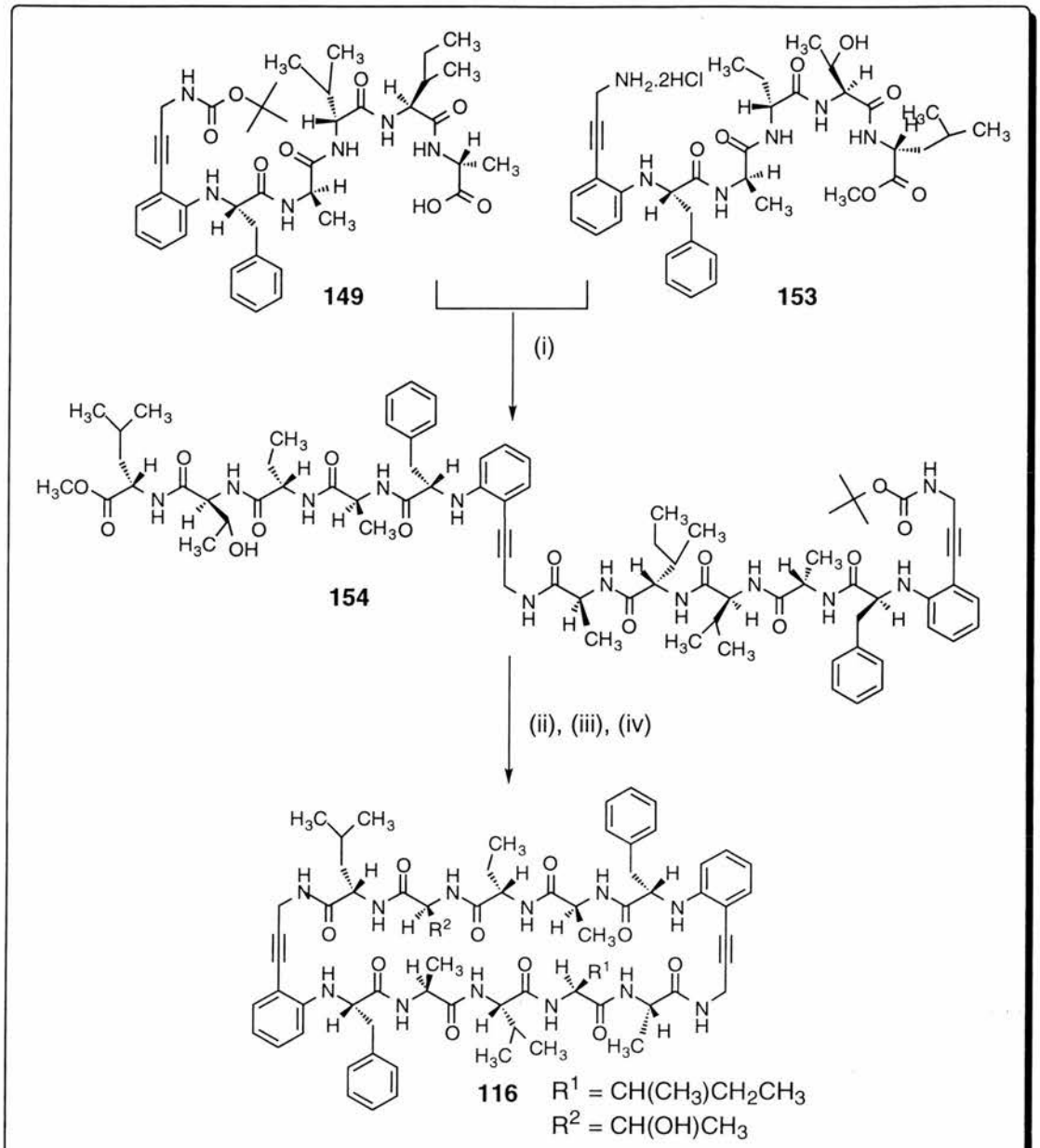

Reagents and Conditions: (i) EDCI, HOBt, DIEA, DMF, 0 °C → rt, 12 h, 35%; (ii) LiOH (1 mol dm^{-3}), MeOH, DMSO, rt, 48 h, 83%; (iii) HCl (g), EtOAc, -20°C, 15 min, 99%; (iv) DPPA, $NaHCO_3$, DMF, 0 °C → rt, 108 h, 12%.

Scheme 2.39: *Synthesis of tetradecapeptide **116**; Part (iii)*

Unfortunately, HPLC purification of the cyclised material (**116**) was problematic because of its insolubility in both acetonitrile and water. Indeed, the only solvents in which cyclic tetradecapeptide analogue **116** was soluble were DCM and $CHCl_3$; both are unsuitable solvents for reverse phase phase chromatography and no normal phase

HPLC columns were available at the time of writing. Purification was therefore carried out on a standard silica gel column with an isocratic DCM-MeOH (95:5) solvent mixture as the eluent to give cyclic peptide **116** as a white solid. Mass spectrometry of the purified compound revealed two peaks {*m/z* (ES+) $[M + 2Na]^{2+}$ = 661 and $[M + Na]^{+}$ = 1300} (Fig. 2.19) and some minor impurities, most likely ketone {*m/z* (ES+) $[M + Na]^{+}$ = 1318, 12%} and diketone {*m/z* (ES+) $[M + Na]^{+}$ = 1336, 12%}.

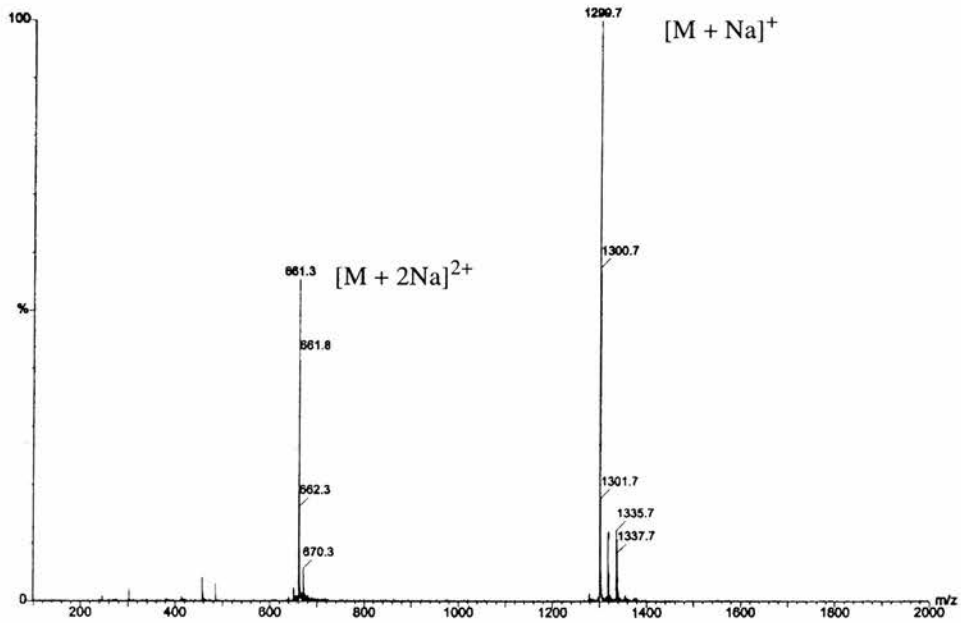

Figure 2.19: *ES+ Spectrum of* ***116***

2.6.4 NOE studies: acyclic and cyclic tetradecapeptide analogues 116 and 154

Like decapeptide analogue **115**, 2D NOE spectroscopy of cyclic tetradecapeptide **154** in d_6-DMSO only revealed sequential NOEs [9 × NH(i) ↔ α-H(i + 1), Ar-H ↔ α-H(Phe) and Ar-H ↔ α-H(Phe)], (Fig. 2.20). We were unable to obtain an NOESY spectrum from cyclic tetradecapeptide analogue **116** for comparison due to the lack of pure material available.

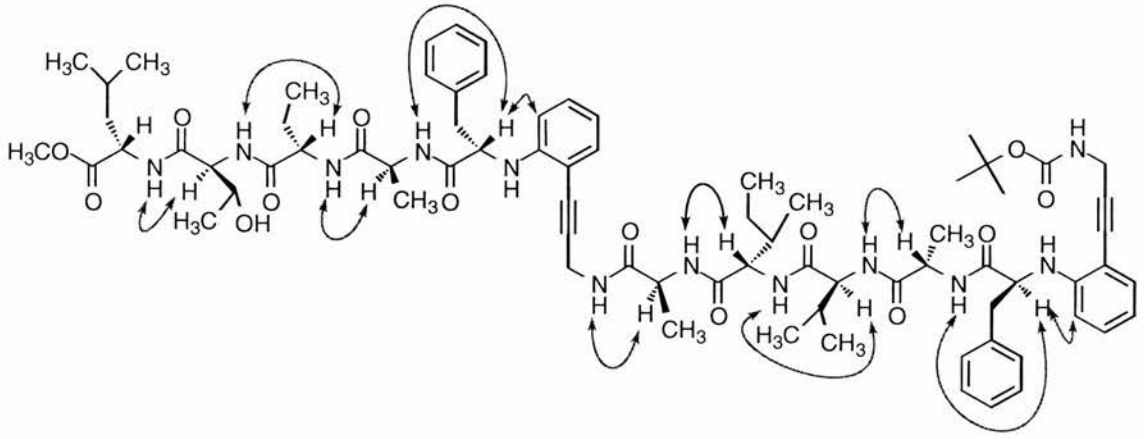

Figure 2.20:*NOE crosspeaks observed for acyclic tetradecapeptide analogue **154** in d_6-DMSO*

Like the acyclic decapeptide analogue **141**, this does not necessarily indicate that intramolecular H-bonding in not present; the molecule may simply be too conformationally mobile in solution to for it to populate a β-sheet structure to any great extent. The fact that the rate of cyclisation of **116**, a large tetradecapeptide analogue, is comparable to decapeptide analogue **115** and hexapeptide analogue **114**, suggests that β-sheet pre-formation is present to some extent in the acyclic precursor, increasing the likelihood that the *N* and *C*-termini will be in close proximity and therefore improving the rate of cyclisation.

2.7 Conclusions and Future Work.

2-(3'-Aminopropynyl)-aniline, a novel reverse turn mimic, has been successfully synthesised and incorporated into three cyclic peptides; hexapeptide analogue **114**, decapeptide analogue **115** and tetradecapeptide analogue **116**. Two of these analogues, the hexapeptide **114** and decapeptide **115**, generate spectroscopic NOE data in $CDCl_3$ solution which is consistent with a β-sheet structure.

In the future it should be possible to introduce side-chains at the 3' position of the propynyl moiety in 2-(3'-aminopropynyl)-aniline (Fig. 2.21). This will enable us to explore the effect, if any, on the ability of different analogues of this turn to stabilise β-sheets. A side-chain could also provide a means of immobilising β-sheet models into resin, thus enabling the creation of resin-bound bioseparation media based on β-sheet interactions.[204]

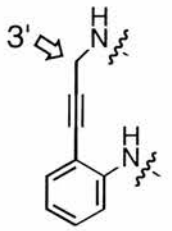

Figure 2.21: *Possible site for the introduction of functional groups and side-chains on* ***66***

A potential synthetic route would involve the coupling of 2-iodoaniline with acetylene in a palladium catalysed Heck reaction to produce amine **161** (Scheme 2.40). This could then be treated with trialkyltin chloride to give the alkenyltributyl stannane **162** to which α-halo amide **159** can be coupled in the presence of zinc chloride to produce diamine **163**.[205]

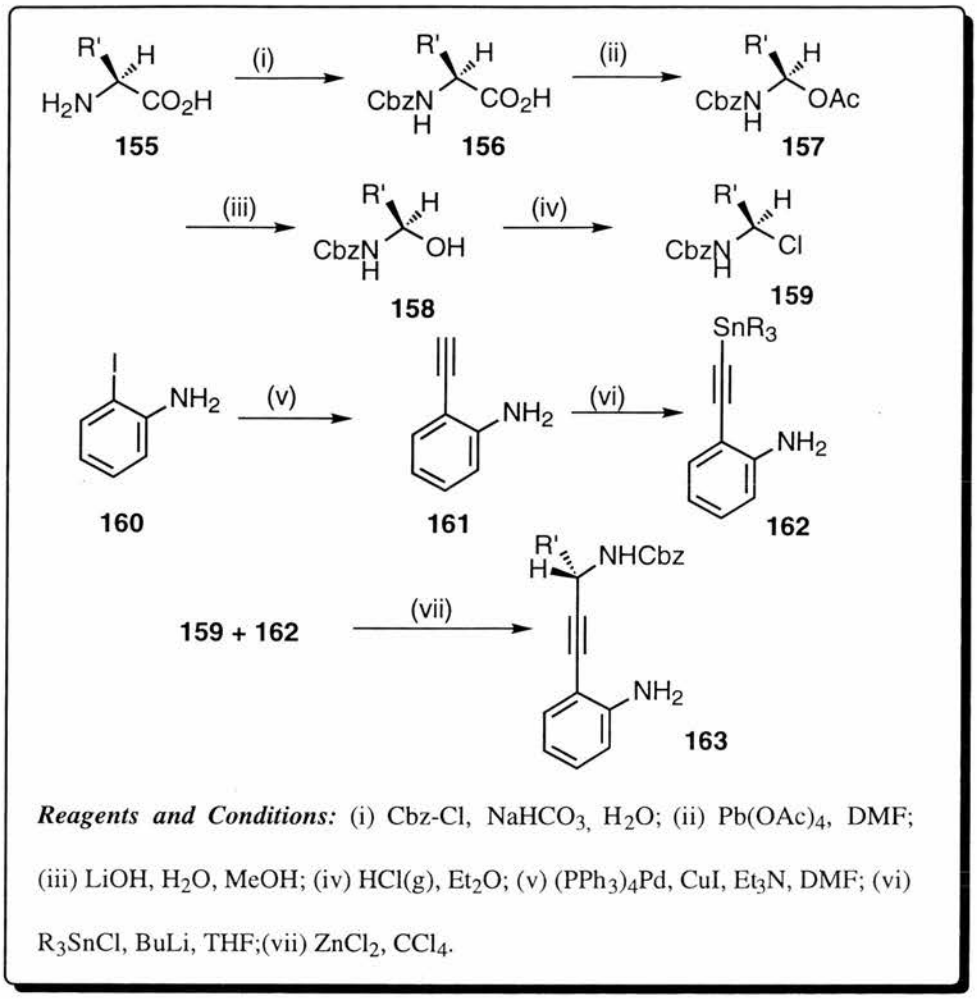

Scheme 2.40: *Introduction of functionality at the 3' position of diamine* ***66***

The mechanism of this latter reaction proceeds by attack of the acetylene π system on the cationic species generated from the halo acetal and the Lewis acid ($ZnCl_2$). Development of the positive charge on the β-acetylenic carbon can be stabilised by the adjacent trialkyltin moiety which will eventually be captured by a halide ion to generate acetylene **167** (Scheme 2.41).[206]

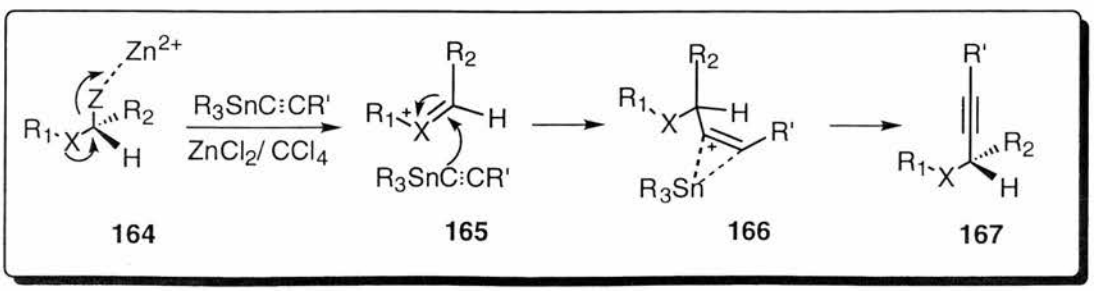

Scheme 2.41: *Mechanism of alkenylation of α-halo amides*

A range α-haloamides could be prepared by the treatment of Cbz protected amino acids with lead tetraacetate in dry dimethylformamide to form *O*-acetyl-*N*,*O*-acetals (**157**). These could then be hydrolysed in aqueous lithium hydroxide solution to furnish the non-acetylated *N*,*O*-acetals (**158**) from which α-haloamides (**159**) could be prepared by treatment with hydrochloric acid gas in diethyl ether.[207]

Ultimately, it is our intention to develop a system in which we can measure the binding interations between two complementary, cyclic β-sheet peptides and to progress to the immobilisation, on resin, of one of the partners, perhaps leading eventually to the development of novel resin-based bioseparation media. The work described in this thesis, not only provides a strong foundation for the development of this idea, but makes a useful contribution towards our understanding of β-sheet structure and protein folding.

3. EXPERIMENTAL

Experimental

Melting points were determined on an Electrothermal melting point apparatus and are uncorrected. Optical rotations were measured between 18 and 25 °C on an Optical Activity AA-1000 polarimeter using 2.5, 5 or 10 cm path length cell and are given in 10^{-1} deg cm^2 g^{-1}. Elemental microanalyses were performed in the departmental microanalytical laboratory. IR spectra were recorded on a Perkin-Elmer 1710 f.t. IR spectrometer. The samples were prepared as Nujol mulls, thin films between sodium chloride discs or KBr discs. The frequencies (υ) of absorption maxima are given in wavenumbers (cm^{-1}) relative to a polystyrene standard. NMR spectra were recorded on a Brüker AM-300 (^1H, 300 MHz; ^{13}C, 74.76 MHz), Varian 300 (^1H, 300 MHz; ^{13}C, 75.44 MHz) or Varian gemini 200 (^1H, 200 MHz; ^{13}C, 50.31 MHz) spectrometers. Chemical shifts are described in parts per million downfield from $SiMe_4$ and are reported consecutively as position (δ_H or δ_C), relative integral, multiplicity (s, singlet; d, doublet; t, triplet; q, quartet; dd, doublet of doublets; m, multiplet and br, broad), coupling constant (*J*/Hz) and assignment (numbering according to the IUPAC nomenclature for the compound). ^1H-NMR spectra were referenced internally on DOH (δ 4.68), $CHCl_3$ (δ 7.27) or DMSO (δ 2.47). ^{13}C-NMR spectra were referenced on CH_3OH (δ 49.3), $CDCl_3$ (δ 77.5), or DMSO (δ 39.7). Carbon and proton resonances of amino acids in NMR spectra are assigned as α, β, γ and δ according to normal convention. Mass spectra and accurate mass measurements were recorded on a VG 70-250 SE or a Kratos MS-50. Fast atom bombardment spectra were recorded using glycerol as a matrix. Major fragments were given as percentages of the base peak intensity (100%).

All experiments were performed at room temperature (20–25 °C) unless otherwise stated. Flash chromatography was performed according to the method of Still *et al.*[208] using Fluka C 60 (40-60 mm mesh) silica gel. Analytical thin layer chromatography was carried out on 0.25 mm precoated silica gel plates (Macherey-Nagel SIL G/UV_{254}) and compounds were visualised using UV fluorescence, iodine vapour or ninhydrin.

The solvents used were either distilled or of analar quality. Light petroleum ether refers to that portion boiling between 40 and 60 °C and ether refers to diethyl ether. Solvents were dried according to literature procedures. Ethanol and methanol were dried using magnesium turnings. DMF, CH_2Cl_2 and pyridine were distilled over CaH_2. THF and ether were dried over sodium/benzophenone and distilled under nitrogen. Thionyl chloride was distilled over sulfur and the initial fractions were always discarded. *N*-Methylmorpholine was distilled over ninhydrin. All other reagents were used without further purification.

In general, compound purity was confirmed by elemental microanalysis. In cases were a reliable microanalysis result was not possible, ^{13}C NMR spectroscopy was used as a guide to ensure that all compounds were at least 95% pure.

_N_-Benzyloxycarbonyl-5-amino-3-pentyn-1-ol (49)

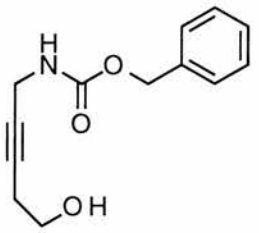

To a stirred solution of liquid ammonia (250 cm^3) at -78 °C under an atmosphere of nitrogen was added sodium metal (2.57 g) followed by a catalytic amount of $FeCl_3.6H_2O$ (40 mg). The cold bath and nitrogen supply were removed and the reaction mixture was allowed to warm up to -35 °C and allowed to stir under reflux for a further 2 h. The reaction mixture was re-cooled to -78 °C while flushing with nitrogen. Propargylamine (5.1 g, 90.0 mmol) was added *via* a glass syringe to the deep blue coloured solution of sodium amide and the reaction mixture was again refluxed at -35 °C for a further 3 h. Ethylene oxide (8.0 g, 180.0 mmol) was then added at -78 °C and the mixture was stirred under reflux for 5 h at -35 °C. The excess ammonia was gradually allowed to evaporate off over a period of 8 h. The residue was dissolved in ethanol (50 cm^3), filtered and concentrated under reduced pressure to afford a crude brown oil which resisted further purification (8.2 g, 90%).

The crude amino alcohol was dissolved in an aqueous solution of sodium carbonate (30 cm^3) and after the addition of benzyl chloroformate (17.05 g, 0.10 mol) the solution was stirred overnight at room temperature. The reaction mixture was partitioned between ethyl acetate (50 cm^3) and aqueous HCl (1 mol dm^{-3}, 50 cm^3) and the aqueous layer washed with ethyl acetate (2 × 50 cm^3). The combined organic layers were dried (Na_2SO_4) and then concnetrated under reduced pressure to afford a brown oil. Purification by flash chromatography on silica gel using ethyl acetate-light petroleum (2:3) as the eluent gave*N*-benzyloxycarbonyl-5-amino-3-pentyn-1-ol (**49**) as a colourless oil (4.3 g, 57%); (HRMS: found $[M+H]^+$, 234.1128. $C_{13}H_{16}NO_3$ requires 234.1130); υ_{max}(Nujol)/cm^{-1} 3450-3300 [OH (H-bonded) and NH, urethane],

2253 (C≡C) 1727 (C=O, urethane), 1554 (NH, urethane), 1250-1270 (C-O and C-N) and 1054 (C-OH); δ_H(200 MHz; $CDCl_3$) 2.40 (2 H, m, CH_2CH_2OH), 2.88 (1 H, br s, OH), 3.67 (2 H, t, *J* 6.2, CH_2OH), 3.91-3.94 (2 H, m, CH_2NH), 5.10 (2 H, s, CH_2Ph), 5.35 (1 H, br s, NH) and 7.33 (5 H, m, Ar-H); δ_C(75.4 MHz; $CDCl_3$) 22.98 (CH_2CH_2OH), 31.23 (CH_2NH), 60.94 (CH_2OH), 67.05 (CH_2Ph), 77.77 (C≡$C$$CH_2CH_2OH$), 80.72 ($C$≡$CCH_2CH_2OH$), 127.11, 127.71, 128.33 and 128.68 (Ar-CH), 136.46 (Ar-C, *ipso*) and 156.22 (CO, urethane); *m/z* (CI) 234 (31%, $[M + H]^+$), 152 (59, $[PhCH_2CO_2NH + H]^+$) and 91 (100, $PhCH_2^+$).

_N_-Benzyloxycarbonyl-5-amino-3-pentynoic acid (50)

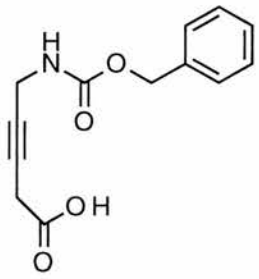

To a stirred solution of alcohol **49** (6.0 g, 24.0 mmol) in dry acetone (150 cm^3), cooled to 0 °C, was added an excess of chromic acid (41 cm^3, 0.67 mol dm^{-3}). The solution was allowed to warm to room temperature, stirred for a further 30 min and then isopropanol (30 cm^3) was added. Acetone was removed under reduced pressure and the residue was dissolved in aqueous HCl (1 mol dm^{-3}, 50 cm^3). The aqueous layer was extracted into ethyl acetate (2 × 100 cm^3) and the combined organic layers were dried (Na_2SO_4), filtered and concentrated under reduced pressure to afford the title acid as a yellow oil. Crystallisation from ethyl acetate-pet. ether afforded the acid **50** as pale yellow crystals (4.5 g, 67%), mp 85-86 °C; (HRMS: found $[M + H]^+$, 248.0928. $C_{13}H_{14}NO_4$ requires 249.0923); υ_{max}(Nujol)/cm^{-1} 3440 (NH, urethane), 2600-3110 (OH), 2280 (C≡C), 1724 (C=O, acid) 1681 (C=O, urethane), 1540 (NH, urethane) and 1250-1270 (C-O and C-N); δ_H(200 MHz; $CDCl_3$) 3.32 (2 H, s,

CH_2CO_2H), 4.01 (2 H, m, CH_2NH), 5.15 (2 H, s, CH_2Ph), 6.55 (1 H, br s, NH), 7.20-7.40 (5 H, m, Ar-H) and 8.75 (1 H, br s, CO_2H); δ_C(75.4 MHz; $CDCl_3$) 26.36 (CH_2CO_2H), 31.18 (CH_2NH), 67.25 (CH_2Ph), 74.90 and 79.68 (C≡C), 128.32, 128.40 and 128.69 (Ar-CH), 136.29 (Ar-C, *ipso*), 156.37 (C=O, urethane) and 173.06 (CO, acid); *m/z* (CI) 248 (100%, $[M + H]^+$), 204 (100, $[M - CO_2H + H]^+$), 147 (39), 136 (26), 114 (23), 96 (22) and 91 (45).

_N_-Benzyloxycarbonyl propargylamine (52)

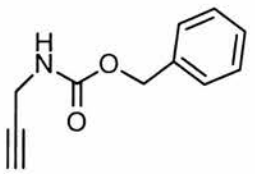

To a vigorously stirred solution of $NaHCO_3$ (4.2 g, 40 mmol) in water (25 cm^3) was added, dropwise, propargylamine (3.72 g, 20 mmol). The mixture was cooled to 0 °C and then benzylchloroformate (3.11 cm^3, 20 mmol) was then added dropwise over a period of 1 h. The resultant reaction mixture was then stirred overnight at room temperature before being partitioned between ethyl acetate (20 cm^3) and aqueous HCl (1 mol dm^{-3}, 25 cm^3). The aqueous layer was extracted further with ethyl acetate (2 × 50 cm^3) and the combined organic layers were dried (Na_2SO_4), filtered and concentrated under reduced pressure to give a colourless oil. Recrystallisation from ethyl acetate-pet. ether gave the *N*-benzyloxycarbonyl propargylamine (**52**) as white crystals (2.72 g, 80%), mp 36.5 °C; (HRMS: found M^+, 189.0781. $C_{11}H_{11}NO_2$ requires 189.0790); υ_{max}(Nujol)/cm^{-1} 3340 (CH, acetylene), 3320 and 3220 (NH, urethane), 3055 (CH, aromatic), 2118 (C≡C), 1721 (C=O, urethane), 1520-1530 (NH, urethane), 1220-1315 (C-O and C-N); δ_H(200 MHz; $CDCl_3$) 2.25 (1 H, s, C≡CH), 3.95 (2 H, s, CH_2NH), 5.05-5.15 (3 H, m, OCH_2Ph and NH) and 7.35 (5 H, m, Ar-H); δ_C(50.31 MHz; $CDCl_3$) 31.30 (CH_2NH), 67.57 (CH_2Ph), 72.11 (C≡CH), 80.40

($C{\equiv}CCH_2$), 128.72 and 129.05 (Ar-CH), 136.75 (Ar-C, *ipso*) and 156.59 (CO); *m/z* (EI) 189 (9%, M^+), 107 (16, OCH_2Ph^+), 91 (100, CH_2Ph^+) and 77 (14, Ph^+).

N-tert-Butyloxycarbonyl propargylamine (63)

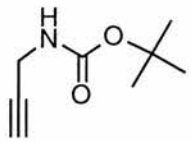

To a stirred solution of $Na_2CO_3.10H_2O$ (5.15 g, 18.0 mmol) in water (20 cm^3) and dioxane (10 cm^3) was added propargylamine (1.16 cm^3, 18.0 mmol). The reaction mixture was cooled to 0 °C and di-*tert*-butylpyrocarbonate (2.4 g, 11.0 mmol) was added and stirring continued at room temperature for 30 min. The solution was concentrated under reduced pressure to 30% of its original volume, cooled to 0 °C and extracted with ethyl acetate (2 × 20 cm^3). The organic extracts were washed with aqueous HCl (0.5 mol dm^{-3}, 30 cm^3), dried (Na_2SO_4) and concentrated under reduced pressure to give a white solid which was recrystallised from ethyl acetate-pet. ether (1:1) to give *N-tert*-butyloxycarbonyl propargylamine (**63**) as white crystals (2.1 g, 79%), mp 40-42 °C; (Found: C, 62.2; H, 8.5; N, 9.1. $C_8H_{13}NO_2$ requires C, 61.9; H, 8.4; N 9.0%); υ_{max}(Nujol)/cm^{-1} 3300 (CH, acetylene), 3270 (NH, urethane), 2129 (C≡C), 1677 (C=O, urethane) 1540 (NH, urethane) and 1260-1300 (C-O and C-N); δ_H(200 MHz; $CDCl_3$) 1.36 [9 H, s, $C(CH_3)_3$], 2.17 (1 H, s, C≡CH), 3.84 (2 H, s, CH_2NH), and 5.11 (1 H, br s, NH); δ_C(74.76 MHz; $CDCl_3$) 28.24 [$C(CH_3)_3$)], 30.21 (CH_2N), 71.14 (HC≡C), 79.89 and 80.23 [$C(CH_3)_3$ and HC≡C] and 155.48 (CO); *m/z* (CI) 156 (10%, $[M + H]^+$), 140 (3, $[M + H - CH_4]^+$) and 100 (100, $[M + 2H - C_4H_9]^+$).

2-(3'-*tert*-Benzyloxycarbonylamino-prop-1'-ynyl)-phenylamine (64)

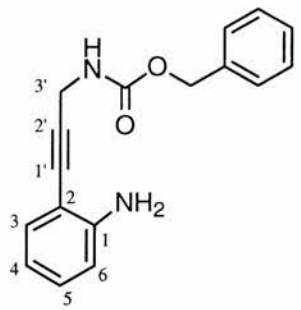

To a mixture of DMF (10 cm^3) and diisopropylamine (5 cm^3) was added 2-iodoaniline (1.0 g, 3.0 mmol) followed by bis(triphenylphosphine) palladium dichloride (0.1 g, 0.1 mmol), *N*-benzyloxycarbonyl propargylamine (**52**) (0.5 g, 3.0 mmol) and copper (I) iodide (0.05 g, 0.25 mmol). The reaction mixture was then stirred at room temperature, in the absence of light, for 5 h under nitrogen. The resulting brown solution was concentrated under reduced pressure to give a dark brown liquid. Saturated ammonium chloride solution (100 cm^3) was added to the reaction mixture and the resulting brown suspension was extracted into ethyl acetate (2×75 cm^3). The combined organic extracts were washed with water (2×75 cm^3), brine (50 cm^3), dried (Na_2SO_4) and then concentrated under reduced pressure to yield a brown oil. Purification of the crude product by flash chromatography on silica gel using ethyl acetate-petroleum ether (1:4) as the eluent afforded 2-(3'-*tert*-benzyloxycarbonylamino-prop-1'-ynyl)-phenylamine (**64**) as a pale yellow solid (0.6 g, 78%), mp 80-83 °C; (HRMS: found M^+, 280.1219. $C_{17}H_{16}N_2O_2$ requires 280.1212); υ_{max}(Nujol)/cm^{-1} 3300 and 3400 (NH_2), 1680 (C=O, urethane), 1540 (NH, urethane) and 1230-1260 (C-O and C-N); δ_H(200 MHz; $CDCl_3$) 4.10-4.30 (4 H, m, PhNH_2 and CH_2NH), 5.15 (2 H, m, CH_2Ph), 5.40 (1 H, br s, NH, urethane), 6.60-6.75 (2 H, m, 4-CH and 6-CH), 7.12 (1 H, m, 5-CH), 7.25 (1 H, m, 3-CH) and 7.35 (5 H, m, Ar-H, Cbz); δ_C(50.30 MHz; $CDCl_3$) 32.40 (CH_2N), 67.56 (CH_2Ph), 74.94 and 80.51 (C≡C), 107.59 (2-C), 114.70 (6-CH), 118.22 (4-CH), 128.01 and 128.06 (Ar-CH, Cbz), 130.33 (5-CH), 132.70 (3-CH) 136.77 and 148.72 [Ar-C, *ipso* (Cbz and 1-C)] and 158.52 (CO); *m/z* (EI) 280 (75%, M^+), 189 (70), 145 (80) and 91 (100).

2-(3'-*tert*-Butoxycarbonylamino-prop-1'-ynyl)-phenylamine (65)

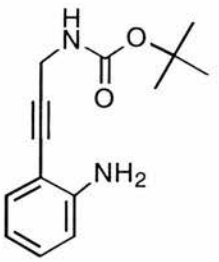

This compound was prepared in a manner identical to that for 2-(3'-*tert*-benzyloxycarbonylamino-prop-1'-ynyl)-phenylamine (**64**), using *N*-*tert*-butyloxycarbonyl propargylamine (**63**) (1.0 g, 6.45 mmol). The crude product was purified by flash chromatography on silica gel using ethyl acetate-petroleum ether (1:4) as the eluent to give 2-(3'-*tert*-butoxycarbonylamino-prop-1'-ynyl)-phenylamine (**65**) as a yellow solid (1.2 g, 77%), mp 80-83 °C; (Found: C, 68.2; H, 7.5; N, 11.4. $C_{14}H_{18}N_2O_2$ requires C, 68.3; H, 7.5; N, 11.4%); υ_{max}(Nujol)/cm^{-1} 3390-3450 (NH_2), 2225 (C≡C), 1674 (C=O, urethane), 1575 (NH, urethane) and 1240-1320 (C-O and C-N); δ_H(200 MHz, $CDCl_3$); 1.46 [9 H, s, $C(CH_3)_3$], 4.16 (2 H, m, CH_2NH), 4.25 (2 H, br s, NH_2), 4.98 (1 H, br s, NH, urethane), 6.65 (2 H, m, 4-CH and 6-CH), 7.10 (1 H, t, *J* 7.7, 5-CH) and 7.22 (1 H, d, *J* 7.7, 3-CH); δ_C(74.76 MHz, $CDCl_3$), 28.88 [$C(CH_3)_3$], 31.95 (CH_2NH), 80.32, 80.40 and 91.35 [$C(CH_3)_3$ and C≡C], 107.50 (2-C), 114.75 (6-CH), 118.18 (4-CH), 130.21 (5-CH), 132.64 (3-CH), 148.72 (1-C) and 156.00 (CO); *m/z* (EI) 246 (33%, M^+), 190 (36, [M - C_4H_9 + H]$^+$), 130 (83, [M - $NHCO_2C_4H_9$]$^+$) and 49 (100).

2-(3'-amino-prop-1'-ynyl)-phenylamine (66)

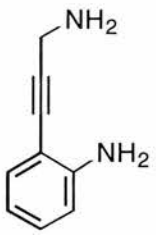

To a stirred solution of 2-(3'-*tert*-benzyloxycarbonylamino-prop-1'-ynyl)-phenylamine (**64**) in dichloromethane (60 cm^3) was added dimethylsulfide (15.6 cm^3) and $BF_3.Et_2O$ (10.1 cm^3). An additional amount of dimethylsulfide was added after 1 h and the solution was stirred at room temperature for a further 3 h. The volatile materials were removed under reduced pressure and the residue was partitioned between aqueous HCl (1 mol dm^{-3}, 50 cm^3) and ethyl acetate (50 cm^3). The aqueous layer was treated with aqueous ammonia solution (30 cm^3, 10% w/v) and extracted with ethyl acetate (2 × 50 cm^3). The latter organic phases were combined, washed with brine (50 cm^3), dried (Na_2SO_4) and then concentrated under reduced pressure to give the diamine **66** as a pale yellow oil (0.93 g, 78%); (HRMS: found M^+, 146.0838. $C_9H_{10}N_2$ requires 146.0844); υ_{max}(Thin film)/cm^{-1} 3250-3500 (NH_2), 2750-3000 (ArC-H and C'-H) and 1940-2100 (C≡C); δ_H(200 MHz; $CDCl_3$) 1.40-1.90 (2 H, br s, CH_2NH_2), 3.65 (2 H, m, CH_2NH_2), 3.90-4.30 (2 H, br s, $PhNH_2$), 6.65 (2 H, m, 6-CH and 4-CH), 7.10 (1 H, m, 3-CH) and 7.22 (1 H, m, 5-CH); δ_C(50.30 MHz; $CDCl_3$) 32.15 (CH_2NH_2), 79.23 and 95.44 (C≡C), 107.99 (2-C), 114.42 (6-CH), 118.02 (4-CH), 129.58 (5-CH), 132.30 (3-CH) and 147.97 (1-C); *m/z* (EI) 146 (87%, M^+), 130 (100, $[M - NH_2]^+$), 117 (46, $[M - CH_2NH_2 + H]^+$), 102 (23), 89 (22) and 77 (19).

Methyl (2*S*)-2-hydroxy-4-methyl pentanoate (85)

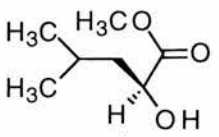

(2*S*)-Leucine (15 g, 114 mmol) was added in one portion to a solution of sulfuric acid (180 cm^3, 0.5 mol dm^{-3}). Upon cooling to 0 °C, a solution of sodium nitrite (11.9 g, 346.5 mmol) in water (145 cm^3) was added dropwise over 2 h and the mixture then warmed to room temperature for a further 12 h. The pH was adjusted to 6 with solid sodium bicarbonate and the solution concentrated under vacuum to 30 cm^3 (bath temperature 50 °C). The pH was adjusted to 3 with phosphoric acid (40% v/v) and the product extracted with tetrahydrofuran (3 × 100 cm^3). The combined organic extracts were then washed with brine (2 × 100 cm^3), dried (Na_2SO_4) and reconcentrated twice from toluene to give an oil that solidified on standing. The solid was triturated with pet. ether and dried under vacuum to yield (2*S*)-2-hydroxy-4-methyl pentanoic acid (**82**) as a colourless, crystalline solid (11.2 g, 75%); δ_H(200 MHz; $CDCl_3$) 0.95 [6 H, m, $CH_2CH(CH_3)_2$], 1.59 [2 H, m, $CH_2CH(CH_3)_2$], 1.86 [1 H, m, $CH_2CH(CH_3)_2$)], 4.28 (1 H, m, $CHCO_2H$), 7.88 and 7.89 (2 H, br s, CO_2H and OH); δ_C(75.44 MHz; $CDCl_3$) 21.83 and 23.69 [$(CH_3)_2CHCH_2$], 24.91 [$(CH_3)_2CHCH_2$], 43.49 [$(CH_3)_2CHCH_2$], 69.44 and 128.10 (CF_3) and 180.53 (CO_2H).

To an ice-cooled solution of (2*S*)-2-hydroxy-4-methyl pentanoic acid (**82**) (9.42 g, 71 mmol) in dry methanol (30 cm^3) was added, dropwise, thionyl chloride (6.2 cm^3, 85.0 mmol) over a period of 30 min. The reaction mixture was then refluxed for a further 2 h, allowed to cool and the pH adjusted to 6 with solid sodium bicarbonate. The resulting suspension was then concentrated under reduced pressure to give a residue which was partitioned between water (150 cm^3) and diethyl ether (150 cm^3). The aqueous phase was extracted further with diethyl ether (3 × 150 cm^3), and the organic extracts combined, dried (Na_2SO_4) and concentrated under reduced pressure (bath temperature: 20 °C) to yield a yellow liquid; Kugelrohr distillation under

reduced pressure afforded ester **85** as a colourless oil (8.2 g, 79%), bp 75-85 °C (~10 mmHg); $[\alpha]_D^{18}$ -4.5 (*c* 5.0, CH_2Cl_2) [lit.,[209] -4.2 (*c* 5.0, CH_2Cl_2)]; δ_H(200 MHz; $CDCl_3$) 0.92 [6 H, m, $(CH_3)_2CH$], 1.53 [2 H, m, $CH_2CH(CH_3)_2$], 1.85 [1 H, m, $CH_2CH(CH_3)_2$], 2.50 (1 H, s, OH), 3.75 (3 H, s, OCH_3) and 4.19 (1 H, m, $CHCO_2CH_3$); δ_C(75.44 MHz; $CDCl_3$) 21.45 and 23.10 [$CH(CH_3)_2$], 24.29 [$CH_2CH(CH_3)_2$], 43.43 [$CH_2CH(CH_3)_2$], 52.33 (OCH_3), 69.06 ($CHCO_2CH_3$) and 176.46 (CO_2CH_3); *m/z* (EI) 147 (4%, $[M + H]^+$), 87 (76, $[M - CO_2CH_3]^+$), 69 (100, $[M - CO_2CH_3 - H_2O]^+$), 50 (10) and 43 (73).

Benzyl 2-[2'-(3''-*tert*-Benzyloxycarbonylamino-prop-1''-ynyl)-phenylamino]-ethanoate acid (89)

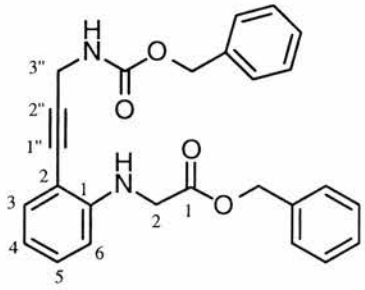

Glycolic acid (10.0 g, 0.13 mol) and triethylamine (18.1 cm^3, 0.13 mol) were dissolved in ethyl acetate (60 cm^3) and the reaction mixture treated with benzyl chloride (13.4 cm^3, 0.12 mol). After 6 h of reflux, the resulting white precipitate was filtered off and the filtrate concentrated under reduced pressure to give a colourless oil which was purified by flash chromatography on silica [eluent: pet. ether-ethyl acetate (4:1)] to give benzyl 2-hydroxy ethanoate (**83**) as a colourless oil (12.65 g, 58%); δ_H(200MHz, $CDCl_3$) 2.86-2.92 (1 H, m, OH), 4.21 (2 H, d, *J* 5.8, CH_2OH), 5.22 (2 H, s, CH_2Ph) and 7.37 (5 H, m, Ar-H); δ_C(50.30 MHz; $CDCl_3$) 61.19 (CH_2OH), 67.73 (CH_2Ph), 129.01, 129.16, and 129.20 (Ar-CH), 135.54 (Ar-C, *ipso*) and 173.80 (CO).

A solution of benzyl 2-hydroxy ethanoate (**83**) (1.4 g, 8.43 mmol) in dichloromethane (40 cm^3) was cooled to -78 °C and 2,6-lutidine was added (1.1 cm^3), followed by slow addition of trifluoromethane sulphonic anhydride (1.5 cm^3, 9.43

mmol). After 0.5 h, the red mixture was added to water (50 cm^3) and the organic phase separated, dried (Na_2SO_4), concentrated under reduced pressure and purified by column chromatography [eluent: pet. ether-dichloromethane (2:1)] to give benzyl (2*S*)-2-[(trifluoromethylsulfonyl)oxy] ethanoate (**86**) as a colourless oil with the expected spectroscopic and analytical properties (1.98 g, 79%); δ_H(200MHz, $CDCl_3$) 4.94 (2 H, s, CH_2OTf), 5.29 (2 H, s, CH_2Ph) and 7.41 (5 H, m, Ar-H); δ_C (50.30 MHz; $CDCl_3$) 68.80 (CH_2OTf), 69.43 (CH_2Ph), 110-124 (CF_3), 129.15, 129.28 and 129.49 (Ar-CH), 134.72 (Ar-C, *ipso*) and 164.97 (CO).

A solution of triflate **86** (0.07g, 0.22 mmol), phenylacetylene **64** (0.06g, 0.21 mmol) and 2,6-lutidine (0.03 cm^3, 0.23 mmol) in 1,2-dichloroethane (7 cm^3) was stirred and heated at 70 °C for 7 h. After cooling to room temperature, the solution was applied directly to a flash silica column and eluted with ethyl acetate-pet. ether (1:3) to give benzyl ester **89** as a colourless oil (57.7 mg, 63%); (HRMS: found M^+, 428.1727. $C_{26}H_{24}N_2O_4$ requires 428.1736); $\upsilon_{max}(CH_2Cl_2)/cm^{-1}$ 3250-3470 (NH, urethane and amine), 2810-2950 (ArC-H and CH), 1675-1790 (C=O, urethane and ester); δ_H(300 MHz; $CDCl_3$) 4.00 (2 H, d, *J* 5.7, $CH_2CO_2CH_2Ph$), 4.27 (2 H, d, *J* 5.5, CH_2NH), 5.20 (5 H, m, 2 × CH_2Ph and N*H*Ph), 6.44 (1 H, d, *J* 8.3, 6'-CH), 6.68 (1 H, t, *J* 7.4, 4'-CH), 7.18 (1 H, m, 5'-CH), 7.29 (1 H, m, 2'-CH) and 7.40 (10 H, m, Ar-H, Cbz and Bn); δ_C(50.30 MHz; $CDCl_3$) 32.43 (CH_2NH), 45.95 ($CH_2CO_2CH_2Ph$), 67.62 (2 × CH_2Ph), 80.48 and 91.53 (C≡C), 108.01 (Ar-C2), 110.13 (Ar-CH6), 117.74 (Ar-CH4), 128.69, 128.92, 129.05 and 129.16 (Ar-CH, Cbz and Bn), 130.58 (Ar-CH5), 132.79 (Ar-CH3), 136.80 [Ar-C, *ipso* (Cbz and Bn)], 148.47 (1'-C), 156.00 (CO, urethane) and 171.12 (CO, benzyl ester); *m/z* (EI) 428 (15%, M^+), 293 (10) and 91 (100, CH_2Ph^+).

Benzyl (2*R*)-2-[2'-(3''-*tert*-benzyloxycarbonylamino-prop-1''-ynyl)-phenylamino]-propanoate (90)

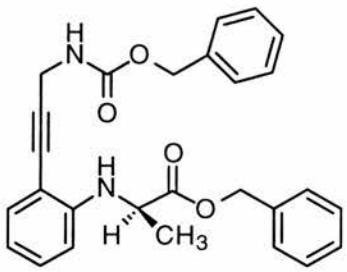

To a stirred solution of (2*S*)-lactic acid (10.0 g, 0.11 mol) and thionyl chloride (1.6 cm^3, 22.0 mmol) in dry toluene (200 cm^3) was added benzyl alcohol (45.5 cm^3). After stirring for 1 h, the solution was heated at reflux with continuous water removal (Dean-Stark trap) for 10 h. An additional amount of thionyl chloride (1.6 cm^3, 22.0 mmol) was added and the reaction continued for a further 10 h. After cooling, the solution was diluted with ether (200 cm^3) and washed successively with sodium bicarbonate solution (100 cm^3, 1 mol dm^{-3}), water (100 cm^3) , brine (100 cm^3) and then dried (Na_2SO_4). The organic extract was then concentrated under reduced pressure to give an oil which was subsequently purified flash silica column chromatography using pet. ether-ethyl acetate (2:1) as the eluent to afford **84** as a colourless oil (8.91 g, 55%); δ_H(200MHz, $CDCl_3$) 1.42 (3 H, m, CH_3), 3.32 (1 H, m, OH), 4.35 (1 H, m, C*H*CH_3), 5.20 (2 H, s, CH_2Ph) and 7.37 (5 H, m, Ar-H); δ_C (50.30 MHz; $CDCl_3$) 21.00 (CH_3), 67.20 and 67.90 (*C*H_2Ph and *C*HCH_3), 128.00-130.00 (Ar-CH and Ar-C, *ipso*) and 176.00 (CO).

A solution of benzyl (2*S*)-2-hydroxy propanoate (**84**) (0.5 g, 2.78 mmol) in dichloromethane (10 cm^3) was cooled to -78 °C and 2,6-lutidine was added (0.42 cm^3), followed by slow addition of trifluoromethane sulphonic anhydride (0.5 cm^3, 2.78 mmol). After 30 min, the red mixture was added to water (50 cm^3) and the organic phase separated, dried (Na_2SO_4), concentrated under reduced pressure. The resulting crude oil was purified by flash silica column chromatography using pet. ether-dichloromethane (2:1) as the eluent to give benzyl (2*S*)-2-

[(trifluoromethylsulfonyl)oxy] propanoate **87** as a colourless oil (0.67 g, 77%); δ_H(200 MHz; $CDCl_3$) 1.71 (3 H, d, *J* 6.87, CH_3), 5.26 (3 H, m, CH_2Ph and C*H*CH_3) and 7.36-7.39 (5 H, m, Ar-H); δ_C(75.44 MHz; $CDCl_3$) 18.02 (CH_3), 68.36 (CH_2Ph), 80.05 (*C*HCH_3), 128.57, 128.89 and 129.00 (Ar-CH), 135.50 (Ar-C, *ipso*) and 167.46 (CO).

A stirred solution of triflate **87** (0.11g, 0.34 mmol), phenylacetylene **64** (0.09 g, 0.32 mmol) and 2,6-lutidine (0.04 cm^3, 0.35 mmol) in 1,2-dichloroethane (15 cm^3) was heated at 70 °C for 7 h. After cooling to room temperature, the solution was applied directly to a silica column and elution with ethyl acetate-pet. ether (1:3) gave benzyl propanoate **90** as a colourless oil (0.12 g, 85%); (HRMS: found M^+, 442.1887. $C_{27}H_{26}N_2O_4$ requires 442.1892); $[\alpha]_D^{18}$ -4.0 (*c* 0.1, CH_2Cl_2); υ_{max}(Thin film)/cm^{-1} 3050-3575 (NH, urethane and amine), 2850-2970 (ArC-H and CH), 1655-1750 (C=O, urethane and ester); δ_H(300 MHz; $CDCl_3$) 1.55 (3 H, d, CH_3), 4.24 (3 H, m, CH_2N and C*H*CH_3), 5.19 (6 H, m, 2 × C*H*$_2$Ph and NH, urethane and amine), 6.49 (1 H, m, 6'-CH), 6.65 (1 H, m, 4'-CH), 7.15 (1 H, m, 5'-CH) and 7.21-7.42 (11 H, m, Ar-H, Cbz and Bn, and 3'-CH); δ_C(75.44 MHz; $CDCl_3$) 18.74 (CH_3), 31.98 (CH_2N), 51.86 (*C*HCH_3), 67.01 and 67.12 (2 × CH_2Ph), 80.13 and 91.12 (C≡C), 107.79 (2'-C), 110.17 (6'-CH), 117.36 (4'-CH), 128.32, 128.53, 128.70 and 128.76 (Ar-CH, Cbz and Bn), 130.19, (5'-CH), 132.62 (3'-CH), 135.69 and 136.49 [Ar-C, *ipso* (Cbz and Bn)], 147.81 (1'-C), 156.50 (CO, urethane) and 174.16 (CO, Bn); *m/z* (EI) 442 (15%, M^+), 307 (32, [M - CO_2CH_2Ph]$^+$), 280 (45), 248 (72), 192 (100), 162 (35), 134 (85) and 91 (55, CH_2Ph^+).

Methyl (2*R*)-2-[2'-(3''-*tert*-benzyloxycarbonylamino-prop-1'-ynyl)-phenylamino]-4-methyl-pentanoate (91)

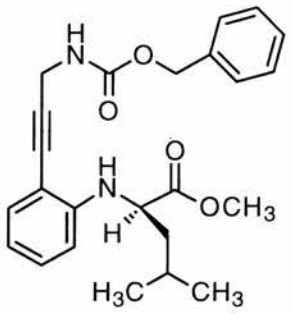

To a stirred solution of methyl (2*S*)-2-hydroxy-4-methyl pentanoate (**85**) (0.75 g, 5.14 mmol) in dry dichloromethane (20 cm^3), cooled to -78 °C and under an N_2 atmosphere, was added 2,6-lutidine (0.78 cm^3, 6.67 mmol), followed by the slow addition of trifluromethanesulfonic anhydride (0.9 cm^3, 5.14 mmol). After 1 h, the red mixture was warmed to room temperature and poured into water (50 cm^3). The organic phase was separated, dried (Na_2SO_4), and concentrated under reduced pressure to an oil. Purification by flash silica chromatography using dichloromethane-pet. ether (1:2) as the eluent, gave methyl (2*S*)-2-[(trifluoromethylsulfonyl)oxy]-4-methyl pentanoate (**88**) as a colourless oil (1.1 g, 77%).

A stirred solution of triflate **88** (0.7 g, 2.52 mmol), phenylacetylene **64** (0.67 g, 2.4 mmol) and 2,6-lutidine (0.3 cm^3, 2.64 mmol) in 1,2-dichloroethane (10 cm^3) was heated at 80 °C for 24 h, under an nitrogen atmosphere. After cooling to room temperature, the solution was applied directly to a silica column and elution with ethyl acetate-pet. ether (1:3) gave the title ester **91** as a colourless oil (0.67 g, 69%); (HRMS: found M^+, 408.2058. $C_{24}H_{28}O_4N_2$ requires 408.2049); $[\alpha]_D^{25}$ -7.6 (*c* 0.5, CH_2Cl_2); υ_{max}(Thin film)/cm^{-1} 3350-3450 (NH, urethane and amine), 2810-2875 (ArCH and CH), 2221 (C≡C), 1650-1750 (C=O, ester and urethane), 1250 (C-N, urethane), 1166 (C-O, ester); δ_H(300 MHz; $CDCl_3$) 0.97 (6 H, dd, J_1 11.8, J_2 6.2, 2 × CH_3, Leu), 1.70-1.90 (3 H, m, β-H_2 and γ-H, Leu), 3.70 (3 H, s, OCH_3), 4.07-4.16 (1 H, m, α-H, Leu), 4.26 (2 H, d, *J* 5.8, CH_2NH), 4.91 (1 H, m, NH, amine), 5.15 (3 H, m, CH_2Ph and NH, urethane), 6.52 (1 H, d, *J* 8.24, 6'-CH), 6.64 (1 H, m, 4'-CH), 7.16

(1 H, m, 3'-CH) and 7.25 (1 H, m, 5'-CH) and 7.30-7.40 (5 H, m, Ar-H, Cbz); δ_C(50.30 MHz; $CDCl_3$) 22.27 and 22.70 (2 × CH_3, Leu), 24.94 (γ-C, Leu) 31.92 (CH_2N), 41.99 (β-C, Leu), 52.13 (OCH_3), 54.97 (α-C, Leu), 67.07 (CH_2Ph), 80.09 and 90.99 (C≡C), 107.70 (2'-C), 110.03 (6'-CH), 117.27 (4-CH), 128.26, 128.32 and 128.67 (Ar-CH, Cbz), 130.21 (5'-CH), 132.62 (3'-CH), 136.46 [Ar-C, *ipso* (Cbz)], 148.15 (1'-C), 156.00 (CO, urethane) and 174.86 (CO, ester); *m/z* (EI) 408 (65%, M^+), 349 (95, $[M - CO_2CH_3]^+$) and 91 (100, $PhCH_2^+$).

Methyl 2-[2'-(3''-*tert*-butoxycarbonylamino-prop-1''-ynyl)-phenylamino]-ethanoate (106)

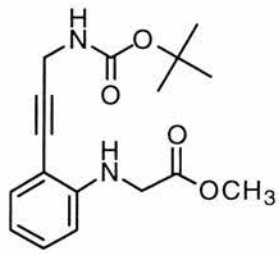

A stirred solution of glycolic acid (10.0 g, 0.13 mol) in dry methanol (25 cm^3) was cooled on an ice-bath and then thionyl chloride (13 cm^3) was added dropwise over a period of 30 min. The reaction mixture was then refluxed for a further 2 h, allowed to cool and the pH adjusted to 6 with solid sodium bicarbonate. The resulting suspension was concentrated under reduced pressure to give a residue which was partitioned between water (150 cm^3) and diethyl ether (150 cm^3). The aqueous phase was extracted further with diethyl ether (3 × 100 cm^3), and the organic extracts combined, dried (Na_2SO_4) and concentrated under reduced pressure (bath temperature: 30 °C). The resulting yellow oil was distilled under reduced pressure to yield methyl glycolate (**97**) as a colourless oil (7.37 g, 63%); υ_{max}(Thin film)/cm^{-1} 1744 (C=O, ester) and 3399 (O-H); δ_H(300 MHz; $CDCl_3$) 3.20 (1 H, m, OH), 3.75 (3 H, s, OCH_3) and 4.22 (2 H, br s, CH_2); δ_C(50.30 MHz; $CDCl_3$) 52.72 (OCH_3), 60.94 (CH_2) and 174.30 (CO, ester).

Under an N_2 atmospshere, a stirred solution of methyl glycolate (0.92 g, 0.01 mmol) in dry dichloromethane was cooled to -78 °C and 2,6-lutidine (1.5 cm^3, 0.93 mmol) was added followed by slow addition of trifluromethanesulfonic anhydride (1.8 cm^3, 10.71 mmol). After 1 h, the red mixture was warmed to room temperature and poured into water. The organic phase was separated, dried (Na_2SO_4), and concentrated to an oil under reduced pressure. Purification by flash silica chromatography using dichloromethane-pet. ether (1:2) as the eluent afforded methyl (2*R*)-2-[(trifluoromethylsulfonyl)oxy] ethanoate as a colourless oil (1.73 g, 78%).

A portion of this compound (0.32 g, 1.46 mmol) was added to a stirred solution of 2-(3'-*tert*-butoxycarbonylamino-prop-1'-ynyl)-phenylamine (**65**) (0.36 g, 1.46 mmol) and 2,6-lutidine (0.18 g, 1.6 mmol) in 1,2-dichloroethane (11 cm^3). The mixture was heated at 75 °C for 21 h and then cooled to room temperature. The solution was applied directly to a silica column and elution with ethyl acetate-pet. ether (1:5) gave the title compound **106** as a colourless oil. (0.22 g, 77%); (HRMS: found: $[M + Na]^+$ 341.1466. $C_{17}H_{22}N_2O_4Na$ requires 341.1477); υ_{max}(Thin film)/cm^{-1} 3440-3470 (NH, urethane and amine), 2060 (C≡C), 1713-1750 (C=O, ester and urethane), 1170-1200 (C-O, ester and urethane); δ_H(300 MHz; $CDCl_3$) 1.47 [9 H, s, $(CH_3)_3C$], 3.79 (3 H , s, OCH_3), 3.98 (2 H, m, $CH_2CO_2CH_3$), 4.21 (2 H, d, *J* 3.9, CH_2NH), 4.86 (1 H, br s, PhNH), 5.21 (1 H, br s, NH, urethane), 6.45 (1 H, m, 6'-CH), 6.67 (1 H, m, 4'-CH), 7.19 (1 H, m, 5'-CH) and 7.28 (1 H, m, 3'-CH); δ_C(75.44 MHz; $CDCl_3$) 28.34 [$(CH_3)_3C$], 46.20 (C≡CCH_2N), 52.25 (OCH_3), 56.60 ($CH_2CO_2CH_3$), 79.66, 91.51 and 100.07 [$(C(CH_3)_3$ and C≡C], 107.90 (2'-C), 109.45 (6'-CH), 117.17 (4'-CH), 130.05 (5'-CH), 132.35 (3'-CH), 148.10 (1'-C), 155.50 (CO, urethane) and 171.63 (CO, ester); *m/z* (EI) 318 (20%, M^+), 262 (40, $[M - C_4H_9 + H]^+$), 203 (45), 142 (75), 130 (100), 57 (80) and 41 (85).

Methyl (2*R*)-2-hydroxy-*n*-butyrate (100)

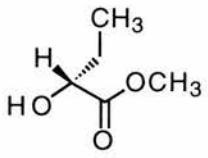

This compound was prepared in a manner identical to that for methyl (2*S*)-2-hydroxy-4-methyl pentanoate (**85**) using (2*R*)-2-amino-*n*-butyric acid (2 g, 19.42 mmol) to give initially (2*R*)-2-hydroxy-*n*-butyric acid (**96**) as a colourless, crystalline solid [(1.4 g, 69%); δ_H(200 MHz; $CDCl_3$) 1.01 (3 H, m, CH_3), 1.80 (2 H, m, CH_2), 4.26 (1 H, m, C*H*CO_2CH_3), 7.05 (2 H, br s, CO_2H and OH); δ_C(50.31 MHz, $CDCl_3$) 8.87 (CH_3), 27.15 (CH_2), 71.33 (C*H*CO_2CH_3) and 179.67 (CO, carboxylic acid)] and then ester **100** as a colourless oil after distillation under reduced pressure (0.7 g, 57%), bp 40 °C (~10 mmHg) [lit.,[210] 73-75 °C (33 mmHg)]; $[\alpha]_D^{18}$ 4.1 (neat) [lit.,[210] 5.1 (neat)]; δ_H(300 MHz; $CDCl_3$) 0.95 (3 H, m, CH_3), 1.70 (2 H, m, C*H*$_2CH_3$), 2.89 (1 H, br s, OH), 3.75 (3 H, s, OCH_3), 4.15 (1 H, m, CHCO); δ_C(75.44 MHz; $CDCl_3$) 8.84 (CH_3), 27.39 (CH_2), 52.42 (COH), 71.44 (OCH_3) and 175.87 (CO); *m/z* (EI) 119 (4%, [M + H]$^+$), 91 (4), 75 (7) and 45 (100).

Methyl (2*S*)-2-[2'-(3''-*tert*-butoxycarbonylamino-prop-1''-ynyl)-phenylamino]-butanoate (109)

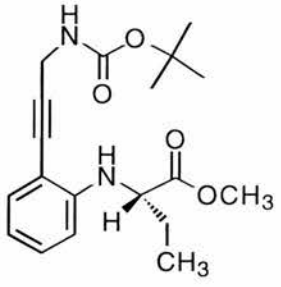

To a stirred solution of methyl (2*R*)-2-hydroxy-butanoate (**100**) (0.30 g, 2.54 mmol) in dry dichloromethane (50 cm^3), cooled to -78 °C, and under an N_2 atmosphere, was added 2,6-lutidine (0.3 cm^3, 2.60 mmol), followed by slow addition of trifluromethanesulfonic anhydride (0.41 cm^3, 2.54 mmol). After 1 h, the red mixture

was warmed to room temperature and poured into water (50 cm^3). The organic phase was separated, dried (Na_2SO_4), and concentrated under reduced pressure to give a colourless oil. Column chromatography with dichloromethane-pet. ether (1:2) as the eluent, yielded methyl (2*R*)-2-[(trifluoromethylsulfonyl)oxy]-butanoate (**104**) as a colourless oil (0.48 g, 75%).

A portion of this compound (0.21 g, 0.84 mmol) was added to a stirred solution of 2-(3'-*tert*-butoxycarbonylamino-prop-1'-ynyl)-phenylamine (**65**) (0.21 g, 0.85 mmol) and 2,6-lutidine (0.11 cm^3, 0.93 mmol) in 1,2-dichloroethane (8 cm^3). The mixture was heated at 60 °C for 7 h and then cooled to room temperature. The solution was applied directly to a silica column and elution with ethyl acetate-pet. ether (1:5) furnished ester **109** as a colourless oil which solidified on standing (0.22 g, 77%), mp 75-77 °C; (HRMS: found: M^+, 346.1900. $C_{19}H_{26}N_2O_4$ requires 346.1892); $[\alpha]_D^{18}$ 15.2 (*c* 0.42, CH_2Cl_2); υ_{max}(KBr disc)/cm^{-1} 3310-3475 (NH, urethane and amine), 2876-3011 (ArCH and CH), 2225 (C≡C), 1686 and 1734 (CO, ester and urethane) and 1130-1290 (C-O, ester and urethane and C-N, urethane); δ_H(300 MHz; $CDCl_3$) 1.02 (3 H, t, *J* 7.42, CH_3CH_2), 1.47 [9 H, s, $(CH_3)_3C$], 1.93 (2 H, m, CH_2CH_3), 3.72 (3 H, s, OCH_3), 4.04 (1 H, t, *J* 6.23, $CHCO_2CH_3$), 4.20 (2 H, d, *J* 5.5, CH_2NH), 4.86 (1 H, br s, PhNH), 5.79 (1 H, m, NH, urethane), 6.51 (1 H, m, 6'-CH), 6.62 (1 H, m, 4'-CH), 7.16 (1 H, m, 5'-CH) and 7.30 (1 H, m, 3'-CH); δ_C(75.44 MHz; $CDCl_3$) 9.88 (CH_3CH_2), 25.90 (CH_3CH_2), 28.34 [$(CH_3)_3C$], 31.42 (CH_2N), 52.18 (OCH_3), 57.50 ($CHCO_2CH_3$), 79.66, 80.01 and 91.51 [$C(CH_3)_3$ and C≡C], 107.90 (2'-C), 110.04 (6'-CH), 117.17 (4'-CH), 130.05 (5'-CH), 132.55 (3'-CH), 147.01 (1'-CH), 155.48 (CO, urethane) and 174.23 (CO, ester); *m/z* (EI) 346 (45%, M^+), 287 (26, $[M - CO_2CH_3]^+$), 273 (10, $[M - C_3H_9CO]^+$), 231 (100), 188 (35, $PhNHC_3H_6CO_2CH_3^+$) and 57 (26, $C_4H_9^+$).

(2*S*)-2-[2'-(3''-*tert*-Butoxycarbonylamino-prop-1''-ynyl)-phenylamino]-butanoic acid (132)

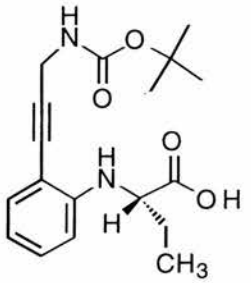

To a stirred solution of methyl (2*S*)-[2'-(3''-*tert*-butoxycarbonylamino-prop-1''-ynyl)-phenylamino]-butanoate (**109**) (0.9 g, 2.6 mmol) in methanol (42 cm^3) was added 1 mol dm^{-3} LiOH solution (13 cm^3, 13 mmol) and the solution stirred for 2 days. The reaction mixture was then cooled in ice, acidified to pH 3 with citric acid solution (10% w/v) and extracted with ethyl acetate (3 × 30 cm^3). The organic extracts were combined, washed with water (4 × 90 cm^3), brine (50 cm^3), dried (Na_2SO_4) and concentrated under reduced pressure to yield acid **132** as a white sticky foam (0.78 g, 91%); (HRMS: found: $[M + Na]^+$, 355.1641 $C_{18}H_{24}O_4N_2Na$ requires 355.1634); $[\alpha]_D^{25}$ 30.0 (*c* 1.04, CH_2Cl_2); υ_{max}(KBr disc)/cm^{-1} 3190-3500 (NH, urethane and amine), 2878-2975 (ArCH and CH), 2223 (C≡C), 1625-1760 (CO, carboxylic acid and urethane), 1165, 1252 and 1283 (C-O, acid and urethane, and C-N, urethane); δ_H(300 MHz; $CDCl_3$) 1.04 (3 H, t, *J* 6.7, CH_3CH_2), 1.46 [9 H, s, $(CH_3)_3C$], 1.90-2.00 (2 H, m, CH_2CH_3), 4.03 (1 H, m, $CHCO_2H$), 4.17 (2 H, m, CH_2N), 4.95 (1 H, br s, PhNH), 6.10-6.60 (2 H, br s, CO_2H and $NHCO_2$), 6.52 (1 H, d, *J* 8.2, 6'-CH), 6.65 (1 H, t, *J* 7.4, 4'-CH), 7.16 (1 H, t, *J* 7.8, 5'-CH) and 7.26 (1 H, d, *J* 7.7, 3'-CH); δ_c(74.76 MHz; $CDCl_3$) 9.81 (CH_3CH_2), 25.65 (CH_3CH_2), 28.24 [$(CH_3)_3C$], 31.31 (CH_2NH), 57.53 ($CHCO_2H$), 79.44, 80.13 and 91.49 [$C(CH_3)_3$ and C≡C], 108.00 (2'-C), 110.28 (6'-CH), 117.41 (4'-CH), 130.12 (5'-CH), 132.44 (3'-CH), 147.77 (1'-C), 155.64 (CO, urethane) and 177.83 (CO_2H); *m/z* (ES+) 377 (10%, $[M + 2Na - H]^+$), 355 (50, $[M + Na]^+$), 299 (100, $[M + Na - C_4H_9 + H]^+$), 277 (10, $[M - C_2H_6CO_2C + 2Na]^+$) and 255 (25, $[M + Na - C_3H_9CO_2 + H]^+$).

Methyl (2*R*)-2-[2'-(3''-*tert*-butoxycarbonylamino-prop-1''-ynyl)-phenylamino]-propanoate (107)

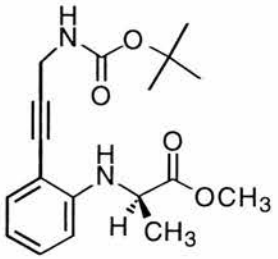

Methyl (2*S*)-2-hydroxypropanoate (**94**) was prepared in a manner identical to methyl glycolate (**97**) using lactic acid (8.0 g, 0.09 mol) to give methyl (2*S*)-2-hydroxy-propanoate (**94**) as a colourless oil (3.5 g, 37%); δ_H(300 MHz; $CDCl_3$) 1.37 (3 H, d, *J* 7.0, CH_3CH), 3.73 (4 H, m, OCH_3 and OH) and 4.26 (1 H, q, *J* 7.0, CH_3CH); δ_C(75.44 MHz; $CDCl_3$) 20.25 (CH_3CH), 52.47 (CH_3CH), 66.76 (OCH_3) and 176.12 (CO).

In a manner identical to the preparation of triflate **104**, methyl (2*S*)-2-hydroxy-propanoate (**94**) (2.0 g, 19.0 mmol) was converted into the triflate **102** (3.18 g, 71%).

A portion of triflate **102** (0.5 g, 2.12 mmol) was then coupled to 2-(3'-*tert*-butoxycarbonylamino-prop-1'-ynyl)-phenylamine (**65**) (0.48 g, 2.02 mmol) in a manner identical to the ethanoate analogue **106** to give ester **107** as a colourless oil (0.54 g 81%); (HRMS: found M^+, 332.1730. $C_{18}H_{24}N_2O_4$ requires 332.1736); $[\alpha]_D^{18}$ -39.2 (*c* 0.5, CH_2Cl_2); υ_{max}(Thin film)/cm^{-1} 3020-3470 (NH, urethane and amine), 2810-3020 (ArC-H and C-H), 2221.9 (C≡C), 1670-1775 (C=O, ester and urethane), 1130-1279 (C-O, acid and urethane, and C-N, urethane); δ_H(300 MHz; $CDCl_3$) 1.44 [9 H, s, $C(CH_3)_3$], 1.51 (3 H, d, *J* 7.0, CH_3CH), 3.71 (3 H, s, OCH_3), 4.16 (1 H, m, CH_3CH), 4.18 (2 H, m, CH_2NH), 5.05 (2 H, br s, NHCO and PhNH), 6.44 (1 H, m, 6'-CH), 6.61 (1 H, m, 4'-CH), 7.11 (1 H, m, 5'-CH), 7.15 (1 H, m, 3'-CH); δ_C(75.44 MHz; $CDCl_3$) 18.71 (CH_3CH), 28.34 [$(CH_3)_3C$], 31.39 (CH_2N), 51.65 (OCH_3), 52.31 ($CHCH_3$), 79.55, 79.92 and 91.67 [($C(CH_3)_3$) and C≡C], 107.85 (2'-C), 109.90 (6'-CH), 117.21 (4'-CH), 130.04 (5'-CH), 132.56 (3'-CH), 147.72 (1'-C), 155.58 (CO,

urethane), 174.82 (CO, ester); *m/z* (EI) 332 (72%, M^+), 273 (45, $[M - CO_2CH_3]^+$), 217 (100), 174 (70), 156 (71) and 144 (42).

(2*R*)-2-[2'-(3''-*tert*-Butoxycarbonylamino-prop-1''-ynyl)-phenylamino]-propanoic acid (119)

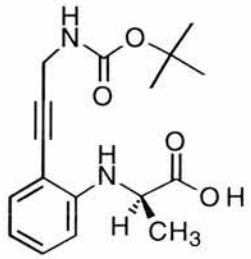

To a stirred solution of methyl (2*R*)-2-[2'-(3''-*tert*-butoxycarbonylamino-prop-1''-ynyl)-phenylamino]-propanoate (**107**) (0.30 g, 0.90 mmol) in methanol (4.0 cm^3) was added aqueous sodium hydroxide solution (2.0 cm^3, 1 mol dm^{-3}). The reaction mixture was stirred for 3 h and then concentrated under reduced pressure to produce a colourless oil which was dissolved in water (20 cm^3). The pH 2 was adjusted to 2 with aqueous HCl solution (5 mol dm^{-3}) and the solution extracted with ethyl acetate (3×50 cm^3). The organic extracts were washed with brine (50 cm^3), dried (Na_2SO_4) and then concentrated under reduced pressure to give acid **119** as a white flocculant solid which slowly darkened when left at room temperature (0.25 g, 84%); (HRMS: found: M^+, 318.1580. $C_{17}H_{22}N_2O_4$ requires 318.1588); $[\alpha]_D^{18}$ -22.8 (*c* 0.6, CH_2Cl_2); υ_{max}(Thin film)/cm^{-1} 3190-3685 (NH, urethane and amine, and O-H), 2910-3030 (ArC-H and C-H), 2225 (C≡C), 1620-1780 (C=O, acid and urethane) and 1130-1280 (C-O, urethane and ester, and C-N, urethane); δ_H(300 MHz; $CDCl_3$) 1.46 [9 H, s, $(CH_3)_3C$], 1.52 (3 H, d, *J* 6.6, CH_3CH), 4.11 (1 H, m, $CHCH_3$), 4.16 (2 H, m, CH_2NH), 4.92 (1 H, br s, PhNH), 6.20-6.60 (2 H, br s, NH, urethane and OH, carboxylic acid), 6.50 (1 H, m, 6'-CH), 6.66 (1 H, m, 4'-CH), 7.17 (1 H, m, 5'-CH), 7.25 (1 H, m, 3'-CH); δ_C(75.44 MHz; $CDCl_3$) 18.64 (CH_3CH), 28.32 [$(CH_3)_3C$], 31.44 (CH_2N), 51.76 ($CHCH_3$), 79.49, 80.75 and 91.60 [($C(CH_3)_3$ and (C≡C)], 108.01 (2'-C), 110.20 (6'-CH), 117.62 (4'-CH), 130.15 (5'-CH), 132.62 (3'-CH),

147.57 (1'-C), 158.50 (CO, urethane) and 178.76 (CO, carboxylic acid); *m/z* (EI) 318 (10%, M^+), 274 (30, $[M - CO_2H + H]^+$), 246 (19, $[M - C_3H_9CO + H]^+$), 217 (55, $[M - CO_2C_3H_9]^+$), 190 (24), 174 (35), 156 (26), 144 (45), 130 (66) and 57 (100, $C_4H_9^+$).

Methyl (2*R*)-[2'-(3''-*tert*-butoxycarbonylamino-prop-1'-ynyl)-phenylamino]-4-methyl-pentanoate (105)

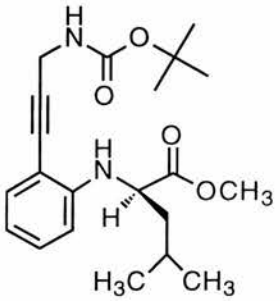

A stirred solution of methyl (2*S*)-2-hydroxy-4-methyl pentanoate (**85**) (6.44 g, 44 mmol) in dry dichloromethane was cooled to -78 °C and, under an N_2 atmosphere, 2,6-lutidine (6.75 cm^3, 58 mmol) was added followed by slow addition of trifluromethanesulfonic anhydride (7.88 cm^3, 48 mmol). After 1 h, the red mixture was warmed to room temperature and poured into water. The organic phase was separated, dried (Na_2SO_4), and concentrated under reduced pressure to an oil. Purification by flash silica using DCM-pet. ether (1:2) as the eluent afforded methyl (2*S*)-2-[(trifluoromethylsulfonyl)oxy]-4-methyl pentanoic acid, methyl ester (**88**) as a colourless oil (7.6 g, 82%).

A stirred solution of triflate **88** (1.6 g, 5.7 mmol), 2-(3'-*tert*-butoxycarbonylamino-prop-1'-ynyl)-phenylamine (**63**) (1.33 g, 5.4 mmol) and 2,6-lutidine (0.67 cm^3, 5.7 mmol) in 1,2-dichloroethane (20 cm^3), under an nitrogen atmosphere, was heated at 70 °C for 7 h, . After cooling to room temperature, the solution was applied directly to a silica column and elution with ethyl acetate-pet. ether (1:5) gave the title ester **105** as a colourless oil (1.7 g, 84%); (HRMS: found: M^+, 374.2200. $C_{21}H_{30}N_2O_4$ requires 374.2205); $[\alpha]_D^{25}$ 8.5 (*c* 1.0, CH_2Cl_2); υ_{max}(Thin film)/cm^{-1} 3250-3500 (NH, urethane and ester), 2870-2958 (ArC-H and C-H), 2220.0 (C≡C), 1650-1780 (C=O,

ester and urethane) 1167, 1249 and 1283 (C-O, ester and urethane, and C-N, urethane); δ_H(200 MHz; $CDCl_3$) 0.97 [6 H, m, $CH_2CH(CH_3)_2$], 1.48 [9 H, s, $(CH_3)_3C$], 1.76-1.81 (3 H, m, $CH_2CH(CH_3)_2$ and $CH_2CH(CH_3)_2$], 3.70 (3 H, s, OCH_3), 4.09-4.17 (1 H, m, $CHCO_2CH_3$), 4.18 (2 H, m, CH_2N), 4.88 (1 H, br s, PhNH), 4.92 (1 H, br s, NH, urethane), 6.50 (1 H, m, 6'-CH), 6.66 (1 H, m, 4'-CH), 7.11 (1 H, m, 5'-CH) and 7.25 (1 H, m, 3'-CH); δ_C(50.31 MHz; $CDCl_3$) 22.78 and 23.23 [$CH_2CH(CH_3)_2$], 25.45 [$CH_2CH(CH_3)_2$], 28.86 [$(CH_3)_3C$], 31.90 (CH_2N), 42.45 [$CH_2CH(CH_3)_2$], 52.61 ($CHCO_2CH_3$), 55.43 (CO_2CH_3), 80.00, 80.25 and 91.99 [$C(CH_3)_3$ and C≡C], 108.24 (2'-CH), 110.3 (6'-CH), 117.61 (4'-CH), 130.45 (5'-CH), 132.92 (3'-CH), 148.4 (1'-C), 158.86 (CO, urethane) and 175.18 (CO, ester); *m/z* (EI) 374 (35%, M^+), 315 (38, [M - CO_2CH_3]$^+$), 259 (100, [M- $NHCO_2C(CH_3)_3$]$^+$), 216 (32), 84 (31) and 49 (44).

Methyl (2*R*)-[2'-(3''-amino-prop-1''-ynyl)-phenylamino]-4-methyl-pentanoate dihydrochloride (118)

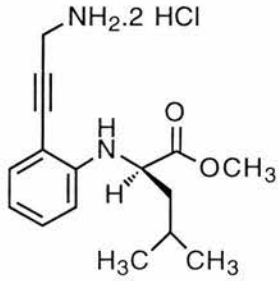

A stirred solution of methyl (2*S*)-[2'-(3''-*tert*-butoxycarbonylamino-prop-1-ynyl)-phenylamino]-4-methyl-pentanoate (**105**) (1.56 g, 4.17 mmol) in dry ethyl acetate (21 cm^3) was cooled to -20 °C, and dry HCl gas was bubbled continuously through the solution until the reaction was judged to be complete by TLC. The reaction mixture was then immediately purged with argon and concentrated under reduced pressure to produce the title dihydrochloride salt **118** as a pale yellow oil (1.45 g, 99%); (HRMS: found: M^+, 274.1688. $C_{16}H_{22}N_2O_2$ requires 274.1681); $[\alpha]_D^{18}$ 12.4 (*c*

1.3, CH_2Cl_2); υ_{max}(Thin film)/cm^{-1} 2850-3000 (ArC-H, C-H, NH_3^+ and NH_2^+), 2225 (C≡C), 1737 (C=O, ester) and 1167 (C-O, ester); δ_H(200 MHz; $CDCl_3$) 0.89 [6 H, 2 × d, *J* 6.2, $(CH_3)_2CH$], 1.63-1.83 [2 H, m, $(CH_3)_2CHCH_2$], 2.05 [1 H, m, $(CH_3)_2CHCH_2$], 3.68 (3 H, s, CO_2CH_3), 4.05 [3 H, m, $CH_2NH_3^+$, and $CHCH_2CH(CH_3)_2$] 6.42 (1 H, m, 6'-CH), 6.56 (1 H, m, 4'-CH), 7.11 (1 H, m, 5'-CH), 7.25 (1 H, m, 3'-CH) and 8.50-8.90 (5 H, m, NH_2^+ and NH_3^+); δ_C(75.44; $CDCl_3$) 21.71 and 22.81 $[CH_2CH(CH_3)_2]$, 24.94 $[CH_2CH(CH_3)_2]$, 30.60 (CH_2N), 41.00 $[CH_2CH(CH_3)_2]$, 52.42 ($CHCO_2CH_3$), 54.89 (CO_2CH_3), 84.05 and 86.16 (C≡C), 106.38 (2'-C), 109.86 (6'-CH), 117.24 (4'-CH), 130.84 (5'-CH), 133.70 (3'-CH), 148.47 (1'-C), 176.18 (CO_2CH_3); *m/z* (EI) 274 (54%, M^+), 215 (53), 198 (100), 156 (61), 142 (33), 130 (31), 115 (28) and 49 (33).

Methyl (2*S*)-[2'-(3''-{2*S*-[2'''-(3''''-*tert*-butoxycarbonylamino-prop-1''''-ynyl)-phenylamino]-propionylamino}-prop-1''-ynyl)-phenylamino]-4-methyl-pentanoate (120)

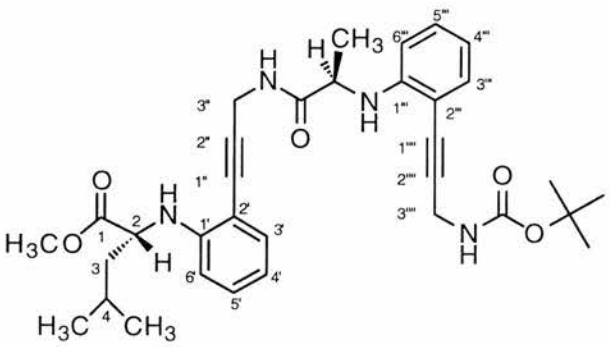

A stirred solution of carboxylic acid **119** (0.60 g, 1.89 mmol) and HOBt (0.39 g, 2.84 mmol) in dry DMF (25 cm^3) was cooled to -5 °C under an N_2 atmosphere. To the reaction mixture was added EDCI (0.83, 2.84 mmol) and a solution of dihydrochloride **118** (0.60 g, 1.93 mmol) and DIEA (1.34 cm^3, 7.72 mmol) in DMF (50 cm^3). The reaction mixture was stirred for 2 h at 0 °C, the DIEA salt filtered off and the filtrate concentrated under reduced pressure. The resulting dark yellow oil

was re-dissolved in ethyl acetate (100 cm^3), washed with citric acid solution (50 cm^3, 10% w/v), $NaHCO_3$ solution (50 cm^3, 0.5 mol dm^{-3}), brine (50 cm^3) and further concentrated under reduced pressure to yield an oil which was re-concentrated from DCM to give the crude hexapeptide analogue **120** as a yellow oil. Purification by flash silica chromatography using MeOH-CH_2Cl_2 (3:97) gave hexapeptide analogue **120** as a pale yellow oil (0.52 g, 48%); (HRMS: found $[M + H]^+$, 575.3225. $C_{33}H_{43}N_4O_5$ requires 575.3233); $[\alpha]_D^{18}$ -40 (*c* 0.2, CH_2Cl_2); υ_{max}(Thin film)/cm^{-1} 3160-3470 (NH, amine, amide and urethane), 2830-3015 (ArC-H and C-H), 2160-2210 (2 × C≡C), 1620-1750 (CO, ester, amide and urethane) 1200-1300 (C-O, urethane, and C-N, urethane and amide) and 1166 (C-O, ester); δ_H(300 MHz; $CDCl_3$) 0.93 [6 H, m, $CH_2CH(CH_3)_2$], 1.45 [9 H, s, $(CH_3)_3C$], 1.57 [3 H, d, CH_3 (Ala)], 1.70 [3 H, m, β-H and γ-H (Leu)], 3.35 (1 H, m, α-H, Leu), 3.67, (3 H, s, OCH_3), 3.82 (1 H, m, α-H, Ala), 4.07 [2 H, m, $CH_2NH(CO)CH(CH_3)$], 4.16 (2 H, m, CH_2NHCO_2), 4.95 (2 H, m, 2 × PhNH), 6.18 (1 H, br s, NH, urethane), 6.46-6.71 (4 H, m, Ar-H), 6.95 (1 H, br s, NH, amide) and 7.03-7.30 (4 H, m, Ar-H); δ_C(75.44 MHz; $CDCl_3$) 19.25 (CH_3, Ala), 22.06 and 22.58 (2 × CH_3, Leu), 24.82 (γ-C, Leu), 28.20 [$C(CH_3)_3$], 29.92 [$CH_2NHCH(CH_3)$], 31.27 (CH_2NHCO_2), 41.78 (β-C, Leu), 51.95 (α-C, Ala), 54.78 (α-C, Leu), 55.02 (CO_2CH_3), 79.12, 79.71 , 80.08, 90.54 and 92.03 [2 × C≡C and $C(CH_3)_3$], 107.66 and 108.23 (2'-C and 2'''-C), 109.93 and 111.07 (6'-CH and 6'''-CH), 117.17 and 118.35 (4'-CH and 4'''-CH), 130.17 and 130.31 (5'-CH and 5'''-CH), 132.38 and 132.70 (3'-CH and 3'''-CH), 147.82 and 148.14 (1'-C and 1'''-C), 155.51 (CO, urethane), 173.87 (CO, amide) and 174.49 (CO, ester); *m/z* (CI) 575 (22%, $[M + H]^+$), 365 (100), 256 (79) and 58 (45, $C_3H_{10}^+$).

(2*S*)-[2'-(3''-{2*S*-[2'''-(3''''-*tert*-butoxycarbonylamino-prop-1''''-ynyl)-phenylamino]-propionylamino}-prop-1''-ynyl)-phenylamino]-4-methyl-pentanoic acid (123)

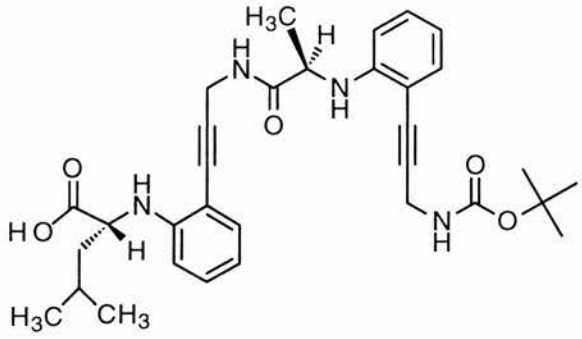

To a stirred solution of the hexapeptide analogue **120** (0.33 g, 0.58 mmol) in methanol (70 cm^3) was added, dropwise, 1 mol dm^{-3} lithium hydroxide solution (3.5 cm^3). The reaction mixture was stirred for 36 h (until the reaction was judged complete by TLC) buffered with saturated ammonium chloride solution and then concentrated under reduced pressure. The residue was re-dissolved in water (30 cm^3), the aqueous solution was acidified to pH 3 with citric acid solution (10%, w/v) and the aqueous layer extracted with ethyl acetate (2 × 50 cm^3). The pooled organic extracts were washed with water (4 × 50 cm^3), dried (Na_2SO_4) and then concentrated under reduced pressure to give the free acid as a pale yellow foam (0.30 g, 93%); (HRMS: found [M + Na] $^+$, 583.2895. $C_{32}H_{40}N_4O_5Na$ requires 583.2896); $[\alpha]_D^{18}$ 12.0 (*c* 0.1, CH_2Cl_2); υ_{max}(KBr disc)/cm^{-1} 3240-3525 (NH, amine, urethane and amide), 2840-3090 (ArC-H and C-H), 2220-2225 (2 × C≡C), 1630-1740 (C=O, carboxylic acid, amide and urethane) and 1168-1280 (C-N, amide and urethane, and C-O, urethane); δ_H(300 MHz; CD_3OD) 0.93 and 1.00 [6 H, 2 × d, *J* 6.8, 2 × CH_3, Leu), 1.45 [9 H, s, $(CH_3)_3C$], 1.49 (3 H, m, CH_3, Ala), 1.61-1.85 (3 H, m, β-CH_2 and γ-CH, Leu), 3.95 (1 H, m, α-H, Ala), 4.08 (3 H, m, α-H, Leu and CH_2NHCO_2), 4.22 [2 H, m, $CH_2NH(CO)CH(CH_3)$], 6.40-6.80 (4 H, m, Ar-H) and 7.00-7.30 (4 H, m, Ar-H); δ_C(75.4 MHz; CD_3OD) 18.12 (CH_3, Ala), 21.11 and 21.91 (2 × CH_3, Leu), 24.79 (γ-

C, Leu), 27.38 [(CH$_3$)$_3$C], 29.14 and 30.33 (2 × CH$_2$N), 41.48 (β-C, Leu), 53.41 (α-C, Leu), 53.84 (α-C, Ala), 78.36, 78.70, 79.10, 90.58 and 91.78 [C(CH$_3$)$_3$ and 2 × C≡C], 107.75 and 108.16 (2'-C and 2'''-C), 109.83 and 110.31 (6'-CH and 6'''-CH), 116.65 and 117.21 (4'-CH and 4'''-CH), 129.65 (5'-CH and 5'''-CH), 131.94 and 132.12 (3'-CH and 3'''-CH), 147.88 and 148.41 (1'-C and 1'''-C), 156.80 (CO, urethane), 175.65 (CO, amide) and 176.56 (CO$_2$H); *m/z* (ES+) 583 (100, [M + Na]$^+$).

(2*S*)-[2'-(3''-{2*S*-[2'''-(3''''-amino-prop-1''''-ynyl)-phenylamino]-propionylamino}-prop-1''-ynyl)-phenylamino]-4-methyl-pentanoic acid hydrochloride (117)

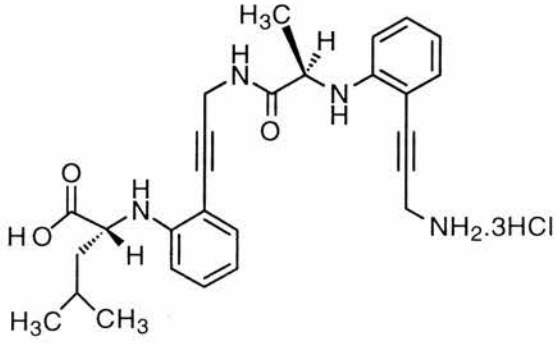

A stirred solution of carboxylic acid **123** (0.25 g, 0.45 mmol) in dry ethyl acetate (50 cm^3) was cooled to -20 °C and dry HCl gas was bubbled through the solution. The reaction mixture was stirred at -20 °C until the reaction was judged to be complete by analytical TLC (~10 min). The solvent was removed under reduced pressure to give the trihydrochloride salt **117** as an off-white solid which was not purified further (0.21 g, 99%), mp 91-97 °C (decomp.); (HRMS: found [M + Na]$^+$, 483.2381. $C_{27}H_{32}N_4O_3Na$ requires 483.2372); $[\alpha]_D^{18}$ -32 (*c* 0.5, CH_2Cl_2); υ_{max}(KBr disc)/cm^{-1} 3500-3270 (NH, amide), 3110-3000 (ArC-H and C-H), 2870-3000 (NH_2^+ and NH_3^+), 1940-2075 (2 × C≡C), 1682 and 1731 (C=O, amide and acid), 1510 (NH, amide), 1169-1319 (C-N, amide, and C-O, acid); δ_H[300 MHz; $(CD_3)_2SO$] 0.88 and 0.96 (6 H, 2 × d, *J* 5.81, 2 × CH_3, Leu), 1.44 (3 H, d, *J* 6.6, CH_3, Ala), 1.65-1.83 (3 H, m, β-H and γ-H, Leu), 4.02 (4 H, m, $CH_2NH_3^+$, α-H, Leu and α-H, Ala), 4.16 (2 H, m, CH_2NHCO), 4.16-5.00 (7 H, br s, 2 × NH_2^+ and NH_3^+), 6.72-8.10 (8 H, m, Ar-H),

8.63-8.77 (2 H, NH, amide, and OH, acid); δ_C[75.44; $(CD_3)_2SO$] 18.41 (CH_3, Ala), 21.58 and 22.47 (2 × CH_3, Leu), 24.30 (γ-C, Leu), 29.00 (2 × CH_2N), 40.57 (β-C, Leu), 52.00 (α-C, Ala), 53.74 (α-C, Leu) 78.08, 82.62, 87.69 and 92.27 (2 × C≡C), 105.67 and 106.76 (2'-C and 2'''-C), 109.67 and 110.20 (6'-CH and 6'''-CH), 116.24 and 116.32 (4'-CH and 4'''-CH), 129.71 and 130.38 (5'-CH and 5'''-CH), 131.62 and 132.09 (3-CH and 3'''-CH), 148.00 and 148.08 (1'-C and 1'''-C), 173.27 and 174.95 (CO, amide and CO_2H); *m/z* (ES+) 483 (100, $[M + Na]^+$).

(3 *R*, 16 *R*)-2,5,15,18-tetraaza-9,22-dibenzo-16-(2-methylpropyl)-3-methyl-4,17-dioxo-7,20-diyne-tricyclo [20.4 .0 .$0^{9,14}$] hexacosane (114)

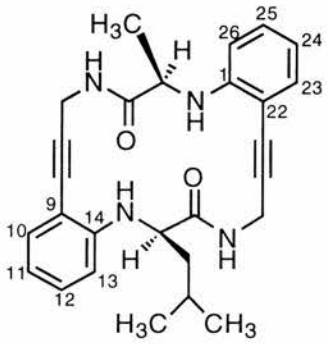

A solution of the deprotected linear hexapeptide analogue **117** (0.22 g, 0.39 mmol) in dry DMF (200 cm^3) was cooled to 0 °C. To this stirred solution was added solid $NaHCO_3$ (0.23g, 2.73 mmol) and diphenylphosphoryl azide (DPPA) (0.43g, 1.56 mmol) and the suspension was stirred at room temperature under an atmosphere of nitrogen. A further 3 equivalents of DPPA was added after 72 h and the reaction was stirred for a further 96 h. The reaction mixture was then added to dichloromethane (100 cm^3), washed with water (4 × 75 cm^3), $NaHCO_3$ solution (25 cm^3, 5% w/v), brine (25 cm^3), dried (Na_2SO_4) and concentrated under reduced pressure to give a yellow oil which was purified by flash silica chromatography using ethyl acetate-hexane (2:5) as the eluent to give the cyclic hexapeptide analogue **114** as a colourless oil which solidified on standing (0.05 g, 28%), mp 116-118 °C (decomp.); (HRMS:

found $[M + H]^+$ 443.2447. $C_{27}H_{31}N_4O_2$, requires 443.2451); $[\alpha]_D^{18}$ 7.2 (*c* 0.05, MeOH); υ_{max}(KBr disc)/cm^{-1} 3200-3600 (2 × NH, amide, and 2 × NH, amine), 2810-3000 (ArC-H and C-H), 2100 and 2220 (2 × C≡C) and 1660-1670 (2 × CO, amide); δ_H(300 MHz; $CDCl_3$) 0.92 and 1.03 (6 H, 2 × d, *J* 6.2, 2 × CH_3, Leu), 1.56 (3 H, d, *J* 6.6, CH_3, Ala), 1.86-1.90 (3 H, m, β-CH_2 and γ-CH, Leu), 3.91 (3 H, m, α-H, Leu and CH_2N), 4.03 (1 H, t, *J* 7.1, α-H, Leu), 4.62 (2 H, m, CH_2NH), 5.32 and 5.42 (2 H, m, 2 × PhNH), 6.52 (2 H, m, Ar-H13 and Ar-H26), 6.66 (2 H, m, Ar-H11 and Ar-H24), 6.80 (1 H, br s, NH, amide) and 7.17-7.27 (5 H, m, Ar-H10, 12, 24 and 26 and NH, amide); δ_C(74.76 MHz; $CDCl_3$) 19.08 (CH_3, Ala), 22.05 and 22.88 (2 × CH_3, Leu), 25.19 (γ-C, Leu), 30.70 and 30.93 (2 × CH_2NH), 42.34 (β-C, Leu), 52.90 (α-C, Leu), 56.76 (α-C, Ala), 80.79, 80.87, 91.25 and 91.32 (2 × C≡C), 107.37 and 107.68 (9-C and 22-C), 109.55 and 109.66 (13-CH and 26-CH), 117.15 (11-CH and 24-CH), 130.13 and 130.43 (12-CH and 25-CH), 131.22 and 131.40 (10-CH and 23-CH), 147.40 and 148.48 (14-C and 1-C), 173.49 and 174.70 (2 × CO, amide); *m/z* (CI) 443 (41%, $[M + H]^+$), 241 (92, $[M + H - C_{12}H_{13}N_2O]^+$) and 57 (100, $C_4H_9^+$).

Methyl (2*R*)-hydroxy-3-phenyl propanoate (99)

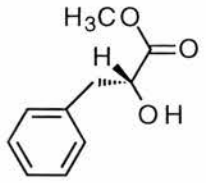

(2*R*)-Hydroxy-3-phenyl propanoic acid (**95**) was prepared from phenylalanine in a manner identical to that described for (2*R*)-2-hydroxy-*n*-butyric acid (**96**) to yield, after trituration with hexanes, the product as a white solid (6.0 g, 60%).

To an ice-cooled, stirred solution of acid **95** (6.0 g, 0.04 mol) in dry methanol (20 cm^3) was added, dropwise, thionyl chloride (3.44 cm^3, 0.05 mol). The reaction mixture was refluxed for 2 h, allowed to cool, and the pH adjusted to 6 with saturated sodium bicarbonate solution. The resulting suspension was concentrated to half its original volume under reduced pressure and partitioned between water (100 cm^3) and

diethyl ether (100 cm^3). The aqueous phase was extracted further with diethyl ether (3 × 50 cm^3). The organic extracts were pooled, washed with brine, dried (Na_2SO_4) and concentrated under reduced pressure to give a colourless oil which was triturated with light petroleum to give ester **99** as a white solid which was not purified further (6.5 g, 82%), mp 43-45 °C (lit.,[211] 47-48 °C); (Found: C, 66.9; H, 6.9. $C_{10}H_{12}O_3$ requires C, 66.6; H, 6.7%); $[\alpha]_D^{25}$ -2.8 (*c* 1.2, MeOH) [lit.,[212] -4.0 (*c* 1.2, MeOH)]; δ_H(300 MHz; $CDCl_3$) 2.29 (1 H, br s, OH), 3.05 (2 H, m, CH_2Ph), 3.77 (3 H, s, OCH_3), 4.46 (1 H, m, C*H*OH) and 7.20-7.33 (5 H, m, Ar-H); δ_C(74.76 MHz; $CDCl_3$) 40.44 (CH_2Ph), 52.34 (OCH_3), 71.23 (CHOH), 126.93, 128.46 and 129.48 (Ar-CH), 136.36 (Ar-C, *ipso*) and 174.66 (CO); *m/z* (CI) 181 (100, $[M + H]^+$), 162 (64, $[M - H_2O]^+$), 121 (53) and 91 (44).

Methyl (2*S*)-valinate ester hydrochloride (134)

Thionyl chloride (13.0 cm^3, 0.18 mol) was added dropwise to a stirred solution of (2*S*)-valine (10.0 g, 0.08 mmol) in dry methanol (100 cm^3) at 0 °C. The reaction mixture was then refluxed for 3 h and the solvent removed under reduced pressure to give a white solid which was recrystallised from hot methanol to give ester **134** as white crystals (10.9 g, 77%), mp 156 °C (lit.,[213] 158-160°C); $[\alpha]_D^{25}$ 26.9 (*c* 1.0, MeOH) [lit.,[214] 24.2 (*c* 1.0, MeOH)]; δ_H(200 MHz; D_2O) 0.94 (6 H, d, *J* 6.8, 2 × CH_3, Val), 2.25-2.45 (1 H, m, β-H, Val), 3.75 (3 H, s, OCH_3) and 4.06 (1 H, α-H, Val); δ_C(74.76 MHz; D_2O) 20.44 (2 × CH_3, Val), 32.30 (β-C, Val), 56.52 (α-C, Val), 61.34 (OCH_3) and 173.05 (CO); *m/z* (EI) 132 (1%, $[M + H]^+$), 88 (48, $[M - C_3H_6]^+$), 72 (100, $[M - C_3H_6 - NH_2]^+$) and 55 (45).

(2*S*)-*N*-(*tert*-butoxycarbonyl) alanine (133)

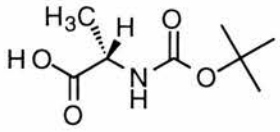

To a stirred solution of (2*S*)-alanine (5.00 g, 56.0 mmol) in NaOH solution (100 cm^3, 1 mol dm^{-3}) at 0 °C was added a solution of di-*tert*-butylpyrocarbonate (13.53 g, 62.0 mmol) in dioxane (100 cm^3). The reaction mixture was allowed to warm to room temperature and the pH adjusted to 11 with sodium hydroxide solution (5 mol dm^{-3}). After stirring for 12 h, the volume of the solution was reduced to 100 cm^3, the mixture cooled to 0 °C, covered with ethyl acetate (75 cm^3), acidified to pH 3 with sodium hydrogen sulphate solution (5% w/v), and the aqueous phase extracted further with ethyl acetate (2 × 75 cm^3). The combined organic extracts were washed with saturated brine, dried ($MgSO_4$), and concentrated under reduced pressure to give **133** as a colourless oil which solidified on standing (9.0 g, 85%), mp 75-77°C (lit.,[215] 73-74°C); $[\alpha]_D^{18}$ -21.9 (*c* 1.6, CH_2Cl_2) [lit.,[216] -19.6 (*c* 1.6, CH_2Cl_2)]; δ_H(300 MHz; $CDCl_3$) (approx. 1:1 mixture of *cis* and *trans* isomers) 1.35-1.45 [12 H, m, $(CH_3)_3C$ and CH_3, Ala], 4.12 and 4.31 (*c* and *t*, 1 H, m, α-H), 5.22 and 6.89 (*c* and *t*, 1 H, m, NH) and 11.56 (1 H, br s, CO_2H); δ_c(74.76 MHz; $CDCl_3$) 18.28 (CH_3), 28.17 [$(CH_3)_3C$], 48.99 and 50.12 (*c* and *t*, α-C), 80.10 and 82.05 [*c* and *t*, $(CH_3)_3C$], 155.36 and 157.50 (*c* and *t*, CO, urethane), 177.75 and 178.31 (*c* and *t*, CO_2H); *m/z* (CI) 207 (100, $[M + NH_4]^+$) and 190 (4, $[M + H]^+$).

Methyl *N*-(*tert*-butoxycarbonyl)-(2*S*)-alanyl-(2*S*)-valinate (135)

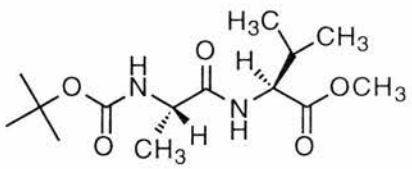

To a stirred solution of alanine **133** (4.0 g, 21.0 mmol) in dry acetonitrile (100 cm^3) was added methyl (2*S*)-valinate ester hydrochloride (**134**) (3.5 g, 21.0 mmol), DIEA

(11.0 cm^3, 63.0 mmol) and TBTU (7.1 g, 22.0 mmol). The reaction mixture was then stirred at 0 °C for 1 h under a nitrogen atmosphere. A solution of saturated brine (200 cm^3) was added to the reaction mixture and the crude dipeptide extracted into ethyl acetate (3 × 70 cm^3). The organic extracts were pooled and washed successively with water (100 cm^3), $NaHCO_3$ solution (100 cm^3, 1 mol dm^{-3}), citric acid solution (100 cm^3, 10% w/v), brine (100 cm^3), dried (Na_2SO_4) and then concentrated under reduced pressure to give a white solid. The crude dipeptide was recrystallised from ethyl acetate-light petroleum to give dipeptide **135** as white needles (5.13 g, 81%), mp 81-84 °C (lit.,[217] 65-66 °C); (Found: C, 55.4; H, 8.75; N, 9.3. $C_{14}H_{26}N_2O_5$ requires C, 55.6; H, 8.65; N, 9.3%); $[\alpha]_D^{22}$ -56.9 (*c* 1.0, MeOH) [lit.,[217] -49.4 (*c* 0.35, MeOH)]; υ_{max}(KBr disc)/cm^{-1} 3333 and 3418 (NH, amide and urethane), 2876-3020 (C-H), 1754 (C=O, ester), 1693 (C=O, urethane), 1665 (C=O, amide), 1255 (C-N, amide), 1159 (C-O, ester); δ_H(300 MHz; $CDCl_3$); 0.90 (6 H, 2 × d, *J* 6.87, 2 × CH_3, Val), 1.35 (3 H, d, *J* 6.87, CH_3, Ala), 1.41 (9 H, s, $(CH_3)_3C$), 2.03-2.07 (1 H, m, β-H, Val), 3.72 (3 H, s, OCH_3), 4.10 (1 H, br s, α-H, Ala), 4.38-4.44 (1 H, m, α-H, Val), 5.13 (1 H, br s, NH, urethane) and 6.71 (1 H, br s, NH, amide); δ_c(74.76 MHz; $CDCl_3$) 17.54 and 18.75 (2 × CH_3, Val), 17.81 (CH_3, Ala), 28.15 [$(CH_3)_3C$], 31.00 (β-C, Val), 49.85 (α-C, Ala), 51.92 (α-C, Val), 57.00 (OCH_3), 79.72 [$(CH_3)_3C$], 155.70 (CO, urethane), 172.37 (CO, amide) and 173.13 (CO_2CH_3); *m/z* (ES+) 325 (100%, $[M + Na]^+$) and 225 (62, $[M - C_4H_9O_2 + H + Na]^+$).

Methyl (2*S*)-[2'-(3''-*tert*-butoxycarbonyl-amino-prop-1''-ynyl)-phenylamino]-3-phenyl-propanoate (108)

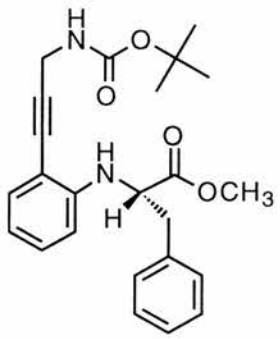

A stirred solution of methyl (2*R*)-hydroxy-3-phenylpropanoate (**99**) (6.0 g, 0.03 mol) in dry dichloromethane (40 cm^3) was cooled to -78 °C and, under an N_2 atmosphere, 2,6-lutidine (4.68 cm^3) was added followed by slow addition of trifluromethanesulfonic anhydride (5.24 cm^3). After 1 h, the red mixture was warmed to room temperature and poured into water. The organic phase was separated, dried (Na_2SO_4), and concentrated to an oil. Purification by flash silica chromatography with DCM-pet. ether (1:2) as the eluent afforded methyl (2*R*)-[(trifluoromethylsulfonyl)oxy]-3-phenylpropanoate (**103**) as a colourless oil (7.4 g, 79%).

A stirred solution of triflate **103** (6.24 g, 0.02 mol), 2-(3'-*tert*-butoxycarbonylamino-prop-1'-ynyl)-phenylamine (**65**) (5.0 g, 0.02 mol) and 2,6-lutidine (2.56 cm^3, 0.02 mol) in 1,2-dichloroethane (150 cm^3), under an N2 atmosphere, was heated at 75 °C for 24 h. After cooling to room temperature, the solution was applied directly to a silica column and elution with ethyl acetate-pet. ether (1:5) gave the title ester **108** as a colourless oil (5.0 g, 62%); (HRMS: found: $[M + H]^+$, 409.2117. $C_{24}H_{29}N_2O_4$ requires 409.2127); $[\alpha]_D^{18}$ -30.0 (*c* 1.3, CH_2Cl_2); $\upsilon_{max}(CHCl_3)/cm^{-1}$ 3375-3460 (NH, urethane and amine), 2950-3095 (ArC-H and C-H), 2060 (C≡C), 1695-1740 (C=O, urethane and ester) and 1167-1263 (C-N, urethane, and C-O, ester and urethane); δ_H(300 MHz; $CDCl_3$) 1.56 [9 H, s, $(CH_3)_3C$], 3.25 (2 H, m, CH_2Ph), 3.87 (3 H, s, OCH_3), 4.17 (2 H, m, CH_2NH), 4.41 (1 H, m,

C*H*CH_2Ph), 4.85 (1 H, br s, NH, urethane), 5.10 (1 H, m, NH, amine), 6.51 (1 H, m, 6'-CH), 6.68 (1 H, m, 4'-CH) and 7.15-7.40, (7 H, 3'-CH, 5'-CH and Ar-H, Phe); δ_C(74.76 MHz; $CDCl_3$) 28.36 [(CH_3)$_3$C], 31.42 (CH_2NH), 38.54 (CH_2Ph), 52.18 (CO_2CH_3), 57.40 ($CHCO_2CH_3$), 79.65, 79.95 and 91.38, [(CH_3)$_3$*C* and C≡C], 108.13 (2'-C), 110.17 (6'-CH), 117.41 (4'-CH), 127.28 (5'-CH), 128.72, 129.10 and 130.04 (Ar-CH, Phe), 132.49 (3'-C), 136.28 [Ar-C, *ipso* (Phe)], 147.58 (1'-C), 155.42 (CO, urethane) and 173.41 (CO, ester); *m/z* (CI) 409 (49%, [M + H]$^+$) and 353 (100, [M - C_4H_9]$^+$).

Methyl (2*S*)-[2'-(3''-*tert*-Butoxycarbonyl-amino-prop-1''-ynyl)-phenylamino]-3-phenyl-propanoate (129)

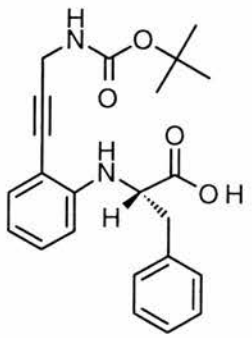

To a stirred solution of tripeptide analogue (**108**) (4.4 g, 0.01 mmol) in methanol (175 cm^3) was added aqueous LiOH solution (45 cm^3, 1 mol dm^{-3}). The solution was stirred for 24 h and then cooled in ice, acidified to pH 3 with citric acid solution (10%, w/v) and extracted into ethyl acetate (3 × 100 cm^3). The organic extracts were pooled, washed with water (4 × 100 cm^3), brine (50 cm^3), dried (Na_2SO_4) and concentrated under reduced pressure to yield acid **129** as a yellow oil which was refractory to recrystallisation (3.42 g, 79%); (HRMS: found M$^+$, 394.1899. $C_{23}H_{26}N_2O_4$ requires 394.1892); $[\alpha]_D^{18}$ -26.4 (*c* 0.5, CH_2Cl_2); υ_{max}(CH_2Cl_2)/cm^{-1} 3440-3490 (C-N, urethane, and C-O, urethane and acid), 2305-2395 (C≡C), 1660-1760 (C=O, urethane and acid), 1280-1370 (C-N, urethane, and C-O, urethsane and acid); δ_H(300 MHz; $CDCl_3$) 1.49 [9 H, s, (CH_3)$_3$C)], 3.22 (2 H, m, CH_2Ph), 4.12 (2 H, m, CH_2NH), 4.35 (1 H, m, C*H*CH_2Ph), 4.85 (2 H, br s, PhNH and NH, amide),

6.50 (1 H, m, 6'-CH), 6.65 (1 H, m, 4'-CH), 7.15 (1 H, m, 5'-CH) and 7.20-7.36 [6 H, 3'-CH and Ar-H (Phe)]; δ_C(74.76 MHz; $CDCl_3$) 28.36 [(CH_3)$_3$C], 31.38 (CH_2NH), 38.20 (CH_2Ph), 57.33 ($CHCO_2H$), 79.52, 80.25 and 91.38 [$C(CH_3)_3$ andC≡C], 108.26 (2'-C), 110.40 (6'-CH), 117.70 (4'-CH), 127.37 (5'-CH), 128.79, 129.56 and 130.08 (Ar-CH, Phe), 132.55 (3'-CH), 136.10 [Ar-C, *ipso*, (Phe)], 147.49 (1'-C), 155.98 ($NHCO_2$) and 177.44 (CO_2H) *m/z* (EI) 394 (15%, M^+), 349 (8, $[M - CO_2H]^+$), 293 (35, $[M + H - CO_2H - C_4H_9]^+$) and 57 (100, $C_4H_9^+$).

Methyl 2'-(3''-*tert*-butoxycarbonylamino-prop-1''-ynyl)-phenyl-1'-(2*S*)-phenylalanyl-(2*S*)-alanyl-(2*S*)-valinate (127)

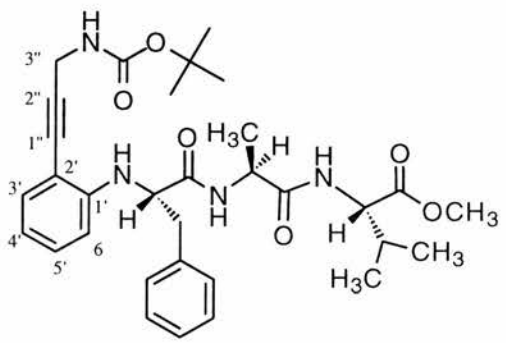

To a cooled solution of hydrogen chloride gas in dry ethyl acetate (0 °C, 100 cm^3) was added dipeptide **135** (0.9 g, 3.0 mmol) and the solution stirred for 30 min at room temperature. Concentration under reduced pressure gave the dipeptide hydrochloride salt **130** as a colourless oil which was refractory to recrystallisation (0.71 g, 99%); δ_H(300 MHz; D_2O) 0.86 (6 H, m, 2 × CH_3, Val), 1.46 (3 H, m, CH_3, Ala), 2.13 (1 H, m, β-H, Val), 3.69 (3 H, s, OCH_3), 4.07 (1 H, m, α-H, Ala) and 4.26 (1 H, d, *J* 5.8, α-H, Val); δ_C(74.76 MHz; D_2O) 16.53 and 18.09 (2 × CH_3, Val), 17.25 (CH_3, Ala), 27.52 (β-C, Val), 48.86 (α-C, Ala), 52.75 (α-C, Val), 58.70 (OCH_3), 171.31 (CO, amide) and 173.89 (CO_2CH_3).

To a solution of carboxylic acid **129** (0.55 g, 1.4 mmol) in dry acetonitrile (50 cm^3) and triethylamine (0.77 cm^3) was added dipeptide hydrochloride salt **130** (0.66 g, 2.77 mmol). The reaction mixture was then cooled to 0 °C, TBTU was added (0.48

g, 1.5 mmol) and the reaction mixture was left to stir at 0 °C for 1 h under a nitrogen atmosphere. Saturated brine was added (50 cm^3) and the solution extracted into ethyl acetate (3 × 100 cm^3). The combined organic extracts were successively washed with water (50 cm^3), citric acid (50 cm^3, 10% w/v), $NaHCO_3$ solution (50 cm^3, 1 mol dm^{-3}), brine (50 cm^3) and dried (Na_2SO_4). Concentration under reduced pressure gave the crude product as a yellow solid; recrystallisation from ethyl acetate-hexane gave the title peptide analogue **127** as a white solid (0.49 g, 60%), mp 63-65 °C (decomp.); (Found: C, 66.3; H, 7.2; N, 9.6. $C_{32}H_{42}N_4O_6$ requires C, 66.4; H, 7.3; N, 9.7%); (HRMS: found $[M + Na]^+$, 601.3019. $C_{32}H_{42}N_4O_6Na$ requires 601.3002); $[\alpha]_D^{18}$ 12.6 (*c* 1.1, CH_2Cl_2); υ_{max}(KBr disc)/cm^{-1} 3210-3460 (NH, amide and urethane), 2870-3065 (ArC-H and C-H), 2160-2250 (C≡C), 1644-1736 (C=O, amide, ester and urethane) and 1165-1271 (C-O, ester and urethane, and C-N, urethane); δ_H(300 MHz; $CDCl_3$) 0.82 [3 H, d, *J* 7.1, one of $(CH_3)_2$, Val], 0.86 [3 H, d, *J* 6.9, one of $(CH_3)_2$, Val], 1.30 (3 H, d, *J* 6.9, CH_3, Ala), 1.49 [9 H, s, $(CH_3)_3C$], 2.09 (1 H, m, β-H, Val), 3.20 (1 H, m, one of PhCH_2, Phe), 3.35 (1 H, m, one of PhCH_2, Phe), 3.74 (3 H, s, OCH_3), 4.03 (1 H, m, α-H, Phe), 4.16 (2 H, d, *J* 5.5, CH_2N), 4.46 (1 H, m, α-H, Val), 4.50 (1 H, m, α-H, Ala), 4.75 (1 H, br s, NH, amine), 4.89 (1 H, m, NH, urethane), 6.46 (1 H, d, *J* 8.5, 6'-CH), 6.68 (2 H, m, 4'-CH and NH, Val), 6.95 (1 H, m, NH, Ala), 7.12 (1 H, m, 5'-CH), 7.23 (1 H, d, *J* 6.3, 3'-CH) and 7.23-7.36 (5 H, m, Ar-H, Phe); δ_C(74.76 MHz; $CDCl_3$) 17.23 (CH_3, Ala), 17.57 [one of $(CH_3)_2$, Val], 18.79 [one of $(CH_3)_2$, Val], 28.27 [$(CH_3)_3C$], 30.95 (β-CH, Val), 31.23 (CH_2NH), 38.64 (CH_2Ph), 48.93 (α-C, Ala), 52.01 (OCH_3), 57.06 (α-C, Val), 59.97 (α-C, Phe), 79.12, 80.07 and 91.63 [$C(CH_3)_3$ and C≡C], 108.43 (2'-C), 110.87 (6'-CH), 118.50 (4'-CH), 127.44, 128.88 and 129.34 (Ar-CH, Phe), 130.26 (5'-CH), 132.37 (3'-CH), 136.11 [Ar-C, *ipso* (Phe)], 147.56 (1'-C), 155.32 (CO, urethane), 171.56 (CO, Val), 172.17 (CO, Phe) and 173.05 (CO, Ala); *m/z* (FAB) 601 (100%, $[M + Na]^+$), 579 (24, $[M + H]^+$), 349 (33, $[M + H - C_{10}H_{17}N_2O_4]^+$) and 293 (100, $C_{10}H_{16}N_2O_2^+$).

Methyl 2'-(3''-amino-prop-1''-ynyl)-phenyl-1'-(2*S*)-phenylalanyl-(2*S*)-alanyl-(2*S*)-valinate dihydrochloride (136)

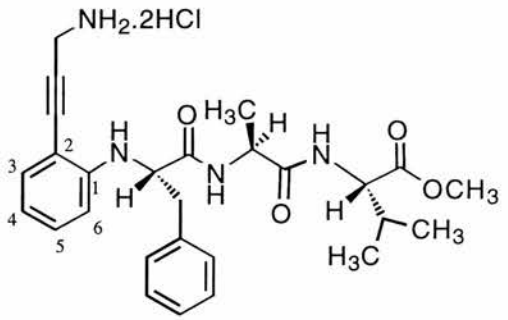

A stirred solution of pentapeptide analogue **127** (0.2 g, 0.35 mmol) in dry ethyl acetate (20 cm^3) was cooled to -10 °C and dry HCl gas bubbled continuously through the solution until the reaction was judged to be complete by TLC. The reaction mixture was then purged with argon and concentrated under reduced pressure to produce the title hydrochloride salt **136** as a white solid which was not purified further (0.19 g, 99%), mp 105-107 °C (decomp.); (HRMS: found $[M + Na]^+$, 501.2469. $C_{27}H_{34}N_4O_4Na$ requires 501.2478); $[\alpha]_D^{18}$ -5.4 (*c* 0.6, CH_2Cl_2); υ_{max}(KBr disc)/cm^{-1} 2966-3388 (ArC-H, C-H, NH_2^+, NH_3^+ and NH, amide), 2220 (C≡C), 1651-1741 (C=O, ester and 2 × amide) and 1159 (C-O, ester); δ_H(300 MHz; $CDCl_3$) 0.76 (6 H, d, *J* 6.87, 2 × CH_3, Val), 1.34 (3 H, d, *J* 5.77, CH_3, Ala), 2.00 (1 H, m, β-H, Val), 3.29 (2 H, m, CH_2Ph), 3.66 (3 H, s, OCH_3), 3.99 (2 H, m, CH_2N), 4.10 (1 H, m, α-H, Phe), 4.32 (1 H, m, α-H, Val), 4.54 (1 H, m, α-H, Ala), 6.47-6.55 (2 H, m, 4'-CH and 6'-CH) and 7.04-7.31 (7 H, m, Ar-H, Phe, 3'-CH and 5'-CH) and 7.80-8.90 (5 H, m, NH_2^+ and NH_3^+); δ_C(74.76 MHz; $CDCl_3$) 17.33 (CH_3, Ala), 17.59 and 18.74 (2 × CH_3, Val), 30.50 (CH_2NH), 30.81 (β-C, Val), 38.50 (CH_2Ph), 49.92 (α-C, Ala), 52.10 (OCH_3), 57.44 (α-C, Val), 60.64 (α-C, Phe), 84.25 and 86.10 (C≡C), 106.25 (2'-C), 110.74 (6'-CH), 117.44 (4'-CH), 126.95, 128.57 and 129.30 (Ar-CH, Phe), 131.97 (5'-CH), 132.76 (3'-CH), 137.12 [Ar-C, *ipso* (Phe)], 148.12 (1'-C), 171.98, 173.05 and 174.01 (CO, ester and 2 × CO, amide); *m/z* (FAB) 479 (40%, M^+), 501 (100, $[M + Na - H]^+$) and 959 (45, $[2M + H]^+$).

Methyl (2*S*)-leucinate ester hydrochloride (137)

To a stirred solution of (2*S*)-leucine (5.12 g, 39.0 mmol) in dry methanol (58 cm^3) at 0 °C was added, dropwise, thionyl chloride (11.33 cm^3, 0.16 mol) and the reaction mixture was refluxed for 2 h. Concentration under reduced pressure gave a white solid which was recrystallised from hot methanol to give the ester hydrochloride **137** as white crystals (5.14 g, 72%), mp 131 °C (lit.,[218] 138-140 °C); $[\alpha]_D^{25}$ 11.2 (*c* 2.0, H_2O) [lit.,[219] 12.6 (*c* 2.0, H_2O)]; δ_H(200 MHz; D_2O) 0.81 (6 H, m, 2 × CH_3, Leu), 1.52-1.76 (3 H, m, β-H and γ-H, Leu), 3.68 (3 H, s, OCH_3) and 3.99 (1 H, m, α-H, Leu); δ_C(74.76 MHz; $CDCl_3$) 22.51 and 22.78 (2 × CH_3, Leu), 22.97 (γ-C), 39.93 (β-C), 52.28 (OCH_3), 53.95 (α-C) and 170.76 (CO).

Methyl *N*-(*tert*-butoxycarbonyl)-(2*S*)-threonyl-(2*S*)-leucinate (139)

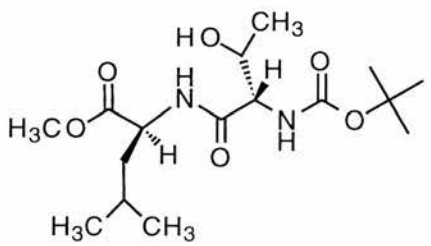

To a stirred solution of *N*-BOC-(2*S*)-threonine (3.3 g, 0.02 mol) in dry acetonitrile (150 cm^3) was added methyl (2*S*)-leucinate ester hydrochloride (**137**) (2.7 g, 0.02 mol), DIEA (7.8 cm^3, 0.04 mol) and TBTU (5.0 g, 0.02 mol). The reaction mixture was then stirred at 0 °C for 1 h under a nitrogen atmosphere. A solution of saturated brine (100 cm^3) was added to the clear solution and the resulting suspension extracted into ethyl acetate (3 × 100 cm^3). The organic extracts were pooled and washed successively with water (150 cm^3), $NaHCO_3$ solution (150 cm^3, 1 mol dm^{-3}), citric acid solution (150 cm^3, 10% w/v), brine (150 cm^3) and dried (Na_2SO_4). Concentration under reduced pressure gave the dipeptide **139** as a colourless oil (6.2 g, 90%); (HRMS: found $[M + H]^+$, 347.2172. $C_{16}H_{31}N_2O_6$ requires 347.2182); $[\alpha]_D^{20}$ -32.1 (*c* 1.4, MeOH) [lit.,[152] -39.3 (*c* 3.0, MeOH)]; υ_{max}(Thin film)/cm^{-1} 3322-3500,

(NH, amide and O-H), 2872-2959 (C-H), 1745 (C=O, ester), 1720 (C=O, urethane), 1659 (C=O, amide), 1207-1249 (C-N and C-O, urethane) and 1167 (C-O, ester); δ_H(200 MHz; $CDCl_3$) 0.88 (6 H, m, 2 × CH_3, Leu), 1.15 (3 H, m, CH_3, Thr), 1.40 [9 H, s, $(CH_3)_3C$)], 1.55 (1 H, m, γ-H, Leu), 1.57 (2 H, m, β-H, Leu), 3.67 (3 H, s, OCH_3), 4.10 (1 H, m, α-H, Leu), 4.25 (1 H, m, α-H, Thr), 4.52 (2 H, m, β-H, Thr and OH, Thr), 5.61 (1 H, m, NH, urethane) and 7.12 (1 H, m, NH, amide); δ_c(74.76 MHz; $CDCl_3$) 20.23 (γ-C, Thr), 22.10 and 23.33 (2 × δ-C, Leu), 25.18 (γ-C, Leu), 28.73 [$(CH_3)_3C$], 38.03 (β-C, Leu), 41.37 (OCH_3), 51.23 (β-C, Thr), 58.36 (α-C, Leu), 67.41 (α-C, Thr), [80.72 $(CH_3)_3C$], 156.85 (CO, urethane), 171.80 (CO, ester) and 173.67 (CO, ester); *m/z* (FAB+) 347 (100%, $[M + H]^+$) and 269 (45, $[M - C_5H_9O_2 + Na + H]^+$) and 146 (16).

Methyl 2'-(3''-*tert*-butoxycarbonylamino-prop-1''-ynyl)-phenyl-1'-(2*S*)-aminobutyryl-(2*S*)-threonyl-(2*S*)-leucinate (128)

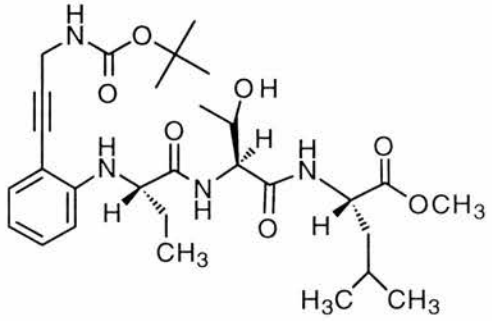

To a cooled solution of hydrogen chloride gas in dry ethyl acetate (0 °C, 70 cm^3) was added dipeptide **139** (1.46 g, 4.38 mmol) and the solution stirred for 30 min at room temperature. Concentration under reduced pressure gave the peptide hydrochloride **131** as a colourless oil which was refractory to recrystallisation (1.19 g, 99%); δ_H(300 MHz; D_2O) 0.81 (6 H, m, 2 × CH_3, Leu), 1.26 (3 H, d, *J* 6.0, CH_3, Thr), 1.57 (3 H, m, β-H, Leu and γ-H, Leu), 2.70 (3 H, s, OCH_3), 3.78 (1 H, α-H, Thr), 4.02 (1 H, m, α-H, Thr) and 4.39 (1 H, t, *J* 7.14, α-H, Leu); δ_C(74.76 MHz; D_2O) 18.70 (CH_3, Thr), 20.62 and 21.94 (2 × CH_3, Leu), 24.25 (γ-C, Leu), 39.07 (β-C, Leu), 51.72 (α-C,

Leu), 52.88 (OCH_3), 58.63 (α-C, Thr), 66.35 (β-C, Thr), 168.09 (CO, amide) and 174.59 (CO, ester).

To a solution of carboxylic **132** (0.8 g, 2.41 mmol) in dry acetonitrile and triethylamine (1.0 cm^3) was added dipeptide hydrochloride salt **131** (0.68 g, 2.41 mmol). The reaction mixture was then cooled to 0 °C, TBTU was added (0.8 g, 2.51 mmol) and the reaction mixture was left to stir at 0 °C for 1.5 h under a nitrogen atmosphere. Saturated brine (100 cm^3) was added and the reaction mixture extracted into ethyl acetate (3 × 100 cm^3). The combined organic extracts were successively washed with water (100 cm^3), citric acid solution (100 cm^3, 10% w/v), $NaHCO_3$ solution (100 cm^3, 1 mol dm^{-3}), brine (50 cm^3) and dried (Na_2SO_4). Concentration under reduced pressure gave the crude product as a yellow solid. Recrystallisation from ethyl acetate-hexane gave the title peptide as a pale yellow solid (1.22 g, 87%), mp 80-85 °C; (HRMS: found $[M + H]^+$, 561.3296. $C_{29}H_{45}N_4O_7$ requires 561.3288); $[\alpha]_D^{18}$ +20.0 (*c* 0.1, MeOH); υ_{max}(KBr disc)/cm^{-1} 3305-3500 (NH, amide, amine and urethane), 2873-3075 (ArC-H and C-H), 2240 (C≡C), 1649-1744 (C=O, amide, ester and urethane) and 1168-1279 (C-O, ester and urethane, and C-N, urethane); δ_H(300 MHz; $CDCl_3$) 0.81-0.88 (6 H, m, 2 × CH_3, Leu), 1.05 (3 H, t, *J* 7.4, CH_3, Abu), 1.11 (3 H, d, *J* 6.3, CH_3, Thr), 1.43 [9 H, s, $(CH_3)_3C$], 1.53 (2 H, m, β-H, Leu), 1.63 (1 H, m, γ-H, Leu), 1.80 (2 H, m, β-H, Abu), 3.68 (3 H, s, OCH_3), 3.70-3.72 (2 H, m, α-H, Abu and β-H, Thr), 4.16 (2 H, m, CH_2N), 4.34-4.51 (3 H, m, 2 × α-H, Leu and Thr, and OH, Thr), 4.91 (1 H, m, NH, Abu), 5.14 (1 H, br s, NH, urethane), 6.43 (1 H, d, *J* 8.2, 6'-CH), 6.67 (1 H, t, *J* 7.20, 4'-CH), 6.89 (1 H, m, NH, amide), 7.11 (1 H, t, *J* 7.8, 5'-CH), 7.25 (1 H, d, *J* 5.5, 3'-CH) and 7.46 (1 H, m, NH, amide); δ_C(74.76 MHz; $CDCl_3$) 10.46 (CH_3, Abu), 20.16 (CH_3, Thr), 21.68 and 23.14 (2 × CH_3, Leu), 24.54 (γ-C, Leu), 26.34 (β-H, Abu), 28.62 [$(CH_3)_3C$], 30.85 (CH_2NH), 39.97 (β-H, Leu), 50.56 (α-C, Leu), 52.26 (OCH_3), 58.00 (α-C, Abu), 58.40 (α-C, Thr), 67.04 (β-C, Thr), 78.63, 78.76 and 93.63 [$C(CH_3)_3$ and C≡C], 108.54 (2'-C), 110.65 (6'-CH), 118.27 (4'-CH), 130.13 (5'-CH), 132.51 (3'-CH), 147.89 (1'-C),

155.97 (CO, urethane), 170.70, 173.06 and 173.36 (3 × CO); *m/z* (CI) 561 (31%, [M + H]$^+$), 505 (14, [M - C_4H_9 + 2H]$^+$), 460 (70, [M + H - $C_5H_9O_2$]$^+$), 362 (100) and 57 (57, $C_4H_9^+$).

2'-(3''-*tert*-butoxycarbonylamino-prop-1''-ynyl)-phenyl-1'-(2*S*)-aminobutyryl-(2*S*)-threonyl-(2*S*)-leucine (140)

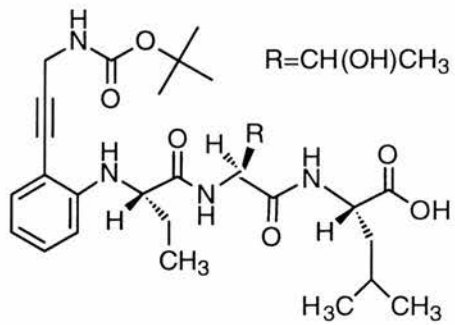

To a solution of methyl pentapeptide analogue **128** (1.15 g, 2.0 mmol) in methanol (100 cm^3) was added LiOH solution (12 cm^3, 1 mol dm^{-3}) and the solution was stirred for 1.5 days. The reaction mixture was cooled in ice, acidified to pH 3 with citric acid solution (10% w/v) and extracted into ethyl acetate (3 × 100 cm^3). The organic extracts were pooled, washed with water (4 × 80 cm^3), brine (50 cm^3) and dried (Na_2SO_4). Concentration under reduced pressure gave **140** as yellow oil which was refractory to recrystallisation (1.06 g, 97%); (HRMS: found [M + Na]$^+$, 569.2944. $C_{28}H_{42}N_4O_7Na$ requires 569.2951); υ_{max}(Thin film)/cm^{-1} 3327-3550 (NH, amide and urethane, and OH, acid and Thr), 2873-3076 (ArC-H and C-H), 2210 (CC), 1654-1740 (C=O, amide, acid and urethane) and 1167-1280 (C-O, urethane and acid, and C-N, urethane); $[\alpha]_D^{25}$ 21.4 (*c* 1.0, CH_2Cl_2); δ_H(300 MHz; $CDCl_3$) 0.86 (6 H, m, 2 × CH_3, Leu), 1.04 (6 H, m, CH_3, Abu and CH_3, Thr), 1.44 [10 H, s, $(CH_3)_3C$ and γ-H, Leu], 1.65 (2 H, β-H, Leu), 1.82-2.03 (2 H, m, β-H, Abu), 3.80 (1 H, m, α-H, Abu), 4.18 (4 H, m, CH_2N, α-H and β-H, Thr), 4.24-4.50 (3 H, m, α-H, Leu, OH, Thr, and NH, amine), 5.20 (1 H, br s, NH, urethane), 6.48 (1 H, m, 6'-CH), 6.65 (1 H, m, 4'-CH), 7.12 (1 H, m, 5'-CH), 7.25 (2 H, m, 3'-CH and NH, amide), 7.30-7.60 (1

H, br s, OH, acid) and 7.71 (1 H, m, NH, amide); δ_C(74.76 MHz; $CDCl_3$) 10.25 (CH_3, Abu), 17.98 (CH_3, Thr), 21.52 and 22.60 (2 × CH_3, Leu), 24.67 (γ-C, Leu), 26.43 (β-H, Abu), 28.20 [(CH_3)$_3$C], 31.19 (CH_2NH), 40.44 (β-H, Leu), 50.80 (α-C, Abu), 56.80 (α-C, Leu), 60.46 (β-C, Thr), 66.84 (α-C, Thr), 79.16 80.06 and 91.87 [C(CH_3)$_3$ and C≡C], 108.41 (2'-C), 110.76 (6'-CH), 118.10 (4'-CH), 130.07 (5'-CH), 132.48 (3'-CH), 147.86 (1'-C), 155.76 (CO, urethane), 170.78, 174.89 and 175.35 (2 × CO, amide, and CO, acid); *m/z* (ES+) 591 (32, [M + 2Na - H]$^+$) and 569 (100%, [M + Na]$^+$).

Methyl 2'-{3''-[2'''-(3''''-*tert*-butoxycarbonylamino-prop-1'''-ynyl)-phenyl-1'''-(2*S*)-phenylalanyl-(2*S*)-methyl-(2*S*)-valinylamino]-prop-1''-ynyl}-phenyl-1'-(2*S*)-aminobutyryl-(2*S*)-threonyl-(2*S*)-leucinate (141)

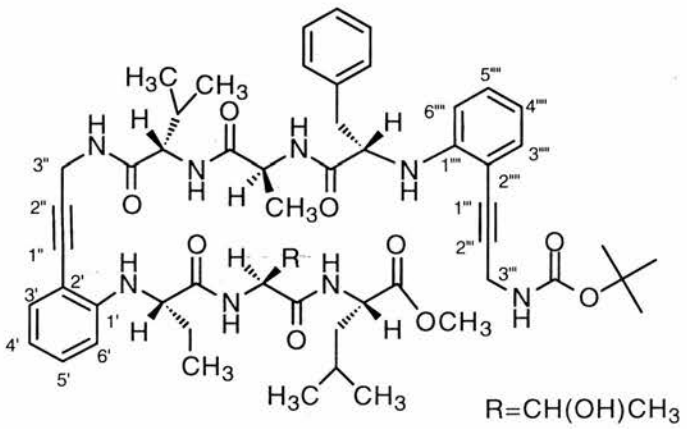

A solution of carboxylic acid **140** (0.31 g, 0.57 mmol) and EDCI hydrochloride (0.16 g, 0.85 mmol) in dry DMF (20 cm^3) was stirred at room temperature for 5 min. To this solution was added HOBt (0.11 g, 0.85 mmol) and the reaction mixture was stirred for a further 2 min at 0 °C under a nitrogen atmosphere. A solution of methyl ester dihydrochloride **136** (0.32 g, 0.57 mmol) and TEA (0.32 cm^3, 2.3 mmol) in DMF (20 cm^3) was added*via* cannula and the reaction mixture was allowed to warm up to room temperature over a period of 12 h. Saturated brine (50 cm^3) and ethyl acetate (50 cm^3) were added and the organic phase separated and washed with citric

acid (50 cm^3, 10% w/v), $NaHCO_3$ (50 cm^3, 5% w/v), water (4 × 50 cm^3), saturated brine (50 cm^3), dried (Na_2SO_4) and concentrated under reduced pressure to yield a brown oil. Purification by flash silica chromatography using MeOH-CH_2Cl_2 (3:97) as the eluent gave acyclic decapeptide analogue **141** as a pale yellow oil (0.47 g, 81%); (HRMS: found $[M + H]^+$ 1007.5567. $C_{55}H_{75}N_8O_{10}$, requires 1007.5606); $[\alpha]_D^{18}$ 24.0 (*c* 0.4, CH_2Cl_2); υ_{max}(KBr disc)/cm^{-1} 3250-3560 (NH, amide, urethane and amine), 2931-3080 (ArC-H and C-H), 2225 (2 × C≡C), 1651-1730 (C=O, amide, ester and urethane) and 1165-1275 (C-O, ester and urethane, and C-N, urethane); δ_H(300 MHz; $CDCl_3$) 0.84-0.94 (12 H, m, 2 × CH_3, Val and 2 × CH_3, Leu), 1.03-1.08 (6 H, m, CH_3, Thr and CH_3, Abu), 1.29 (3 H, d, *J* 6.87, CH_3, Ala), 1.40 (2 H, m, β-H, Leu), 1.45 [9 H, s, $(CH_3)_3C$], 1.73-1.92 (1 H, m, γ-H, Leu), 2.00-2.10 (2 H, m, β-H, Leu), 2.13-2.17 (1 H, m, β-H, Val), 3.18 (2 H, d, *J* 6.32, β-H, Phe), 3.72 (4 H, m, OCH_3 and β-H, Thr), 3.99-4.06 {1 H, m, one of CH_2NH(CO)CH[$CH(CH_3)_2$]}, 4.14-4.23 (5 H, m, CH_2NCO_2, α-H, Phe, α-H, Thr and OH, Thr), 4.37-4.45 [1 H, m, one of CH_2NH(CO)CH[$CH(CH_3)_2$]}, 4.46-4.58 (3 H, m, α-H, Val, α-H, Leu, and α-H, Abu), 4.74 (1 H, m, α-H, Ala), 4.92, 5.02-5.12 and 5.14 (3 H, m, 2 × NH, amine and NH, urethane), 6.46 (2 H, d, *J* 8.24, 6'-CH and 6''''-CH), 6.60-6.72 (2 H, 2 × t, *J* 7.42, 4'-CH and 4''''-CH), 6.92 (1 H, br s, NH, amide), 7.07-7.29 (12 H, m, 3 × NH, amide, 3'-CH, 3''''-CH, 5'-CH, 5''''-CH and Ar-H, Phe) and 7.52 (1 H, m, NH, amide); δ_C(74.76 MHz; $CDCl_3$) 10.38 (CH_3, Abu), 17.66 and 17.83 (2 × CH_3, Val), 18.48 (CH_3, Thr), 18.92 (CH_3, Ala), 21.59 and 22.95 (2 × CH_3, Leu), 24.72 (γ-C, Leu), 26.56 (β-C, Abu), 28.30 [(CH_3)$_3$C], 28.85 and 30.12 (2 × CH_2N), 30.95 (β-C, Val), 38.99 (CH_2Ph), 40.11 (β-C, Leu), 48.83 (α-C, Ala), 51.52 (α-C, Abu), 52.10 (OCH_3), 56.95 (α-C, Leu), 57.25 (α-C, Val), 59.54 (α-C, Phe), 61.01 (β-C, Thr), 67.04 (α-C, Thr), 79.10 79.62 and 80.05 [2 × C≡C and $C(CH_3)_3$], 108.36 and 108.67 (2'-C and 2''''-C), 110.84 (6'-CH and 6''''-CH), 117.95 and 118.48 (4'-CH and 4''''-CH), 127.33, 128.81 and 129.41 (Ar-CH, Phe), 130.14 and 130.96 (5'-CH and 5''''-CH), 132.15 and 132.63 (3'-CH and 3''''-CH), 136.31 [Ar-C, *ipso* (Phe)], 147.53 and 147.96 (1'-C and 1''''-C) 155.50 (CO, urethane), 170.11, 171.44, 171.93, 172.19, 172.92 and 174.57 (5

× CO, amide and CO, ester); *m/z* (FAB) 1030 (100, $[M + Na]^+$) and 1007 (19%, $[M + H]^+$).

(3*S*, 6*S*, 9*S*, 22*S*, 25*S*, 28*S*)-2,5,8,11,21,24,27,30-octaaza-15, 34-dibenzo-3-benzyl-6-methyl-9-isopropyl-22-ethyl-25-[(2*S*)-hydroxyethyl]-28-(2-methypropyl)-4, 7, 10, 23, 26, 29-hexaoxo-13,32-diyne-tricyclo [32.4.0.0^{15,20}] octatriacontane (115)

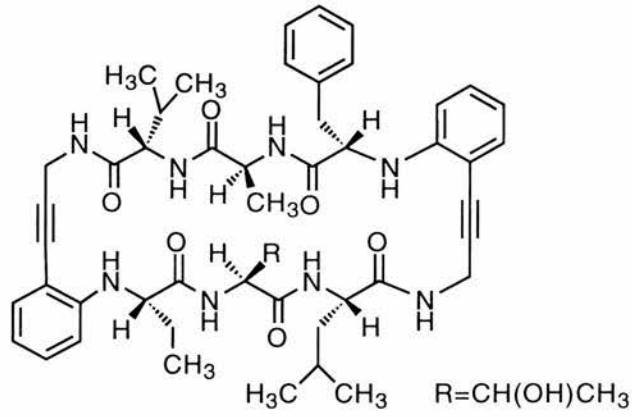

To a stirred solution of the acyclic decapeptide analogue **141** (150 mg, 0.15 mmol) in THF, water and methanol (1:1:2, 20 cm^3) was added aqueous LiOH solution (1 mol dm^{-3}, 1.18 cm^3). The reaction mixture was then stirred for 7 h . The pH was adjusted to 3 with citric acid solution (10%, w/v) and the solution extracted with ethyl acetate (3 × 50 cm^3). The organic extracts were combined, washed with water (4 × 50 cm^3), brine (50 cm^3) and dried (Na_2SO_4). Concentration under reduced pressure yielded the free acid as a white flocculant (124 mg, 84%).

A stirred solution of this acid (120 mg, 0.12 mmol) in dry ethyl acetate (13 cm^3) was cooled to -15 °C and dry HCl gas bubbled through the solution for 10 min. The solution was then purged with argon and concentrated under reduced pressure to give the *N* and *C*-deprotected decapeptide analogue as a trihydrochloride salt (120 mg, 99%)

Under an atmosphere of nitrogen, a portion of this compound (110 mg, 0.12 mmol) was dissolved in dry DMF (100 cm^3) and the solution cooled to 0 °C. $NaHCO_3$ (0.12 g, 1.4 mmol) and diphenylphosphoryl azide (DPPA) (0.24 g, 0.86

mmol) were added and the reaction mixture stirred at 0 °C for 2 h and then allowed to slowly warm up to room temperature. A further 3 equivalents of DPPA was added after 2 days and the reaction was stirred for a further 24 h. $CuSO_4$ solution (1 mol dm^{-3}, 100 cm^3) was added and the reaction mixture extracted into dichloromethane (100 cm^3). The organic extracts were washed with water (4 × 50 cm^3), $NaHCO_3$ solution (25 cm^3, 5% w/v), brine (25 cm^3), dried (Na_2SO_4) and concentrated under reduced pressure to give a brown oil which was purified by column chromatography [eluent: dichloromethane-methanol (95:5)] to give the cyclised material as a yellow oil. Further purification on a Vydac semi-preparative C-18 reverse phase column using an acetonitrile-water gradient yielded the title compound **115** as a sticky white foam (0.02 g, 20%); (HRMS: found $[M + Na]^+$ 897.4648. $C_{49}H_{62}N_8O_7$,Na requires 897.4639); δ_H(500 MHz; $CDCl_3$) 0.73 (3 H, m, 1 × CH_3, Val), 0.83 (3 H, m, 1 × CH_3, Val), 0.89-0.95 (9 H, m, CH_3, Abu and 2 × CH_3, Leu), 1.00 (3 H, d, CH_3, Thr), 1.26 (3 H, m, CH_3, Ala), 1.66 (1 H, m, γ-H, Leu), 1.82-1.92 (3 H, m, one of CH_2, Abu, and β-H, Leu), 1.93-2.09 (2 H, m, one of CH_2, Abu, and β-H, Val), 3.21 (2 H, d, β-H, Phe), 3.80-3.87 (2 H, m, OH, Thr, and one of CH_2N), 4.01-4.08 (2 H, m, β-H, Thr and α-H, Abu), 4.08-4.19 (2 H, m, α-H, Phe, and one of CH_2N), 4.27 (1 H, m, 1 H of CH_2N), 4.41 (1 H, m, α-H, Val), 4.46 (1 H, m, one of CH_2N), 4.58 (1 H, m, α-H, Leu), 4.64 (1 H, m, α-H, Thr), 4.71 (1 H, m, α-H, Ala), 5.35 (1 H, d, NH, Phe), 5.71 (1 H, d, NH, Abu), 6.42 (1 H, m, Ar-H6), 6.53 (1 H, m, Ar-H6'), 6.57 (1 H, m, Ar-H4'), 6.61 (1 H, m, Ar-H4), 6.86 (1 H, m, NH, Thr), 7.07-7.36 (12 H, m, Ar-H5, Ar-H5', Ar-H3, Ar-H3', Ar-H, Phe, NH, Ala, NH, Val and $CH_2N\mathit{H}$), 7.43 (1 H, m, $CH_2N\mathit{H}$) and 7.60 (1 H, m, NH, Leu); δ_c(74.76 MHz; $CDCl_3$) 9.20 (CH_3, Abu), 17.90 and 18.46 (2 × CH_3, Val), 19.00 (CH_3, Thr), 19.84 (CH_3, Ala), 21.43 and 22.99 (2 × CH_3, Leu), 24.80 (γ-C, Leu), 25.74 (β-C, Abu), 30.81 and 31.07 (2 × CH_2N), 31.42 (β-C, Val), 39.19 (CH_2Ph), 39.46 (β-C, Leu), 48.62 (α-C, Ala), 51.29 (α-C, Abu), 57.17 (α-C, Leu), 57.90 (α-C, Val), 58.45 (α-C, Phe), 59.56 (β-C, Thr), 67.69 (α-C, Thr), 80.48, 81.63 91.04 and 91.39 (2 × C≡C), 107.70 and 107.96 (15-C and 34-C), 110.35 (19-CH and 35-CH), 116.74 and 117.06 (12-CH and 36-CH), 126.90, 128.47

and 129.38 (Ar-H, Phe), 129.72 (18-CH and 37-CH), 130.72 and 131.33 (16-CH and 35-CH), 136.97 [Ar-C, *ipso* (Phe)], 147.94 and 148.39 (20-C and 1-C), 170.64, 170.81, 171.20, 172.72, 173.08 and 173.86 (6 × CO, amide); *m/z* (ES) 897 (100, $[M + Na]^+$) and 875 (25%, $[M + H]^+$).

(2*S*)-Alanyl-(2*S*)-isoleucinyl-(2*S*)-valinyl-(2*S*)-alanine, trifluoroacetic acid (146)

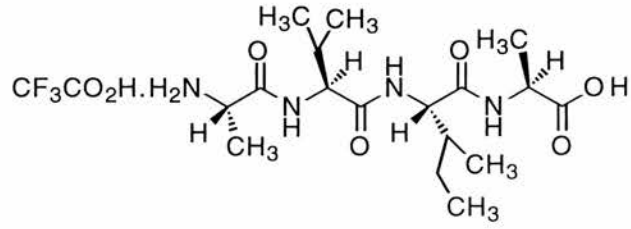

This compound was prepared in the manner described in appendix one using Fmoc-Ala-Wang (0.68 g, 0.5 mmol), Fmoc-Ile (0.71 g, 2.0 mmol), Fmoc-Val (0.68 g, 2.0 mmol) and Fmoc-Ala (0.62 g, 2.0 mmol) to give, after lyophilisation, the peptide trifluoroacetate salt **146** as a white powder (0.23 g, 95%), mp >280 °C (decomp.); (HRMS: found $[M + Na]^+$, 395.2265. $C_{17}H_{32}N_4O_5Na$ requires 395.2270); $[\alpha]_D^{18}$-60 (*c* 0.1, MeOH); υ_{max}(KBr disc)/cm^{-1} 2950-3448 (O-H, NH_3^+ and C-H) and 1630-1654 (C=O, amide and carboxylic acid); δ_H(300 MHz; D_2O) 0.66-0.78 (12 H, m, 2 × CH_3, Ile and 2 × CH_3, Val), 0.98-1.07 (1 H, m, one of γ-CH_2, Ile), 1.21 (3 H, d, *J* 7.2, CH_3, Ala), 1.33 (4 H, m, CH_3, Ala, and one of γ-CH_2, Ile), 1.67 (1 H, m, β-H, Ile), 1.84 (1 H, m, β-H, Val), 3.96 (3 H, m, α-H, Ala, Val and Ile) and 4.08 (1 H, q, *J* 7.2, α-H, Ala); δ_C[50.30 MHz; $(CD_3)_2SO$] 10.90 (δ-C, Ile), 15.24 (γ-C, Ile), 17.02 (CH_3, Ala), 17.20 (CH_3, Val), 17.81 (CH_3, Ala), 19.01 (CH_3, Val), 24.28 (CH_2, Ile), 30.68 (β-H, Ile), 36.31 (β-H, Val), 47.36, 47.88, 57.04 and 57.11 (4 × α-C), 169.27, 170.27, 170.35 and 173.72 (3 × CO, peptide, and CO, acid); *m/z* (ES+) 395 (100%, $[M + Na]^+$).

Methyl (2*S*)-Alanyl-(2*S*)-isoleucinyl-(2*S*)-valinyl-(2*S*)-alanate, hydrochloride (147)

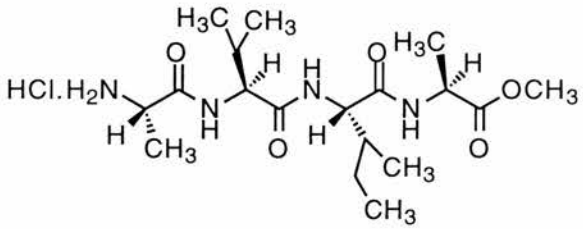

Tetrapeptide **146** (0.30 g, 0.62 mmol) was dissolved in dimethoxypropane (10.4 cm^3) and methanol (2.0 cm^3) and to this solution was added concentrated hydrochloric acid (1.3 cm^3). The reaction mixture was stirred for 18 h at rt, concentrated under reduced pressure and triturated with dry diethyl ether to yield a white semi-solid which was subsequently lyophilised to produce the dry tetrapeptide methyl ester **147** as a white solid (0.26 g, 99%), mp >250 °C (decomp.); (HRMS: found $[M + Na]^+$, 409.2416. $C_{18}H_{34}N_4O_5Na$ requires 409.2427); $[\alpha]_D^{18}$ -46.0 (*c* 0.2 MeOH); υ_{max}(KBr disc)/cm^{-1} 3285-3540 (NH, amide), 2830-2963 (C-H), 1639-1745 (C=O, amide and ester) and 1218 (C-O, ester); δ_H(300 MHz; D_2O) 0.67-0.78 (12 H, m, 2 × CH_3, Ile and 2 × CH_3, Val), 1.05 (1 H, m, one of γ-CH_2, Ile), 1.23 (3 H, d, *J* 7.4, CH_3CHNH_2.HCl), 1.33 (4 H, m, $CH_3CHCO_2CH_3$ and one of γ-CH_2, Ile), 1.67 (1 H, m, β-H, Ile), 1.85 (1 H, m, β-H, Val), 3.57 (3 H, s, OCH_3), 3.92-4.01 (3 H, m, α-H, Ala, Val and Ile), and 4.20 (1 H, m, $CH_3CHCO_2CH_3$); δ_C(100 MHz; D_2O) 12.59 (CH_3, Ile), 17.21 (γ-C, Ile), 18.50 (CH_3, Ala), 19.20 (CH_3, Val), 20.37 (CH_3, Ala), 20.73 (CH_3, Val), 27.13 (CH_3, Ile), 32.78 (β-C, Ile), 38.61 (β-C, Val), 51.29 and 51.43 (2 × α-C), 55.40 (OCH_3), 60.98 and 61.77 (2 × α-C), 173.24, 175.29, 175.74 and 177.41 (3 × CO, amide and CO, ester); *m/z* (ES+) 409 (100%, $[M + Na]^+$).

(2*S*)-Alanyl-(2*S*)-aminobutyryl-(2*S*)-threonyl-(2*S*)-leucine, trifluoroacetic acid (150)

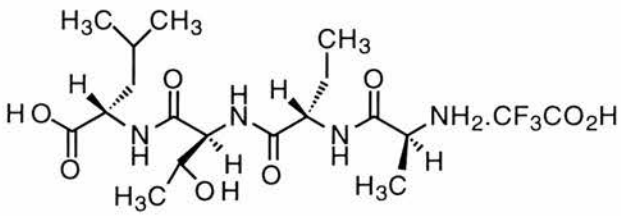

This compound was prepared in the manner described in appendix one using Fmoc-Leu-Wang (1.0 g, 0.44 mmol), Fmoc-Thr (0.6 g, 1.76 mmol), Fmoc-Abu (0.57 g, 1.76 mmol) and Fmoc-Ala (0.55g, 1.76 mmol) to give, after lyophilisation, the dry peptide **150** as the trifluoroacetate salt (210 mg, 95%), mp >165 °C (decomp.); (HRMS: found $[M + Na]^+$, 411.2202. $C_{17}H_{32}O_6N_4Na$ requires 411.2220); $[\alpha]_D^{18}$ -8.4 (*c* 0.1, MeOH); υ_{max}(KBr disc)/cm^{-1} 3300 and 2966-3082 (O-H, NH_3^+ and C-H) and 1651-1740 (C=O, amide and carboxylic acid); δ_H(300 MHz; D_2O) 0.68-0.79 (9 H, m, 2 × CH_3, Leu, and CH_3, Abu), 1.06 (3 H, d, *J* 6.2, CH_3, Thr), 1.36 (3 H, d, *J* 7.2, CH_3, Ala), 1.54 (3 H, m, β-H, Abu and γ-H, Leu), 1.60 (2 H, m, β-H, Leu), 3.92-3.97 (2 H, m, α-H, Ala and β-H, Thr), 4.11-4.15 (2 H, m, α-H, Leu and Thr) and 4.20 (1 H, m, α-H, Abu); δ_C(50.30 MHz; D_2O) 11.95 (CH_3, Abu), 19.12 (CH_3, Ala), 21.37 (CH_3, Thr), 23.13 and 24.70 (2 × CH_3, Leu), 26.96 (γ-C, Leu), 27.10 (β-C, Leu), 41.96 (β-C, Abu), 51.44 (α-C, Ala), 54.16 (α-C, Abu), 57.91 (α-C, Leu), 61.63 (α-C, Thr), 69.70 (β-C, Thr), 173.32, 173.94, 176.38 and 178.89 (3 × CO, amide, and CO, acid); *m/z* (ES+) 411 (100, $[M + Na]^+$) and 389 (11%, $[M + H]^+$).

Methyl (2*S*)-Alanyl-(2*S*)-aminobutyryl-(2*S*)-threonyl-(2*S*)-leuciate, hydrochloride (151)

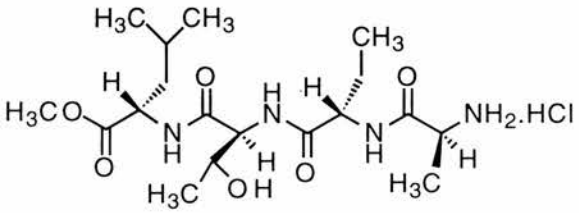

Tetrapeptide **150** (0.47 g, 0.88 mmol) was dissolved in a 10% (v/v) solution of methanol in dimethoxypropane (27 cm^3) and to this solution was added concentrated hydrochloric acid (1.0 cm^3). The reaction mixture was stirred for 18 h at rt, concentrated under reduced pressure and triturated with dry diethyl ether to yield a white semi-solid which was subsequently lyophilised to produce the dry tetrapeptide methyl ester **151** as a white solid (0.38 g, 99%), m.p >190 °C (decomp.); (HRMS: found $[M + Na]^+$, 425.2368. $C_{18}H_{34}N_4O_6Na$ requires 425.2376); $[\alpha]_D^{18}$ -36.0 (*c* 0.1 MeOH); υ_{max}(KBr disc)/cm^{-1} 2964-3253 (NH_3^+, NH, amide, and C-H), 1674-1745 (C=O, ester and amide); δ_H(300 MHz; D_2O) 0.71-0.79 (9 H, m, 2 × CH_3, Leu and CH_3, Abu), 1.26 (3 H, d, *J* 6.6, CH_3, Thr), 1.38 (3 H, d, *J* 7.2, CH_3, Ala), 1.50 (2 H, m, CH_2, Abu), 1.72 (1 H, m, γ-H, Leu), 1.81 (2 H, m, CH_2, Leu), 3.56 (1 H, s, OCH_3), 3.95 (1 H, q, *J* 7.2, α-H, Ala), 4.07 (1 H, d, *J* 4.6, α-H, Thr), 4.22-4.33 (2 H, m, α-H, Leu and α-H, Abu), and 5.25 (1 H, m, β-H, Thr); δ_C(50.30 MHz; D_2O) 11.81 (CH_3, Abu), 18.33 (CH_3, Thr), 19.21 (CH_3, Ala), 23.29 and 24.52 (2 × CH_3, Leu), 26.48 (β-C, Leu), 26.86 (γ-C, Leu) 41.79 (β-C, Abu), 51.44 (α-C, Ala), 54.32 (α-C, Abu), 55.48 (OCH_3), 56.84 (α-C, Leu), 58.46 (α-C, Thr), 72.61 (β-C, Thr), 169.02, 173.34, 174.01 and 176.64 (3 × CO, amide and CO, ester); *m/z* (ES+) 425 (100%, $[M + Na]^+$) and 385 (32, $[M - H_2O + H]^+$).

Methyl 2'-(3''-*tert*-butoxycarbonylamino-prop-1''-ynyl)-phenyl-1'-(2*S*)-phenylalanyl-(2*S*)-alanyl-(2*S*)-aminobutyryl-(2*S*)-threonyl-(2*S*)-leucinate (152)

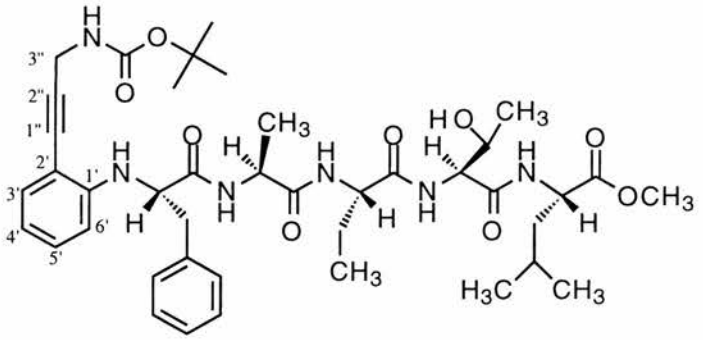

This compound was prepared in a manner identical to that for decapeptide analogue **141**, using tetrapeptide methyl ester **151** (0.12 g, 0.27 mmol) and carboxylic acid **129** (0.11 g, 0.27 mmol). The crude product was obtained as a pale yellow oil which was subsequently triturated with cold ethyl acetate-diethyl ether (1:1) to yield heptapeptide analogue **152** as a yellow solid. This material was purified further by flash silica chromatography using DCM-MeOH (98:2) as the eluent to yield the pure heptapeptide analogue as a white solid (0.11 g, 52%), mp >170 °C (decomp.). This procedure was repeated several times to obtain enough material for the remaining steps; (HRMS: found $[M + Na]^+$, 801.4155. $C_{41}H_{58}N_6O_9$ requires 801.4163); $[\alpha]_D^{18}$ 104.0 (*c* 0.1, DMSO); υ_{max}(KBr disc)/cm^{-1} 3302-3575 (NH, amide and urethane, and NH, amine), 2873-3064 (Ar-C-H and C-H), 2200 (C≡C), 1642-1745 (C=O, amide and ester) and 1165-1272 (C-O, ester and urethane, and C-N, urethane); δ_H[300 MHz; $(CD_3)_2SO$] 0.75-0.85 (9 H, m, 2 × CH_3, Leu and CH_3, Abu), 1.01 (3 H, d, *J* 6.2, CH_3, Thr), 1.18 (3 H, d, *J* 7.0, CH_3, Ala), 1.38 [9 H, s, $(CH_3)_3C$], 1.43-1.63 (5 H, m, CH_2, Abu and Leu, γ-H, Leu), 2.90-3.10 (2 H, m, CH_2, Phe), 3.56 (3 H, s, OCH_3), 3.85 (1 H, m, β-H, Thr), 4.00 (2 H, m, CH_2N), 4.10-4.40 (5 H, m, α-H, Leu, Abu, Thr, Ala and Phe), 4.80 (1 H, m, OH, Thr) and 5.15 (1 H, m, NH, Phe), 6.40 (1 H, m, 6'-CH), 6.50 (1 H, m, 4'-CH) 7.00-7.44 (8 H, m, Ar-H, Phe, NH, urethane, 3'-CH and 5'-CH), 7.70 (1 H, m, NH, Thr), 8.03 (2 H, m, NH, Leu and Abu) and 8.29 (1 H, m, NH, Ala); δ_C[100.60 MHz; $(CD_3)_2SO$] 9.50 (CH_3, Abu), 18.00 (CH_3, Ala), 19.80 (CH_3, Thr),

21.30 and 22.90 (2 × CH_3, Leu), 24.4 (γ-CH, Leu), 25.10 (β-C, Abu), 28.80 [$(CH_3)_3C$], 30.90 (CH_2N), 39.00-40.00 (β-CH_2, Leu and β-C, Phe), 48.30 and 50.50 (2 × α-C), 52.20 (OCH_3), 54.10 and 58.20 (3 × α-C), 67.40 (β-C, Thr), 78.00, 78.10 and 93.50 [$C(CH_3)_3$ and C≡C], 107.50 (2'-C), 110.00 (6'-CH), 116.00 (4'-CH), 126.00, 128.70 and 129.70 (Ar-H, Phe), 130.00 (5'-CH), 131.8 (3'-CH), 138.10 [Ar-C, *ipso* (Phe)], 148.00 (1'-C), 156.10 (CO, urethane) and 169.60-172.50 (4 × CO, amide, and CO, ester); *m/z* (FAB) 801 (100%, $[M + Na]^+$).

Methyl 2'-(3''-*tert*-butoxycarbonylamino-prop-1''-ynyl)-phenyl-1'-(2*S*)-phenylalanyl-(2*S*)-alanyl-(2*S*)-valinyl-(2*S*)-isoleucinyl-(2*S*)-alanate (148)

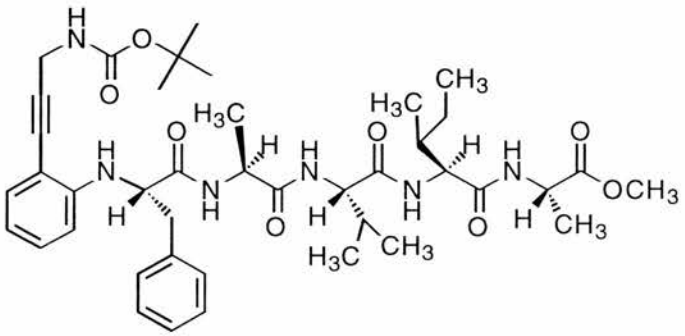

This compound was prepared in a manner identical to that for pentapeptide analogue **127**, using tetrapeptide **147** (0.43 g, 1.02 mmol) and carboxylic acid **129** (0.4 g, 1.02 mmol). The crude product was obtained as a pale yellow oil which was subsequently triturated with cold diethyl ether to yield heptapeptide analogue **148** as a white solid (0.74 g, 95%), mp >210 °C (decomp.); (HRMS: found $[M + Na]^+$, 785.4223. $C_{41}H_{58}N_6O_8Na$ requires 785.4214); $[\alpha]_D^{18}$ -96.0 (*c* 0.1, CD_3SO); υ_{max}(KBr disc)/cm^{-1} 3288-3590 (NH, amide and urethane, and NH, amine), 2860-3075 (Ar-C-H and C-H), 2250 (C≡C), 1638-1740 (C=O, amide and ester) and 1165-1350 (C-O, ester and urethane, and C-N, urethane); δ_H[300 MHz; $(CD_3)_2SO$] 0.65-0.81 (12 H, m, 2 × CH_3, Ile and 2 × CH_3, Val), 1.02-1.13 (1 H, m, one of γ-CH_2, Ile), 1.17 (3 H, d, *J* 7.0, CH_3, Ala), 1.22 (4 H, m, CH_3, Ala and one of γ-CH_2, Ile), 1.38 [9 H, s, $(CH_3)_3C$], 1.68 (1 H, m, β-H, Val), 1.91 (1 H, m, β-H, Ile), 2.84-3.09 (2 H, m, CH_2, Phe), 3.54 (1 H, s,

OCH_3), 4.00 (2 H, m, CH_2NH), 4.14-4.20 (4 H, m, α-H, Ala, Ile, Val and Phe), 4.36 (1 H, m, α-H, Ala), 5.12 (1 H, d, *J* 7.3, NH, Phe), 6.38 (1 H, d, *J* 8.3, 6'-CH), 6.49 (1 H, t, *J* 7.4, 4'-CH), 7.00-7.10 (2 H, m, 5'-CH and 3'-CH), 7.14, 7.23 and 7.29 (5 H, 3 × m, Ar-H, Phe), 7.42 (1 H, m, NH, urethane), 7.76 (1 H, d, *J* 8.8, NH, Val), 7.93 (1 H, d, *J* 8.8, NH, Ile), 8.41 (1 H, d, *J* 6.6, NH, Ala) and 8.46 (1 H, d, *J* 7.5, NH, Ala); δ_C(50.30 MHz; $CDCl_3$) 10.87 (δ-C, Ile), 15.06 (γ-C, Ile), 16.72 (CH_3, Ala), 18.00 (CH_3, Val), 18.34 (CH_3, Ala), 19.08 (CH_3, Val), 24.07 (CH_2, Ile), 28.19 [$C(CH_3)_3$], 30.28 (β-CH, Ile), 30.40 (CH_2N), 36.79 (β-CH, Val), 38.48 (β-CH_2, Phe), 47.47 and 48.03 (2 × α-CH), 51.64 (CO_2CH_3), 56.27, 57.69 and 57.83 (3 × α-CH), 78.05, 78.25 and 92.99 [$C(CH_3)_3$ and C≡C], 107.12 (2'-CH), 109.00 (6'-CH), 116.35 (4'-CH), 126.32, 128.10 and 129.30 (Ar-CH, Phe), 129.58 (5'-CH), 131.52 (3'-CH), 137.68 [Ar-C, *ipso* (Phe)], 147.93 (1'-C), 155.30 (CO, urethane), 170.44, 170.62, 171.46, 171.85 and 172.68 (4 × CO, amide and CO, ester); *m/z* (FAB) 785 (100%, $[M + Na]^+$).

2'-(3''-*tert*-butoxycarbonylamino-prop-1''-ynyl)-phenyl-1'-(2*S*)-phenylalanyl-(2*S*)-alanyl-(2*S*)-valinyl-(2*S*)-isoleucinyl-(2*S*)-alanine (149)

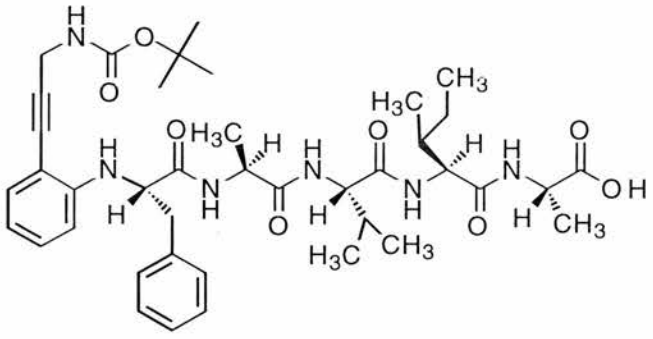

To a solution of heptapeptide analogue **148** (0.30 g, 0.36 mmol) in methanol (36 cm^3), THF (12 cm^3) and water (12 cm^3) was added LiOH solution (2.88 cm^3, 1 mol dm^{-3}). The reaction mixture was stirred for 1 h, cooled in ice, acidified to pH 3 with citric acid solution (10%, w/v) and extracted into ethyl acetate (3 × 70 cm^3). The organic extracts were pooled, washed with water (4 × 70 cm^3), brine (50 cm^3), dried

(Na_2SO_4) and concentrated under reduced pressure to yield acid **149** as a pale yellow foam (0.21 g, 79%), mp >125 °C (decomp.); (HRMS: found $[M + Na]^+$, 771.4053. $C_{40}H_{56}O_8N_6Na$ requires 771.4057); $[\alpha]_D^{18}$ -48 (*c* 0.1, CD_3SO); υ_{max}(KBr disc)/cm^{-1} 3289-3500 (NH, amide, urethane and amine), 2876-3076 (ArC-H and C-H), 2210 (C≡C), 1639-1730 (C=O, amide and ester) and 1164-1248 (C-O, ester and urethane, and C-N, urethane); δ_H[300 MHz; $(CD_3)_2SO$] 0.74-0.82 (12 H, m, 2 × CH_3, Ile and 2 × CH_3, Val), 0.99-1.10 (1 H, m, 1 H of γ-CH_2, Ile), 1.16-1.26 (6 H, m, 2 × CH_3, Ala), 1.16-1.26 (1 H, m, 1 H of γ-CH_2, Ile), 1.38 [9 H, s, $(CH_3)_3C$], 1.68 (1 H, m, β-H, Val), 1.92 (1 H, m, β-H, Ile), 2.88-3.08 (2 H, m, β-H, Phe), 4.06 (2 H, m, CH_2NH), 4.01-4.20 (4 H, m, α-H, Ala, Ile, Val and Phe), 4.38 (1 H, m, α-H, Ala), 5.12 (1 H, d, *J* 7.3, NH, Phe), 6.38 (1 H, d, *J* 8.3, 6'-CH), 6.50 (1 H, t, *J* 7.4, 4'-CH), 7.01-7.09 (2 H, m, 5'-CH and 3'-CH), 7.13-7.38 (5 H, m, Ar-H, Phe), 7.40 (1 H, m, NH, urethane), 7.68 (1 H, d, *J* 8.6, NH, Val), 7.89 (1 H, d, *J* 8.8, NH, Ile), 8.18 (2 H, d, *J* 6.8, NH, Ala, and OH, acid) and 8.33 (1 H, d, *J* 7.5, NH, Ala); δ_C(50.30 MHz; $CDCl_3$) 11.02 (δ-CH_3, Ile), 15.24 (γ-CH_3, Ile), 17.12 (CH_3, Ala), 18.10 (CH_3, Val), 18.55 (CH_3, Ala), 19.24 (CH_3, Val), 24.14 (γ-CH_2, Ile), 28.30 [C(*C*H_3)$_3$], 30.39 (β-CH, Ile), 30.51 (CH_2N), 36.93 (β-CH, Val), 38.55 (β-CH_2, Phe), 47.54, 48.03, 51.24, 56.36, 57.71 (5 × α-CH), 78.13, 78.38 and 93.13 [*C*$(CH_3)_3$ and C≡C], 107.18 (2'-C), 110.03 (6'-CH), 116.49 (4'-CH), 126.49, 128.26 and 129.42 (Ar-CH, Phe), 129.75 (5'-CH), 131.65 (3'-CH), 137.79 [Ar-C, *ipso* (Phe)], 148.05 (1'-C), 155.40 (CO, urethane), 170.61, 171.56, 171.98, 171.85 and 173.97 (4 × CO, amide and CO, ester); *m/z* (FAB) 793 (79%, $[M + 2Na - H]^+$) and 771 (100, $[M + Na]^+$).

Methyl 2'-{3''-[2'''-(3''''-*tert*-butoxycarbonylamino-prop-1'''-ynyl)-phenyl-1'''-(2*S*)-phenylalanyl-(2*S*)-methyl-(2*S*)-valinylamino]-prop-1''-ynyl}-phenyl-1'-(2*S*)-aminobutyryl-(2*S*)-threonyl-(2*S*)-leucinate (154)

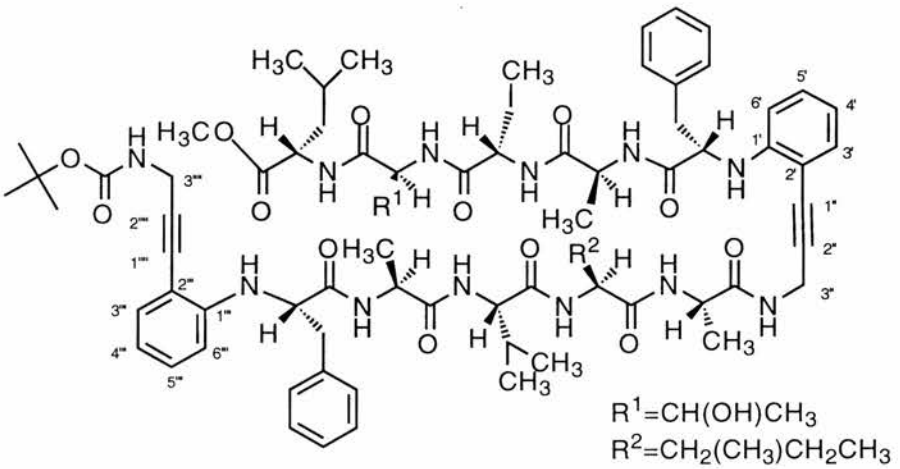

A stirred solution of heptapeptide analogue (**152**) (100 mg, 0.13 mmol) in dry ethyl acetate (13 cm^3) was cooled to -15 °C and dry HCl gas bubbled continuously through the solution for 10 min. The reaction mixture was then purged with argon concnetrated under reduced pressure to furnish the *N*-deprotected peptide analogue **153** as a dihydrochloride salt (97 mg, 99%). This procedure was repeated twice to obtain enough material for the next step.

Dihydrochloride salt **153** (140 mg, 0.2 mmol) was coupled to carboxylic acid **149** (147 mg, 0.2 mmol) in a manner identical to that for acyclic decapeptide analogue **141**. On completion of the reaction, saturated brine was added directly to the reaction mixture and the resulting suspension extracted with 1:1 ethyl acetate-THF (70 cm^3). The organic phase was washed with citric acid (10%, w/v), $NaHCO_3$ solution (5%, w/v), water (50 cm^3), brine (50 cm^3), dried (Na_2SO_4) and concentrated to a colourless oil. Trituration with dry ether yielded the title compound as an off-white solid. The crude material was stirred in methanol for 20 min, the excess solvent decanted off, and the remaining methanol removed under reduced pressure to give the acyclic tetadecapeptide analogue **154** as a white solid (98 mg, 35%), mp >225 °C (decomp.);

$[\alpha]_D^{18}$ -30 (*c* 0.1, CD_3SO); υ_{max}(KBr disc)/cm^{-1} 3289-3628 (NH, amide, urethane and amide), 2875-3066 (ArC-H and C-H), 2223 (2 × C≡C), 1636-1720 (C=O, amide and ester); δ_H[400 MHz; $(CD_3)_2SO$] 0.70-0.90 (24 H, m, CH_3, Abu, 2 × CH_3, Ile, CH_3, Ala, 2 × CH_3, Leu and 2 × CH_3, Val), 1.00-1.11 [4 H, m, 1 H of β-CH_2, Abu and CH_3, Thr), 1.17-1.24 (6 H, m, 2 × CH_3, Ala), 1.41 [10 H, m, $(CH_3)_3C$ and 1 H of β-CH_2, Abu], 1.47-1.76 (6 H, m, γ-H, Leu, β-H, Val, and CH_2, Leu), 1.90-2.02 (1 H, m, 1 H of β-CH, Ile), 2.87-3.13 (4 H, m, 2 × CH_2Ph), 3.59 (3 H, s, OCH_3), 3.87-3.95 (1 H, m, β-H, Thr), 4.02 (2 H, m, CH_2NH), 4.11-4.35 (10 H, m, 8 × α-H and CH_2NH), 4.36-4.49 (2 H, m, 2 × α-H), 4.85 (1 H, br s, OH, Thr), 5.12-5.22 (2 H, 2 × d, 2 × NH, amine), 6.39-6.48 (2 H, 2 × m, 6'-CH and 6'''-CH), 6.49-6.56 (2 H, 2 × m, 4'-CH and 4'''-CH), 6.99-7.41 (15 H, m, 2 × Ar-H, Phe, 5'-CH, 5'''-CH, 3'-CH, 3'''-CH, and NH, urethane) and 7.72-8.45 (9 H, m, 9 × NH, amide); δ_C(50.30 MHz; CD_3SO) 9.92 (CH_3, Abu), (CH_3, Ala), 10.85 (δ-C, Ile), 15.19 (γ-CH_3, Ile), 17.99 (1 × CH_3, Val), 18.10 (CH_3, Ala), 18.43 (CH_3, Ala), 19.10 (1 × CH_3, Val), 19.67 (CH_3, Thr), 21.20 and 22.66 (2 × CH_3, Leu), 24.04 (γ-CH, Leu), 24.15 (CH_2, Abu), 25.23 (CH_2, Ile), 28.19 [$(CH_3)_3C$], 29.16 (CH_2N), 30.35 (CH_2N and β-CH, Ile), 36.50 (β-CH, Val), 38.46 (2 × CH_2Ph), 40.01 (CH_2, Leu), 47.94 and 50.12 (4 × α-CH), 51.71 (OCH_3), 56.51, 57.53, 57.63 57.90 and 58.10 (6 × α-CH), 66.47 (β-CH, Thr), 78.06, 78.27 and 78.50, 92.14 and 93.00 [2 × C≡C and $(CH_3)_3C$], 107.04 and 107.16 (Ar-C2 and Ar-C2'), 110.03 (Ar-C6 and Ar-C6'), 116.40 (Ar-C4 and Ar-C4'), 126.35, 128.12 and 129.30 (2 × Ar-CH, Phe), 129.59 (Ar-C5 and Ar-C5'), 131.54 (Ar-C3 and Ar-C3'), 137.59 [2 × Ar-C, *ipso* (Phe)], 147.92 and 148.05 (Ar-C1 and Ar-C1') 155.31 (CO, urethane), 170.00, 170.34 170.66, 171.25, 171.45, 171.53, 171.68, 171.87, 171.88 and 172.6 (9 × CO, amide) and CO, ester); *m/z* (ES+) 1431.8 (90%, $[M + Na]^+$) and 727.3 (100, $[M + 2Na]^{2+}$).

(3*S*, 6*S*, 9*S*, 12*S*, 15*S*, 28*S*, 31S, 34*S*, 37*S*, 40*S*)-2, 5, 8, 11, 14, 17, 27, 30, 33, 36, 39, 42-dodecaaza-21, 46-dibenzo-3, 28-dibenzyl-6, 31, 40-trimethyl-9-ethyl-12-(hydroxyethyl)-15-(2-methylpropyl)-34-isopropyl-37-(1-methylpropyl)-4, 7, 10, 13, 16, 29, 32, 35, 38, 41-decaoxo-19,14-diyne-tricyclo [44.4.0.0$^{21, 26}$] pentacontane (116)

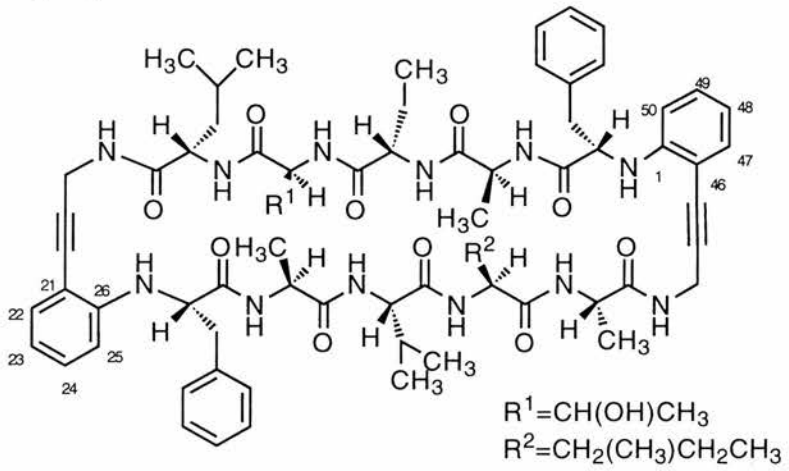

A solution of the acyclic tetradecapeptide analogue **154** (70 mg, 0.05 mmol) in DMSO (0.76 cm^3), methanol (3.0 cm^3) and water (3.5 cm^3) was added to aqueous LiOH (1 mol dm^{-3}) and the reaction mixture was stirred at room temperature for 36 h. A mixture of ethyl acetate and (10%, w/v) citric acid solution (1:1, 20cm^3) was added to the reaction mixture, the organic phase removed, washed with water (4 × 50 cm^3), brine (50 cm^3), dried (Na_2SO_4) and concentrated under reduced pressure to give a colourless oil which was triturated with ether-hexane (1:1) to give the carboxylic acid as a pale yellow solid (59.5 mg, 83%). A suspension of this material (51.3 mg) in dry ethyl acetate (4 cm^3) was cooled to -15 °C and dry HCl gas bubbled through the reaction mixture for 10 min. The resulting clear solution was concentrated under reduced pressure to yield the hydrochloride salt of the fully deprotected tetradecapeptide analogue as an off-white solid (49 mg, 99%). A solution of this material (43 mg, 0.032 mmol) in dry DMF (25 cm^3) was cooled to 0 °C. To this solution was added solid $NaHCO_3$ (32 mg, 0.38 mmol) and diphenylphosphoryl azide (DPPA) (63 mg, 0.23 mmol). The reaction mixture was stirred and allowed to slowly warm up to room temperature under an atmosphere of nitrogen. After 4.5 days, the

reaction mixture was directly added to dichloromethane (50 cm^3), washed with water (4 × 40 cm^3), $NaHCO_3$ solution (20 cm^3, 5% w/v), brine (20 cm^3), dried (Na_2SO_4) and concentrated under reduced pressure to give a yellow oil. A portion of of this material (20 mg) was purified by flash silica chromatography using DCM-MeOH (98:2) as the eluent to give the cyclic teradecapeptide analogue **116** as a white solid (5 mg, 12%); δ_H[400 MHz; $(CD_3)_2SO$] 0.43-0.91 (24 H, m, CH_3, Abu, 2 × CH_3, Ile, CH_3, Ala, 2 × CH_3, Leu and 2 × CH_3, Val), 0.97-1.26 (10 H, m, 2 × CH_3, Ala, CH_3, Thr, and one of CH_2, Ile), 135-1.64 (7 H, m, CH_2, Leu, one of CH_2, Ile, β-CH, Val, γ-CH, Leu, and β-CH_2, Abu), 1.91 (1 H, m, β-CH, Ile), 2.94-3.11 (4 H, m, 2 × CH_2, Phe), 3.63-5.11 (16 H, m, 10 × α-CH, 2 × C*H*$_2$NH, OH, and β-CH, Thr), 5.68 (1 H, m, NH, amine), 6.42-6.71 (5 H, m, 23-CH, 25-CH, 48-CH and 50-CH and NH, amine), 6.88-7.38 [14 H, 2 × Ar-H (Phe), 24-CH, 49-CH, 22-CH and 47-CH] and 8.20-8.79 (10 H, m, 10 × CO, amide); *m/z* (ES+) 1300 (100%, $[M + Na]^+$) and 661 (57, $[M + 2Na]^{2+}$).

APPENDICES

Appendix 1

Solid-phase peptide synthesis

The peptides were prepared using a Rainin P53 automated solid phase peptide synthesiser. The resin (Wang-type) and all amino acids (Fmoc protected) were purchased from Novabiochem Ltd. PyBOP was used as the coupling reagent and was also purchased from Novabiochem. Piperazine in DMF (20%, v/v) was used as the deprotection solution and NMM in DMF (0.4 mol dm^{-3}) was used as the activation solution. The peptides were prepared on a 0.1 mmol scale with coupling times of 60 min used throughout the synthesis.

The peptides were cleaved from the resin using a mixture of TFA, water and triethylsilane (95:2.5:2.5 respectively) and left for 2 h at 25 °C. Excess TFA, water and triethylsilane were removed under reduced pressure and the resultant oil was triturated with dry diethyl ether to furnish the peptides as white solids. These were subsequently lyophilised under high vacuum and the dry peptides stored at -20 °C.

The purity of the peptides was checked by HPLC. The dry peptide (1 mg) was dissolved in water (1 cm^3), filtered and injected (10µl) onto a C_{18} column equilibrated with water containing TFA (0.1%). The peptides were eluted with 0-99% acetonitrile over 30 min and monitored at 214 nm.

Appendix 2

Crystallography data

2.1: Cystallographic Data for 65

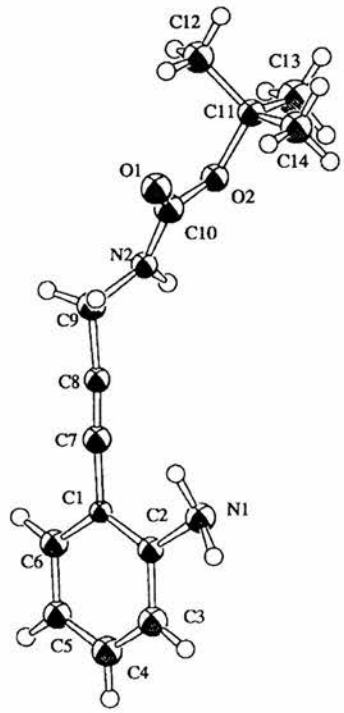

$C_{14}H_{18}N_2O_2$, M = 246.31, monoclinic, space group $P2_1/n$ (#14), a = 10.316(5), b = 5.192(5), c = 25.000(4) Å, β = 96.95(3)°, V=1329(1) $Å^3$, Z=4, D_{calc}=1.231 g cm^{-3}, T=293 K. 1301 unique reflections were collected on a Rigaku AFC7S diffractometer employing Mo-Kα radiation (λ = 0.71069) of which 757 [I>3.00σ(I)] were used for refinement. Convergence at R_1 = 4.5%, wR_2 = 3.0% for 164 variable parameters.

Table 3.1: *Bond lengths (Å) and angles (°) for* ***65***

O(1)-C(10)	1.207(6)	O(2)-C(10)	1.365(6)
O(2)-C(11)	1.491(6)	N(1)-C(2)	1.396(6)
N(2)-C(9)	1.454(6)	N(2)-C(10)	1.349(6)
C(1)-C(2)	1.406(7)	C(1)-C(6)	1.380(7)
C(1)-C(7)	1.439(7)	C(2)-C(3)	1.410(7)
C(3)-C(4)	1.370(7)	C(4)-C(5)	1.383(7)
C(5)-C(6)	1.392(7)	C(7)-C(8)	1.174(7)
C(8)-C(9)	1.471(7)	C(11)-C(12)	1.501(7)
C(11)-C(13)	1.528(7)	C(11)-C(14)	1.508(7)
N(1)-H(16)	1.08	N(1)-H(17)	1.11
N(2)-H(18)	1.23	C(3)-H(1)	0.95
C(4)-H(2)	0.95	C(5)-H(3)	0.95
C(6)-H(4)	0.95	C(9)-H(5)	0.95
C(9)-H(6)	0.95	C(12)-H(7)	0.96

C(12)-H(8)	0.95	C(12)-H(9)	0.95
C(13)-H(10)	0.95	C(13)-H(11)	0.95
C(13)-H(12)	0.95	C(14)-H(13)	0.95
C(14)-H(14)	0.95	C(14)-H(15)	0.96

C(10)-O(2)-C(11)	119.1(4)	C(9)-N(2)-C(10)	119.4(4)
C(2)-C(1)-C(6)	119.5(5)	C(2)-C(1)-C(7)	118.8(5)
C(6)-C(1)-C(7)	121.8(6)	N(1)-C(2)-C(1)	121.7(5)
N(1)-C(2)-C(3)	119.8(6)	C(1)-C(2)-C(3)	118.3(5)
C(2)-C(3)-C(4)	120.7(5)	C(3)-C(4)-C(5)	121.5(5)
C(4)-C(5)-C(6)	118.0(5)	C(1)-C(6)-C(5)	122.1(5)
C(1)-C(7)-C(8)	117.9(7)	C(7)-C(8)-C(9)	175.5(6)
N(2)-C(9)-C(8)	112.2(5)	O(1)-C(10)-O(2)	125.7(5)
O(1)-C(10)-N(2)	125.9(5)	O(2)-C(10)-N(2)	108.4(5)
O(2)-C(11)-C(12)	110.1(4)	O(2)-C(11)-C(13)	101.7(4)
O(2)-C(11)-C(14)	109.3(4)	C(12)-C(11)-C(13)	110.9(5)
C(12)-C(11)-C(14)	114.0(5)	C(13)-C(11)-C(14)	110.2(5)
C(2)-N(1)-H(16)	106.0	C(2)-N(1)-H(17)	104.4
H(16)-N(1)-H(17)	111.3	C(9)-N(2)-H(18)	121.5
C(10)-N(2)-H(18)	119.1	C(2)-C(3)-H(1)	119.3
C(4)-C(3)-H(1)	120.0	C(3)-C(4)-H(2)	118.8
C(5)-C(4)-H(2)	119.7	C(4)-C(5)-H(3)	121.2
C(6)-C(5)-H(3)	120.8	C(1)-C(6)-H(4)	118.9
C(5)-C(6)-H(4)	119.0	N(2)-C(9)-H(5)	109.1
N(2)-C(9)-H(6)	108.9	C(8)-C(9)-H5)	108.7
C(8)-C(9)-H(6)	108.5	H(5)-C(9)-H(6)	109.4
C(11)-C(12)-H(7)	109.6	C(11)-C(12)-H(8)	110.6
C(11)-C(12)-H(9)	110.7	H(7)-C(12)-H(8)	108.1
H(7)-C(12)-H(9)	108.3	H(8)-C(12)-H(9)	109.3
C(11)-C(13)-H(10)	109.1	C(11)-C(13)-H(11)	109.2
C(11)-C(13)-H(12)	109.4	H(10)-C(13)-H(12)	109.6
H(10)-C(13)-H(12)	109.6	H(11)-C(13)-H(14)	110.0
C(11)-C(14)-H(13)	110.5	C(11)-C(14)-H(14)	110.3
C(11)-C(14)-H(15)	109.8	H(13)-C(14)-H(14)	109.2
H(13)-C(14)-H(15)	108.6	H(14)-C(14)-H(15)	108.3

Table 3.2: *Torsion angles (°) for* ***65***

O(1)-C(10)-O(2)-C(11)	-2.2(9)
O(2)-C(10)-N(2)-C(9)	-176.5(4)
N(1)-C(2)-C(1)-C(7)	-5.0(8)
N(2)-C(9)-C(8)-C(7)	-169(8)
C(1)-C(2)-C(3)-C(4)	0.7(8)
C(1)-C(7)-C(8)-C(9)	-122(15)
C(2)-C(1)-C(7)-C(8)	10(17)
C(3)-C(2)-C(1)-C(6)	0.0(8)
C(3)-C(4)-C(5)-C(6)	0.8(9)
C(6)-C(1)-C(7)-C(8)	-170(17)
C(10)-O(2)-C(11)-C(12)	-62.3(6)
C(10)-O(2)-C(11)-C(14)	63.6(6)
O(1)-C(10)-N(2)-C(9)	6.5(9)
N(1)-C(2)-C(1)-C(6)	175.5(5)
N(1)-C(2)-C(3)-C(4)	-174.9(5)
N(2)-C(10)-O(2)-C(11)	-179.2(4)
C(1)-C(6)-C(5)-C(4)	-0.1(9)

C(2)-C(1)-C(6)-C(5)	-0.3(8)
C(2)-C(3)-C(4)-C(5)	-1.1(9)
C(3)-C(2)-C(1)-C(7)	179.5(5)
C(5)-C(6)-C(1)-C(7)	-179.8(5)
C(8)-C(9)-C(2)-C(10)	-147.9(5)
C(10)-C(2)-C(11)-C(13)	-179.8(5)

2.2: Cystallographic Data for 109

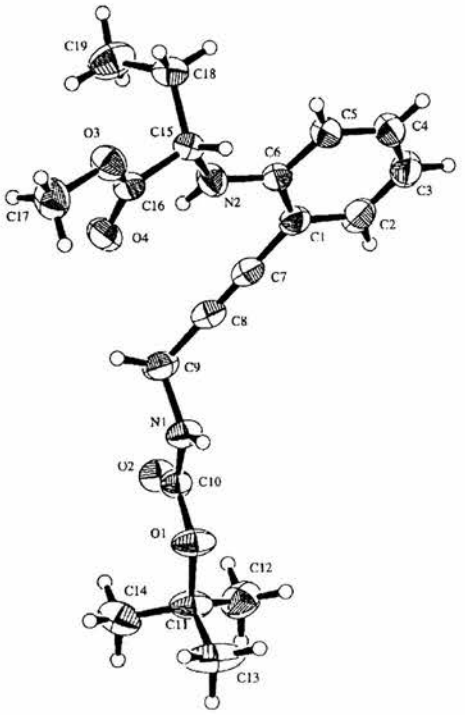

$C_{19}H_{26}N_2O_4$, M = 346.42, orthorhombic, space group $P2_12_12_1$, a = 14.0436(3), b = 26.816(3), c = 5.2108(5) Å, $\alpha = 90°$, $\beta = 90°$, $\gamma = 90°$, V=1963 Å^3, Z=4, D_{calc}=1.173 g cm^{-3}, T=293 K. 3243 unique reflections were collected on a Rigaku RAxisII diffractometer employing Mo-Kα radiation (λ = 0.71069) of which 3243 [I>2.00σ(I)] were used for refinement. Convergence at R_1 = 4.8%, wR_2 = 11.3% for 226 variable parameters.

Table 3.3: *Bond lengths (Å) and angles (°) for* ***109***

C(1)-C(10)	1.348(2)	C(1)-C(7)	1.437(3)
C(1)-C(11)	1.476(2)	C(1)-C(3)	1.380(4)
C(2)-C(10)	1.207(3)	C(1)-C(4)	1.374(5)
C(3)-C(16)	1.320(3)	C(1)-C(5)	1.379(4)
C(3)-C(17)	1.448(3)	C(1)-C(6)	1.398(3)
C(4)-C(16)	1.200(3)	C(1)-C(8)	1.189(3)
N(1)-C(10)	1.344(3)	C(1)-C(9)	1.462(3)
N(1)-C(9)	1.463(3)	C(1)-C(14)	1.508(4)
N(2)-C(6)	1.371(3)	C(1)-C(12)	1.512(4)
N(2)-C(15)	1.439(3)	C(1)-C(13)	1.522(4)

C(1)-C(2)	1.388(3)	C(1)-C(16)	1.512(3)
C(1)-C(6)	1.409(3)	C(1)-C(18)	1.537(3)
C(1)-C(19)	1.497(4)		

C(10)-O(1)-C(11)	119.8(2)	O(2)-C(10)-N(1)	125.0(2)
C(16)-O(3)-C(17)	116.4(2)	C(2)-C(10)-O(1)	125.8(2)
C(10)-N(1)-C(9)	119.9(2)	N(1)-C(10)-O(1)	109.2(2)
C(6)-N(2)-C(15)	125.4(2)	O(1)-C(11)-C(14)	109.9(2)
C(2)-C(1)-C(6)	120.1(2)	O(1)-C(11)-C(12)	109.5(2)
C(2)-C(1)-C(7)	120.0(2)	C(14)-C(11)-C(12)	112.9(2)
C(6)-C(1)-C(7)	119.8(2)	O(1)-C(11)-C(13)	102.2(2)
C(3)-C(2)-C(1)	121.0(3)	C(14)-C(11)-C(13)	110.9(3)
C(4)-C(3)-C(2)	118.7(3)	C(12)-C(11)-C(13)	110.9(3)
C(3)-C(4)-C(5)	121.8(3)	N(2)-C(15)-C(16)	107.2(2)
C(4)-C(5)-C(6)	120.1(3)	N(2)-C(15)-C(18)	114.4(2)
N(2)-C(6)-C(5)	123.1(2)	C(16)-C(15)-C(18)	111.4(2)
N(2)-C(6)-C(1)	118.8(2)	O(4)-C(16)-O(3)	124.1(2)
C(5)-C(6)-C(1)	118.1(2)	O(4)-C(16)-C(15)	124.3(2)
C(8)-C(7)-C(1)	178.5(2)	O(3)-C(16)-C(15)	111.6(2)
C(7)-C(8)-C(9)	178.5(3)	C(19)-C(18)-C(15)	113.8(2)
C(8)-C(9)-N(1)	112.1(2)		

REFERENCES

References

1. J. S. Richardson, *Adv. Prot. Chem.*, 1981, **34**, 170-175.
2. D. G. Hardie, '*Biochemical Messengers - Hormones, Neurotransmitters and Growth Factors*' , ed. Chapman and Hall, London, 1991, 21-69.
3. J. Hughes, T. W. Smith, H. W. Kosterlitz, L. A. Fothergill, B. A. Morgan and H. R. Morris, *Nature*, 1975, **258**, 577-579.
4. Y. Audigier, H. Mazarguil, R. Gout and J. Cros, *Eur. J. Pharm.*, 1980, **63**, 35-46.
5. A. Saran, M. M. Dhingra and Y. U. Sasidhar, *Journal of Molecular Structure (Theochem)*, 1991, **233**, 315-334.
6. B. Gardner, H. Nakanishi and M. Kahn, *Tetrahedron*, 1993, **49**, 3433-3448.
7. B. P. Roques, C. Garbay-Jaureguiberry, R. Oberlin, M. Anteunis and A. K. Lala, *Nature*, 1976, **262**, 778-779.
8. C. R. Jones, W. A. Gibbons and V. Garsky, *Nature*, 1976, **262**, 779-782.
9. A. Giannis and T. Kolter, *Angew. Chem. Int. Ed. Engl.*, 1993, **1993**, 1244-1267.
10. W. T. Heller, A. J. Waring, R. I. Lehrer and H. W. Huang, *Biochemistry*, 1998, **37**, 17331-17338.
11. L. Stryer, '*Biochemistry*' , ed. W. H Freeman and Company, New York, 1988, 302-303.
12. S. E. V. Phillips, *J. Mol. Biol.*, 1980, **142**, 531-554.
13. A. McPherson, G. Brayer, D. Cascio and R. Williams, *Science*, 1986, **232**, 765-768.
14. S. J. Singer and G. L. Nicolson, *Science*, 1972, **175**, 720-730.
15. G. V. Heijne, *BioEssays*, 1995, **17**, 25-29.
16. R. Henderson and P. N. T. Unwin, *Nature*, 1975, **257**, 28-32.
17. L. P. Liu and C. M. Deber, *Bioorg. Med. Chem.*, 1999, **7**, 1-7.
18. R. D. Long and K. D. Moeller, *J. Am. Chem. Soc*, 1997, **119**, 12394-12395.

19. L. Pauling and R. B. Corey, *Nature*, 1951, **168**, 550-551.

20. IUPAC-IUB Commission on Biochemical Nomenclature. Description of Conformations of Polypeptide Chains, 1970, **9**, 3471-3479.

21. G. L. Marshall, *Tetrahedron*, 1993, **49**, 3547-3558.

22. P. Y. Chou and G. D. Fasman, *Biochemistry*, 1974, **13**, 211-222.

23. P. Y. Chou and G. D. Fasman, *Adv. Enzymol.*, 1978, **47**, 45-148.

24. A. Chakrabartty, T. Kortemme and R. L. Baldwin, *Protein Science*, 1994, **3**, 843-852.

25. S. Padmanabhan and R. L. Baldwin, *Protein Science*, 1994, **3**, 1992-1997.

26. A. Yang and B. Honig, *J. Mol. Biol.*, 1995, **252**, 351-365.

27. L. Serrano, J. Neira, J. Sancho and A. R. Fersht, *Nature*, 1992, **356**, 453-455.

28. L. G. Presta and G. D. Rose, *Science*, 1988, **240**, 1632-1641.

29. J. S. Richardson and D. C. Richardson, *Science*, 1988, **240**, 1648-1652.

30. S. Dasgupta and J. A. Bell, *Int. J. Pept. Protein Res.*, 1993, **41**, 499-511.

31. L. Serrano and A. R. Fersht, *Nature*, 1989, **342**, 296-299.

32. B. Forood, E. J. Feliciano and K. P. Nambiar, *Proc. Natl. Acad. Sci. USA*, 1993, **90**, 838-842.

33. M. Narita, S. Isokawa, M. Doi and R. Wakita, *Bull. Chem. Soc. Jpn.*, 1986, **59**, 3547-3552.

34. K. M. Armstrong, R. Fairman and R. L. Baldwin, *J. Mol. Biol.*, 1993, **34**, 284-291.

35. B. M. P. Huyghues-Depointes, T. M. Klinger and R. L. Baldwin, *Biochemistry*, 1995, **34**, 13267-13271.

36. R. L. Baldwin, *Biophysical Chemistry*, 1995, **55**, 127-135.

37. A. Lewis, M. D. Ryan and D. Gani, *J. Chem. Soc., Perkin Trans. 1*, 1998, 3767-3775.

38. D. S. Kemp, J. G. Boyd and C. C. Muendel, *Nature*, 1991, **352**, 451-454.

39. D. P. Fairlie, M. L. West and A. K. Wong, *Current Medicinal Chemistry*, 1998, **5**, 29-62.

40. K. Bode, M. Goodman and M. Mutter, *Helv. Chim. Acta.*, 1985, **68**, 705-714.

41. J. M. Ramanjulu and M. M. Joullie, *Tett. Lett.*, 1996, **37**, 311-314.

42. D. A. Tinker, E. A. Krebs, I. C. Feltham, S. K. Attah-Poku and V. S. Ananthanarayanan, *J. Biol. Chem.*, 1988, **263**, 5024-5026.

43. B. Imperiali, K. L. Shannon and K. W. Rickert, *J. Am. Chem. Soc.*, 1992, **114**, 7942-7944.

44. G. Boussard and M. Marraud, *J. Am. Chem. Soc.*, 1985, **107**, 1825-1828.

45. K. Yu, G. Rajakumar, L. K. Srivastava, R. K. Mishra and R. L. Johnson, *J. Med. Chem.*, 1988, **31**, 1430-1436.

46. G. Liang, C. J. Rito and S. H. Gellman, *J. Am. Chem. Soc.*, 1992, **114**, 4440-4442.

47. S. H. Gellman, G. P. Dado, G. Liang and B. R. Adams, *J. Am. Chem. Soc.*, 1991, **113**, 1164-1173.

48. J. B. Ball, R. A. Hughes, P. F. Alewood and P. R. Andrews, *Tetrahedron*, 1993, **49**, 3467-3478.

49. K. D. Kopple, A. Go and D. R. Pilipauskas, *J. Am. Chem. Soc.*, 1975, **97**, 6830-6838.

50. J. B. Ball, P. R. Andrews, P. F. Alewood and R. A. Hughes, *FEBS Lett.*, 1990, **237**, 15-18.

51. H. Dürr, M. Goodman and G. Jung, *Angew. Chem. Int. Ed. Engl.*, 1992, **31**, 785-787.

52. C. L. Nesloney and J. W. Kelly, *Bioorg. & Med. Chem.*, 1996, **4**, 739-766.

53. I. L. Karle, S. K. Awasthi and P. Balaram, *Proc. Natl. Acad. Sci. USA*, 1996, **93**, 8189-8193.

54. R. Kaul and P. Balaram, *Bioorg. Med. Chem.*, 1999, **7**, 105-117.

55. M. Ramirez-Alvarado, T. Kortemme, F. J. Blanco and L. Serrano, *Bioorganic and Medicinal Chemistry*, 1999, **7**, 93-103.

56. F. J. Blanco, M. A. Jiménez, J. Herranz, M. Rico, J. Santoro and J. L. Nieto, *J. Am. Chem. Soc.*, 1993, **115**, 5887-5888.

57. C. Das, S. Raghothama and P. Balaram, *J. Am. Chem. Soc.*, 1998, **120**, 5812-5813.

58. J. Späth, F. Stuart, L. Jiang and J. A. Robinson, *Helv. Chim. Acta.*, 1998, **81**, 1726-1738.

59. S. H. Gellman, *Current Opinion in Chemical Biology*, 1998, **2**, 717-725.

60. E. deAlba, M. A. Jimenez and M. Rico, *J. Am. Chem. Soc.*, 1997, **119**, 175-183.

61. P. T. Lansbury, *Acc. Chem. Res.*, 1996, **29**, 317-321.

62. J. D. Harper and P. T. Lansbury, *Annu. Rev. Biochem.*, 1997, **66**, 385-407.

63. K. C. Chou, M. Pottle, G. Nemethy, Y. Ueda and H. Scheraga, *J. Mol. Biol.*, 1982, **162**, 89-112.

64. C. K. Smith and L. Regan, 1997, **30**, 153-161.

65. J. S. Richardson, E. D. Getzoff and D. C. Richardson, *Biochemistry*, 1978, **75**, 2574-2578.

66. D. S. Kemp and Z. Q. Li, *Tetrahedron Lett.*, 1995, **36**, 4179-4180.

67. Y. Bai and S. W. Englander, *Proteins: Struct., Funct., Genet.*, 1994, **18**, 262.

68. H. Y. Xiong, B. L. Buckwalter, H. M. Shieh and M. H. Hecht, *Proc. Natl. Acad. Sci. USA*, 1995, **92**, 6349-6353.

69. J. F. Callahan, K. A. Newlander, J. L. Burges, D. S. Eggleston, A. Nichols, A. Wong and W. F. Huffman, *Tetrahedron*, 1993, **49**, 3479-3488.

70. B. Schmidt and C. Kühn, *Synlett.*, 1998, 1240-1242.

71. D. D. Kemp and J. S. Carter, *Tetrahedron Lett.*, 1987, **28**, 4645-4648.

72. R. Escher and P. Bunning, *Angew. Chem. Int. Ed. Engl.*, 1986, **25**, 277-278.

73. B. Schmidt, S. Lindman, W. Tong, G. Lindeberg, A. Gogoll, Z. Lai, M. Thornwall, B. Synnergren, A. Nilsson, C. J. Welch, M. Sohtell, C.

Westerlund, F. Nyberg, A. Karlen and A. Hallberg, *J. Med. Chem.*, 1997, **40**, 903.

74. C. Kuhn, G. Lindeberg, A. Gogoll, A. Hallberg and B. Schmidt, *Tetrahedron*, 1997, **53**, 12497.

75. E. D. Thorsett, E. E. Harris, S. D. Aster, E. R. Peterson, J. P. Snyder, J. P. Springer, J. Hirshfield, E. W. Tristram, A. A. Patchett, E. H. Ulm and T. C. Vassil, *J. Med. Chem.*, 1986, **29**, 251-260.

76. V. J. Hruby, F. A. Obeidi and W. Kazmierski, *Biochem. J.*, 1990, **268**, 249-262.

77. G. Gacel, M. C. Fourine-Zaluski and B. P. Roques, *FEBS Lett.*, 1980, **118**, 245.

78. J. M. Hambrook, B. A. Morgan, M. J. Rance and C. F. C. Smith, *Nature*, 1976, **262**, 782-783.

79. A. S. Horn and J. R. Rodgers, *Nature*, 1976, **260**, 795-797.

80. Y. Shimohigashi and C. H. Stammer, *Int. J. Peptide Protein Res.*, 1982, **20**, 199-206.

81. Y. Shimohigashi, M. L. English and C. H. Stammer, *Biochem. and Biophys. Res. Comm.*, 1982, **104**, 583-590.

82. Y. Shimohigashi and C. H. Stammer, *J. Peptide Protein Res.*, 1982, **19**, 54-62.

83. S. F. Martin, C. J. Oalmann and S. Liras, *Tetrahedron,* 1993, **49**, 3521-3532.

84. M. Pellegrini, I. S. Weitz, M. Chorev and D. F. Mierke, *J. Am. Chem. Soc.*, 1997, **119**, 2430-2436.

85. N. DeLaFiguera, M. Martín-Martinez, R. Herranz, M. T. García-López, M. Latorre, E. Cenarruzabeitia, J. DelRío and R. González-Muñiz, *Bioorg. Med. Chem. Lett.*, 1999, **9**, 43-48.

86. P. C. Belanger, C. Dufresne, J. Scheigetz, R. N. Young, J. P. Springer and G. I. Dmitrienko, *Can. J. Chem.*, 1982, **60**, 1019-1029.

87. M. Kahn and B. Chen, *Tetrahedron Lett.*, 1987, **28**, 1623-1626.

88. C. Toniolo, *Biopolymers*, 1989, **28**, 247-257.

89. D. Jiao, K. C. Russell and V. J. Hruby, *Tetrahedron*, 1993, **49**, 3511-3520.

90. X. Qian, K. E. Kover, M. D. Shenderovich, B. Lou, A. Misicka, T. Zalewska, R. Horvath, P. Davis, E. J. Bilsky, F. Porreca, H. I. Yamamura and V. J. Hruby, *J. Med. Chem.*, 1994, **37**, 1746-1757.

91. U. Bhatt, N. Mohamed and G. Just, *Tetrahedron Lett.*, 1997, **38**, 3679-3682.

92. U. Schopfer, M. Stahl, T. Brandl and R. W. Hoffmann, *Angew. Chem. Int. Ed. Engl.*, 1997, **36**, 1745-1747.

93. D. B. A. DeBont, K. M. Sliedregt-Bol, L. J. F. Hofmeyer and R. M. J. Liskamp, *Bioorg. Med. Chem.*, 1999, **7**, 1043-1047.

94. M. Kahn and B. Devens, *Tetrahedron Lett.*, 1986, **27**, 4841-4844.

95. S. Borman, *C & EN*, 1993, 27-28.

96. A. Boumendjel, J. C. Roberts, E. Hu and P. V. Pallai, *J. Org. Chem.*, 1996, **61**, 4434-4438.

97. M. M. Hann, P. G. Sammes, P. D. Kennewel and J. B. Taylor, *J. Chem. Soc. Perkin Trans. 1*, 1982, 307-314.

98. M. Hagihara, N. J. Anthony, T. J. Stout, J. Clardy and S. L. Schreiber, *J. Am. Chem.*, 1992, **14**, 6568-6570.

99. A. Lecoq, G. Boussard and M. Marraud, *Tetrahedron Lett.*, 1992, **33**, 5209-5212.

100. R. J. Simon, R. S. Kania, R. N. Zuckermann, V. D. Huebner, D. A. Jewell, S. Banville, S. Ng, L. Wang, S. Rosenberg, C. K. Marlowe, D. C. Spellmeyer, R. Tan, A. D. Frankel, D. V. Santi, F. E. Cohen and P. A. Bartlett, *Proc. Natl. Acad. Sci. USA*, 1992, **89**, 9367-9371.

101. W. C. Ripka, G. V. DeLucca, A. C. Bach, R. S. Pottorf and J. M. Blaney, *Tetrahedron*, 1993, **49**, 3609-3628.

102. A. Wlodawer, A. Miller, M. Jaskolski, B. Sathyanarayana, E. Baldwin, I. Weber, L. Selk, L. Clawson, J. Schneider and S. Kent, *Science*, 1989, **245**, 616-621.

103. R. Zutshi, J. Franciskovich, M. Shultz, B. Schweitzer, P. Bishop, M. Wilson and J. Chmielewski, *J. Am. Chem. Soc.*, 1997, **119**, 4841-4845.

104. G. D. Fasman and C. D. Moore, *Proc. Natl. Acad. Sci.*, 1994, **91**, 11232-11235.

105. M. Kahn, *Synlett*, 1993, 821-826.

106. R. M. J. Liskamp, *Recl. Trav. Chim. Pays-Bas*, 1994, **113**, 1-19.

107. A. Lewis, J. Wilkie, T. J. Rutherford and D. Gani, *J. Chem. Soc., Perkin Trans. 1*, 1998, 3777-3793.

108. A. Lewis, J. Wilkie, T. J. Rutherford, T. Jenn and D. Gani, *J. Chem. Soc., Perkin Trans. 1*, 1998, 3795-3806.

109. A. D. Piscopio, J. F. Miller and K. Koch, *Tetrahedron*, 1999, **55**, 8189-8198.

110. U. Nagai and K. Sato, *Tetrahedron Lett.*, 1985, **26**, 647-650.

111. W. Li and K. Burgess, *Tetrahedron Lett.*, 1999, **40**, 6527-6530.

112. D. S. Kemp and P. E. McNamara, *J. Org. Chem.*, 1985, **50**, 5834-5838.

113. D. S. Kemp and E. T. Sun, *Tetrahedron Lett.*, 1982, **23**, 3759-3760.

114. F. Jean, E. Buisine, O. Melnyk, H. Drobecq, B. Odaert, M. Hugues, G. Lippens and A. Tartar, *J. Am. Chem. Soc.*, 1998, **120**, 6076-6083.

115. R. M. Freidinger, D. S. Perlow and D. F. Veber, *J. Org. Chem.*, 1982, **47**, 104-109.

116. M. J. Genin, W. H. Ojala, W. B. Gleason and R. L. Johnson, *J. Org. Chem.*, 1993, **58**, 2334-2337.

117. W. C. Ripka, G. V. DeLucca, A. C. Bach, R. S. Pottorf and J. M. Blaney, *Tetrahedron*, 1993, **49**, 3593-3608.

118. B. L. Currie, J. L. Krstenansky, Z. Lin, J. Ungwitayatorn, Y. Lee, M. Rosario-Chow, W. Sheu and M. E. Johnson, *Tetrahedron*, 1993, **49**, 3489-3500.

119. A. Geyer, D. Bockelmann, K. Weissenbach and H. Fischer, *Tetrahedron Lett.*, 1999, **40**, 477-478.

120. D. S. Kemp, B. R. Bowen and C. C. Muende, *J. Org. Chem.*, 1990, **55**, 4650-4657.

121. A. B. Smith, M. C. Guzman, P. A.Sprengeler, T. P. Keenan, R. C. Holcomb, J. L. Wood, P. J. Carroll and R. Hirschmann, *J. Am Chem. Soc.*, 1994, **116**, 9947-9962.

122. A. B. Smith, D. A. Favor, P. A. Sprengeler, M. C. Guzman, P. J. Carroll, G. T. Furst and R. Hirschmann, *Bioorganic and Medicinal Chemistry*, 1999, **7**, 9-22.

123. T. Schrader and C. Kirsten, *Chem. Commun.*, 1996, 2089-2090.

124. D. L. Minor and P. S. Kim, *Nature*, 1994, **371**, 264-267.

125. A. J. Maynard, G. J. Sharman and M. S. Searle, *J. Am. Chem. Soc.*, 1998, **120**, 1996-2007.

126. G. J. Sharman and M. S. Searle, *J. Am. Chem. Soc.*, 1998, **120**, 5291-5300.

127. Y. Yan and B. W. Erickson, *Protein Science*, 1994, **3**, 1069-1073.

128. J. S. Nowick, E. M. Smith and M. Pairish, *Chem. Soc. Rev.*, 1996, 401-415.

129. M. Feigel, *J. Am. Chem. Soc.*, 1986, **108**, 181-182.

130. V. Brandmeier, M. Feigel and M. Bremer, *Angew. Chem. Int. Ed. Engl.*, 1989, **28**, 486-488.

131. V. Brandmeier, W. H. B. Sauer and M. Feigel, *Helv. Chim. Acta.*, 1994, **77**, 70-85.

132. H. Bekele, C. L. Nesloney, K. W. McWilliams, N. M. Zacharias, P. Chitnumsub and J. W. Kelly, *J. Org. Chem.*, 1997, **62**, 2259-2262.

133. H. Díaz, K. Y. Tsang, D. Choo, J. R. Espina and J. Kelly, *J. Am. Chem. Soc.*, 1993, **115**, 3790-3791.

134. K. Y. Tsang, H. Díaz, N. Graciani and J. W. Kelly, *J. Am. Chem. Soc.*, 1994, **116**, 3988-4005.

135. A. J. Doig, *Chem. Commun.*, 1997, 2153-2154.

136. T. Kortemme, M. Ramirez-Alvarado and L. Serrano, *Science*, 1998, **281**, 253-256.

137. J. H. Tsai, A. S. Waldman and J. S. Nowick, *Bioorganic and Medicinal Chemistry*, 1999, **7**, 29-38.

138. J. S. Nowick, M. Pairish, I. Q. Lee, D. L. Holmes and J. W. Ziller, *J. Am. Chem. Soc.*, 1997, **119**, 5413-5424.

139. E. M. Smith, D. L. Holmes, A. J. Shaka and J. S. Nowick, *J. Org. Chem.*, 1997, **62**, 7906-7907.

140. M. J. Soth and J. S. Nowick, *J. Org. Chem.*, 1999, 276-281.

141. D. S. Kemp and Z. Q. Li, *Tetrahedron Lett.*, 1995, **36**, 4175-4178.

142. T. D. Clark, J. M. Buriak, K. Kobayashi, M. P. Isler, D. E. McRee and M. R. Ghadiri, *J. Am. Chem. Soc.*, 1998, **120**, 8949-8962.

143. T. D. Clark, K. Kobayashi and M. R. Ghadiri, *Chem. Eur. J.*, 1999, **5**, 782-792.

144. G. B. Fields, *Bioorganic and Medicinal Chemistry*, 1999, **7**, 75-81.

145. C. Vita, J. Vizzavona, E. Drakopoulou, S. Zinn-Justin, B. Gilquin and A. Ménez, *Biopolymers*, 1998, **4**, 93-100.

146. I. Ernest, J. Kalvoda, C. Sigl, G. Rihs, H. Fritz, M. J. J. Blommers, F. Raschdorf, E. Francotte and M. Mutter, *Hel. Chim. Acta.*, 1993, **76**, 1539-1563.

147. S. Peluso, P. Dumy, I. M. Eggleston, P. Garouste and M. Mutter, *Tetrahedron*, 1997, **53**, 7231-7236.

148. M. Mutter and G. Tuchscherer, *Cell. Mil. Life Sci.*, 1997, **53**, 851-863.

149. J. M. Humphrey and A. R. Chamberlin, *Chem. Rev.*, 1997, **97**, 2243-3366.

150. G. W. Anderson, J. E. Zimmerman and F. M. Callahan, *J. Am. Chem. Soc.*, 1967, **89**, 5012-5017.

151. H. T. Huang and C. Niemann, *J. Am. Chem. Soc.*, 1950, **72**, 921-922.

152. V. Dourtoglou and B. Gross, *Synthesis*, 1984, 572-574.

153. S. T. Chen, S. H. Wu and K. T. Wang, *Synth. Commun.*, 1989, 37-38.

154. L. Carpino and A. El-Faham, *J. Org. Chem.*, 1995, **60**, 3561-3564.

155. L. A. Carpino, *J. Am. Chem. Soc.*, 1993, **115**, 4397-4398.

156. C. Bisang, C. Weber, J. Inglis, C. A. Schiffer, W. F. VanGunsteren, I. Jelesarov, H. R. Bosshard and J. A. Robinson, *J. Am. Chem. Soc.*, 1995, **117**, 7904-7915.

157. Y. M. Angell, C. García-Echeverría and D. H. Rich, *Tetrahedron Lett.*, 1994, **35**, 5981-5984.

158. Y. M. Angell, T. L. Thomas, G. R. Flentke and R. D. H., *J. Am. Chem. Soc.*, 1995, **117**, 7279-7280.

159. L. A. Carpino, A. El-Faham, C. A. Minor and F. Albericio, *J. Chem. Soc., Chem. Commun.*, 1994, 201-203.

160. T. Shioiri, K. Ninomiya and S. Yamada, *J. Am. Chem. Soc.*, 1972, **94**, 6203-6205.

161. S. Zimmer, E. Hoffmann, G. Jung and H. Kessler, *Lieigs Ann. Chem.*, 1993, 497-501.

162. M. M. Lenman, *Ph. D Thesis*, St. Andrews University, 1995.

163. M. D. Ryan, M. Donnelly, A. P. Mehrotra, J. Wilkie and D. Gani, *Bioorg. Chem.*, 1999, **27**, 55-79.

164. A. Lewis, *Ph. D Thesis*, St. Andrews University, 1998.

165. J. P. Schneider and J. W. Kelly, *Chem. Rev.*, 1995, **95**, 2169-2187.

166. V. Brandmeier and M. Feigel, *Tetrahedron*, 1989, **45**, 1365-1376.

167. B. Hartzoulakis, T. J. Rutherford, M. D. Ryan and D. Gani, *Tetrahedron Lett.*, 1996, **37**, 6911-6914.

168. R. D. Allan, H. W. Dickenson, G. A. R. Johnston, R. Kazlauskas and H. W. Tran, *Aust. J. Chem.*, 1985, **38**, 1651-1656.

169. R. F. Heck, *J. Am. Chem. Soc.*, 1969, **91**, 6707-6714.

170. W. Cabri and I. Candiani, *Acc. Chem. Res.*, 1995, **28**, 2-7.

171. A. deMeijere and F. E. Meyer, *Angew. Chem. Int. Ed. Engl.*, 1994, **33**, 2379-2411.

172. D. L. Thorn and R. Hoffmann, *J. Am. Chem. Soc.*, 1978, **100**, 2079-2089.

173. J. Kabbara, C. Hoffmann and D. Schinzer, *Synthesis*, 1995, 299-302.

172. D. L. Thorn and R. Hoffmann, *J. Am. Chem. Soc.*, 1978, **100**, 2079-2089.

173. J. Kabbara, C. Hoffmann and D. Schinzer, *Synthesis*, 1995, 299-302.

174. A. G. Myers, M. M. Alauddin, M. M. Fuhry, P. S. Dragovich, N. S. Finney and P. M. Harrington, *Tetrahedron Lett.*, 1989, **30**, 6997-7000.

175. A. G. Myers and P. S. Dragovich, *Org. Synth.*, 1995, **72**, 104-111.

176. N. Ono, T. Yamada, T. Saito, K. Tanaka and A. Kaji, *Bull. Chem. Soc. Jap.*, 1978, **51**, 2401-2404.

177. S. N. Filigheddu and M. Taddei, *Tetrahedron Lett.*, 1998, **39**, 3857-3860.

178. K. Fuji, T. Kawabata and E. Fujita, *Chem. Pharm. Bull.*, 1980, **28**, 3662-3664.

179. C. D. Mudaliar and S. H. Mashraqui, *J. Chem. Res.*, 1994, 174-175.

180. F. Fache, F. Valot, A. Milenkovic and M. Lemaire, *Tetrahedron*, 1996, **52**, 9777-9784.

181. F. Effenberger, U. Burkard and J. Willfahrt, *Angew. Chem. Int. Ed. Engl.*, 1983, **22**, 65-66.

182. C. D. Beard, K. Baum and V. Grakauskas, *J. Org. Chem.*, 1973, **38**, 3673-3677.

183. T. P. Kogan, T. C. Somers and M. C. Venuti, *Tetrahedron*, 1990, **46**, 6623-6631.

184. E. Leete, *Tetrahedron Lett.*, 1968, **55**, 5793-5794.

185. S. Yamada, T. Kitagawa and K. Achiwa, *Tetrahedron Lett.*, 1967, **31**, 3007-3011.

186. R. Frank and M. Schutkowski, *Chem. Commun.*, 1996, 2509-2510.

187. F. A. Etzkorn, T. Guo, M. A. Lipton, S. D. Goldbergand and P. A. Bartlett, *J. Am. Chem. Soc.*, 1994, **116**, 10412-10425.

188. A. Lombardi, G. D'Auria, O. Maglio, F. Nastri, L. Quartara, C. Pedone and V. Pavone, *J. Am. Chem. Soc.*, 1998, **120**, 5879-5886.

189. D. Ranganathan, V. Haridas and I. L. Karle, *J. Am. Chem. Soc.*, 1998, **120**, 2695-2703.

190. J. S. Nowick, *Acc. Chem. Res.*, 1999, **32**, 287-296.

191. D. H. Williams and I. Fleming, '*Spectroscopic Methods in Organic Chemistry*', ed. McGraw-Hill, 1995, 102-105.

192. F. Adrián, M. I. Burguete, S. V. Luis, J. F. Miravet, M. Querol and E. GarciaEspana, *Tetrahedron Lett.*, 1999, **40**, 1039-1040.

193. C. J. Salomon, E. G. Mata and O. A. Mascaretti, *Tetrahedron*, 1993, **49**, 3691-3748.

194. M. E. Jung and M. A. Lyster, *J. Am. Chem. Soc.*, 1977, **99**, 968-969.

195. T. Ho and G. A. Olah, *Angew. Chem. Int. Ed. Engl.*, 1976, **15**, 774-775.

196. G. A. Olah and S. C. Narang, *Tetrahedron*, 1982, **38**, 2225-2277.

197. R. S. Lott, V. S. Chauhan and C. H. Stammer, *J. C. S. Chem. Comm.*, 1979, 495-496.

198. G. A. Olah, S. C. Narang, B. G. B. Gupta and R. Malhotra, *J. Am. Chem. Soc.*, 1979, **44**, 1247-1251.

199. J. Diago-Meseguer, A. L. Palomo-Coll, J. R. Fernandez-Lizarbe and A. Zugaza-Bilbao, *Synth. Commun.*, 1980, 547-551.

200. R. D. Tung and D. H. Rich, *J. Am. Chem. Soc.*, 1985, **107**, 4342-4343.

201. L. Qian, Z. Sun, T. Deffo and K. B. Mertes, *Tetrahedron Lett.*, 1990, **31**, 6469-6472.

202. N. Pitt and D. Gani, *Tetrahedron Lett.*, 1999, **40**, 3811-3814.

203. J. R. Rachele, *J. Org. Chem.*, 1963, **28**, 2898.

204. F. Emery, C. Bisang, M. Favre, L. Jiang and J. A. Robinson, *Chem. Commun.*, 1996, 2155-2156.

205. R. M. Williams, D. J. Aldous and S. C. Aldous, *J. Org. Chem.*, 1990, **55**, 4657-4663.

206. D. Zhai, W. Zhai and R. M. Williams, *J. Am. Chem. Soc.*, 1988, **110**, 2501-2502.

207. R. C. Corcoran and J. M. Green, *Tetrahedron Lett.*, 1990, **47**, 6827-6830.

208. W. C. Still, M. Khan and A. Mitra, *J. Org. Chem.*, 1978, **43**, 2923-2925.

209. T. Kolasa and M. J. Miller, *J. Org. Chem.*, 1987, **52**, 4978-4984.

210. K. Mori, M. Sasaki, S. Tamada, T. Suguro and S. Masuda, *Tetrahedron*, 1979, **35**, 1601-1605.

211. G. Bitan and C. Gilon, *Tetrahedron*, 1995, **51**, 10513-10522.

212. S. Kano, Y. Yuasa, T. Yokomatsu and S. Shibuya, *J. Org. Chem.*, 1988, **53**, 3865-3868.

213. K. Y. Zee-Cheng and C. C. Cheng, *J. Med. Chem.*, 1972, **15**, 13-16.

214. D. S. Lingenfelter, R. C. Helgeson and D. J. Cram, *J. Org. Chem.*, 1981, **46**, 393-406.

215. M. Fujino and C. Hatanaka, *Chem. Pharm. Bull.*, 1967, **15**, 2015-2016.

216. A. Sutherland and C. L. Willis, *J. Org. Chem.*, 1998, **63**, 7764-7769.

217. A. Ahmed, N. Taniguchi, H. Fukuda, H. Kinoshita, K. Inomata and H. Kotake, *Bull. Chem. Soc. Jap.*, 1984, **57**, 781-786.

218. F. Weygand and W. Swodenk, *Chem. Ber.*, 1960, **93**, 1693-1696.

219. B. D. White, J. Mallen, K. A. Arnold, F. R. Fronczek and R. D. Gandour, *J. Org. Chem.*, 1989, **54**, 937-947.